# COBALT, NICKEL AND SELENIUM IN TASMANIAN ORE MINERALS

by

G. D. LOFTUS-HILLS, B.Sc. (Hons.)

Submitted in partial fulfillment of the requirements

for the degree of Doctor of Philosophy.

UNIVERSITY OF TASMANIA

HOBART

1968

This thesis contains no material which has been accepted for the award of any other degree or diploma in any University and, to the best of my knowledge and belief, contains no copy or paraphrase of material previously published or written by another person, except where due reference is made in the text of the thesis.

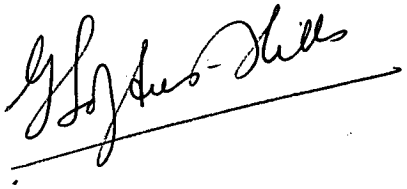

G. D. LOFTUS-HILLS.

University of Tasmania,
November, 1968.

# ABSTRACT

Analyses of Co, Ni and Se in pyrites and other minerals from a wide variety of Tasmanian ore deposits support a genetic relationship between the Mt. Lyell (pyritic - Cu) and Rosebery (banded Zn-Pb-Cu) deposits, and the Cambrian eugeosynclinal volcanic rocks in which they occur.

The concentration trends for all the ores due to fundamental availability contain smaller-scale components due to depositional processes, which, except in one case, do not interfere with these trends. The components include impoverishment of Co (and Ni) during remobilization of sulphides, increase in Ni and decrease in Co away from the centre of zoned deposits, impoverishment of Ni (and Co) in replacement as compared with vein lodes, and regular and irregular partitioning of respectively Co-Ni and Se between coexisting minerals.

The trends of Co-Ni in pyrite due to availability include the following:

(a) The sedimentary-diagenetic pyrites generally contain Co/Ni < 0.5, but show no correlation of Co-Ni values with rock type, age, or degree of recrystallization.

(b) Pyrites in the Cambrian acid-intermediate igneous rocks have Co/Ni ratios ranging 1-150, and contain up to 0.8% Co.

(c) Pyrites from Devonian hypogene replacement and vein deposits show two main trends - 0-1500 ppm Ni, with Co/Ni < 1; and 0-400 ppm Co, with Ni ranging 10-100 ppm.

The Se contents of sulphides associated with Cambrian and Devonian acid-intermediate igneous activity are indistinguishable, but the Savage River magnetite ore, the Cuni Cu-Ni ore, and particularly the Mt. Lyell ore are all enriched in Se, whereas the Rosebery ore is impoverished.

The Co-Ni values in the Mt. Lyell and Rosebery ores follow the trend for pyrites in the Cambrian acid-intermediate igneous rocks. The dispersion of Se at Mt. Lyell is consistent with the postulated open-cast origin for the massive ores, and within the Rosebery lode, the stratification of the Co-Ni values, and their gradation between lode and normal sedimentary types, strongly suggest a sedimentary origin. These and other collated data suggest that ores associated with geosynclinal vulcanism may be characterized by (i) high to very high Co/Ni ratios, and often marked impoverishment in Ni, (ii) greater Co and Ni concentrations associated with Cu than with Pb-Zn ores, both within and between deposits, and (iii) a tendency for Co to correlate with Cu within deposits.

In Tasmania, Se and $\delta S^{34}$ values are more closely controlled than Co-Ni in their fundamental availability by other than genetic factors, and within deposits they show less variation due to depositional processes.

Selenium was analyzed by X-ray fluorescence spectrography, and Co and Ni by atomic absorption spectrophotometry. In the latter technique, because Fe caused both non-atomic absorption and chemical interferences in the flame, it was extracted with di-isopropyl ether.

CONTENTS

LIST OF FIGURES

## LIST OF PLATES

LIST OF TABLES

# 1. INTRODUCTION

Tasmanian ore deposits are unusual in their variety and richness. They have been subjected to scientific examination for over eighty years, but the origin of some of them is still unclear. This thesis forms part of the continuing investigation of the deposits by the group led by Dr. M. Solomon at the University of Tasmania. In addition to using standard field and laboratory research techniques, the group is specializing in mineral thermometry and barometry, isotope geology, and geochemistry.

## SCOPE OF THE THESIS

The initial aim of the investigation was to determine the extent to which the trace Co, Ni and Se contents of ore minerals could be used to elucidate the genesis of some Tasmanian ore deposits. In order to define trace-element concentration trends which were empirically useful as genetic discriminants, as many as possible of the potentially interfering non-genetic trends, due to local effects at the deposition site and post-depositional changes, had first to be accounted for. This has yielded results of general geochemical significance, and has helped to solve some specific geological problems.

Part of this work has been undertaken in collaboration with Mr. D. I. Groves (Tasmanian Department of Mines). While most of the Co and Ni work is mine, the study of Cd in sphalerite was mainly Groves',

and the Se analytical work was equally shared. The only analytical data listed in the body of the thesis are those produced wholly or partly by myself. The analyses of Cd and Fe in sphalerite are listed in Appendix 2. The development of original analytical techniques is described in Chapter 4, but the detailed procedures are described in Appendices.

## ACKNOWLEDGEMENTS

I wish to express my appreciation of the sustained inspiration, guidance, and practical assistance of Dr. Michael Solomon during the course of this study. Mr. David Groves' energetic cooperation in our joint investigations is very much appreciated. Mr. Ramsay Ford has been a source of expert advice on all matters geochemical. Discussion with other Departmental staff, and fellow graduate students, has been most stimulating.

Thanks are due to the following for invaluable advice on atomic absorption technique and theory: Dr. K.L. Williams and Dr. C.S. Rann (A.N.U.), Mr. B.S. Rawling (Zinc Corporation, Broken Hill), Dr. D.J. David (CSIRO, Canberra), and Prof. T.S. West (Imperial College, London). Dr. J.F. Lovering (A.N.U.) kindly arranged for analyses of pyrite specimens on the electron microprobe. Dr. P.W. Smith (University of Tasmania), Prof. H.P. Schwarcz (McMaster) and Dr. J.B. Goodenough (M.I.T.) gave helpful advice on crystal field theory, and Mr. B.D. Johnson and Dr. V.P. St. John generously devoted time to developing computer programmes. Mr. A. Grassia (CSIRO, Hobart) and J.P. McKibben helped in elucidating some statistical problems.

For permission to sample, and for assistance in the field, I am indebted to the Mt. Lyell Co. and Messrs. R. G. Elms and K. O. Reid; the Electrolytic Zinc Co. and Mr. R. B. Brathwaite; Renison Ltd. and Mr. R. Shakesby; the Storey's Creek Tin Mining Co.* and Mr. C. Kingsbury; the Broken Hill Proprietary Co. and Mr. C. E. Gee; and Pickands Mather & Co. and Mr. A. Munro. Samples were also collected by Dr. R. George, and Messrs. M. R. Banks, A. Brown, C. E. Gee, A. B. Gulline, J. P. McKibben, J. Jago, M. Rubenach, and D. Patterson. I wish to thank Dr. M. Solomon, Mr. C. E. Gee and Mr. P. Gourley, for assistance in the field. The assistance with some of the drafting of Mrs. Helen Quilty and the Tasmanian Mines Department is gratefully acknowledged.

The research was supported by the Australian Research Grants Committee (grant to Dr. M. Solomon) and by the University of Tasmania research funds.

For laboratory and typing assistance, and for sustained encouragement, I am greatly indebted to my wife.

---

* The spelling of the town, from which the mine takes its name, has been changed to "Story's Creek".

# 2. THE STUDY OF TRACE ELEMENTS IN ORE MINERALS

## DISPERSION OF TRACE ELEMENTS

All naturally crystallizing minerals incorporate, by various mechanisms, traces of elements foreign to the mineral. The trace element content of an ore mineral is controlled by a large number of variables, which may be divided into those acting at the source of the transporting medium, during transport, during deposition, and after deposition (during metamorphism or diagenesis). Rose (1967) has given an extensive list of possible variables in a magmatic-hydrothermal ore-depositing system. In such a system the individual variables at source and during transport are not all accessible for systematic investigation, and trace element concentration due to their combined effect is referred to here as "availability". Even when the source and transport mechanisms can be examined, as with some minerals formed by surface processes, so many variables are acting that it is often still necessary to describe their effect in terms of empirical availability.

Trace elements may be held in various structural sites in a mineral e.g. in diadochic substitution, in interstitial sites, in lattice defects (Goni and Guillemin, 1964), or in growth zones (Grigor'ev, 1961; Tauson, 1965). In addition, trace minerals may be captured during the growth of the host mineral, or may exsolve during its cooling, and these may interfere in those trace element studies which require single-mineral rather than whole-ore analysis (Loftus-Hills and Solomon, 1967). It should be noted with respect to the following discussions that some older single-mineral trace element analyses do not record any monitoring of, in particular, trace mineral contamination.

## APPLIED STUDIES

Trace element studies in sulphides have usually been directed towards one or more of the following objectives : determination of metallogenic provinces, of general environment of deposition, or of detailed conditions of deposition (Loftus-Hills and Solomon, 1967). The studies as listed require examination of successively shorter wavelengths in the concentration-distance distribution pattern, but different combinations of trace elements and minerals have different patterns. The elements most suitable for study of availability are those that show little control by depositional and post-depositional variables, thus allowing the larger scale patterns to emerge. Conversely, if an element is a good discriminant of the local variables, it may thereby be a poor indicator of availability. The usefulness of various trace elements in these studies will be examined in following sections.

### Metallogenic Provinces

The dispersion of metals in space and time over large areas has been studied on many different scales and with varying emphases, but the evident difficulties in defining criteria for classification of metallogenic provinces and epochs (Turneaure, 1955) has somewhat inhibited quantitative studies. On the scale of continental structures genetic relationships cannot generally be demonstrated, and the investigations are mainly empirical. Within tectonic units, however, it becomes possible to relate the distribution of metals to magmatic, tectonic and sedimentary stages of geosynclinal development (Bilibin, 1955; McCartney, 1965; Solomon, 1965a), and genetic associations such as Cu-Ni sulphides in early geosynclinal ultramafics, and Sn in later granites, are well known.

It has long been recognized (DeLaunay and Urbain, 1910) that trace concentrations of metals can be used to supplement and expand classification of metallogenic provinces and epochs based on mineral concentrations. Stoiber (1940) and Schroll (1950, 1951) found that the trace element composition of, respectively, sphalerite, and galena and sphalerite, was distinctive for certain metallogenic provinces. Warren and Thompson (1945) and Burnham (1959) have subdivided large, mineral-defined provinces on the basis of trace elements in sphalerite, and sphalerite and chalcopyrite. On a smaller scale, Rose (1967) used trace elements in sphalerite and chalcopyrite to classify in space and time the mineralization within the Central district, New Mexico, and the Bingham district, Utah. In each of these studies it was shown, at least qualitatively, that the discriminating elements had appropriate distribution patterns. Burnham (1959) demonstrated this distribution quantitatively by calculating that the variance of tin in chalcopyrite was greater between districts than within districts.

In Australia the only attempt to relate trace element distributions to evolutionary stages in the development of a geosyncline has been by Harris (1965), who studied galena, sphalerite and chalcopyrite in southeastern New South Wales, within the Tasman Geosyncline. His study suffered from inadequate sampling, and no firm conclusions can be drawn from it.

## Environments and conditions of deposition

The many attempts to relate trace element distribution in ore minerals to the origin and depositional conditions of the ores can be classified as follows:

(i) Single minerals have been analyzed in attempts to correlate temperature of formation with the concentration of individual elements. The concentrations of Cd, Mn, Ge, In, Ga and other elements in sphalerite (e.g. Fryklund and Fletcher, 1956), Re in molybdenite (Fleischer, 1959; Badalova et al., 1962; Paganelli, 1963), and Ag, Sb and Bi in galena (Fleischer, 1955; El Shazly et al., 1957), have been extensively tested for such correlations. It has gradually been realized that there should be no direct temperature-control of concentrations, as the trace elements are undersaturated with respect to the host mineral. Nevertheless, certain types of ore appear to develop within certain temperature ranges, and thus the trace and major element composition may indicate the approximate temperature of deposition. It is clear, however, that the single element-single mineral approach is applicable only over restricted areas.

More useful are sets of several trace elements, which can for example "fingerprint", if only empirically, certain environments of deposition, in the same way that sets can characterize metallogenic provinces (Taylor, 1965). Fruth and Maucher (1966) have used the technique in a stratiform Pb-Zn deposit in the Bergamo Alps, Italy, to correlate two distinctive trace element sets with two sedimentary facies of the host rock, and they consider that this evidence supports a syngenetic origin for the ore.

(ii) Of greater significance for temperature determination is the analysis of pairs of coexisting minerals for single elements.

The partition coefficient defining equilibrium concentrations of the element in the two minerals is a quantitative function of temperature, and can be determined experimentally (Friedman, 1949; McIntire, 1963; Barton and Skinner, 1967). Numerous attempts to show consistent partition in natural ores (summary in Fleischer, 1955; Fryklund and Harner, 1955; Fryklund and Fletcher, 1956; Wilson and Anderson, 1959; Doe, 1962; Rose, 1967) have indicated that apparently coexisting ore minerals are rarely in trace element equilibrium.

This could be explained either by the minerals incorporating the trace elements in non-equilibrium amounts, or by the minerals not being deposited contemporaneously. More successful studies with silicate pairs suggest that in order to produce equilibrium partition, it may be necessary to anneal the ore for times comparable with those involved in regional metamorphism. Some metamorphosed ores show more consistent partition between minerals than unmetamorphosed ores (Roscoe, 1965).

(iii) One mineral may be analyzed for a selected pair of elements. This approach is used in petrological studies, where ratios such as Rb/K, Ni/Co, Ni/Mg, Hf/Zr, Ba/Sr (Taylor, 1965) have proved powerful tools for investigating the geochemistry of igneous rock series. The pairs consist either of a trace and a major element which are chemically similar, the former substituting for the latter; or two trace or minor elements that are similar enough to enter the same host mineral, but show different sensitivities to environmental or depositional variables.

In studies of ores, Troshin (1962) has used Ga/In ratios in sphalerite to qualitatively define temperature ranges of ore deposition. However the two most promising ratios - Co/Ni and Se/S* - have been found most useful in defining environments of deposition (see Chapter 3).

(iv) The spatial pattern of trace-element distribution within a deposit can not only indicate gradients of temperature, etc. during deposition; it can also reflect the environment of deposition of the ore. One might expect, for example, a stratification of trace element values parallel to bedding in a sedimentary mineral deposit. However the existence of such a relationship would be insufficient evidence for assigning a sedimentary origin to a deposit.

As Cambel and Jarkovsky (1967) have stressed, it is pointless, if only because of sampling requirements, to attempt determination of environments of deposition by trace element studies without a thorough knowledge of the geology and mineralogy of the sampled areas. The better this knowledge, the greater is the possibility that the trace element dispersion shown by each deposit, and the differences between deposits, might be explained geochemically, rather than by empirical availability. Especially within deposits, the dispersions are meaningless without being tested against predetermined parameters such as spatial interval, mineralogical zoning, temperature gradients, time

---

* There is no advantage in also analyzing S where single monometallic sulphides, rather than mixed sulphides or concentrates, are being studied. Analyses for Se only would then be classified in group (i).

intervals (e.g. textural sequences), differences in wallrock, etc. By systematic elimination of variables it may then be possible to approach unique interpretations of data.

## PROBLEMS OF INVESTIGATION

Many trace element investigations of hypogene ore deposits have been at least partly directed towards the interpretation of the data in terms of temperature control. However, not only are temperature gradients difficult to establish independently, due to the paucity of ore thermometers, but interfering variables may be impossible to define, much less account for quantitatively. This complexity is shown, for example, by zoning of trace elements within single crystals (e.g. Muravyeva et al., 1964). Rose (1967), after analyzing zones in a large sphalerite crystal for Mn, Cd, Co, In, Ni and Fe, inferred that at least four factors were necessary to explain the concentration variations across the crystal. Such studies suggest that the elucidation of detailed processes of trace element dispersion should improve with the number of elements analyzed. The use of multi-element sets has been encouraged by the existence of techniques of multivariate analysis such as factor analysis (e.g. Spencer, 1966).

It is not immediately apparent that single-mineral analyses are to be preferred to analyses of whole-ore in every type of investigation. In the study of availability, for example, although the use of a single mineral ensures a constant host matrix, any dilution effect due to other trace-accommodating minerals in the deposit remains undefined. Gavelin and Gabrielson (1947) and Burnham (1959) found that

characteristic values in one mineral were accompanied by similarly high or low values in associated minerals. It cannot be assumed, however, that dilution is unlikely under all conditions of ore deposition, and in this study, although the sample sets are biased towards a single mineral, check-analyses have been performed on associated, where possible coexisting, minerals.

In single-mineral studies the minimum size of specimens is determined by the concentration of the mineral in the ore, combined with the efficiency of the separation procedures, and the sensitivity of the analytical technique. When the ore is locally about 100% single mineral (allowing sampling from polished sections), or the trace element concentrations come within the range of an electron microprobe, it is possible to keep sample-volumes very small in order to avoid trace mineral contamination. This procedure may be disadvantageous in practice, as more analyses will be required to delineate variation of a given wavelength, and in general a compromise must be reached between analyzing many small samples relatively easily, and analyzing fewer large samples demanding lengthier preparation.

The problems of properly designing a sampling programme in single-mineral trace element investigations are formidable. Not only is constant sample size impossible to maintain, because of variable concentration of the mineral in the ore, and discontinuity of mineralization; but the sampling interval, which is usually already variable due to difficulty of access and irregularity of distribution of the single mineral, cannot be optimised without some prior knowledge of the distribution of the trace element in the ore. In particular, the type of

serial correlation (Agterberg, 1965) would have to be established for each deposit, as the surface defining the limits of mutual dependence of trace element concentrations in specimens close together may be highly asymmetrical in three dimensions. Finally, if the intention is to specify the trace element content of a whole ore deposit, and the sampling technique cannot be systematized, then the existence of gross concentration gradients, combined with the serial correlation effects, can only be allowed for by quantity rather than quality of samples. It may be noted that in many cases where the ideas on the origin of an orebody have changed, the original sampling in older trace element investigations, and therefore the data, may be inappropriate for testing the new hypotheses.

## THE STUDY OF TASMANIAN ORES

The ore deposits of Tasmania, and particularly of western Tasmania, are highly suitable for trace element investigations, for the following reasons:-

(i) The regional geology and tectonics is well known, and the detailed geology of many of the mines is adequately documented.

(ii) Uncertain relationships between some igneous rocks and nearby ores have been reduced by extensive radiometric dating of the former.

(iii) The small size of the area should minimize gross variations in deep-seated trace element availability for any metallogenic unit.

(iv) Pyrite occurs in every one of the major deposits, and most of the small ones, allowing comparative studies within a constant matrix.

There are two main clases of ore deposit in Tasmania which are suitable targets for trace-element investigation:

(a) The large deposits at Rosebery and Mt. Lyell have until this decade been regarded as Devonian magmatic-hydrothermal replacement deposits. However, both these deposits occur within Cambrian volcanic rocks, and in common with many similar ore deposits throughout the world, a genetic association of the ores with their host rocks is becoming increasingly apparent. The empirical data of trace elements in ore minerals could therefore provide further evidence for or against such an association.

(b) There are several smaller vein deposits which, when examined by standard geological techniques, do not clearly reveal their origin. A trace element study could well do so.

The trace elements chosen for investigating the Tasmanian environments of deposition were Co, Ni and Se. These elements are present in reasonably high concentrations, are less likely than some other elements such as Pb, Zn, Cu, As, and Sn to contaminate as trace minerals, and have previously been successful as environmental indicators (see Chapter 3). Minerals other than pyrite were analyzed for these elements where pyrite was absent, or where dilution or partition effects required study. If mineral separation was impossible with available equipment, whole-ore samples were used. The overall availability trend for each deposit was investigated for interfering components due to within-deposit variables by testing the trace element concentrations against all possible independent local parameters. The valid trends were then used for genetic discrimination.

Tasmanian metallogenesis may be divided into five units: one probably Precambrian, two Cambrian (one mafic-ultramafic igneous, one acid igneous), and two Devonian (one in the west, one in the north-east). The procedure has been to establish the trace element distribution both within and between deposits of known origin in each of these units; to determine the background sedimentary-diagenetic values in a wide variety of sedimentary rocks; and then to compare these with the distributions for the deposits of uncertain origin. The results of the empirical correlations have then been compared with similar empirical evidence from Cd in sphalerites (Appendix 2), and from S-isotope data.

# 3. DISPERSION OF COBALT, NICKEL, SELENIUM AND CADMIUM

## COBALT AND NICKEL

### Crystal Chemistry

To facilitate interpretation of the analytical data, an attempt has been made to determine orders of preference for accommodation of Co and Ni in the structures of minerals used in this study. The best approach would have been to use quantitative crystal field stabilization energy (CFSE) data for the elements and structures involved, but such data does not yet exist for the transition metal sulphides. It was therefore necessary to compile all available experimental and empirical data in an attempt to give a qualitative order of accommodation.

A reasonable interpretation from the data is given in Figure 3.1, which suggests how Co and Ni should partition between arsenopyrite, pyrite, pyrrhotite, chalcopyrite, magnetite and hematite, assuming mutual equilibrium. This interpretation is based on evidence of widely varying quality; in general the orders of accommodation in the individual minerals are more firmly based than the differences in accommodation between minerals. Several different types of explanation are available for some of these relationships, but the most fundamental reasoning applicable to each is as follows:-

Figure 3.1

Suggested partition of Co and Ni between ore minerals. The orders of accommodation, assuming mutual equilibrium, between arsenopyrite, pyrite, pyrrhotite, chalcopyrite, magnetite and hematite, are derived from empirical results and from crystal chemistry.

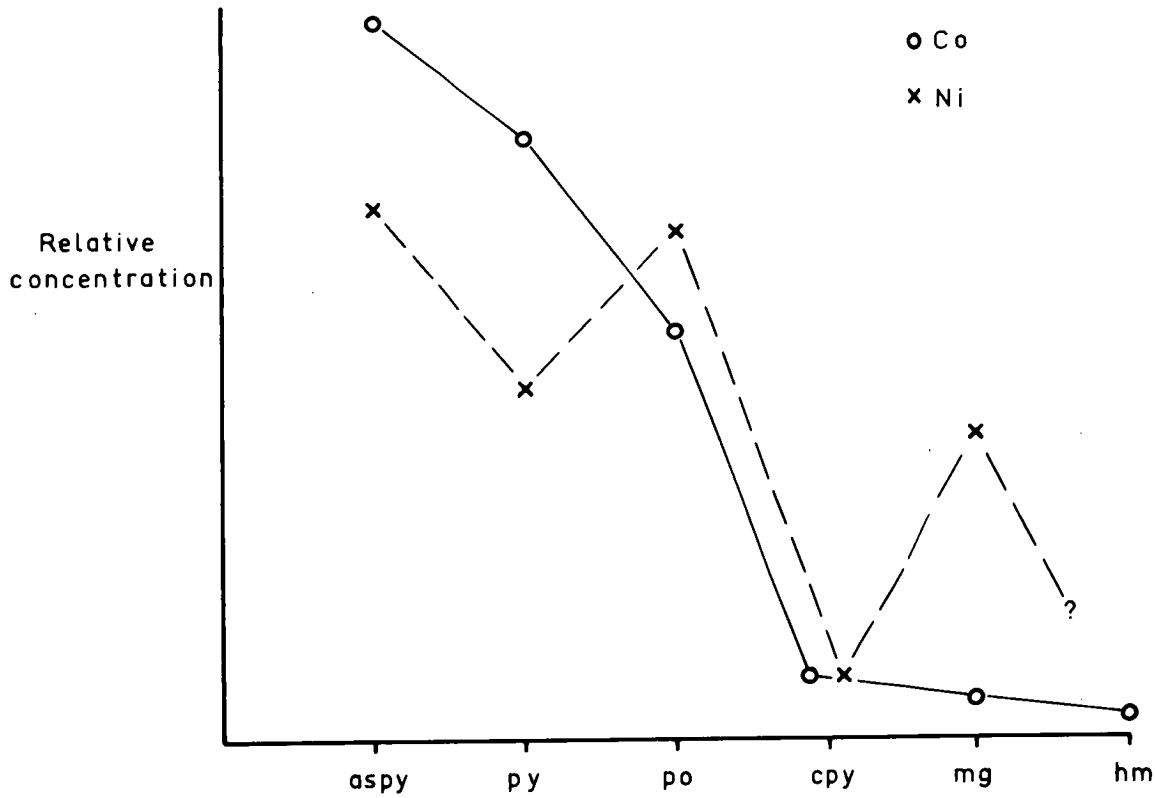
o Co
× Ni
Relative concentration
?
aspy
py
po
cpy
mg
hm

Arsenopyrite : Co > Ni : There is a Co equivalent of arsenopyrite - glaucodot, (Co,Fe)AsS - and there may be a solid solution series between arsenopyrite and glaucodot (Dana, 1944). However there is no equivalent orthorhombic Ni-As sulphide.

Pyrite : Co > Ni : Elliott (1960) and Burns and Fyfe (1967) show that the bond length $M^{2+}$ - S decreases in the order $NiS_2$ - $CoS_2$ - $FeS_2$. As the CFSE is proportional to the closeness of packing, and the $M^{2+}$ - S distance may be taken as a measure of this closeness (Schwarcz, 1967), the Co atom is thus more stable than the Ni atom in the $MS_2$ configuration. This order of stability is reflected in the greater degree of solid solubility in the system $CoS_2$ - $FeS_2$ (complete) than in the system $NiS_2$ - $FeS_2$ (limited) in natural minerals.

Pyrrhotite : Ni > Co : (a) There is a Ni equivalent of pyrrhotite - millerite - but no valid equivalent Co mineral species, as jaipurite, CoS, has not been confirmed (Dana, 1944).

(b) An inspection of the symmetries of all the Fe, Co and Ni sulphides reveals that Co does not readily form structures of lower symmetry, whereas Ni more easily accommodates in such structures. This suggests that Ni is preferentially stabilized in less symmetrical structures, such as pyrrhotite.

Chalcopyrite : Co = Ni ? : As very little evidence can be adduced for the relationships in chalcopyrite, there being no Co or Ni equivalents of $CuFeS_2$, no basis exists for predicting an order of accommodation.

Magnetite : Ni > Co : Magnetite is an inverse spinel, and the $M^{2+}$ sites are therefore in octahedral coordination. The CFSE data are

known for the oxides, and reveal that $Ni^{2+}$ is more stabilized than $Co^{2+}$ in octahedral sites (Schwarcz, 1967).

Hematite : Co only ? : The existence of Ni in the +3 oxidation state has not been established, although higher oxidation states can be produced (Sisler, Vanderwerf and Davidson, 1949). This suggests that, small though the amount of Co entering the hematite lattice appears to be, the Ni content should be even smaller, and where present, probably not held in diadochic substitution.

The relative concentrations of Co and Ni between minerals must be justified mainly on empirical grounds. The exceptions are: (a) Crystal chemical considerations show that transition metals will be much more readily accommodated in sulphides than in oxides because (i) they are in the more stable low spin configuration in sulphides (Schwarcz, 1967), and (ii) the stabilization of the metals in the sulphide sites is strengthened by π-bond formation (Burns and Fyfe, 1967). (b) The concentration of Co in hematite should be low because the available Co species will probably be in the +2 oxidation state. (c) The concentration of both Co and Ni in chalcopyrite will be lower than in the other sulphides because both the Cu and Fe atoms are in sites of tetrahedral coordination, which are energetically less stable than those octahedrally coordinated, as in arsenopyrite, pyrite and pyrrhotite (J. B. Goodenough, pers. comm.).

The relationships between arsenopyrite, pyrite and pyrrhotite are founded entirely on observational evidence. Much of the pioneering work was based on mineral assemblages which were stated to be in paragenetic sequences, no claim being made for textural equilibrium

(Rost, 1939; Hegemann, 1943; Gavelin and Gabrielson, 1947). Nevertheless the early conclusions have not been substantially varied by later work, although one of the latter (Neumann, 1950), despite the significance given it by Deer, Howie and Zussman (1962, p.149), is based on inadequate sampling. The major qualitative conclusion which may be drawn, particularly from the data of Wager, Vincent and Smales (1957) and Hawley and Nichol (1961), is that pyrite discriminates against Ni more strongly than pyrrhotite discriminates against Co (Fig. 3.1). However some of the Ni and Co in pyrrhotite may be present in intergrown or exsolved pentlandite (Deer, Howie and Zussman, 1962, p.150), and the possibility arises that much of the Ni enrichment commonly found in pyrrhotite is due to trace mineral contamination, which was certainly not allowed for in any of the studies quoted above.

## Primary Dispersion

### Availability

The Co/Ni ratio is low in mafic and ultramafic rocks, but during differentiation the ratio rises, until in late silicic fractions it can be > 1 (Taylor, 1965). It is apparent that Ni is withdrawn from the fluid into crystallizing minerals more rapidly than Co, which is thereby enriched in residual fluids. This is explained by the preferential CFSE of Ni in octahedral oxygen-coordinated sites in silicates and oxides (Schwarcz, 1967). During early crystallization, Ni in particular enters the structures of olivine, pyroxene, and iron oxides, in which it probably substitutes for $Fe^{2+}$ (Ringwood, 1956). Nickel is also enriched in the early fractions of minerals, which can be explained by

inversion of solid-solution trends in Mg-Fe-Ni-Na silicate systems caused by the high octahedral site preference energy of $Ni^{2+}$ (Burns and Fyfe, 1967). The Ni content of later Fe-rich olivines becomes lower due to decreased availability (Wager and Mitchell, 1951). It is not clear whether $Co^{2+}$ substitutes for $Fe^{2+}$, or $Mg^{2+}$, or both, in the ferromagnesian minerals.

If the basic magma contains sufficient S, an immiscible sulphide phase may separate at an early stage, and Ni and Co will partition strongly into this melt from the silicate phase, either before or after silicate crystallization (Kullerud and Yoder, 1965). If the S content is somewhat lower, as in the Skaergaard intrusion (Wager, Vincent and Smales, 1957), the Ni and Co may be almost entirely taken up in silicates before sulphides begin to form. The sulphides are then Ni-Co deficient, and may be Cu-rich.

Granites have low Ni content, and even lower Co. The metals are held in the structures of ferromagnesian minerals such as biotite, which in the Cape Granite, South Africa, contains up to 105 ppm Ni and 57 ppm Co (Kolbe and Taylor, 1966a). There is a definite correlation of Ni with Fe and of Co with Fe and Mg (Carr and Turekian, 1961; Kolbe and Taylor, 1966a), although the concentrations of Ni and Co reduce to undetectable amounts as granites become leucocratic. The overall crustal abundances, and some detailed data, of Co and Ni are listed in Table 3.1.

The concentrations of Co and Ni in sulphides generally acknowledged to be derived from igneous rocks reflect to a certain extent concentrations in the parent bodies. Wilson's (1953) suggestion that

TABLE 3.1

ABUNDANCES OF Co AND Ni IN IGNEOUS ROCKS

Data are of crustal abundances from Turekian and Wedepohl (1961) except where indicated.

| | Co ppm | Ni ppm |
|---|---|---|
| Ultrabasic | 150 | 2000 |
| Basaltic | 48 | 130 |
| Acid granophyre [1] | 5 | 8 |
| Granites and granophyre [2] | - | 22 |
| Granodiorites and adamellites [3] | 13.5 | 15 |
| Gneissic granites [3] | 16 | 27 |
| Leucogranites [3] | < 1 | < 1 |
| Ca-rich granites | 7 | 15 |
| Ca-poor granites | 1 | 4.5 |

[1] At Skaergaard. Wager and Mitchell (1951).

[2] In Bushveld Igneous Complex. Liebenberg (1961).

[3] In New South Wales granites. Kolbe and Taylor (1966b).

pyrite derived from early magmatic melts should have a higher Ni and Co content, and a lower Co/Ni ratio, than pyrite derived from late fluids, was supported by the results of Hawley and Nichol (1961). Noddack and Noddack (see Rankama and Sahama, 1950, p.679) suggested that the average content of Co and Ni in magmatic sulphide ores is 0.21% and 3.14% respectively (Co/Ni = 0.07). Berg and Friedensburg (1944) showed that hydrothermal sulphides have Co/Ni ratios ranging from 0.1 up to, in pyrite, 830. Cambel and Jarkovsky (1967, Figs. 94, 97, 126) describe a range in the Co/Ni ratios of Czechoslovakian hydrothermal pyrites, with twice as many individual deposits containing Ni > Co as containing Co > Ni, the average Co and Ni contents being about 600 ppm.

The Co and Ni concentrations in ore deposits which are interpreted as being related to vulcanism are difficult to relate to the chemical evolution of the postulated source rocks, as the geochemical cycles of possible types of mineralizing solutions in the environment are far from understood. The solutions, and also their metal content, are probably polygenetic, due to admixture of meteoric waters, most obviously at the exhalative stage. For this reason much of the chemical and isotopic investigations of this type of ore deposit have been empirical, an approach made possible by the existence of modern occurrences of mineralization similar to a few of the ore types. In one such occurrence in the Red Sea (Miller et al., 1966) an Fe-Cu-Zn rich submarine discharge of thermal waters is depositing a sediment containing 300 ppm Co and 50 ppm Ni.

Despite the paucity of direct evidence for trace-element abundances in a volcanic environment of ore deposition, there are data for Co-Ni in pyrites from several ores which are associated with volcanic rocks, and can with greater or less certainty be related genetically to the volcanic activity, whether subvolcanic, exhalative, or of obscure environment. A representative sample of these ores is listed in Table 3.2. These pyrites show three outstanding features:

(i) Those from the unmetamorphosed ores, and from some of the metamorphosed ores, have extremely high Co/Ni ratios (up to 100), and remarkably restricted Ni ranges (e.g. 0-10 ppm, 20-50 ppm, 0-100 ppm). The exception is Stordo, which has Co/Ni = 0.1, but still shows negligible variation from 100 ppm Ni. According to Schneiderhohn (1962, p.315) and Routhier (1963, p.955), the Stordo deposit is sedimentary.

(ii) There is a distinct tendency, noted by Cambel and Jarkovsky (1967) both for their own results and those of Hegemann (1943), for Co (and to a much smaller extent Ni) to be more enriched in Cu ores than in Pb-Zn ores, typical concentration ranges being 50-1000 ppm Co and 0-400 ppm Co respectively. A tendency for Co to correlate with Cu is also shown by the Noranda ores (Roscoe, 1965), pyrite in the Zn-rich ores containing less Co (and Ni).

(iii) Some of the metamorphosed pyrites (e.g. Helpa), although having higher Co/Ni ratios, show just as restricted a range for Co as for Ni, probably due to metamorphic homogenization.

TABLE 3.2

SOME ORES OF POSSIBLE VOLCANIC ORIGIN ANALYZED FOR Co AND Ni

Cu deposits

| | Metamorphosed | Not strongly metamorphosed |
|---|---|---|
| Mainly basic vulcanism | Besshi-type (Japan) [5] | Smolnik (Czech.) [1] |
| | Roros-Lokken-type (Norway) [2] | Mnisek (Czech.) [1] |
| | Ergani (Turkey) [2] | Zlate Hory (Czech.) [1,6] |
| | Helpa (Czech.) [1] | Stordo (Norway) [2] |
| Mainly acid vulcanism | Noranda (Canada) [4] | Rio Tinto (Spain) [3] |
| | Falun (Sweden) [2] | |

Zn-Pb deposits

| | Not strongly metamorphosed |
|---|---|
| Acid-basic vulcanism | Stiavnica (Czech.) [1] |
| | Horni Benesov (Czech.) [1] |

References: [1] Cambel and Jarkovsky (1967).

[2] Hegemann (1943).

[3] Hegemann and Leybold (1954).

[4] Roscoe (1965).

[5] Yamaoka (1962).

[6] Gruszczyk and Pouba (1968).

Depositional processes

Goldschmidt (1954, p.668) lists several European workers who claimed a correlation between the Co content of pyrite and temperature of deposition, and Bjørlykke and Jarp (1950) made a similar suggestion for Norwegian pyrites. It was demonstrated by Rose (1967), however, that in chalcopyrite and sphalerite "The general lack of similarity in the behaviour of different elements", including Co, "even in parts of the same crystal, indicates that the trace element content is not dependent on any single environmental variable such as temperature ... Consideration of several factors is necessary to explain the variations" (p.582).

More empirically, several investigators have examined spatial variation of the Co and Ni contents within ore deposits. Suggestions by Auger (1941) that Co and Ni in pyrrhotite vary systematically with depth in the Noranda ore were regarded by Fryklund and Harner (1955) as inconclusive, and their own results on other ores failed to find any systematic trend. Lateral zoning of Co contents of sphalerite averaged over intervals of 2000 ft. has been found by Rose (1967) in the Central District, Utah, the decrease of Co outward from the granitic stocks paralleling a decrease in Zn/Pb ratio of the ores.

## Secondary Dispersion

Sedimentation

The cycles of Co and Ni in normal sedimentary environments have been summarized by Loftus-Hills and Solomon (1967), who emphasized the complexity of the variables controlling the ultimate trace element

content of a sedimentary pyrite crystal. The availability of the trace elements, particularly Ni, seems to be mainly a function of the history of potential adsorbing materials in the transporting medium. These adsorbents include detritus, particularly clays; scavenger Fe and Mn hydrated oxide colloids; and both terrestrial and marine organic compounds, which may form organometallic complexes. For example, terrestrial clays and organic materials with an inherited sorbed trace element component may adsorb further metals during transport, and the final distribution of the trace elements would be closely related to the history of transport and deposition of these carriers. The overall effect is that Ni, and to a less extent Co, correlate significantly with carbonaceous content of a sediment, and tend to be concentrated in shales, although the relative significance of these correlations is not constant (e.g. Krauskopf, 1956; Tourtelot, 1964; Vine, 1966).

The Co and Ni are rearranged during diagenesis, partitioning into any sulphide phase present (particularly pyrite).

Cobalt should be concentrated preferentially to Ni in pyrite, and this has been confirmed by Spencer (1966), who found the pyrite/shale partition for Co to be three to four times that for Ni. The extent to which partitioning of Co and Ni proceeds depends on the abundance and form of the sulphide and of alternative host minerals (clays, carbonaceous material), and on the degree of recrystallization, and can vary widely between rock units (Mohr, 1959; Le Riche, 1959; Nicholls and Loring, 1962; Spencer, 1966).

Despite the many variables, the Co/Ni ratio in sedimentary pyrites is generally < 1 (Table 3.3), and that in the whole-rock

TABLE 3.3

ABUNDANCES OF Co AND Ni IN SEDIMENTARY ROCKS AND PYRITES

| | Co ppm | | | Ni ppm | | |
|---|---|---|---|---|---|---|
| | Rock | Pyrite | Enrichment factor | Rock | Pyrite | Enrichment factor |
| A. Marine | | | | | | |
| Shale | 19 | 13-240 | 6 | 68 | 100-1010 | 8 |
| Sandstone | 0.3 | 10 | 17 | 2.0 | 10-35 | 11 |
| Limestone | 0.1 | 10-35 | 220 | 2.0 | 250-950 | 300 |
| Non-marine | | | | | | |
| Shale | 11* | 20-1050 | 47 | 25* | 100-950 | 21 |
| Sandstone | | 10 | | | 10-28 | |
| Limestone | | 45-200 | | | 560-1040 | |
| B. Undifferentiated | | | | | | |
| Shale | 10-50 | | | 20-100 | | |
| Sandstone | 1-10 | | | 2-10 | | |
| Limestone & dolomite | 0.2-2 | | | 3-10 | | |

A. "Rock" data from Turekian and Wedepohl (1961).

"Pyrite" data from Degens (1965).

"Enrichment factor" is the median of the range of concentrations in pyrite divided by the average abundance in the rock.

* Tourtelot (1964).

B. Krauskopf (1955).

usually even lower. From the data on the average abundances, two main points emerge:

(a) Marine sulphides are generally less enriched in Co and Ni than non-marine sulphides. This is probably a dilution effect caused by the greater weight of sulphides available in marine environments.

(b) The Co and Ni content of iron sulphides is in general markedly dependent on the rock type. A low content of e.g. clay and organic material in a sediment may result in low initial trace-element abundances, but it also means that there are few suitable hosts for the metals other than pyrite, which therefore becomes relatively enriched during diagenesis. Hence the increase in the approximate enrichment factors from shale to limestone in Table 3.3.

A well documented exception is the Silurian graptolitic shale analyzed by Spencer (1966), in which the pyrite averaged 1900 ppm Co and 400 ppm Ni, the Co-enrichment being tentatively explained in terms of the ready transport by colloidal iron hydrated oxides of $Co^{3+}$, supposedly formed at elevated pH and Eh in the absence of soluble organic acids in the early Palaeozoic.

The dispersion of Co and Ni in abnormal sedimentary environments, in which base-metal concentrations are unusually high, is significantly different to that in normal environments. Whole-rock analyses of the Marl Slate by Hirst and Dunham (1963), and of the Kupferschiefer by Deans (1950), Wedepohl (1964, 1965), Wazny (1965) and Knitzschke (1966) generally show Ni > Co, but with Co ranging 0-300 ppm, and Ni 30-500 ppm or 300-1000 ppm. These ranges are greater than those for normal shales quoted by Krauskopf (1955) (Table 3.3). However, as in many normal

shales, Co and Ni, and Ni and non-carbonate C, show good positive correlations, and Co also correlates with Cu.

It might be expected that the greater the base-metal concentration in a sediment, the more abnormal will be its trace element content. If the Rammelsberg and Meggen ores are sedimentary, as postulated by Ehrenberg et al. (1954), Kraume et al. (1955) and Anger et al. (1966), this expectation is confirmed, but the Co-Ni distribution in pyrites from the two deposits (Hegemann, 1943) are completely different:

(i) The more cupriferous Rammelsberg Zn-Pb-Cu deposit has Co > Ni, with Co ranging 10-1000 ppm, and Ni 5-400 ppm, giving a Co-Ni field similar to, but somewhat broader than, those described for the ores of volcanic association. The massive banded ore averages about 150 ppm Co and 20 ppm Ni, and exhibits layering of the trace as well as the major elements (Kraume, 1962).

(ii) The pyritic-Zn deposit of Meggen contains pyrite with Co < Ni, Co ranging 10-50 ppm, and Ni showing a restricted range of concentrations around 100 ppm - an overall distribution very like that for Stordo. Although these fields lie within the range for normal sedimentary pyrite, they show abnormally restricted values of Ni.

Metamorphism

The problem in investigating the effect of metamorphism is the difficulty of sampling both unmetamorphosed and metamorphosed material from the same site. For this reason studies of metamorphic resegregation of trace elements will usually have an inherent error due to the undefined initial availability of the metals. With this proviso, the study of Cambel and Jarkovsky (1965, 1967) reveals some remarkable

trends of Co and Ni concentrations with increasing metamorphism. These authors divided a series of pyritic ores, formed in several different environments during the syngenetic clastic and pyroclastic phase of geosynclinal vulcanism in the Little Carpathians of Czechoslovakia, into three groups based on metamorphic grade (epizone, mesozone, and katazone metamorphism). The unmetamorphosed ores had an average Co/Ni = 0.04. There is a marked increase in Co at constant Ni (about 1000 ppm) with increase of metamorphic grade; but within the highest grade, the Ni content remains constant below a certain threshold value of Co, above which the Ni values drop and become erratic, the Co/Ni ratio becoming > 1. Cambel and Jarkovsky offer no explanation for these trends, but the changes could represent an increased approach to equilibrium partitioning of Co into, and Ni out of, the pyrite structure. However, the possibility cannot be discounted of introduction of additional Co into the recrystallizing sulphides by a fluid phase, which Robinson and Strens (1968) have shown experimentally to be quite feasible.

Roscoe (1965) found a similar trend with increasing metamorphism in the Noranda-Matagami area, the Co content increasing in pyrite, but decreasing in pyrrhotite, and the overall abundances being less variable in the more metamorphosed Matagami area than in the Noranda area.

## Discussion

In areas where both magmatic-hydrothermal and normal sedimentary-diagenetic pyrites have been studied, the latter show much lower Co/Ni ratios (Rost, 1939; Carstens, 1943; Hegemann, 1943; Coleman and

Delevaux, 1957; Roscoe, 1965; Cambel and Jarkovsky, 1967). Several authors have therefore attempted to use the ratio in metallogenic studies (Davidson, 1962; Prokhorov, 1965; Wright, 1965; Darnley, 1966; Saager and Mihalik, 1967), but several of these studies are methodogically unsound.

(i) Davidson argued that, because the statistics he compiled showed the only Co-rich ores of known origin to be hydrothermal, the Co-rich Zambian Cu ores could therefore not be regarded as "sedimentary". This reasoning begs the question by not allowing the possibility of, and therefore not investigating, environments of sulphide deposition other than magmatic hydrothermal or normal sedimentary-diagenetic (Loftus-Hills and Solomon, 1967).

(ii) Wright used several criteria in attempting to prove the syngenesis of pyrite associated with a Canadian iron ore deposit. He cited, for example, a low Co content and Co/Ni ratio, and low Se content, and from broad generalizations from the literature on the general distribution of these elements, inferred a syngenetic origin. The fallacy of this argument is an overdependence on empirical rules, with no testing of the conclusions by analysis of other local pyrites of different genesis.

(iii) One sample of each of two different types of pyrite, intimately intergrown, from the Basal Reef of the Witwatersrand System, were analyzed by Saager and Mahalik. Because one analysis gave Co/Ni < 1, and the other Co > 100 ppm, and the authors considered that these pointed to sedimentary and hydrothermal origins respectively, they concluded that the Co-Ni values could not be used for genetic interpretation. Apart from the inadequate use of the empirical Co-Ni data, it is quite unacceptable to base such a conclusion on two samples.

It is clear, then, that as a technique of investigation, the Co-Ni distribution in sulphides is still fundamentally empirical. Preconceived ideas about dispersion patterns based on work in other areas may therefore be misleading, and applied studies in every case demand establishment of the basic local dispersion patterns, using a sufficiently large number of samples to cover variations caused by processes at the deposition site. Nevertheless, the dispersion patterns described in this section show some remarkably consistent trends between widely separated mineral deposits, and could provide very strong corroborative evidence for discrimination of genetic types of deposits.

## SELENIUM

### Crystal Chemistry

There is no basis either for a quantitative or a qualitative determination of the order of preference for accommodation of Se in ore sulphides. Complete isomorphism has been demonstrated between galena and clausthalite (Earley, 1950; Coleman, 1959), but although several other sulphide-selenide pairs are known to be isostructural, and some of them form limited solid solution series (Earley, 1949; Coleman and Delevaux, 1957; Bethke and Barton, 1961; Sindeeva, 1964), there is insufficient data for ranking the sulphides in their order of preference for Se. Most investigators of Se in sulphides (e.g. Bergenfelt, 1953; Edwards and Carlos, 1954; Zaryan, 1962; Faramazyan and Zaryan, 1964;

Sindeeva, 1964; Ismailov, 1965; Babcan, 1966) have ranked the sulphides they studied in order of Se content, but the discrepancies between their lists suggests that variation in availability of Se during deposition of the mineralogical sequences, as found by Hawley and Nichol (1959) and Zaryan (1962), outweighs effects due to inherent accommodating capabilities of the minerals. The only order which may be generally applicable, and even then availability factors may dominate, is that Cu, Fe, and Mo sulphides tend to be enriched in Se, and sphalerite depleted (Sindeeva, 1964), but exceptions are common (e.g. Ismailov, 1965).

## Primary Dispersion

### Availability

The Clarke Index for Se is 0.14 ppm, based on acid, mafic, and ultramafic rocks (Sindeeva, 1964). The geochemical cycle of Se is entirely controlled by its crystallochemical similarity to S. It substitutes for S in sulphide structures whenever the latter are available, and only in the absence of abundant sulphides, or where the concentration of Se is unusually high, does Se form independent minerals. Selenium is so strongly chalcophile that all classes of igneous rocks contain at most a few ppm Se, and usually < 1 ppm (Turekian and Wedepohl, 1961; Sindeeva, 1964).

It is recognized that certain areas are Se-enriched in both their igneous and sedimentary rocks (e.g. South-western U.S.A.; Tuva, U.S.S.R.), and Se can thus be an excellent metallogenic province indicator.

Despite the uniform depletion of Se in igneous source rocks, different genetic types of mineralization concentrate Se to varying degrees. Volcanic processes in general tend to produce Se-rich gases, sulphur and tuffs (Coleman and Delevaux, 1957; Davidson and Powers, 1959; Rosenfeld and Beath, 1964; Sindeeva, 1964), and pyritic ores associated with volcanic rocks have high Se contents. Magmatic-hydrothermal ores are very variable in Se, with Cu-Mo deposits being enriched (Goldschmidt and Strock, 1935; Edwards and Carlos, 1954), Pb-Zn deposits not so markedly enriched, and Au-quartz deposits showing variable enrichment. In magmatic Ni-Cu ores the vein deposits tend to be more enriched in Se than the disseminated deposits (Sindeeva, 1964). Superimposed on the genetic variability are distinct correlations of Se with Cu (Hawley and Nichol, 1959; Sindeeva, 1964), and with U (Sindeeva, 1964), which cut across the genetic types of deposits.

Depositional processes

Because of varying availability during deposition, and of the imprecise criteria used, most attempts to correlate the concentration of Se with temperature of formation are probably invalid. Goldschmidt and Strock (1935) and Rankama and Sahama (1950, p.746) suggest that there may in some cases be a direct proportionality between Se and temperature, but their data are scanty. Bergenfelt (1953) and Sindeeva (1964) claim a general correlation of Se with low-temperature stages of mineralization, although as Sindeeva notes, temperature may not be the direct control of concentration.

Attempts have been made in two investigations to directly measure the temperature of formation of the host minerals. Pyrites for which the

formation temperature had been estimated by Smith (1948) using his thermoelectric potential method, were analyzed for Se by Hawley and Nichol (1959). They found an inverse relationship between Se concentration and temperature, but admitted the possible effect of other variables. However, various workers have shown the thermoelectric potential method to be invalid (Fischer and Hiller, 1956; Suzuki, 1963). A direct measurement of temperatures of fumarolic S samples by Suzuoki, (1964) showed the Se content to be directly proportional to temperature.

Spatial variation of Se concentration with respect to intrusive igneous rocks was tested by Hawley and Nichol (1959), who found only three cases of systematic dispersion, two examples (dolerites at Noranda and Geco) showing decreased abundance away from the intrusive, and one (quartz porphyry at McIntyre) showing an increase followed by a decrease.

The Cu ores of the Kafan deposit consist both of quartz veins and disseminated ores in volcanics. Zaryan (1962) showed that Se in most ore minerals was enriched in the veins, which could be a natural concentration effect due to different available proportions of sulphides.

## Secondary Dispersion

### Sedimentation

In the weathering-sedimentation cycle, Se separates from S, the latter being largely bound in the sulphate ion, which is concentrated in the hydrosphere. Selenium, however, is trapped by exogenetic processes, and is largely retained by the products of mineral weathering.

The selenite normally produced in weathering is easily reduced to Se metal and Byers et al. (1938) suggest that it is also absorbed by colloidal Fe hydrated oxides. Some Se is transported to the oceans, probably as selenites, on colloidal Fe hydrated oxides, and incorporated in or adsorbed on carbonaceous material, but it is precipitated on reaching the sea, as almost all modern seabottom samples contain Se, whereas its concentration in seawater is < 0.001 ppm (Sindeeva, 1964). Shales, especially where carbonaceous, have the highest Se contents of normal sediments (Turekian and Wedepohl, 1961; Rosenfeld and Beath, 1964), but except in high-Se provinces, sedimentary-diagenetic sulphides, in which the Se and S become reassociated, are reported to contain < 30 ppm Se (Rankama and Sahama, 1950, p.754; Goldschmidt, 1954; Edwards and Carlos, 1954; Sindeeva, 1964).

Metamorphism

Wampler and Kulp (1964) suggest that some enrichment in sedimentary pyrite may occur during metamorphic recrystallization, but studies of Se in metamorphosed ores (Edwards and Carlos, 1954; Cambel and Jarkovsky, 1967) have not been sufficiently detailed to allow testing of this hypothesis.

## Discussion

The genetic implications of Se concentration have been variously argued on the basis of the continually enlarging mass of empirical evidence. Goldschmidt and Hefter (1933), Goldschmidt and Strock (1935) and Carstens (1941) suggested that pyrite of sedimentary origin had a

S/Se ratio of 200,000 or more, whereas pyrite of hydrothermal origin had a ratio of 10,000 to 20,000. The data from a wider range of ore types constrained Edwards and Carlos (1954) to modify this generalization. They refused to consider a sedimentary origin for an ore which contained pyrite with greater than about 10 ppm Se, and concluded, with Williams and Byers (1934), that high Se is caused by hydrothermal or magmatic processes, but that low Se does not rule out a hydrothermal origin. Since the latter work, the relationship of Se and volcanic activity has been more clearly recognized, and the investigation of Coleman and Delevaux (1957) proved that high Se concentrations do not rule out a sedimentary origin, particularly where volcanic material is present and/or where the province is Se-rich. Discrimination between Se-enrichment due to particular processes, and to a general provincial enrichment, must be made in every study by determination of local background concentrations, as in Co-Ni investigations.

## CADMIUM IN SPHALERITE

The crustal abundance of Cd has been estimated at 0.15 ppm (Green, 1959) and 0.08 ppm (Brooks and Ahrens, 1961). Sandell and Goldich (1943) and Vincent and Bilefield (1960) estimate a concentration of 0.13 to 0.18 ppm Cd in basic magma. The latter authors, in a study of fractional crystallization in the Skaergaard intrusion, have shown that Cd remains largely in solution, and that there is only a four-fold increase in concentration in the youngest siliceous differentiates. Zinc has been shown to behave similarly (e.g. Lundergårdh, 1948) and

there should be little difference in the Zn/Cd ratio in a hydrothermal solution from that in the parent magma.

Numerous authors have attempted to relate empirically the Cd content of sphalerite and the Fe content and/or temperature of formation of the sphalerites (Graton and Harcourt, 1935; Stoiber, 1940; Warren and Thompson, 1945; Edwards, 1955; Fryklund and Fletcher, 1956; Kullerud, 1959). Their opinions are about equally divided between Cd correlating directly and inversely with inferred temperature. Some of the later authors, however, have noted that theoretically there can be no temperature control of Cd content due to accommodation constraints by the host ZnS structure, as the latter is not saturated with Cd. Further, the criterion used by Edwards, Fryklund and Fletcher, and Kullerud to determine temperatures - the Fe content of sphalerite - was based on experiments (Kullerud, 1953) which have since proved to be inadequate (e.g. Boorman, 1967; Scott and Barnes, 1967).

Mookherjee (1962) investigated the "enrichment factor" for Cd in sphalerite and found that the enrichment calculated from published data was lower by about two orders of magnitude than the theoretical factor. While the theoretical factor could be obtained experimentally by using pure components, the addition of $Cl^-$ ions, which Mookherjee reasoned from fluid inclusion data to be present in ore-forming fluids, depressed the value to the range actually found in ores. Thus, while the experimental data suggested that the Cd content of the sphalerites was directly proportional to temperature, they showed a much stronger inverse correlation of the Cd content with the salinity. If, therefore, a decrease in salinity happens to be accompanied by a decrease in

temperature, as found in several studies (Roedder, 1960; Groves and Solomon, in press), the Cd content of the sphalerite could appear to have a spurious inverse correlation with temperature. Therein, perhaps, lies yet another explanation for the contradictory temperature correlations obtained by previous workers.

As pointed out in most of the previous studies, however, the variations in Cd content due to local depositional effects are much smaller than variations between districts due to differing availability, and Cd in sphalerites may therefore be used to delineate metallogenic provinces. Ivanov (1964) indicated that Cd values from similar deposits but different provinces may differ by a factor of up to 2.5. Fryklund and Fletcher (1956) suggested a Cd province with Cd contents of sphalerite from 0.40 to 0.45 per cent extending down the west coast of North Amercia, and on a smaller scale Rose (1967) has demonstrated differences in Cd content of sphalerites between districts in Utah.

## SUMMARY

Cobalt and nickel together can in many cases be excellent discriminators of sedimentary and volcanic processes, and in some cases hydrothermal processes. Because their distribution between rock types is reasonably constant, they have not found much use in delineation of metallogenic provinces except in combination with other elements. However their distribution between mineral phases is well enough known for them to be used as empirical discriminators on a local scale, and perhaps as guides to post-depositional changes such as metamorphism.

The dispersion of Se is much less strictly controlled by mineralogy. The dispersion patterns are therefore more empirically based, and it has proved very difficult to distinguish between local effects on concentrations due to variable availability, inherent mineralogical preferences, temperature, etc. However the Se content can broadly reflect mineralizing processes, and is therefore a potential discriminant of genesis. Its enrichment in certain areas of the earth's crust make it useful for delineating metallogenic provinces.

Despite attempts to relate the Cd content of sphalerites to temperature of deposition, it appears from the data of dispersion of Cd that it can most usefully be applied to determination of metallogenic provinces.

# 4. SAMPLING AND ANALYSIS

## SAMPLING

Eight minerals have been used in this study, but most analyses have been performed on pyrite and pyrrhotite, because

(i) pyrite, with or without pyrrhotite, occurs in nearly all the metallogenic environments of interest in Tasmania;

(ii) pyrite and pyrrhotite are by far the most abundant of the Co-Ni-rich minerals in the deposits investigated;

(iii) Edwards and Carlos (1954) concluded that pyrite is the most consistent index mineral for Se distribution.

As specimens could be of optimum use only if they were located accurately with respect to geology, most were chip-samples taken from in situ or from diamond-drill core. Because of difficulty of access, it was not always possible to realize this ideal, and some dump and museum specimens were used. Where conditions permitted, however, sampling was designed to give a set of specimens which could be systematically tested for the scale of trace element variation at the sampling site, from fractions of a millimeter to several meters. On a larger scale, sampling sites were selected within lodes or mineral fields to test spatial variations which might be genetically significant. The number of specimens sampled from each locality (sampling site) is evident from Table 6.1.

## SAMPLE PREPARATION

Pure pyrite samples were ground in a porcelain mortar and pestle, but most multimineralic samples required the use of a mechanical jaw crusher, a rotating disc pulverizer, or a gyratory grinder (Cr-steel head), and sieves. Contamination from these sources was tested using large specimens of clear quartz, with the results listed in Table 4.1.

TABLE 4.1

CONTAMINATION IN SAMPLE PREPARATION : TEST WITH PURE QUARTZ

| Procedure | AAS analysis | |
|---|---|---|
| | Co | Ni |
| Crush (4 cycles), Sieve, Hand grind | 0 ppm | 1 ppm |
| Crush (4 cycles), Sieve, Gyratory grinder | 0 ppm | 5 ppm |
| Crush (4 cycles), Sieve, Disc pulverizer | 1 ppm | 13 ppm |

Very little use was made of the disc pulverizer, and inspection of the ore mineral analyses suggests that in practice the levels of contamination in the quartz test were not reached when comminuting sulphides and oxides: the highest possible contamination (lowest analysis) from the disc pulverizer, for example, was 5 ppm Ni.

Where grain size permitted, the samples were purified by various combinations of micropanning, electromagnetic and hand-magnet separations, differential acid leaching, simple flotation using a detergent, heavy liquid separation, flash-roast magnetization of

chalcopyrite, and hand-picking. The procedure for every sample is listed in the Table of Data (an expansion of Table 6.1) filed in the Geology Department, University of Tasmania.

A few specimens were too fine-grained for purification, and were analyzed whole, polished sections being made for identification of potentially interfering minerals, which, if too abundant, disqualified the sample from analysis.

All purification procedures were continually monitored by binocular microscope, and visual estimates of impurities were made using a grain-count card. Most purification resulted in samples > 95% pure (with respect to ore minerals), and the latter were > 99% pure except where stated otherwise in Table 6.1. Seventy of the more difficult separations were quality-controlled by microscopic examination of polished grain-mounts. Where such examination revealed purifications of < 99%, the grain-count estimate of composition (> 400 grains) is listed in Table 6.1.

## ANALYSIS

A considerable period was spent in establishing satisfactory analytical procedures. The X-ray Spectrograph techniques were developed in collaboration with Mr. R. J. Ford and Dr. M. Solomon of this Department, and Mr. J. Hutton of Adelaide, and the atomic absorption techniques were developed with the help of Dr. K.L. Williams, Dr. C.S. Rann, and Dr. D.J. David at Canberra, and Mr. B.S. Rawling, of Broken Hill.

The techniques used for the various analyses were:

| | |
|---|---|
| Spectrophotometry : | Co in pyrite |
| X-ray Spectrography : | Ni in pyrite |
| | Se in sulphides |
| | Cu, Fe, Zn in sulphides |
| Atomic Absorption Spectrophotometry : | Co and Ni in all samples. |

## Cobalt and Nickel

X-ray fluorescence is not an ideal choice for analyzing sulphide minerals, because of the strong mass absorption of the metalliferous matrix. This absorption lowers sensitivity, an undesirable feature in the determination of trace concentrations. In addition, the fluorescence of the pyrite samples produced a very strong iron spectrum, the $FeK_{\beta}$ line of which seriously interfered with the $CoK_{\alpha}$ line, thus precluding Co analysis. Iron also absorbed Ni radiation, and the sensitivity of Ni analyses decreased accordingly.

Much work on the X-ray spectrograph (Philips PW 1540) was nevertheless directed towards determining Ni in powdered pyrite pressed pills (Norrish and Chappell, 1967), both using Ge as an internal standard, and using the scattered background technique of Andermann and Kemp (1958) as modified by Kalman and Heller (1962). Unfortunately Ge was found to enhance the Ni radiation, and the scattered background technique did not work, as a constant ratio of analytical line to scattered background intensity could not be obtained. The satisfactory value of 78 ppm for W-1 (quoted range 75-82 ppm) derived by the latter method is regarded as fortuitous.

A simple linear calibration technique was therefore used, but the method was limited to samples of approximately constant mass-absorption, i.e. to pure or nearly pure pyrite. The early pyrite-based standards were somewhat unsatisfactory as they were mixed wet, but later standards were mixed dry in a gyratory swing-mill. Operating conditions are presented in Table 4.2. Background at the peak position was estimated by finding the smallest response possible from a series of Analar, supposedly Ni-free chemicals of varying mass absorption, and calculating this response in terms of the mass absorption of pyrite. Figure 4.1 shows that comparable results were obtained for Ni analyses by X-ray spectrography and atomic absorption spectrophotometry.

Spectrophotometry is an excellent technique for Co analysis as Co forms highly coloured complexes susceptible to solvent extraction. The method used was the 2-nitroso-1-naphthol extraction described by Sandell (1959, Vol.3, p.409), and is summarized in Appendix 3. Measurements were made on a Bausch and Lomb "Spectronic 20" spectrophotometer, which gave excellent results, emphasising the sensitivity of the technique (Table 4.3). Analysis of samples determined by both spectrophotometry and atomic absorption agree reasonably well (Fig. 4.2).

All such spectrophotometric techniques have the inherent disadvantage that a separate extraction is usually required for each element, which involves excessive laboratory time. This can be avoided in the technique of atomic absorption spectrophotometry (AAS), which in its simplest form requires only that the sample be taken up into a suitable solution. With the installation of a Techtron AA3 atomic absorption spectrophotometer, the methods discussed previously were used only for accuracy tests.

Figure 4.1

Comparison of Ni analyses of 17 sulphide samples by atomic absorption spectrophotometry (AAS) and X-ray fluorescence spectrography (XRF).

Figure 4.2

Comparison of Co analyses of 6 sulphide samples by atomic absorption spectrophotometry (AAS) and spectrophotometry.

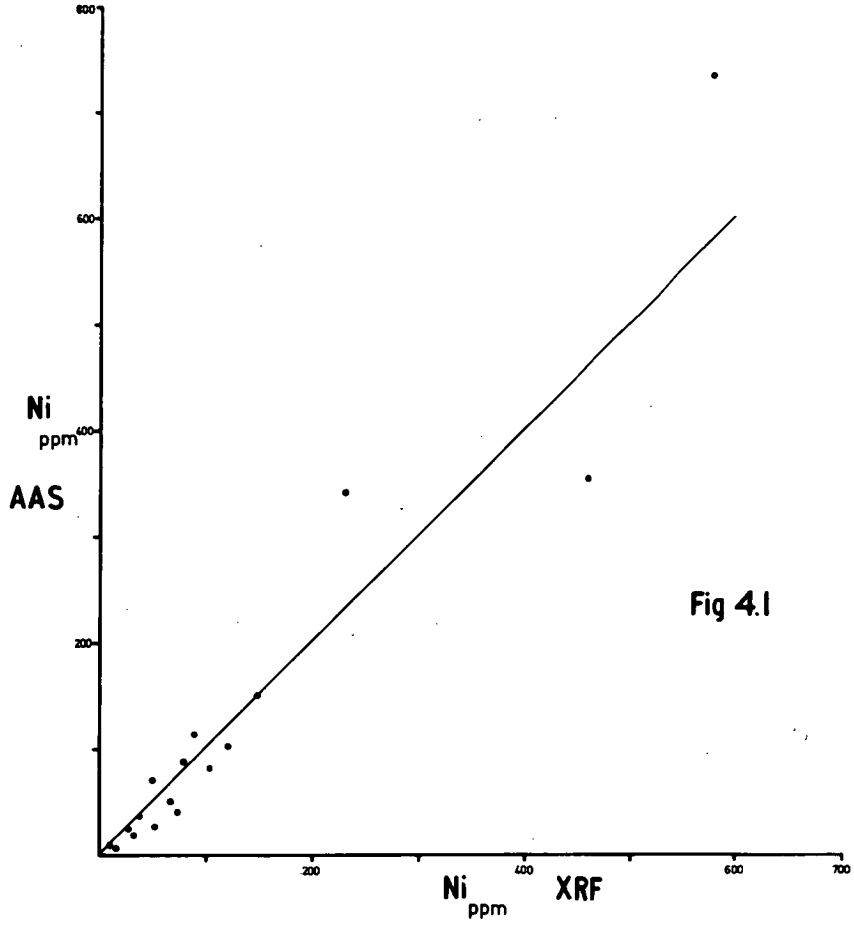
800
600
400
200
Ni
ppm
AAS
200
400
600
700
Ni ppm XRF

Fig 4.1

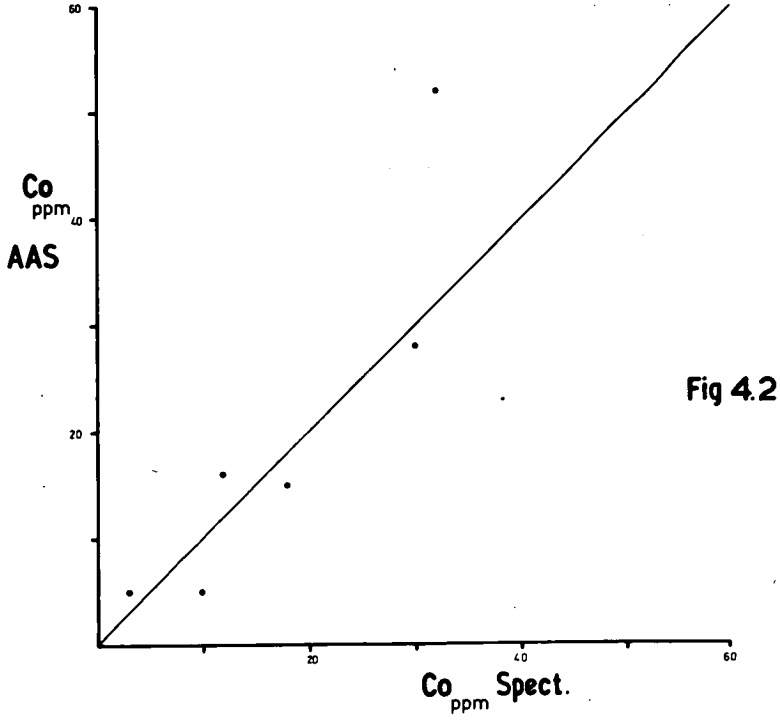
60
40
20
Co
ppm
AAS
20
40
60
Co ppm Spect.

Fig 4.2

TABLE 4.2

Ni ANALYSIS : X-RAY SPECTROGRAPHY OPERATING CONDITIONS

| | |
|---|---|
| Tube | Gold, 48kV, 20 mA |
| Crystal | $LiF_{220}$ |
| Counter | Scintillometer, 860 V |
| Emission line | $NiK_{\alpha}$, 71.26° 2θ |
| Background measurement | 70.20° 2θ |
| Counts above background per ppm (m) | 0.212 c./sec./ppm |
| Counting time (t) | 64 sec. (each measurement) |
| Relative standard counting error | ± 8% at 100 ppm |
| Lower limit of detection (95% confidence)* | 16 ppm |

* $\frac{3}{m}\sqrt{\frac{C_b}{t}}$, where $C_b$ = number of background counts.

TABLE 4.3

Co ANALYSIS : SPECTROPHOTOMETER 2-NITROSO-1-NAPHTHOL METHOD

| | |
|---|---|
| Instrument | Bausch & Lomb "Spectronic 20". |
| Wavelength | 530 mμ |
| Blank reading | Equivalent to 2 ppm in the solid. |
| Sensitivity (average) | 1.14 μg/ml (equivalent to 57 ppm in the solid) for 50% absorption. Absorbance vs. concentration is linear to 80% absorption. |
| Limit of quantitative determination | 2 ppm * |
| Limit of detection | 1 ppm * |
| Precision (as coefficient of variation) | 6%* at 40 ppm |

* Despite the extreme sensitivity of this method, the electronics of the instrument used were insufficiently stable for comparable reading precision.

The Techtron AA3 operates as follows. A stabilized D.C. power supply feeds the appropriate hollow-cathode spectral lamp. The solution to be analyzed is drawn up a plastic capillary and converted by means of a stream of compressed air to a fine spray which, after condensation of oversize droplets on a glass bead, is mixed with acetylene or other gas(es) and burned in the long flame of a stainless steel burner. The light from the lamp, after traversing the flame, and (ideally) undergoing absorption according to the Beer-Lambert Law, enters via an adjustable slit a grating monochromator set at the wavelength of the resonance line of the element being determined. The resolved light beam passes through an adjustable exit slit and falls on a photomultiplier. The light from the lamp is modulated at the mains frequency, and the signal from the photomultuplier is amplified by an A.C. amplifier. The modulation procedure ensures that most light emitted from the flame at the analytical wavelength produces no signal at the amplifier output. For the present work, the amplifier output was fed into one of two servo-recorder systems; either (a) through the amplifier of a Hewlett-Packard DC micro volt-ammeter, into a two-speed Beckman recorder; or (b) into a general purpose Leeds and Northrop Speedomax-H recorder. The standard graph was plotted as absorbance vs. concentration, where absorbance (A) = (2 - log % transmission).

It is not difficult to dissolve the minerals used in this study, but interferences were found in the determination of Co and Ni in Fe-rich solutions. The dissolution techniques most appropriate for the

chemical preparation necessary to overcome these interferences will be described after the following discussion of the interferences.

Although the AAS technique is relatively free of interferences compared with flame photometry or X-ray fluorescence, physical, chemical and spectral interferences can occur (e.g. Slavin, 1964). Contrary to the results obtained by Belcher and Kinson (1964) and Beyer (1965), who found no interferences from Fe in the analysis of Ni in iron and steel, marked interferences were found when Co and Ni were analyzed in very Fe-rich solutions using normal-intensity hollow-cathode lamps.

Type I interference is a blank effect which is constant for constant Fe concentration, and results in parallel calibration curves for varying Fe concentrations (Fig. 4.3a). This interference is commonly referred to as non-atomic absorption (NAA), and ascribed to scattering of light, particularly at short wavelengths, by non-atomized particles in the flame (Willis, 1963). There are, however, two other possibilities, which were investigated by the writer and C.S. Rann on the latter's experimental apparatus, using a narrow band amplifier to minimise effects due to line broadening.

(i) True molecular absorption may occur, due to the presence of undissociated molecules in the flame. Koirtyohann and Pickett (1966a, 1966b) have since emphasised the theoretical probability that this type of absorption will predominate over scattering. However, tests using a Xenon (band spectrum) lamp revealed no absorption at the analytical wavelength.

(ii) The Fe atoms in the flame may absorb energy from the Co

Figure 4.3

Interferences found in the analysis of Co and Ni in Fe-rich solutions by atomic absorption spectrophotometry, using ordinary hollow-cathode spectral lamps.

(a) Interference Type I : non-atomic absorption. Identical interference results from impurities in chemicals.

(b) Interference Type II : Chemical Fe interference.

(c) Combination of interference Types I and II.

(d) Interference Type III : due to non-absorbing lines in the lamp spectrum.

(e) Total interferences.

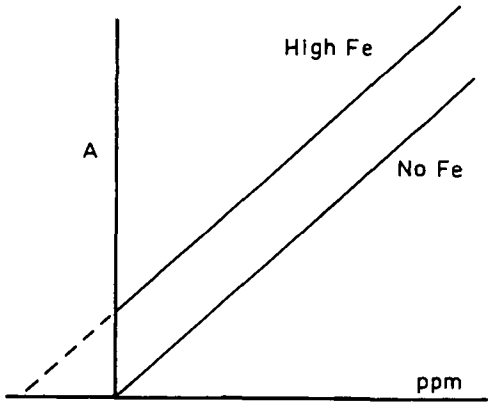


(a) Type I

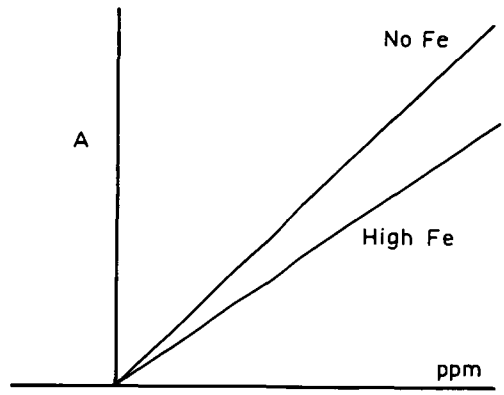


(b) Type II

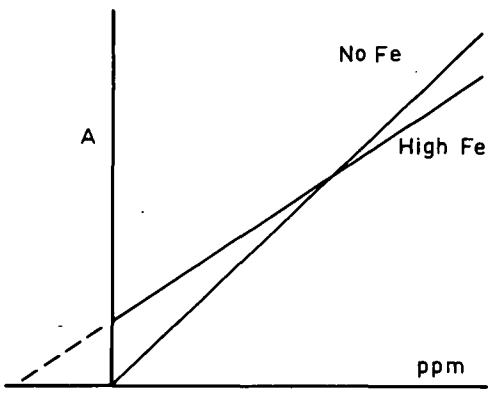


(c) Types I & II

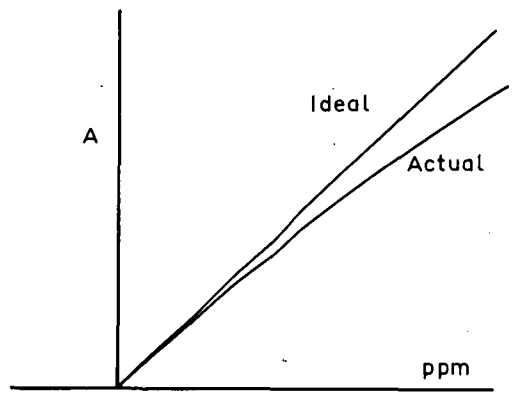


(d) Type III

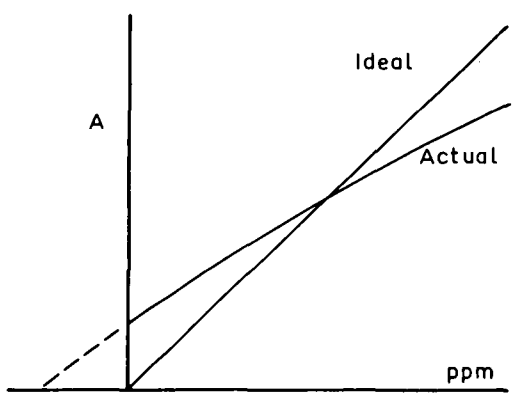


(e) Total

emission spectrum, depending on the coincidence of Co emission and Fe absorption wavelengths. This was tested by investigating every absorption peak of the (Fe + Co) solutions in the vicinity of the analytical wavelength (2407 Å), by aspirating pure Co solutions. No interference was found at 2407 Å, but at 2473 Å the following effects were noted:

Co lamp : Solution of $[(NH_4)_2SO_4.FeSO_4.6H_2O$ + Co] : strong absorption

Solution of (metallic Fe + Co) : strong absorption

Solution of pure Co : no absorption

Xenon lamp : Solution of $[(NH_4)_2SO_4.FeSO_4.6H_2O$ + Co] : no absorption.

The inference is that the absorption is due to Fe, and is atomic. Although this phenomenon did not affect the Co analyses, it has the interesting practical applications pointed out by Frank, Schrenk and Meloan (1966) in that one lamp with an appropriate spectrum can be used to analyze several elements.

As these two possible interferences were absent, it was concluded that the standard method of measuring light-scattering NAA should be adequate. This consists of analyzing the samples at a wavelength close to the resonance (analytical) line, but using a line (not necessarily of the same lamp) which is known not to be absorbing (i.e. a line where no absorption is observed when using a dilute solution containing small quantities of the analyte). The apparent absorption (NAA), when subtracted from the total resonance line absorption, should then give the atomic absorption.

Type II interference is a depressive effect proportional to the amount of Fe in solution (Fig. 4.3b). This is partly caused by lower

atomic density in the flame, due to increased salt-content of the solutions and therefore less efficient atomization of the trace elements in the flame, and is equivalent to the "unspecified matrix interference" of Slavin (1964). Rates of solution aspiration were also tested as a function of Fe concentration, but the change of viscosity is insignificant, the largest change in aspiration rate being due to change of acid concentration.

The major part of this effect, however, must be a specific chemical interference. While Co and Ni exhibit both interference types I and II (Fig. 4.3c), Cr exhibits type II only, and Pb, Bi and Sb only type I (B.S. Rawling, pers. comm.). The effect is probably due to certain trace elements being physically incorporated in refractory compounds of Fe, which are much less readily dissociated in the flame, thus reducing the concentration of the trace element available for atomic absorption. Prof. T.S. West (pers. comm.) found that the effect does not increase above a certain (high) Fe concentration.

Type III interference is spectral rather than chemical, and results in a marked curvature of the standard graphs towards the concentration axis. This is predominantly due to non-absorbing lines in the hollow-cathode spectrum which are not resolved from the analytical lines by the monochromator (Walsh, 1965), and also possibly due to inhomogeneous absorption in the flame (Menzies, 1960; Gilbert, 1962; Rann and Hambly, 1965). The result is an asymptoting of the standard graph towards the value of transmission of the unwanted light. This interference was largely eliminated by using high-intensity lamps, in which the non-absorbing lines are suppressed.

A further serious problem was that the only Fe compounds available at a reasonable price in sufficient quantities for making up the concentrated standard solutions were contaminated with both Co and Ni. Because of this, and of type I interference, the lower parts of the curved standard graphs were never actually delineated by appropriate standards (Fig. 4.3a).

There are two main possibilities for overcoming interference types I and II - (a) to make up standards with an appropriate Fe content, or (b) to remove the Fe from the samples altogether.

In an attempt to salvage the simplicity inherent in the basic analytical method, the analysis of Fe-rich solutions was extensively tested. As it was suspected that manipulation of salt-rich solutions might lead to erratic errors in measurement (e.g. Firman, 1965), dilution tests were performed on Fe-rich standards. Small variations in Fe content gave, within the limits of error, a linear absorbance response, but gross dilution produced a non-linear absorbance curve (Fig. 4.4). Figure 4.4 also illustrates the errors involved in assuming a regular decrease in "total absorption minus non-atomic absorption" with successive dilutions. The dilution behaviour of Zn in Fe-rich solutions is shown to be similarly erratic, even though Zn does not generally exhibit the other interferences listed for Co and Ni. It was therefore concluded that the sample-solutions could not be grossly diluted (to bring high trace element concentrations into the working range of the machine) without preparing strictly equivalent standards.

Figure 4.4

Erratic dilution behaviour of Fe-rich solutions of Co and Zn, illustrating the errors involved in assuming a regular decrease of "total absorption minus non-atomic absorption" with successive dilutions. Ordinary hollow-cathode spectral lamps used.

(a) Co lamp. Atomic abs. : 2407 Å

Non-atomic abs. : 2388 Å

Slit width : 25 microns

x = 0.467 g Fe + 190 µg Co in 50 ml 2.2N HCl.

(b) Zn lamp. Atomic abs. : 2139 Å

Non-atomic abs. : 2099 Å

Slit width : 300 microns

x' = 0.467 g Fe + 15 µg Zn in 50 ml 2.2N HCl.

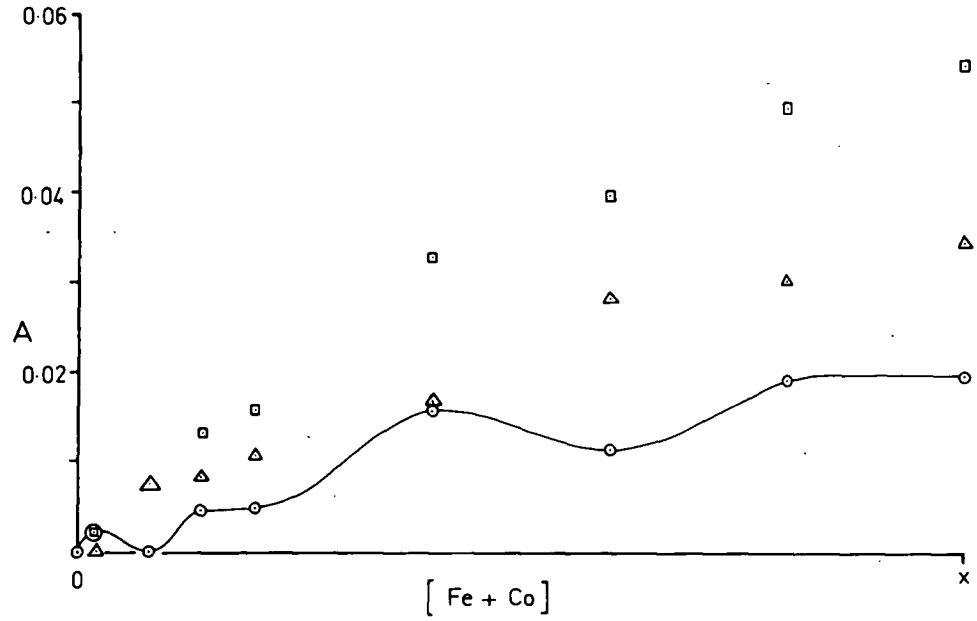
0·06
0·04
A
0·02
0
[ Fe + Co ]
x

(a)

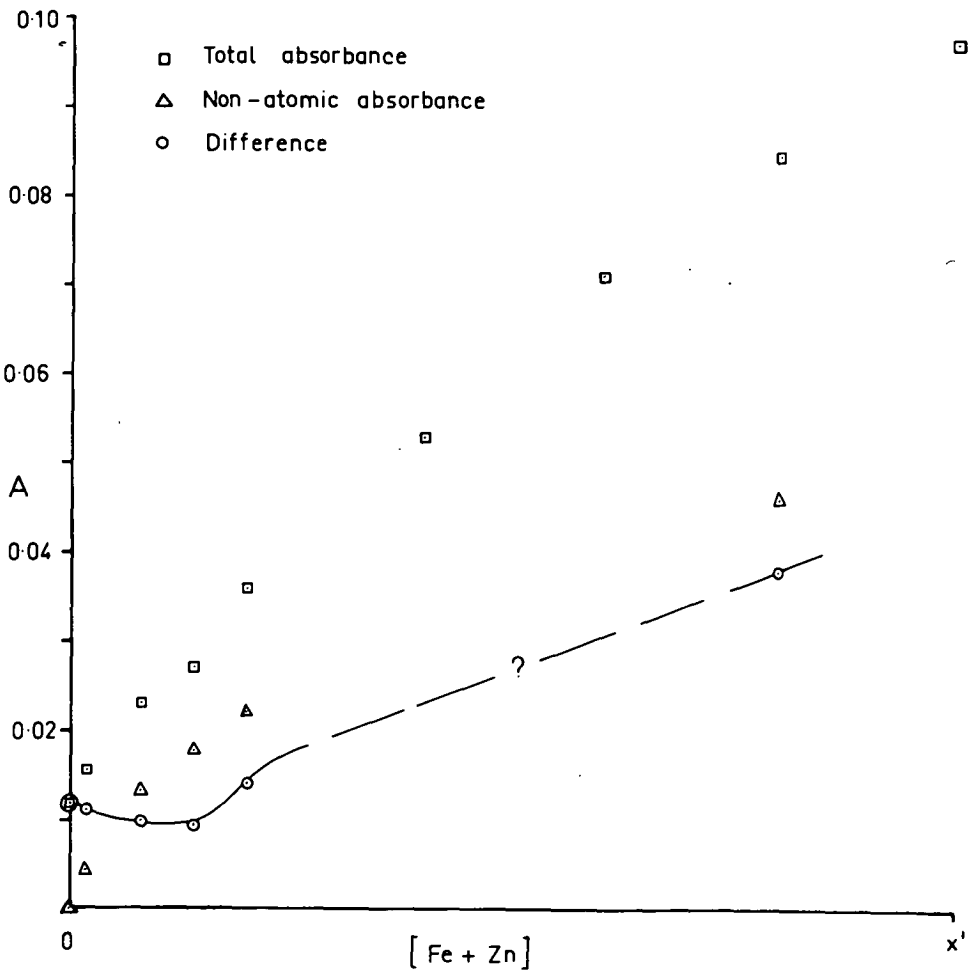
0·10
Total absorbance
Non-atomic absorbance
Difference
0·08
0·06
A
0·04
0·02
?
0
[ Fe + Zn ]
x'

(b)

Ideally, this procedure should have involved a prior determination of the Fe content of the samples. As no Fe spectral lamp was immediately available, the approximation was made that all pyrite samples were pure with the exception of the acid-insoluble residue. Standards were therefore prepared to cover the range of iron concentrations of 1 g (approx.) per 50 ml sample solutions from which varying weights of residues had been filtered. It was found convenient to (i) subtract NAA from both sample and standard absorbances; (ii) read the Co or Ni concentrations from the main standard graph, suitably adjusted for machine drift*; and (iii) calculate the correction for the appropriate Fe concentration. The factor used was ± 3 ppm for ± 10% Fe concentration, derived from standard lines representing Fe concentrations of 70, 80, 90, 100, 110% of a 1 g pyrite per 50 ml concentration. Standards and samples were made up in 2.2 M HCl.

It was eventually realized that this technique gave inaccurate and imprecise answers, especially for Ni. The reason is not clear, but is probably related both to the imprecision of the lower part of the standard graphs, and to the poor monitoring of the Fe concentration, the Fe in the solutions apparently interfering more significantly with the Ni than with the Co. Examples of analyses of sulphide powders by this method and by the following method are given in Table 4.4.

---

* This was considerable, due to burner blockage by Fe salts, and to thermal instability of the diffraction grating mounting in the AA3.

TABLE 4.4

COMPARATIVE SAMPLE ANALYSIS

Examples of sample analysis (i) without extracting Fe, compared with analysis (ii) after ether extraction (Appendix 4):

| Number | Co (i) | Co (ii) | Ni (i) | Ni (ii) |
|---|---|---|---|---|
| 100243 | 7 ppm | 1 ppm | 73 ppm | 6 ppm |
| 100312a | 72 | 61 | 78 | 59 |
| 100397 | 226 | 258 | 795 | 775 |

A technique suitable for removing the Fe from the sample solutions was brought to the attention of the writer by B.S. Rawling. The dissolved and evaporated sample was taken up in strong HCl and the Fe removed by shaking with di-isopropyl ether (Dodson, Forney and Swift, 1936; Nachtrieb and Fryxell, 1948). The final solutions are of $CH_3.COONH_4$ in HCl. Recovery of both Co and Ni was found to be 100%.

Two significant variations were developed to process the samples in this study:

(i) The concentration of the HCl required for optimum extraction of the Fe was found to be 9N HCl, which differs both from that quoted in the literature and from that used by Rawling. This probably reflects the high concentration of Fe in solutions of iron-rich minerals.

(ii) Simple acid digestion of the samples was not used, for reasons which will now be discussed.

Attention was devoted by the writer and by Dr. K.L. Williams to the sulphur, as colloid and/or coagulate, produced in the standard

oxidizing $HNO_3$ dissolution of pyrite. It was thought probable that the free S would interfere with absorption in the flame, and also produce an erratic error due to variable viscosity of the solutions.* Tests by the writer reveal no such interferences, nor were there chemical interferences with the ether extraction, or with Co and Ni recovery.

Four techniques have been used by the writer to dissolve pyrite:

(a) 72% $HClO_4$.

(b) Conc. $HNO_3$.

(c) 8M $HNO_3$, followed by a bromine-hydrogen peroxide mixture (e.g. Sindeeva, 1964).

(d) Roasting to $Fe_2O_3$, followed by solution in HCl.

Method (d) was eventually incorporated in the analytical routine for these reasons:

(i) Methods (a) and (c) are relatively expensive.

(ii) Where the sample was subjected to a two-acid treatment, it was found more difficult to control the pH for ether extractions than with a one-acid treatment.

(iii) Because of various technical difficulties, which could not be overcome in the time available, the sulphur was not completely eliminated using any of the first three methods. Any S which happened to remain in the solution was very slow to clear from the aqueous phase after shaking with ether.

(iv) Most important, the roasting procedure was the most versatile, handling as it could both sulphides of several types, and oxides.

---

* The $S/SO_4$ ratio in the original solution is a function of acid strength, which can vary due to e.g. filtering requirements.

Recovery of Co and Ni from the roast was found to be 100%, but the technique cannot be extended to cover analysis of elements which volatilize at the high operative temperatures. The efficiency of the roasting method depends on the availability of oxygen to the roasting bed. This was tested by roasting samples of a pyrite powder in silica boats in a 1 inch diameter silica tube through which a controlled air current was passed, the tube being heated by two Meker burners. Although all products were shown by XRD to be $Fe_2O_3$, the colour of the product ranged from rust red (highest air flow) to a deep mauve, the former dissolving more readily than the latter. By carrying out the roasting in a reasonably squat crucible, there is sufficient access of air for satisfactory dissolution of the product.

The complete procedure for the preparation of standards and the analysis of samples for Co and Ni is presented in Appendix 4. The operating conditions and reliability tests of the analyses are given in Tables 4.5 and 4.6. After the extraction of the Fe (eliminating interference types I and II), NAA became zero, and the standard graphs could be drawn through the origin. With the introduction of the high-intensity lamps (eliminating interference type III), the graphs were taken as straight lines up to absorbances of about 0.7 (20% transmission). It is inadvisable to work at higher absorbances because of loss of sensitivity and precision, preferred procedures being dilution of the sample solutions, rotation of the slit burner, or use of a less sensitive resonance line.

The coefficients of variation in Table 4.6 indicate that the overall precisions for Co and Ni are very similar. The 95% confidence

TABLE 4.5

Co AND Ni ANALYSES : ATOMIC ABSORPTION SPECTROPHOTOMETER

OPERATING CONDITIONS

| Element | Co | Ni |
|---|---|---|
| Wavelength (Å) | 2407 | 2320 |
| Lamp current (mA) | 14 | 14 |
| Booster setting | 100-200 | 200 |
| Flame | Air/acetylene | Air/acetylene |
| Slit width (μ) | 25 or 50 | 50 or 100 |
| Sensitivity (average maximum): μg/ml for 50% absorption | 6.4* | 6.5* |
| Standards | 0.1-100 μg/ml | 0.1-100 μg/ml |
| Percentage absorption | | |
| - lowest standard | 1% | 1% |
| - lowest sample | 0% | 0% |
| Dilutions used | None | None |
| Limit of quantitative determination (in solid) | 1 ppm | 1 ppm |
| Limit of detection (in solid) | 0.5 ppm | 0.5 ppm |

* Absorbance vs. concentration is linear to 80% absorption.

TABLE 4.6

Co AND Ni ANALYSES : ATOMIC ABSORPTION SPECTROPHOTOMETER

RELIABILITY TESTS

Accuracy (a) : Canadian Standard Sulphide Ore number 1 (triplicate)

| | This study | Mean reported values (Webber, 1965) |
|---|---|---|
| Co : | Av. 523 ppm | 546 ppm |
| Ni : | Av. 12,800 ppm | 13,103 ppm |

Accuracy (b) : Analysis by different techniques:
Refer to Figures 4.1 and 4.2

Accuracy (c) : Independent analysis of pyrite sample from Set 23:
This study : 0.81% Co (Av. of 3).
Mt. Lyell Co.* : 0.83% Co.

Precision (a) : Expressed as coefficients of variation:
At 5 ppm Co : 20% (8 replicates)
At 25 ppm Ni : 6% (8 replicates)
At 523 ppm Co : 5% (3 replicates)

Precision (b) : Time-reproducibility :

| Number | | May 1967 | September 1967 | |
|---|---|---|---|---|
| | | | Run 1 | Run 3 |
| CAAS-1 | Co | 524 ppm | | 509 ppm |
| | Ni | 12,577 | | 12,563 |
| 100224 | Co | | 6 ppm | 5 |
| | Ni | | 49 | 49 |
| 100233 | Co | 15 | | 15 |
| | Ni | 102 | | 103 |

* $HNO_3$-HCl-$Br_2$ digestion, followed by precipitation of Fe, precipitation and resolution of Co, and determination by atomic absorption spectrophotometry. Mt. Lyell Co. Assay Section, Queenstown.

limits for a single determination of either element are then ±ts, where t is Student's* $t_{0.05}$ for the N-1 degrees of freedom on which the estimate of the standard deviation was based (Sullivan, Timms and Young, 1968). The approximate 95% confidence intervals based on the quoted precisions are:

At 5 ppm , ±2 ppm.

At 25 ppm , ±4 ppm..

At 523 ppm, ±108 ppm.

In other words, because of imprecision in sample homogenization, processing, and analysis, the probability that two individual analyses of 21 and 28 ppm are different will be less than 95%.

The final concentrations were calculated by an Algol Elliott 503 computer programme written by B. D. Johnson, two hundred of the analyses having also been calculated manually. A total of 10 parameters for each analysis were fed into this programme, including figures for drift of the equipment as read from the chart record. The calculations were designed to give the following basic information:

(1) $$\frac{\text{(weight of Co or Ni)} \times 10^6}{\text{wt. of original sample - wt. of filtered residue}}$$ ppm

(2) $$\frac{\text{(weight of Co or Ni)} \times 10^6}{\text{weight of original sample}}$$ ppm

(3) The Co:Ni ratio for each sample

For most analyses, the assumption was made (calculation 1) that a filtered residue which had remained visibly inert during sample preparation represented gangue, from which no Co and Ni were extractable. If the filtered residue was a precipitate, say $PbCl_2$, formed during the

chemical preparation, some of the Co and Ni may have been held in trace galena in the sample. The correct concentration in the main mineral would then lie somewhere between answers (1) and (2), thus introducing an uncertainty (which in practice is small; see Table 6.1). This is another reason why the specimens were purified as much as possible before analysis.

## Selenium

X-ray fluorescence spectrography was used for analyzing Se, as the sensitivity was adequate for the ranges of concentrations found in Tasmanian sulphides (see Fig. 6.12). The operating conditions are listed in Table 4.7. To prepare standards, Analar Se metal powder and the appropriate sulphide were mixed in the gyratory swing-mill for 30 seconds.

As with the Ni analyses by XRF, the scattered background technique could not be made to work. Instead an empirical curve was prepared relating peak minus background intensity to variation in composition of accurately proportioned pyrite-quartz standards. It was then assumed that the acid insoluble fraction of the pyrite samples (known from the Co-Ni determinations) had the same mass absorption as $SiO_2$, and a correction factor for the analysis was read from the empirical curve. Concentrations of Se were then calculated with respect to the pyrite fraction of the sample.

For sphalerite analyses, a natural sphalerite (10509) was used as the standard base. The purified sphalerite samples did not vary in

TABLE 4.7

Se ANALYSIS : X-RAY SPECTROGRAPHY OPERATING CONDITIONS

| | |
|---|---|
| Tube | Molybdenum, 48kV, 20mA. |
| Crystal | $LiF_{220}$ |
| Counter | Scintillometer, 890 V. |
| Emission line | $SeK_{\alpha}$, 45.70° 2θ |
| Background measurement | 46.77° 2θ |
| Counts above background per ppm | 0.15 c./sec./ppm (in pyrite) |
| Counting time | 128 seconds (each measurement) |
| Relative standard counting error | ± 33% at 23 ppm to ± 3.5% at 211 ppm |
| Lower limit of detection (95% confidence) | 15 ppm |

mass absorption, except where the Fe contents changed, and as the latter had been previously determined, the mass absorptions were suitably adjusted.

Pure chalcopyrite, pure pyrrhotite, and pentlandite-pyrrhotite ore were analysed using the sphalerite standards and recalculating with respect to mass absorption.

The poor sensitivity of the analytical method was partially overcome by counting for a total of 256 seconds on each sample. The standard counting error varied regularly (Table 4.7), and was equivalent to an uncertainty of ± 7 ppm Se at all measured concentrations.

To test the precision, eight duplicate analyses, covering the range of results, were carried out. The precision was expressed as the relative deviation (C), according to the formula

$$C = \pm \sqrt{\frac{\Sigma d^2}{n-1}}$$

where d is the percentage deviation of each observation from the arithmetic mean of each pair of duplicates, and n is the number of duplicate pairs. This yields a maximum precision of ± 6 ppm for all concentrations, which is an underestimate in view of the level of counting error.

The accuracy of the results was tested by analysis of several specimens by the Department of Mines Assay Laboratories, Tasmania, and by the Australian Mineral Development Laboratories, Adelaide, South Australia (AMDEL). The spectrophotometric method of analysis developed by the Department of Mines is summarized in Appendix 5. The technique used by AMDEL was a spectrophotometric method following separation of the Se by coprecipitation as the metal with Te.

Figure 4.5

Comparison of Se analyses of various sulphides by X-ray fluorescence spectrography (this work), spectrophotometry (Department of Mines Assay Laboratory), and precipitation-spectrophotometry (Australian Mineral Development Laboratories).

Composition of the samples, and details of analyses, are listed in Appendix 5.

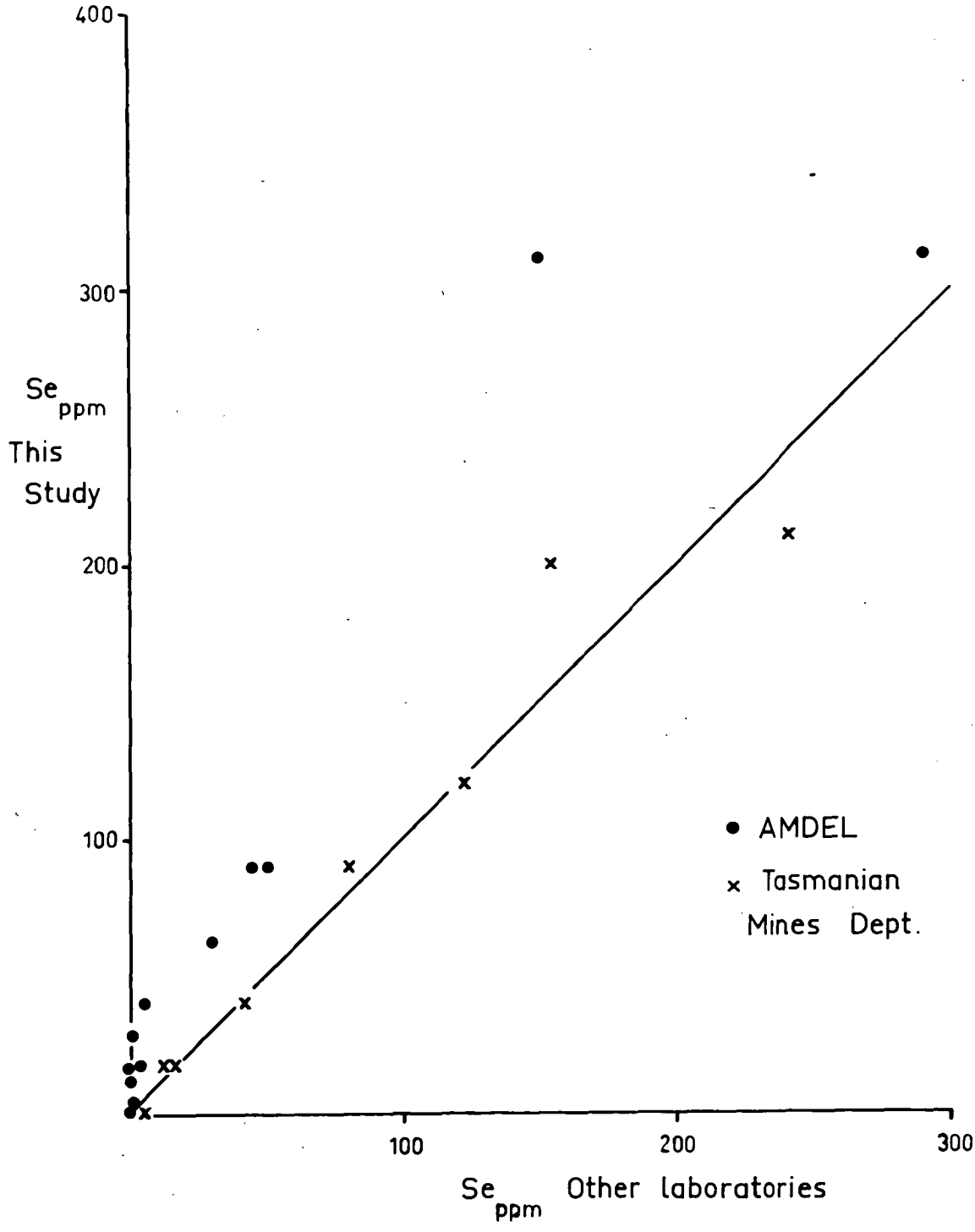
400
300
200
100
Se ppm
This
Study
100
200
300
Se ppm Other laboratories
AMDEL
Tasmanian
Mines Dept.

A comparison of the three sets of analyses is given in Figure 4.5, and in Appendix 5. Only those analyses in which no difficulties were reported by the analysts were included in Figure 4.5. The Se results obtained in this study by XRF, and those obtained by the Department of Mines, are equivalent within the precision of measurement for both groups of analyses below 100 ppm. Above 100 ppm there is less agreement. The results obtained by AMDEL are consistently lower than the other two groups of results, which may be the result of incomplete precipitation of Se.

A further check on accuracy was provided by comparison of the analyses (distillation-colourimetric) of Edwards and Carlos (1954), recalculated to the pure sulphides, of specimens from some of the same localities as those in the present study. These have been plotted in Figure 6.12, and show good agreement.

The accuracy of the analyses thus established is considered adequate for the subsequent interpretations.

## Copper, Iron and Zinc

It was necessary in two investigations to estimate the proportions of pyrite, chalcopyrite and sphalerite in already prepared samples. The powdered and pilled samples were analyzed by X-ray spectrography (linear calibration method) for Cu, Fe and Zn (Table 4.8), and the amounts of the minerals calculated assuming stoichiometric proportions, the average 2% Fe in sphalerite not interfering at the level of accuracy required. The results are listed in Table 6.1.

TABLE 4.8

Cu, Fe AND Zn ANALYSES : X-RAY SPECTROGRAPH OPERATING CONDITIONS

| | Cu | Fe | Zn |
|---|---|---|---|
| Tube | Mo | Mo | Mo |
| Tube settings | 26 kV, 10mA | 26kV, 10 mA | 20 kV, 6mA |
| Crystal | $LiF_{220}$ | $LiF_{220}$ | $LiF_{220}$ |
| Counter | Scintillometer, 860 V | | |
| Emission Line ($K_\alpha$) ($^\circ 2\theta$) | 65.56 | 85.71 | 60.60 |
| Background measurement ($^\circ 2\theta$) | 64.16 | 83.16 | 59.19 |
| Counts above background per % | 356 | 178-212 | 174 |
| Counting time (sec.), each measurement | 32 | 32 | 32 |
| Relative standard counting error | ± 0.2% at 24% | ± 0.3% at 25% | ± 0.3% at 23% |
| Lower limit of detection (95% confidence) | .006% | .010% | .012% |

The standards used were pure pyrite, chalcopyrite, and sphalerite, the Canadian Standard Sulphide Ore number 1, and Cu, Pb and Zn concentrates from the Rosebery Mine analyzed by the Assay Department of the Electrolytic Zinc Company. The standard graphs are shown in Figure 4.6. Variation in iron caused the greatest variation in mass absorption, and where it was known that the sample contained only pyrite and chalcopyrite, an approximate empirical correction was made to the Fe standard graph in terms of previously determined % Cu (Figure 4.6c).

Because strictly quantitative results were not necessary, accuracy and precision tests were not performed. Inspection of Figure 4.6 and Table 4.8 suggests limits of significant error of ± 10% of the Fe content, and lower limits for Cu and Zn.

Figure 4.6

Standard graphs for XRF analysis of Cu, Fe and Zn:

(a) Cu;

(b) Fe;

(c) Conversion graph for Fe in pyrite-chalcopyrite mixtures with respect to % Cu;

(d) Zn.

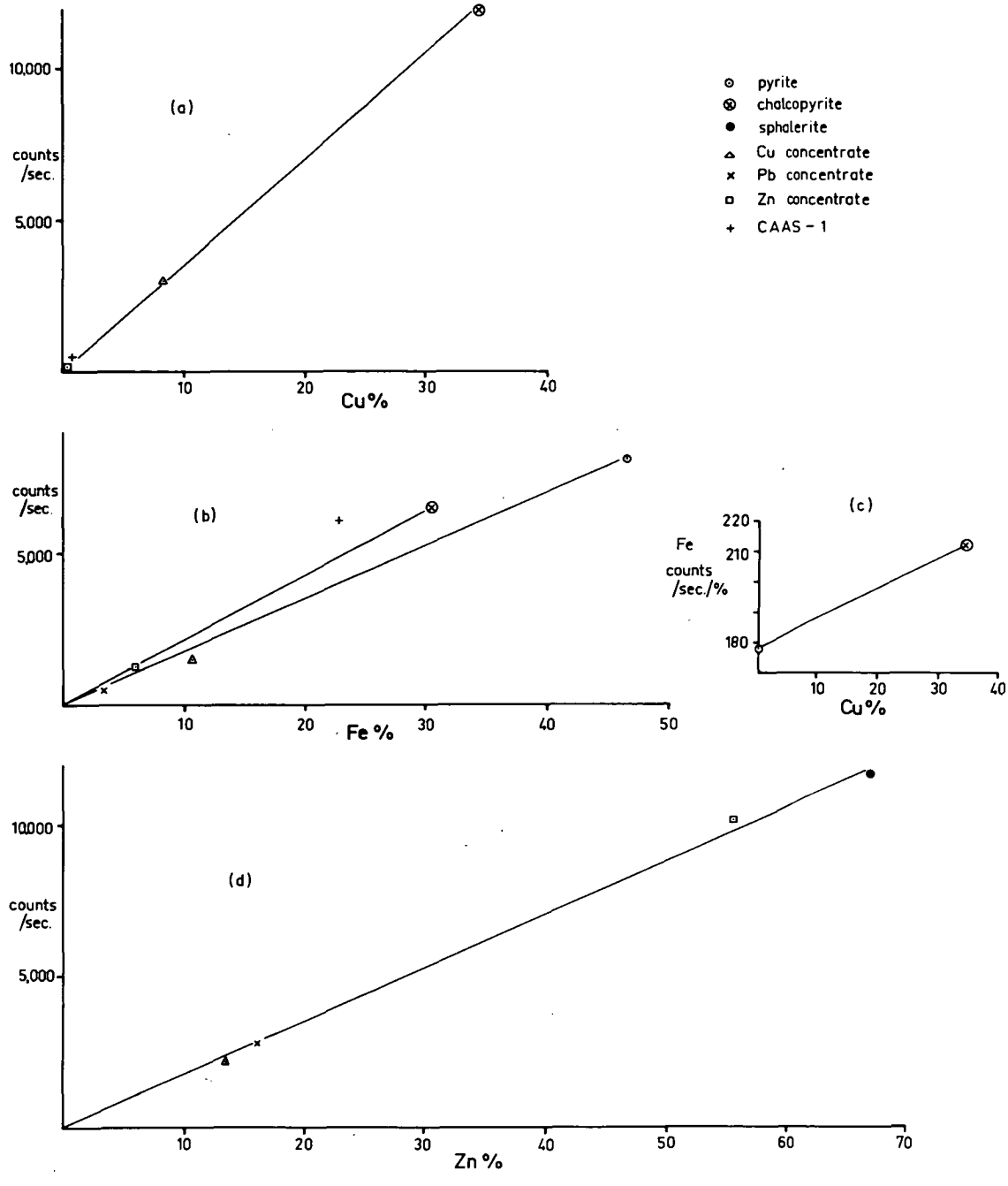
(a)
10,000
counts
/sec.
5,000
10
20
30
40
Cu%
pyrite
chalcopyrite
sphalerite
Cu concentrate
Pb concentrate
Zn concentrate
CAAS - 1
(b)
counts
/sec.
5,000
10
20
30
40
50
Fe %
(c)
220
Fe
210
counts
/sec./%
180
10
20
30
40
Cu%
(d)
10,000
counts
/sec.
5,000
10
20
30
40
50
60
70
Zn %

# 5. METALLOGENESIS OF TASMANIA

Tasmania lies in the southernmost part of the Palaeozoic Tasman Geosyncline, a major structure forming almost the entire eastern seaboard of the Australian continent. It is probable that Tasmania is tectonically related to Victoria, 150 miles to the north (Hills, 1965), but the geological features they share are few. These include Cambrian spilitic vulcanism, and upper Palaeozoic orogenesis and plutonism with associated Au and Sn mineralization. This restricted range of mineralization is confined, however, to Tasmania's north-east corner. The western half of the island is geologically quite unlike Victoria, with large areas of Precambrian and Cambrian rocks, and a great time range (? Precambrian - Devonian), and variation in type (Fe, Ni-Cr, Os-Ir, Cu-Au, Sn-W, Ag-Pb-Zn) of mineralization.

## GEOLOGICAL HISTORY

The geological history of Tasmania has been well synthesized in Spry and Banks (1962), and by Solomon (1965a) and Banks (1965), and the following summary is based partly on these sources.

The geology of the island is shown in Figure 5.1. The outstanding feature is the widespread distribution of essentially horizontal Permian, Triassic and later Systems, unconformably overlying lower Palaeozoic and older rocks which were involved in the Devonian orogenesis. Primary mineralization is restricted to the rocks below the unconformity.

Figure 5.1

Geological map of Tasmania, from Banks (1965).

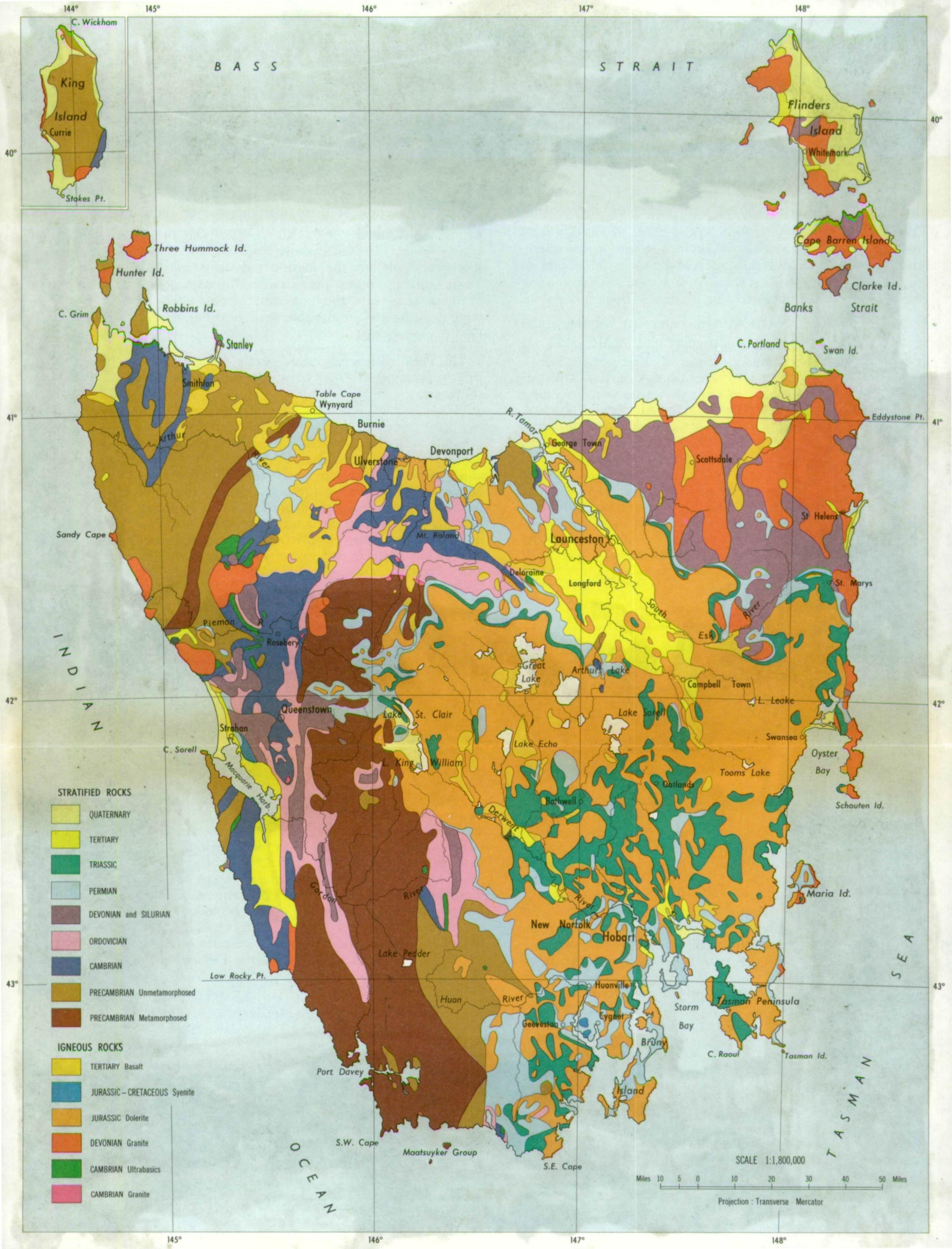
144°
145°
146°
147°
148°
40°
41°
42°
43°
BASS STRAIT
INDIAN OCEAN
TASMAN SEA
C. Wickham
King Island
Currie
Stokes Pt.
Flinders Island
Whitemark
Cape Barren Island
Clarke Id.
Banks Strait
Three Hummock Id.
Hunter Id.
Robbins Id.
C. Grim
Stanley
Smithton
Table Cape
Wynyard
Burnie
Ulverstone
Devonport
R. Tamar
George Town
C. Portland
Swan Id.
Eddystone Pt.
Scottsdale
St Helens
Launceston
Deloraine
Longford
St. Marys
South Esk River
Sandy Cape
Mt. Roland
Arthur River
Pieman R.
Rosebery
Queenstown
Lake St. Clair
Strahan
C. Sorell
Macquarie Harb.
Great Lake
Arthurs Lake
Lake Sorell
Campbell Town
L. Leake
Swansea
Oyster Bay
Schouten Id.
Lake Echo
King William
Tooms Lake
Oatlands
Bothwell
Derwent River
Gordon River
New Norfolk
Hobart
Maria Id.
Lake Pedder
Low Rocky Pt.
Huon River
Huonville
Storm Bay
Tasman Peninsula
Cygnet
Geeveston
Bruny Island
C. Raoul
Tasman Id.
Port Davey
S.W. Cape
Maatsuyker Group
S.E. Cape
STRATIFIED ROCKS
QUATERNARY
TERTIARY
TRIASSIC
PERMIAN
DEVONIAN and SILURIAN
ORDOVICIAN
CAMBRIAN
PRECAMBRIAN Unmetamorphosed
PRECAMBRIAN Metamorphosed
IGNEOUS ROCKS
TERTIARY Basalt
JURASSIC – CRETACEOUS Syenite
JURASSIC Dolerite
DEVONIAN Granite
CAMBRIAN Ultrabasics
CAMBRIAN Granite
SCALE 1:1,800,000
Miles 10 5 0 10 20 30 40 50 Miles
Projection : Transverse Mercator

The Precambrian rocks of western Tasmania are of two types - metamorphosed and relatively unmetamorphosed. Spry (1962a) considered the metamorphosed rocks to be older than the unmetamorphosed, and separated them by the Frenchman Orogeny, an episode of regional metamorphism and basic igneous activity (Fig. 5.2). It has since been found, however, that the age relationships are reversed in north-western Tasmania. The Arthur Lineament, a narrow belt of metamorphosed Precambrian rocks extending from the Pieman River to Wynyard (Figs. 5.1, 5.2, 5.4), consists of psammitic and pelitic schists, with ortho-amphibolites, one of which contains the Savage River magnetite deposit (Fig. 5.4). Gee (1967) has shown that these rocks are metamorphic derivatives of the unmetamorphosed Precambrian rocks, formed in a shear zone during the Penguin Orogeny. The ortho-amphibolites are considered by Gee to be metamorphosed equivalents of albite dolerites occurring in the unmetamorphosed rocks. Some of the dolerites were intruded as dykes and sills during the early part of the Penguin folding, and one of them, the Cooee Dolerite (Spry, 1962b), has been radiometrically dated at 700 m.y. On geological grounds, the Penguin Orogeny is pre-Middle Cambrian, and the combined evidence suggests an uppermost Precambrian age. However its effects seem to have been restricted in area, as discontinuities in the geological record at this time are much less apparent to the south, where the unmetamorphosed Precambrian passes upwards into a distinctive suite of sandstone, siltstone, and dolomite - late Precambrian or early Cambrian - termed by Solomon (1965a) the Success Creek phase (Fig. 5.2).

Figure 5.2

Summary of geological history and mineralization of Tasmania, for the north-west coast (up to the Cambrian), and the mineralized areas of the west coast and north-east coast (up to the Devonian). Partly after Solomon (1965).

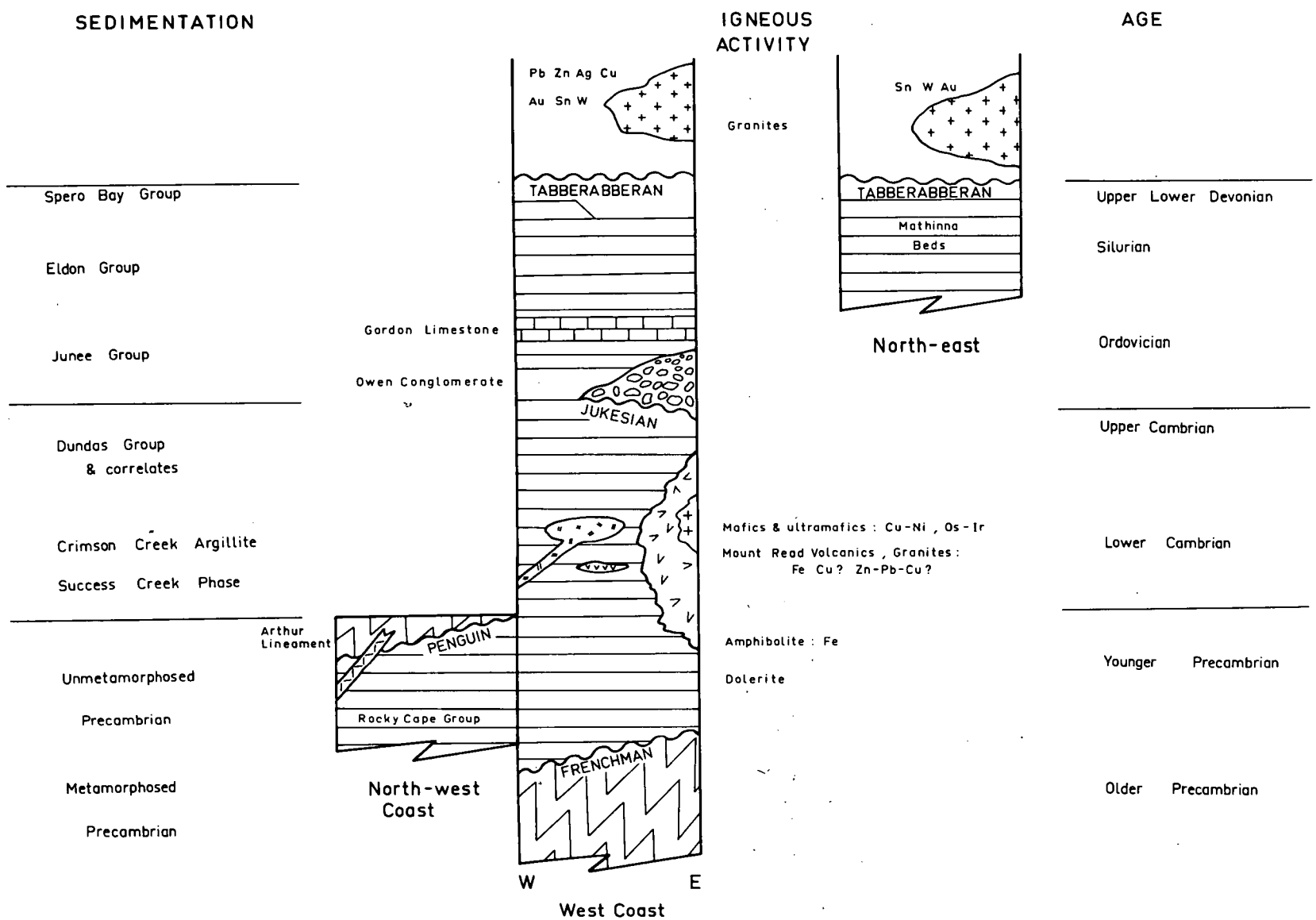
SEDIMENTATION
IGNEOUS ACTIVITY
AGE
Spero Bay Group
Eldon Group
Junee Group
Dundas Group & correlates
Crimson Creek Argillite
Success Creek Phase
Unmetamorphosed Precambrian
Metamorphosed Precambrian
Pb Zn Ag Cu
Au Sn W
Granites
TABBERABBERAN
Gordon Limestone
Owen Conglomerate
JUKESIAN
Mafics & ultramafics : Cu-Ni , Os-Ir
Mount Read Volcanics , Granites :
Fe Cu? Zn-Pb-Cu?
Arthur Lineament
PENGUIN
Amphibolite : Fe
Dolerite
Rocky Cape Group
FRENCHMAN
North-west Coast
W
E
West Coast
Sn W Au
TABBERABBERAN
Mathinna Beds
North-east
Upper Lower Devonian
Silurian
Ordovician
Upper Cambrian
Lower Cambrian
Younger Precambrian
Older Precambrian

Figure 5.3

Locality map for some of the sets of samples used in this study. The set numbers refer to Table 6.1. The locations of sampling areas on the west coast are given in Figure 5.4.

| Locality | Sets |
|---|---|
| Cowrie Point | 2 |
| Arthur River | 3 |
| Franklin River | 4 |
| Branch Creek | 11 |
| Florentine Valley, Woody Island | 14 |
| South Mt. Cameron | 15 |
| Great Mussel Roe Bay | 16 |
| Dove Granite | 23 |
| Low Rocky Point | 24 |
| Story's Creek | 68 |
| Moina | 70, 119 |
| Mt. Remus | 120 |

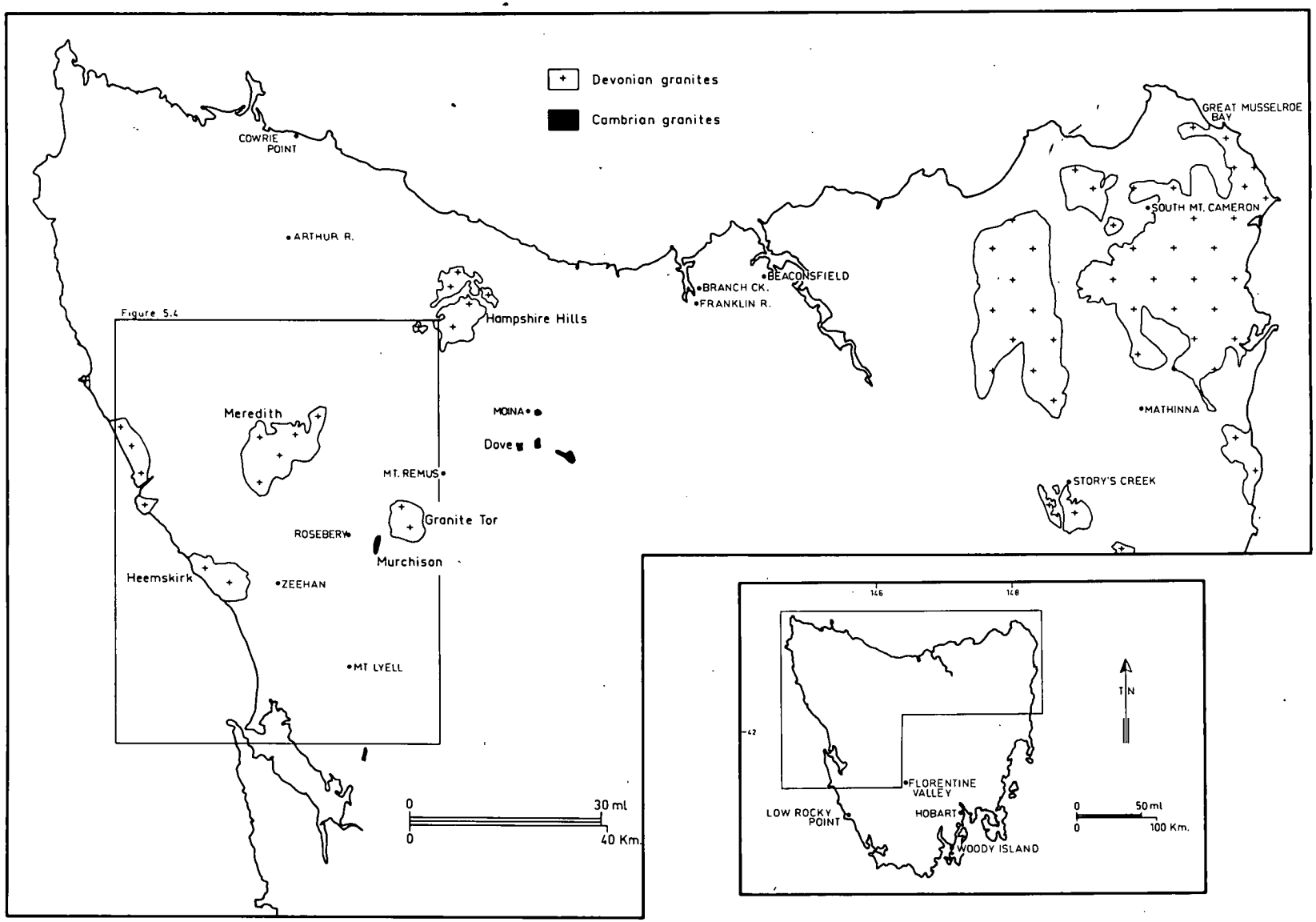
Devonian granites
Cambrian granites
COWRIE POINT
ARTHUR R.
BRANCH CK.
FRANKLIN R.
BEACONSFIELD
GREAT MUSSELROE BAY
SOUTH MT. CAMERON
MATHINNA
STORY'S CREEK
Hampshire Hills
Figure 5.4
Meredith
MOINA
Dove
MT. REMUS
Granite Tor
ROSEBERY
Murchison
Heemskirk
ZEEHAN
MT LYELL
0 30 ml
0 40 Km.
146
148
42
TN
FLORENTINE VALLEY
LOW ROCKY POINT
HOBART
WOODY ISLAND
0 50 ml
0 100 Km.

Figure 5.4

Geological sketch map of the mineralized area of the west coast of Tasmania, from Solomon (1965). The location of this area is shown on Figure 5.3.

| Locality | Sets |
|---|---|
| 1. Mt. Lyell (see Fig. 5.5) | 72-95 |
| 2. Dundas | 60-67 |
| 3. Hercules (see Fig. 5.7) | 117 |
| 4. Cuni | 19 |
| 5. Renison Bell (see Fig. 6.20) | 51-55 |
| 6. Tullah (see Fig. 5.8) | 121-124 |
| 7. Murchison Granite (see Fig. 5.8) | 22 |
| 8. Que River | 12 |
| 9. Valentine's Peak | 71 |
| 10. Mt. Bischoff (see Figs. 6.18, 6.19) | 30-50 |
| 11. Magnet | 118 |
| 12. Cleveland | 69, 128 |
| 13. Savage River | 18 |

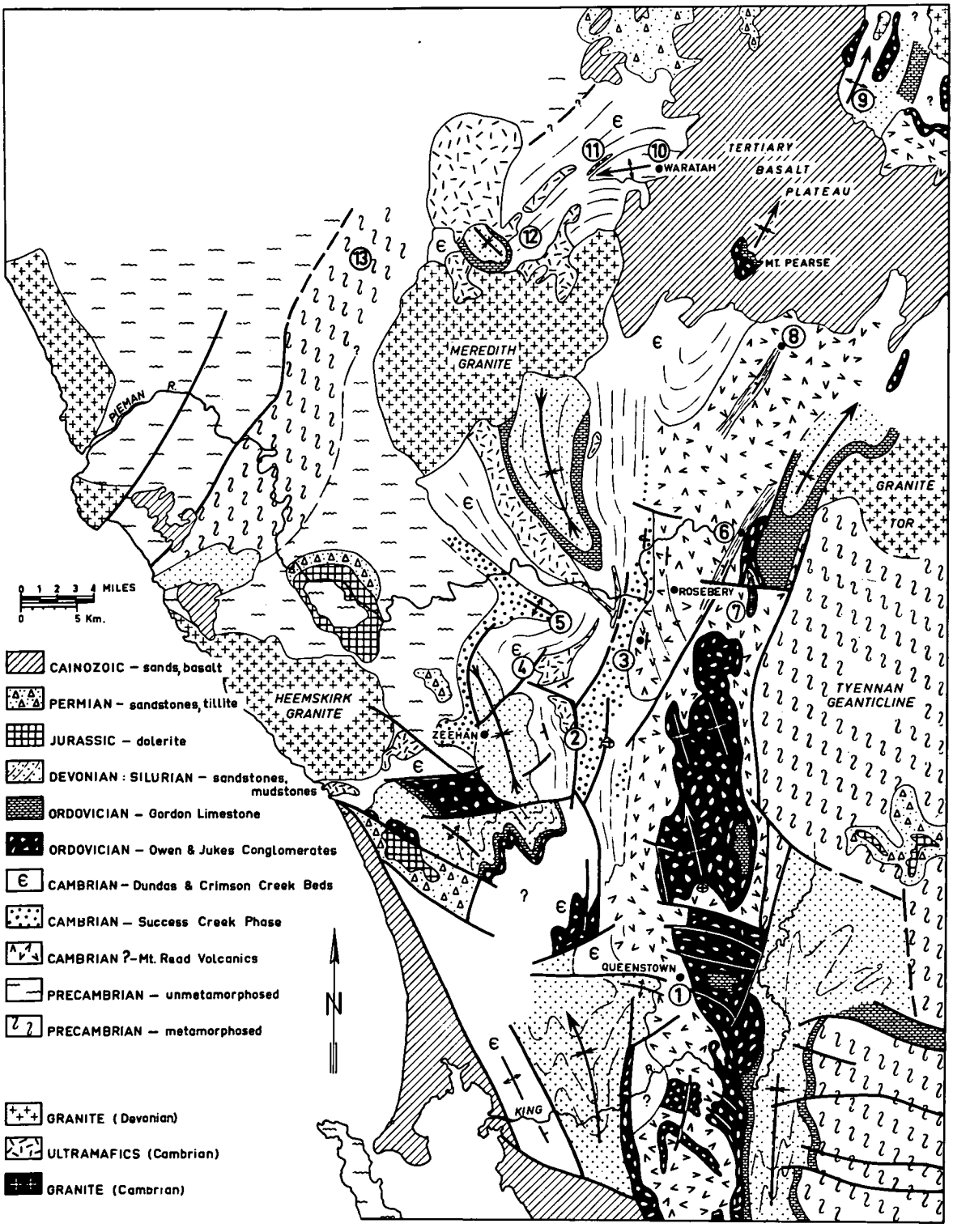
TERTIARY
BASALT
PLATEAU
WARATAH
MT. PEARSE
MEREDITH
GRANITE
PIEMAN R.
HEEMSKIRK
GRANITE
ZEEHAN
ROSEBERY
TOR
GRANITE
TYENNAN
GEANTICLINE
QUEENSTOWN
KING
N
0 1 2 3 4 MILES
0 5 Km.
CAINOZOIC – sands, basalt
PERMIAN – sandstones, tillite
JURASSIC – dolerite
DEVONIAN : SILURIAN – sandstones, mudstones
ORDOVICIAN – Gordon Limestone
ORDOVICIAN – Owen & Jukes Conglomerates
CAMBRIAN – Dundas & Crimson Creek Beds
CAMBRIAN – Success Creek Phase
CAMBRIAN ?–Mt. Read Volcanics
PRECAMBRIAN – unmetamorphosed
PRECAMBRIAN – metamorphosed
GRANITE ( Devonian)
ULTRAMAFICS (Cambrian)
GRANITE (Cambrian)

Whereas the unmetamorphosed successions discussed above were deposited in a widespread miogeosyncline (Spry, 1962a; Solomon, 1965a), in the (?) early Cambrian a eugeosyncline was initiated around the western and northern margins of the Tyennan Geanticline, an emergent block of Precambrian rocks in the mid-west of the island (Fig. 5.1). This trough was filled with perhaps 20,000 feet of conglomerates, greywackes, mudstones, and pyroclastics, and igneous rocks of the spilite-keratophyre association. The mafic-ultramafic igneous activity tended to be concentrated further out in the trough than the acid-intermediate activity, which was confined mainly to a narrow belt (the Mt. Read Volcanic arc) adjacent to the Tyennan Geanticline, although intercalations of the two types occur.

In the Zeehan-Waratah area (Fig. 5.4), the unfossiliferous Crimson Creek Argillite, 10,000 feet thick, concordantly overlying the Success Creek phase, consists of unfossiliferous mudstone, greywacke and shale (Blissett, 1962; Loftus-Hills, 1964), with spilitic lavas and keratophyric tuffs (Solomon, 1965a). It passes upwards into the fossiliferous Dundas Group (lower Middle Cambrian-middle Upper Cambrian), a sequence of variable and impersistent paraconglomerates, greywackes, siltstones, shales and tuffs, which show cyclic deposition. The Cambrian sediments in general become coarser, and contain fewer volcanics towards the top of the succession (Banks, 1965).

Associated with the early Cambrian spilites are mafic-ultramafic complexes containing layered pyroxenites, harzburgites, norites, and bronzitites, with serpentinites, and agglomerates (Jack and Groves, 1964; Groves, 1965; Rubenach, 1967). The McIvor Hill Gabbro west of

Zeehan has been radiometrically dated at 518 ± 133 m.y. (Brooks, 1966). Some of these complexes were exposed to erosion at least by the lower Middle Cambrian, as evidenced in several parts of Tasmania by detritus in immediately overlying sediments, and it is possible that they were wholly extrusive on the sea floor (Solomon, 1965a; Rubenach, 1967). This ophiolite association may be the culmination of a period of basic igneous activity begun in the late Precambrian with the albite dolerite intrusions in the north-west, and spilitic vulcanism in the Zeehan area (Blissett, 1962).

The age of the acid-intermediate igneous rocks - the Mt. Read Volcanics and associated late-stage, high-level, sub-volcanic Darwin, Murchison and Dove Granites - is a major problem. Immediately to the west of Rosebery (Fig. 5.7a), the Volcanics appear to be almost isoclinally folded with the Rosebery "Series", which has been correlated with the Success Creek phase (Loftus-Hills et al., 1967). The Volcanics could therefore be partly Precambrian, but in other parts of Tasmania similar volcanics are known to be Upper Cambrian, and it appears that the suite is regionally diachronous.

The Mt. Read Volcanics, about 10,000 feet thick, are largely sodic quartz keratophyres and albite andesites, and include ignimbrites and tuffs (Solomon, 1964). Coeval marine sedimentation occurred to the west, but the only evidence for a sub-aqueous environment of deposition for the Volcanics is a series of minor siltstone intercalations, one of which contains upper Middle Cambrian marine fossils, and Solomon (Solomon et al., in press) considers that much of the arc was probably sub-aerial. The Volcanics contain the Rosebery, Mt. Lyell and Mt. Farrell orebodies.

Cambrian eugeosynclinal deposition ceased with the onset of the Jukesian Movement. This created local unconformities between several areas of Cambrian and Precambrian rocks, and the succeeding 15,000 - 20,000 feet of continental and marine miogeosynclinal sedimentary rocks. The latter were then deposited without further major disturbance until the upper Lower Devonian. In western Tasmania, these rocks consist of the Ordovician Junee Group, which is comprised in part of the basal Jukes Conglomerate and Owen Conglomerate, and the Lower to Upper Ordovician Gordon Limestone; the Siluro-Devonian Eldon Group; and the Lower Devonian Spero Bay Group. In north-eastern Tasmania the lower Palaeozoic basement of Mathinna Beds, monotonous in lithology and almost unfossiliferous, is Siluro-Devonian, and possibly Ordovician.

In the upper Lower - upper Middle Devonian, the whole of Tasmania was subjected to the two-phase Tabberabberan Orogeny. In the Upper Devonian, high-level post-tectonic granite batholiths and stocks were intruded in a radiometrically dated succession from east (oldest) to west across Tasmania and the small islands to the north (McDougall and Leggo, 1965; Brooks and Compston, 1965).

## METALLOGENIC HISTORY

In the following summary, "set" numbers refer to the sample-groups in Table 6.1, and "ore" refers to economic mineralization. Localities of deposits are shown in Figures 5.3 and 5.4.

The Savage River magnetite deposit (set 18) lies within an ortho-amphibolite in the Arthur Lineament. The age of the original mafic

igneous intrusion has been interpreted as Older Precambrian (Spry, 1964), Upper Precambrian (Gee, 1967), and coeval with the Cambrian mafic-ultramafic complex at Bald Hill, four miles to the east (Urquhart, 1966). Gee and Urquhart have discounted Spry's (1964) conclusion on structural and chemical grounds. Gee's interpretation is the most likely, as both the amphibolites and the Precambrian dolerites lack the Ni-Cu-Cr-Os-Ir mineralization of the Bald Hill complex, but the question is unresolved.

The wall-rocks of the pyritic, titaniferous magnetite ore show varying degrees of alteration to serpentine, magnesite, dolomite, chlorite, and epidote. Tetlow (1960) and Hughes (1961) postulated a magmatic segregation origin for the ore, but Hall and Solomon (1962) commented that because of the small volume of the igneous bodies compared with the size of the ore deposits, the concentration of ore constituents probably occurred prior to emplacement of the host-rock. Banks (1965) notes the further possibility of in situ flowage differentiation. However Urquhart (1966), citing mainly the apparent paragenetic sequence, and the alteration of the amphibolite, proposes a hydrothermal origin from a mafic source rock. The diversity of these views may be more apparent than real, as Singewald (1917) has suggested, and it is now commonly assumed (Park and MacDiarmid, 1964, p.217), that many iron ores, especially titaniferous iron ores, are late-stage magmatic differentiates whose emplacement is assisted by coeval hydrothermal fluids. The amphibolite has undergone at least two periods of metamorphism, and if the ore was syngenetic, it will have been similarly affected.

The mafic-ultramafic igneous suite, which is probably mainly Cambrian, contains extensive, at present sub-economic mineralization.

(i) Samples of magnetite have been taken from the Tenth Legion deposit in the McIvor Hill gabbro (set 21). (ii) Nickel mineralization is not uncommon in several of the complexes, and pyrrhotite-pentlandite ore (set 19) has been analyzed from Cuni, a deposit associated with the Serpentine Hill complex between Zeehan and Renison Bell, mainly to establish the Co/Ni ratio. (iii) Small spherical nodules (0.2 in. diam.) occur in a spilite in the Bald Hill complex (set 20). They have a complex internal structure, a euhedral pyrite nucleus being surrounded by a pure pyrite core, which is succeeded by a subophitic texture of silicate laths and interstitial pyrite. The textures suggest that the nodules grew from a central nucleus, and are coeval with the host spilite.

The Cambrian acid-intermediate volcanic rocks also contain distinctive mineralization which is almost certainly syngenetic. Typical are magnetite-hematite veins, with or without pyrite, chalcopyrite and barite, one of which was sampled at Low Rocky Point (set 24). Pyrite-hematite was also sampled from the Powerful Mine in the Dove Granite (set 23), and disseminated pyrite from the Murchison Granite (set 22). Of less certain origin is mineralization (sets 25 and 26) in the volcanic country rocks enclosing the host-rock shale of the Rosebery Zn-Pb-Cu lode. This mineralization may be genetically related to the main lode, the origin of which is discussed below.

The Mount Lyell deposits at Queenstown are predominantly of pyrite-chalcopyrite, occurring in chloritized and sericitized schistose Mt. Read Volcanics. The ores, which have been described by Wade and Solomon (1958), Solomon and Elms (1965), Solomon (1967), Markham (1968) and Solomon et al.,(in press), are similar to those at Rio Tinto, Spain

(Solomon, pers. comm.). They occur adjacent to the base of upturned and overturned Owen Conglomerate, the contact between the two rock units having been faulted and folded in the Tabberabberan Orogeny.

Six main types of primary mineral concentrations have been sampled in this study (Fig. 5.5):

(i) Massive pyrite with some chalcopyrite (e.g. the Blow, or Mt. Lyell Mine, set 72).

(ii) Pyrite with chalcopyrite disseminated in schist, forming poorly defined, steeply dipping and pitching lenses (e.g. the West Lyell lenses, sets 77-80). Derived from these are remobilized quartz-sulphide lenses in tensional gashes in the schist (sets 81-84).

(iii) Disseminated pyrite without chalcopyrite (e.g. the Blow, sets 73-76; West Lyell, sets 85-88; Cape Horn, sets 89-90).

(iv) Massive irregular chalcopyrite-bornite, with or without pyrite (e.g. the North Lyell - Crown Lyell area, sets 91-93).

(v) Disseminated chalcopyrite, with some stratiform pyrite, and barite (e.g. Lyell Comstock, set 94).

(vi) A small lens of banded Pb-Zn-Cu ore, similar to that at Rosebery (Tasman and Crown Lyell, set 95).

Two main possibilities exist for the origin of the mineralization:

(i) It was associated with Tabberabberan plutonism in the Devonian.

(ii) It was genetically related to the host volcanics, is therefore originally Cambrian, and has been metamorphosed into its present configuration during the Devonian.

The evidence bearing on the age or genesis of the deposits is as follows:

Figure 5.5

Geological and locality map of the Mt. Lyell area, by Solomon (Solomon et al., in press). The grid is the Mt. Lyell Co. mine grid.

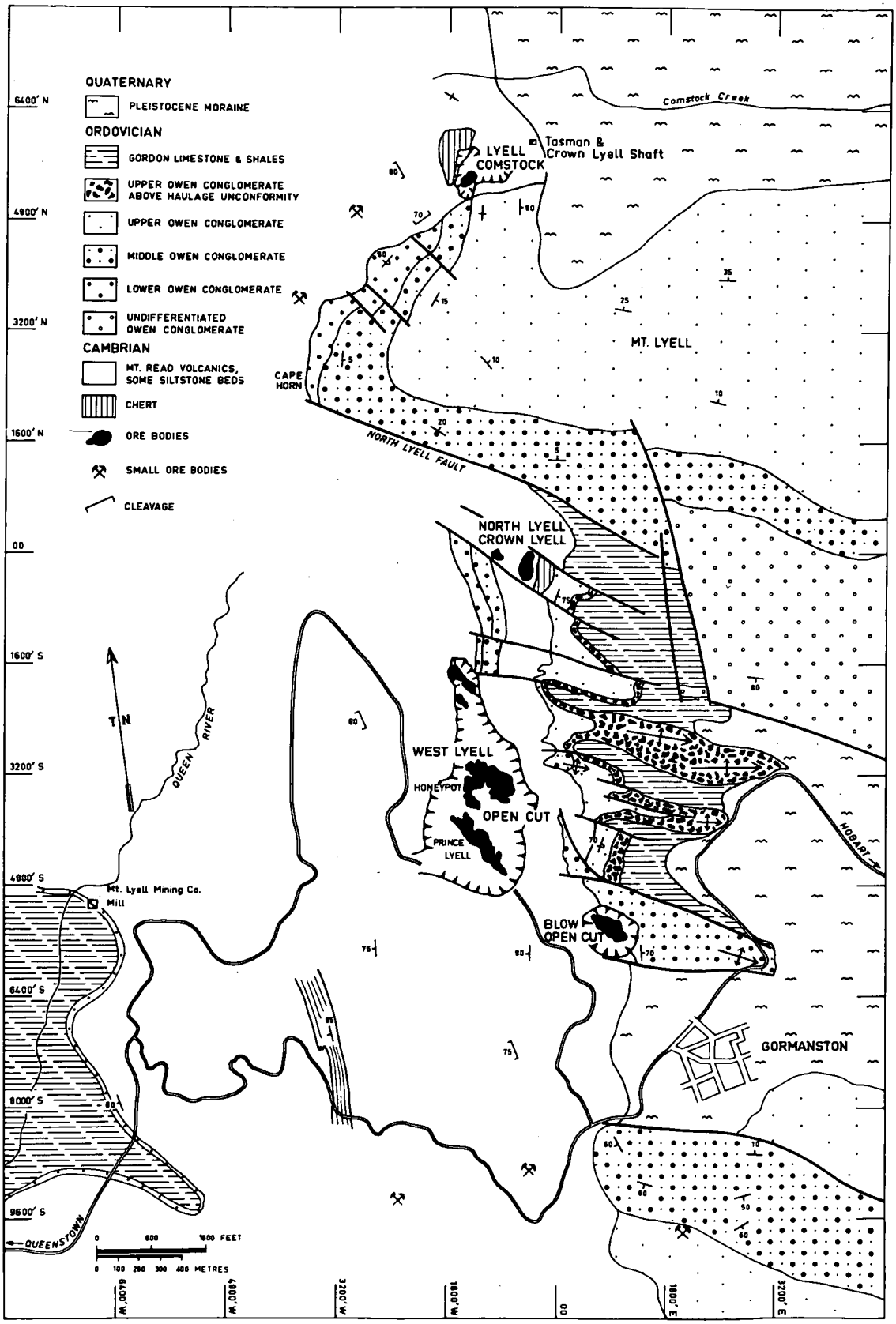
QUATERNARY
PLEISTOCENE MORAINE
ORDOVICIAN
GORDON LIMESTONE & SHALES
UPPER OWEN CONGLOMERATE ABOVE HAULAGE UNCONFORMITY
UPPER OWEN CONGLOMERATE
MIDDLE OWEN CONGLOMERATE
LOWER OWEN CONGLOMERATE
UNDIFFERENTIATED OWEN CONGLOMERATE
CAMBRIAN
MT. READ VOLCANICS, SOME SILTSTONE BEDS
CHERT
ORE BODIES
SMALL ORE BODIES
CLEAVAGE
6400' N
4800' N
3200' N
1600' N
00
1600' S
3200' S
4800' S
6400' S
8000' S
9600' S
6400' W
4800' W
3200' W
1600' W
00
1600' E
3200' E
Comstock Creek
LYELL COMSTOCK
Tasman & Crown Lyell Shaft
MT. LYELL
CAPE HORN
NORTH LYELL FAULT
NORTH LYELL
CROWN LYELL
WEST LYELL
HONEYPOT
OPEN CUT
PRINCE LYELL
BLOW OPEN CUT
HOBART
GORMANSTON
QUEEN RIVER
T N
Mt. Lyell Mining Co. Mill
QUEENSTOWN
0 800 1600 FEET
0 100 200 300 400 METRES

(a) Some of the ore emplacement is post-Lower Ordovician, as part of the Owen Conglomerate in the North Lyell area is mineralized. Further, although the lenses of mineralization types (ii), (iii), and (v) approximately conform to the relict bedding in the volcanics, they also tend to parallel the Devonian cleavage. All these phenomena may, however, be metamorphic effects. There are preserved three examples of stratiform ore, all adjacent to the stratigraphic top of the volcanic sequence (at the Blow, Lyell Comstock, and Tasman and Crown Lyell), which could have been of sedimentary origin (Rafter and Solomon, 1967; Markham, 1968).

(b) Much of the ore is deformed, recrystallized and remobilized on a microscopic scale (Markham, 1968), and the occurrence of stratiform ore at Lyell Comstock is folded on a mesoscopic scale. In addition, the unusually strong development of the Devonian cleavage in the mine area implies that this block of volcanics was previously affected by hydrothermal alteration (Loftus-Hills et al., 1967). These observations suggest that ore emplacement predated the Devonian orogeny.

(c) There is no apparent Devonian igneous source for the mineralization, whereas there is a possible Cambrian igneous source - the volcanic episode.

(d) In other geosynclines there are examples of this type of mineralization occurring in similar volcanics (Markham, 1968).

(e) The sulphur isotope data (Fig. 5.6, from Solomon et al., in press) is not inconsistent with results from sulphides of known volcanic provenance in other countries.

(f) Evidence for a pre-Lower Ordovician age for sulphide mineralization has been presented by Solomon (1967), who suggests that

Figure 5.6

Distribution of S-isotope ratios ($\delta S^{34}$ per mil) from some ores and sedimentary pyrites within the Mt. Read Volcanics; from Solomon *et al.* (in press).

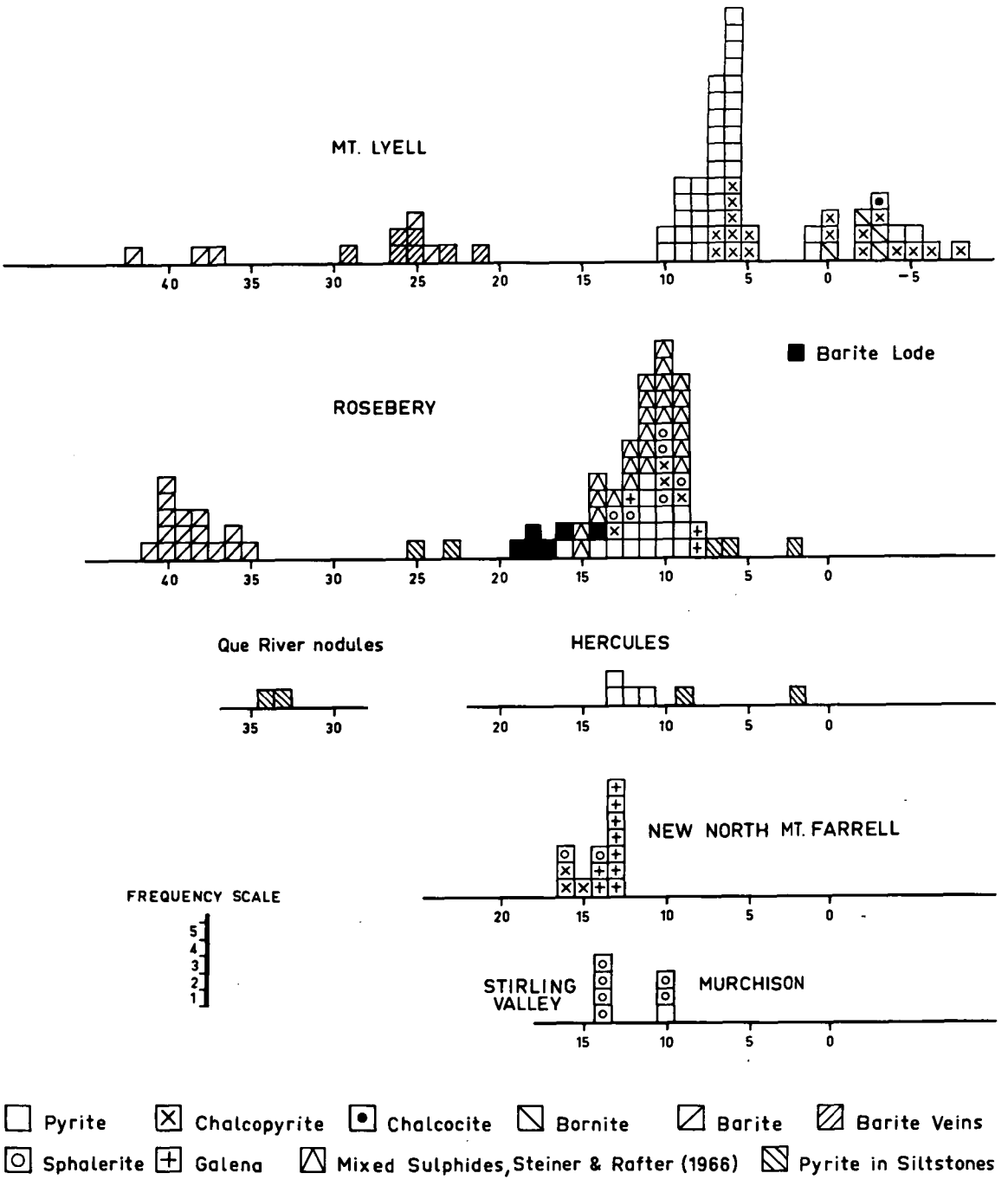
MT. LYELL
40
35
30
25
20
15
10
5
0
−5
Barite Lode
ROSEBERY
40
35
30
25
20
15
10
5
0
Que River nodules
35
30
HERCULES
20
15
10
5
0
NEW NORTH MT. FARRELL
20
15
10
5
0
FREQUENCY SCALE
5
4
3
2
1
STIRLING VALLEY
MURCHISON
15
10
5
0
Pyrite
Chalcopyrite
Chalcocite
Bornite
Barite
Barite Veins
Sphalerite
Galena
Mixed Sulphides, Steiner & Rafter (1966)
Pyrite in Siltstones

hematite bodies at the contact of the volcanics and the overlying Owen Conglomerate could represent dehydrated Ordovician gossans.

It is apparent that there is considerable positive evidence for a Cambrian volcanic origin for the ores.

The Rosebery and (essentially similar) Hercules ore bodies are stratiform banded pyritic Zn-Pb-Cu ores of the Rammelsberg type. The Rosebery lode occurs in a tuffaceous shale lens near the western margin of the Mount Read Volcanics 20 miles north of Mount Lyell. The geology has been summarized by Hall et al. (1953) and Hall et al. (1965).

The host rock shale of the orebodies (Fig. 5.7), which dips east at about $45^{\circ}$, contains sedimentary pyrite (set 7). It is underlain by altered and cleaved pyroclastic phases of the Mount Read Volcanics, containing disseminated mineralization (set 25). Overlying the host rock is a quartz- and carbonate-veined pyritic black shale (sets 5 and 6), followed by pyroclastics and massive lavas (set 26).

There are two spatially and compositionally distinct orebodies in the mine - the banded pyrite-sphalerite-galena-chalcopyrite body, and above it a banded stratiform barite-manganese carbonate orebody, with some hematite-pyrite mineralization (set 107). Both are stratiform, but the barite orebody is less continuous.

The origin of the ore is as problematical as for most similar ores. At Rosebery the mineralization could be syngenetic with the host rock shale, or epigenetic, either in the Cambrian (as a late volcanic episode) or in the Devonian. The present evidence pertaining to genesis, much of which is due to Brathwaite (1967), is as follows:

Figure 5.7

Geology of the Rosebery and Hercules deposits (after mapping and compilation by Brathwaite). The grid is the Tasmanian Transverse Mercator grid.

(a) Geological map of the Rosebery-Hercules area. For detailed discussion of the problem of the relationship between the Rosebery "Series" and the Mt. Read Volcanics, see Loftus-Hills et al. (1967).

(b) Geological cross-section of the Rosebery Mine along the line A-B in (a) above.

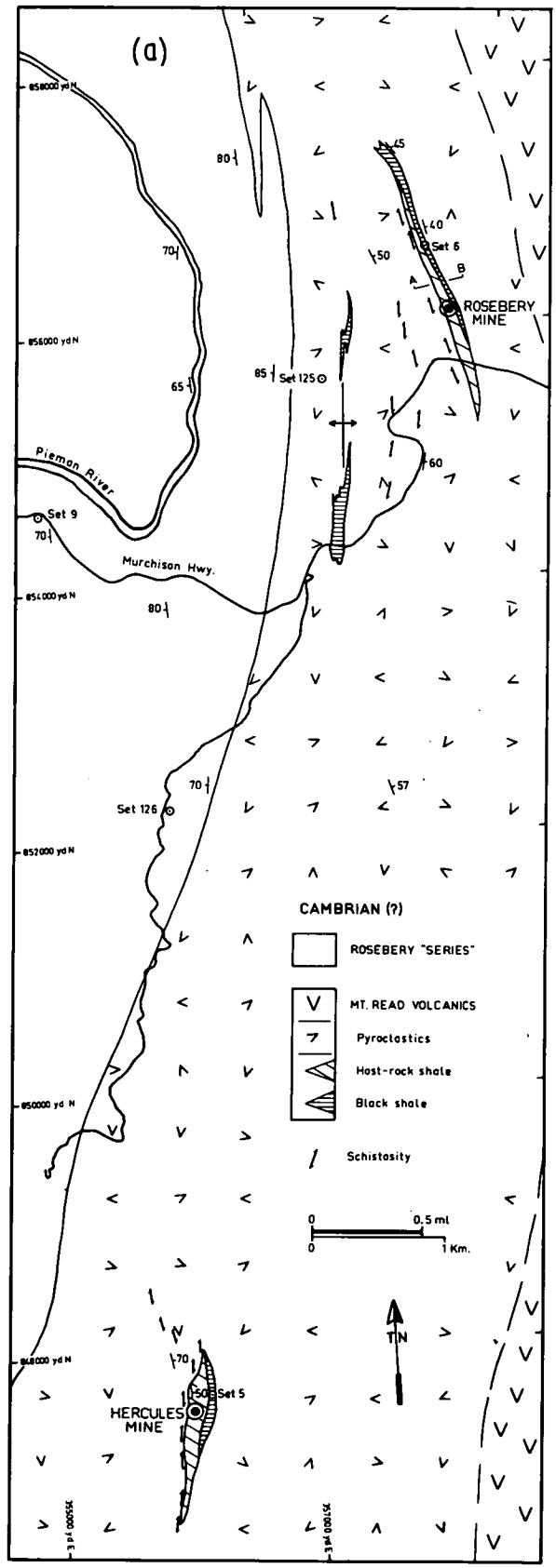
(a)
858000 yd N
856000 yd N
854000 yd N
852000 yd N
850000 yd N
848000 yd N
80
70
65
85
Set 125
45
40
50
Set 6
A
B
ROSEBERY MINE
60
Piemon River
Set 9
Murchison Hwy.
Set 126
57
HERCULES MINE
Set 5
CAMBRIAN (?)
ROSEBERY "SERIES"
MT. READ VOLCANICS
Pyroclastics
Host-rock shale
Black shale
Schistosity
0
0,5 mi
0
1 Km.
TN
352000 mE
357000 mE

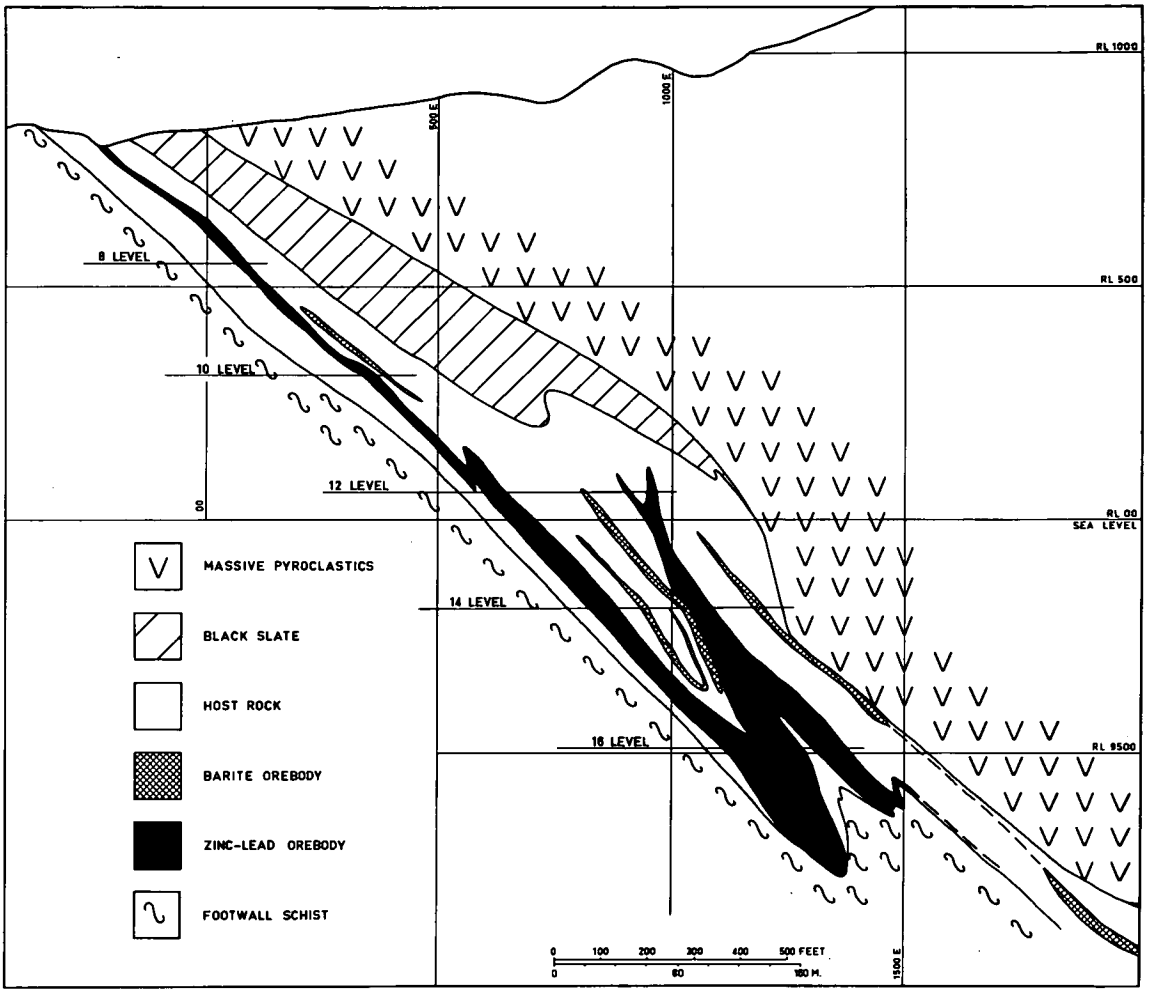
RL 1000
RL 500
RL 00
SEA LEVEL
RL 9500
500 E
1000 E
1500 E
8 LEVEL
10 LEVEL
12 LEVEL
14 LEVEL
16 LEVEL
MASSIVE PYROCLASTICS
BLACK SLATE
HOST ROCK
BARITE OREBODY
ZINC-LEAD OREBODY
FOOTWALL SCHIST
0 100 200 300 400 500 FEET
0 60 180 M.

(b)

(i) There is no outcropping Devonian source for the mineralization, although there is undoubted Devonian mineralization within two miles of the Rosebery Mine. However, volcanic emanations in the Cambrian are another possible source for the metals.

(ii) The lodes were once believed to be en echelon (and due to replacement), but are now known to be a single folded unit, locally disrupted by shearing.

(iii) Fabric analysis indicates that although the Tabberabberan cleavage, the host rock bedding, the ore-host rock contacts, and the banding in the ore, are essentially coplanar, the last three of these show an equally developed degree of preferred orientation, whereas the cleavage shows a much higher degree of preferred orientation. This suggests that the cleavage is independent of the other parameters, which all appear to be related and to predate the cleavage.

(iv) In general the folding is much more intense in the ore than in the wall-rocks, which are progressively less folded away from the ore (Fig. 5.7b). This may be taken as evidence that the ore was emplaced prior to Tabberabberan folding, and acted as an incompetent medium during deformation.

(v) Despite the overall metamorphism of the ore, as shown by crystalloblastic and deformation textures, there remain some framboidal and colloform-like pyrite textures, and oolites occur in the associated carbonate rocks.

(vi) Wall-rock sericitization and chloritization, and cleavage, are most strongly developed below the black shale horizon, and more especially in the footwall of the mine. They are least developed in the hangingwall, and away from the orebody.

(vii) The senior author in Hall et al. (1965) observed that an undeformed basalt dyke in the mine was mineralized by galena and chalcopyrite at its margins, and he deduced a post-Devonian orogeny, epigenetic origin for the ore. However this occurrence is much better explained as preferential rheomorphic mobilization during dyke emplacement.

In summary, the evidence at present seems to favour a pre-deformation origin for the ore, possibly by sedimentary processes syngenetic with host rock formation in the Cambrian, the ore solutions having altered the country rock in their passage to the surface.

Two other occurrences of mineralization near the Rosebery Mine were also sampled (Fig. 5.7a). In the footwall schist to the west of the Rosebery Lode, a pyrite-galena-siderite-cassiterite vein occurs at the Black P.A. Mine (set 125). The mineralogy of the ore suggests it is related to the other Devonian fissure lodes of the region. Further to the south, pyrite is disseminated in the Natone Volcanics, a narrow band of tuff in the "Rosebery Series", which is the group of sediments occurring immediately to the west of the margin of the Mount Read Volcanics at Rosebery (Loftus-Hills et al., 1967). There is no geological avidence for the age of this pyrite.

At Tullah, 5 miles NE of Rosebery, on the opposite margin of the Mount Read Volcanics, a steeply-dipping, probably overturned lens of sediments (the "Farrell Slates") occurs in the Volcanics (Fig. 5.8). This is intruded by a series of Pb-Ag-Cu fissure veins at the New North Mt. Farrell Mine (set 124). Other smaller deposits occur nearby in both the sediments and the adjacent Volcanics, and these have been

Figure 5.8

Geological map of the Tullah area (Mt. Farrell group of mines), after Solomon and Brooks, in Hall and Solomon (1962).

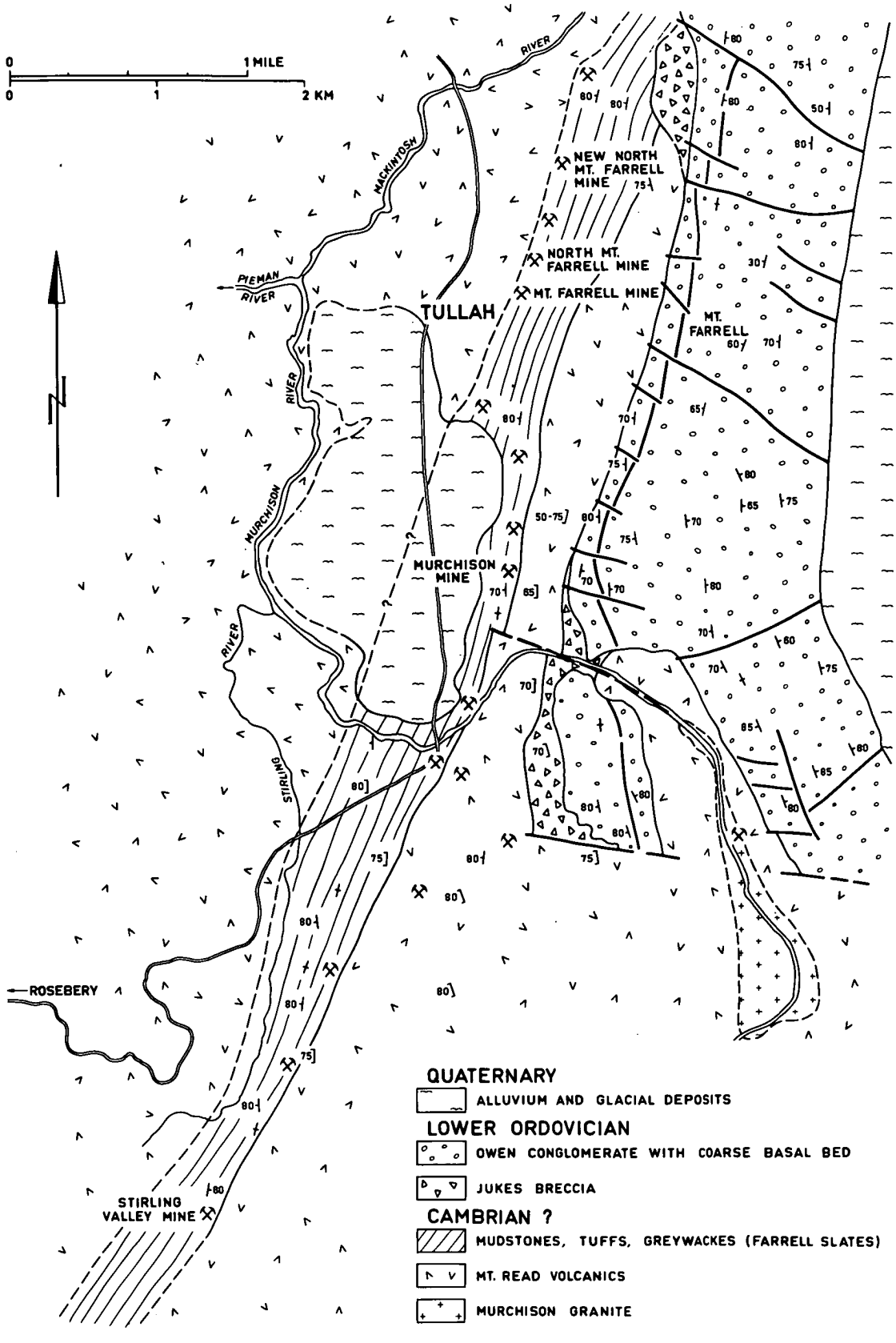
0 1 MILE
0 1 2 KM
MACKINTOSH RIVER
NEW NORTH MT. FARRELL MINE
NORTH MT. FARRELL MINE
MT. FARRELL MINE
PIEMAN RIVER
TULLAH
MT. FARRELL
MURCHISON RIVER
MURCHISON MINE
STIRLING RIVER
ROSEBERY
STIRLING VALLEY MINE
QUATERNARY
ALLUVIUM AND GLACIAL DEPOSITS
LOWER ORDOVICIAN
OWEN CONGLOMERATE WITH COARSE BASAL BED
JUKES BRECCIA
CAMBRIAN ?
MUDSTONES, TUFFS, GREYWACKES (FARRELL SLATES)
MT. READ VOLCANICS
MURCHISON GRANITE

sampled at the Zn-rich Murchison (set 123) and Stirling Valley (set 121) Mines, and at the Tullah Ag-Pb Mine (set 122). All the mines at Tullah are referred to as the Mt. Farrell group.

These ores have previously been grouped on the basis of their mineralogy with the Devonian Pb-Ag-Zn ores at e.g. Zeehan, and assigned a magmatic hydrothermal origin (Solomon, 1965b). Certainly some of the ore has been emplaced later than the Devonian cleavage, but as Solomon et al. (in press) have pointed out, certain characteristics suggest that the ore might have been Cambrian, volcanic, and remobilized in the Devonian:

(i) There is no obvious Devonian igneous source, whereas the ores are associated with Cambrian volcanic rocks.

(ii) The sulphur isotope values are quite different from those in the Pb-Ag-Zn ores at Zeehan, but are similar to those at Rosebery.

At the Magnet Mine, four miles west of Mt. Bischoff, a Pb-Ag-Zn fissure vein system occurs within a complex zone of Cambrian pyroxenites, spilites, and volcanic breccias (Solomon, 1964; Groves and Solomon, 1964). As there is little positive evidence for the age of the deposit, the unlikely possibility that the ore is Cambrian has been investigated by analyzing sphalerite for Se (set 118) and Cd (Appendix 2).

The only highly cobaltiferous Tasmanian mineral occurrence known prior to this study (set 120) was at a Mo prospect at Mt. Remus, between the Rosebery-Tullah and Moina areas (Nye, 1928; Stillwell, 1932). Pyrite-molybdenite veins, some containing quartz, intrude Precambrian schists, and seem to be related to an adjacent system of ramifying acid porphyry dykes. However, the age of these dykes is unknown, as they

could be intrusive phases either of the Cambrian volcanics, which outcrop within half a mile, or of the Devonian Granite Tor granite, which outcrops 5½ miles to the south.

Major mineralization is associated with the Devonian granites intruded after the Tabberabberan Orogeny. Intramagmatic cassiterite and other sulphides occur in the Heemskirk Granite (sets 27-28) and in some types of granite in the north-east. There are several mineral fields adjacent to granitic intrusions:

(a) East of the Heemskirk Granite is the Zeehan Pb-Ag field, (sets 56-59) where the ore occupied fissures in Younger Precambrian to Ordovician rocks. The field is mineralogically zoned with respect to the source granite into cassiterite, pyritic, sidero-pyritic, and sideritic groups (Park, 1955; Both and Williams, 1968). To the east of Zeehan there is further Pb-Ag-Zn-Sb mineralization in the Dundas area (sets 60-67).

(b) Three tin ore deposits occur north of Zeehan. Renison Bell is one mile from a granitic stock outcropping between the Heemskirk and Meredith Granites; Cleveland is adjacent to the northern margin of the Meredith Granite; and nearby Mt. Bischoff contains a porphyry dyke swarm probably related to an apophysis of the Meredith Granite.

At Renison Bell and Mt. Bischoff (sets 30-55) the cassiterite-pyrrhotite-pyrite ore occurs mainly in concordant replacement lenses, particularly in dolomite (upper "Success Creek phase" and, at Renison Bell, lower Crimson Creek Argillite), although there are associated vein deposits (Gilfillan, 1965). The Mt. Bischoff area is mineralogically zoned (Groves and Solomon, 1964; Groves, 1968) from central high-

temperature pyrrhotite replacement Sn ore, to outer lower-temperature pyritic vein Pb-Zn ore (see Chapter 6). At Cleveland (set 69) the mineralogy is similar, with Sn-Cu replacement lodes strictly stratiform in dolomitized Cambrian shales (Cox, 1968).

(c) Further to the north-east is the Hampshire Hills Granite. A pyrite fissure vein in Cambrian (?) sediments associated with a porphyritic phase of this body has been sampled near Valentine's Peak (set 71).

(d) The Moina area, 30 miles east of Mt. Bischoff, contains several small Devonian granites which have associated ores, as at the Shepherd and Murphy Sn-W Mine (set 119) and the Round Hill Pb-Ag Mine (set 70), both in Ordovician rocks. The Shepherd and Murphy samples are from contact metamorphosed Gordon Limestone, and it is not certain whether they represent recrystallized sedimentary pyrite or hypogene material, although the latter origin is more likely.

(e) In the north-east of the island, the lodes adjacent to granites are cassiterite-wolframite-quartz fissure veins in Mathinna Beds. At Story's Creek (set 68) and Aberfoyle, the vein systems are truncated at depth by the parent granites (Kingsbury, 1965).

The Au in quartz veins in Ordovician rocks and Mathinna Beds of the north-eastern region (e.g. at Mathinna and Beaconsfield; Fig.5.3) are not spatially related to outcrops of igneous rocks, but it is reasonably assumed that they are genetically related to Devonian granites at depth.

# 6. COBALT, NICKEL, SELENIUM AND CADMIUM IN ORE MINERALS

In the first part of this Chapter, all the analyses are presented, and the trends of trace-element concentrations for the ores of known origin are discussed. The effect of depositional and post-depositional variables on the dispersion of the trace elements in all the ores is then examined in detail, so that some of the components of the overall trends can be established. It is then possible to evaluate the data for the ores of uncertain origin, and to examine the possibility of delineating metallogenic subprovinces.

All the analyses for Co, Ni and Se are presented in Table 6.1. Analyses of Cd in sphalerite are listed in Appendix II.

TABLE 6.1

ANALYSES OF COBALT, NICKEL AND SELENIUM IN ORE MINERALS

This table contains half of the complete compilation available in the Geology Department, University of Tasmania. Omitted here are calculations of logarithms of analyses, Ni/Co ratios, original weights of specimens, and full details of sample preparations. An example of the omitted pages has been included in this table.

## Arrangement of the Table

| | | Sets |
|---|---|---|
| 1. | Mineral deposits of known age and (usually) origin: | |
| | (a) Sedimentary-diagenetic | 1-17 |
| | (b) Precambrian and Cambrian, intramagmatic in volcanics, granites, mafics and ultramafics | 18-26 |
| | (c) Devonian intramagmatic and hydrothermal | 27-71, 128-132 |
| 2. | Other mineral deposits of uncertain origin: | |
| | (a) Mt. Lyell | 72-95 |
| | (b) Rosebery-Hercules | 96-117 |
| | (c) Magnet Mine | 118 |
| | (d) Shepherd and Murphy Mine | 119 |
| | (e) Mt. Remus prospect | 120 |
| | (f) Tullah area mines (Mt. Farrell group) | 121-124 |
| | (g) Other mineralization near Rosebery | 125-126 |
| | (h) Lake George Mine, Captain's Flat, N.S.W. | 127 |

## Explanatory Notes

SAMPLE Numbers refer to powdered, concentrated samples taken from specimens catalogued in the Geology Department, University of Tasmania, except where stated otherwise.

The numbering system is as follows:

| | |
|---|---|
| 100121 PY<br>100122 PY | From two different specimens |
| 100124A PY<br>100124B PY | From two different parts of the same specimen |

| | | |
|---|---|---|
| 100125A<br>100125B | PY<br>CPY | From two different parts of the same specimen |
| 100126A<br>100126A | PY<br>CPY | Separated from the same sample of the specimen |
| 100127<br>100127 | PY<br>CPY | Separated from the same sample of the specimen |

MIN Mineral abbreviations:

| | |
|---|---|
| ASPY | arsenopyrite |
| CA-R | secondary carbonate, replacement deposit |
| CA-V | vein carbonate |
| CPY | chalcopyrite |
| DOL | primary dolomite |
| HM | hematite |
| MG | magnetite |
| MS | marcasite |
| PO | pyrrhotite |
| PO-M | hand-magnet sensitive |
| PO-N | not PO-M |
| PY | pyrite |
| SL | sphalerite |

The mineral named refers to the powdered concentrate after sample preparation, and is > 95% pure (in most cases > 99% pure) with respect to ore minerals, except where stated otherwise.

CO1 NI1 Co and Ni analyses in ppm. Concentrations in the mineral calculated assuming none of the Co and Ni is in the acid-insoluble residue.

CO2 NI2 Co and Ni analyses in ppm. Concentrations calculated with respect to the whole sample, including acid-insoluble residue.

SE Se analyses in ppm. Calculated concentration in the sulphide component of the sample.

SE/S = Se ppm x $10^5$/ S%. S calculated from the known proportion of sulphide in the sample.

DS34 = $\delta S^{34}$. Sulphur isotope analyses performed for Dr. M. Solomon and Mr. R.A. Both by Dr. T.A. Rafter (Institute of Nuclear Sciences, D.S.I.R., New Zealand). Only those analyses are included here which are of samples of specimens analyzed for Co-Ni and/or Se. Precision is usually ± 0.1 per mil.

FT Diamond drillhole footage for core samples.

COMMENT This usually applies to the original specimen, except that quoted analyses are of processed samples, thus:

PS Polished section grain-count analysis (> 400 points). Percentage quoted is percentage of opaque minerals.

XRF X-ray fluorescence spectrograph analysis. Percentage quoted is percentage of total sample.

* preceding a comment : comment applies to all set samples until next comment.

## Compilation

The table was produced on an Elliot 503 computer, using an Algol programme (U938-3) written by B.D. Johnson to the author's specifications. The programme, explanatory flow chart, and original data are filed in the Geology Department, University of Tasmania.

| SAMPLE | MIN | CO1 | NI1 | CO2 | NI2 | CO/NI | SE | SE/S | DS34 | FT | COMMENT |
|---|---|---|---|---|---|---|---|---|---|---|---|
| 1. METAMORPHOSED SILTSTONES, NAIRNE PYRITE MEMBER, BRUKUNGA FORMATION, KANMANTOO GROUP, NAIRNE, SOUTH AUSTRALIA. PRECAMBRIAN. | | | | | | | | | | | |
| 100630A | PY | 100 | 44 | 94 | 41 | 2.29 | | | | | SEGREGATION PARALLELS BEDS |
| 100630B | PY | 94 | 45 | 89 | 43 | 2.07 | | | | | AS ABOVE, ADJACENT |
| 100630C | PY | 106 | 47 | 93 | 41 | 2.26 | | | | | AS ABOVE, ADJACENT |
| 100630D | PY | 161 | 60 | 153 | 57 | 2.69 | | | | | ORIGINAL IN BEDDING |
| 100631A | PY | 105 | 62 | 100 | 59 | 1.70 | | | | | AS ABOVE |
| 100631B | PY | 119 | 61 | 114 | 59 | 1.94 | | | | | AS ABOVE |
| 100631C | PY | 129 | 55 | 123 | 53 | 2.33 | | | | | AS ABOVE |
| 100631D | PY | 86 | 54 | 83 | 51 | 1.61 | | | | | SEGREGATION CUTTING BEDS |
| 100631E | PY | 87 | 52 | 79 | 47 | 1.68 | | | | | SEGREGATION PARALLELS BEDS |
| 100632A | PY | 401 | 96 | 399 | 96 | 4.17 | | | | * | COARSE CROSS-CUTTING VEIN |
| 100632B | PY | 451 | 102 | 444 | 101 | 4.40 | | | | | |
| 100632C | PY | 449 | 112 | 444 | 110 | 4.02 | | | | | |
| 100632D | PY | 441 | 107 | 436 | 106 | 4.13 | | | | | |
| 100632E | PY | 438 | 149 | 420 | 143 | 2.94 | | | | | |
| 100632E | PO-M | 7 | 536 | 7 | 519 | 0.01 | | | | | |
| 100632E | PO-N | 41 | 622 | 41 | 615 | 0.07 | | | | | |
| 100632F | PY | 379 | 288 | 355 | 270 | 1.32 | | | | | |
| 100632F | PO-M | 6 | 598 | 5 | 564 | 0.01 | | | | | |
| 100632F | PO-N | 39 | 714 | 38 | 707 | 0.05 | | | | | |
| 100632G | PY | 478 | 165 | 472 | 163 | 2.89 | | | | | |
| 100632G | PO-M | 111 | 460 | 104 | 432 | 0.24 | | | | | |
| 100632G | PO-N | 9 | 533 | 9 | 513 | 0.02 | | | | | |
| 100633A | PY | 171 | 63 | 160 | 60 | 2.70 | | | | | ORIGINAL IN BEDDING |
| 100633B | PY | 177 | 59 | 166 | 56 | 2.99 | | | | | AS ABOVE |
| 100633C | PY | 17 | 63 | 16 | 59 | 0.27 | | | | | AS ABOVE |
| 100633D | PO | 6 | 314 | 4 | 184 | 0.02 | | | | | SEGREGATION CUTTING BEDS |
| 100634A | PY | 135 | 43 | 116 | 37 | 3.16 | | | | | AS ABOVE |
| 100634B | PY | 99 | 56 | 82 | 47 | 1.75 | | | | | AS ABOVE |
| 100634C | PY | 185 | 72 | 165 | 64 | 2.58 | | | | | ORIGINAL IN BEDDING |
| 2. SILTSTONE, ROCKY CAPE GROUP, COWRIE POINT, N.W.TAS. PRECAMBRIAN. | | | | | | | | | | | |
| 100227 | PY | 28 | 736 | 28 | 718 | 0.04 | | | | | |
| 100593 | PY | 75 | 630 | 73 | 609 | 0.12 | | | | | |
| 100594 | PY | 32 | 377 | 31 | 369 | 0.08 | | | | | |

| SAMPLE | MIN | CO1 | NI1 | CO2 | NI2 | CO/NI | SE | SE/S | DS34 | FT | COMMENT |
|---|---|---|---|---|---|---|---|---|---|---|---|
| 100595 | PY | 37 | 534 | 36 | 520 | 0.07 | | | | | |
| 100596 | PY | 49 | 598 | 47 | 579 | 0.08 | | | | | |
| 100597 | PY | 104 | 629 | 97 | 590 | 0.16 | | | | | |
| 100598 | PY | 81 | 724 | 74 | 665 | 0.11 | 41 | 7.68 | | | |
| 3. SILTSTONE, ROCKY CAPE GROUP, FORESTRY RD. BRIDGE ACROSS ARTHUR RIVER, NEAR SAVAGE RIVER PIPELINE, 16 ML. S. OF SET 2. PRECAMBRIAN. | | | | | | | | | | | |
| 100642 | PY | 18 | 505 | 14 | 404 | 0.04 | 61 | 11.42 | | | |
| 100643 | PY | 61 | 674 | 58 | 649 | 0.09 | | | | | |
| 4. SILTSTONE, SHALE AND SANDSTONE, FRANKLIN RIVER, 2.5 ML. FROM ESTUARY (PORT SORELL). PRECAMB. | | | | | | | | | | | |
| 100639 | PY | 1398 | 924 | 1304 | 863 | 1.51 | | | | | COARSE SILTST. AND SANDST. |
| 100640 | PY | 1561 | 996 | 1453 | 927 | 1.57 | | | | | DARK GREY SILTSTONE |
| 100641 | PY | 1004 | 829 | 954 | 788 | 1.21 | | | | | FINE KHAKI SILTSTONE |
| 5. SLATE, HERCULES MINE, WILLIAMSFORD, 4 ML. S. OF ROSEBERY. CAMBRIAN(?). | | | | | | | | | | | |
| 33886A | PY | | | | | | | | + 1.6 | | |
| 33886B | PY | | | | | | | | + 8.7 | | |
| 33886C | PY | 15 | 443 | 15 | 425 | 0.03 | 19 | 3.56 | | | |
| 6. HANGINGWALL DARK GREY SHALE, ROSEBERY MINE, 12 LEVEL, P14N CROSSCUT E, 1400N, 770-1020E, RL 70. CAMBRIAN(?). | | | | | | | | | | | |
| 100402 | PY | 418 | 517 | 399 | 494 | 0.81 | | | | | |
| 100402 | PO | 29 | 1067 | 26 | 954 | 0.03 | | | | | |
| 100469 | PY | 407 | 654 | 368 | 592 | 0.62 | | | | | |
| 100521A | PY | 222 | 580 | 130 | 338 | 0.38 | 34 | 6.37 | | | |
| 100521B | PY | 266 | 699 | 143 | 376 | 0.38 | | | | | |
| 100522 | PY | 263 | 333 | 228 | 288 | 0.79 | | | | | |
| 7. SERICITIZED HOST ROCK SHALE OF ROSEBERY BANDED PB-ZN-CU OREBODY. CAMBRIAN(?). | | | | | | | | | | | |
| 100529 | PY | 31 | 304 | 17 | 167 | 0.10 | | | | | 780S 750E RL 9945 13 LEVEL F LENS |
| 100628 | PY | 294 | 688 | 183 | 428 | 0.43 | | | | | DDH R1680 818 FT 1595N 1650E RL 9590 |
| 100629 | PY | 8 | 65 | 3 | 29 | 0.12 | | | | | DDH R1680 828 FT 1595N 1650E RL 9590 |

| SAMPLE | MIN | CO1 | NI1 | CO2 | NI2 | CO/NI | SE | SE/S | DS34 | FT | COMMENT |
|---|---|---|---|---|---|---|---|---|---|---|---|
| 8. FARRELL SLATE, NEW NORTH MT. FARRELL MINE, TULLAH. CAMBRIAN(?). | | | | | | | | | | | |
| 100644 | PY | 605 | 1585 | 581 | 1521 | 0.38 | | | | | |
| 9. MUNRO CREEK SLATE AND QUARTZITE, ROSEBERY SERIES, MURCHISON HIGHWAY, ROSEBERY. CAMBRIAN(?). | | | | | | | | | | | |
| 100396 | PY | 211 | 600 | 206 | 584 | 0.35 | | | | | |
| 100397 | PY | 257 | 775 | 234 | 706 | 0.33 | | | | | |
| 10. CROSS-BEDDED SANDSTONE ADJACENT TO SET 71, A.P.P.M. ROAD, VALENTINES PEAK. CAMBRIAN(?). | | | | | | | | | | | |
| 100733 | PY | 77 | 207 | 64 | 173 | 0.37 | | | | | |
| 11. BLACK CARBONACEOUS SHALE, BRANCH CREEK, E. OF PORT SORELL. CAMBRIAN(?). | | | | | | | | | | | |
| 100590 | PY | 11 | 27 | 11 | 26 | 0.41 | | | | | COMB STRUCTURE IN JOINTS |
| 100591 | PY | 15 | 30 | 14 | 29 | 0.49 | | | | | VERY FINE, IN BEDDING |
| 100592 | PY | 9 | 20 | 9 | 19 | 0.46 | 13 | 2.43 | | | AS ABOVE |
| 12. DARK GREY SILTSTONE, MURCHISON HIGHWAY BRIDGE ACROSS QUE RIVER. UPPER MIDDLE CAMBRIAN. | | | | | | | | | | | |
| 100322 | PY | 63 | 386 | 59 | 360 | 0.16 | | | | | |
| 100326 | PY | 54 | 348 | 51 | 329 | 0.16 | 94 | 17.60 | | | |
| 100328 | PY | 48 | 307 | 46 | 295 | 0.16 | | | | | |
| 100329 | PY | 33 | 222 | 32 | 213 | 0.15 | 83 | 15.54 | | | |
| 100330 | PY | | | | | | 70 | 13.11 | | | |
| 100331 | PY | | | | | | 77 | 14.42 | | | |
| 100332 | PY | 53 | 346 | 51 | 331 | 0.15 | | | | | |
| 100333 | PY | 75 | 233 | 72 | 225 | 0.32 | | | | | |
| 100334 | PY | 62 | 362 | 59 | 346 | 0.17 | | | | | |
| 100335 | PY | 85 | 282 | 82 | 273 | 0.30 | | | | | |
| 100336 | PY | 104 | 392 | 102 | 383 | 0.27 | | | | | |
| 13. GORDON LIMESTONE, LYELL HIGHWAY, LINDA, NEAR GORMANSTON. ORDOVICIAN. | | | | | | | | | | | |
| 100458 | PY | 23 | 111 | 21 | 103 | 0.20 | 0 | 0.0 | | | |
| 14. WOODY ISLAND SILTSTONE, PERMIAN. | | | | | | | | | | | |
| 100231 | PY | 52 | 150 | 46 | 132 | 0.35 | | | | | FLORENTINE VALLEY |
| 100587A | PY | 171 | 391 | 143 | 328 | 0.44 | 90 | 16.85 | | | WOODY ISLAND |
| 100587B | PY | 108 | 303 | 84 | 237 | 0.36 | | | | | WOODY ISLAND |

| SAMPLE | MIN | CO1 | NI1 | CO2 | NI2 | CO/NI | SE | SE/S | DS34 | FT | COMMENT |
|---|---|---|---|---|---|---|---|---|---|---|---|
| 100588 | PY | 25 | 128 | 21 | 111 | 0.19 | | | | | WOODY ISLAND |
| 100589 | PY | 66 | 190 | 48 | 137 | 0.35 | 33 | 6.18 | | | WOODY ISLAND |
| 15. UNCONSOLIDATED DEEP-LEAD NON-MARINE GRAVEL, ENDURANCE TIN MINE, SOUTH MT. CAMERON. MIDDLE TERTIARY. | | | | | | | | | | | |
| 100584 | PY | 57 | 17 | 54 | 16 | 3.42 | | | | | |
| 16. UNCONSOLIDATED MARINE SANDS, BENEATH GREAT MUSSELROE BAY, N.E. TAS. PLEISTOCENE OR RECENT. | | | | | | | | | | | |
| 100459 | PY | 5 | 146 | 3 | 96 | 0.03 | 28 | 5.24 | | | |
| 100460 | PY | 4 | 67 | 4 | 56 | 0.07 | | | | | |
| 100461 | PY | 6 | 113 | 4 | 81 | 0.05 | 31 | 5.81 | | | |
| 100462 | PY | 6 | 134 | 4 | 83 | 0.05 | | | | | |
| 100463 | PY | 5 | 131 | 3 | 84 | 0.04 | | | | | |
| 100464 | PY | 6 | 125 | 3 | 71 | 0.05 | | | | | |
| 17. BASE OF RAISED BEACH, NEAR NARACOOPA, KING ISLAND. PLEISTOCENE OR RECENT. | | | | | | | | | | | |
| 100233 | PY | 15 | 103 | 13 | 91 | 0.15 | | | | | |
| 18. PYRITIC MAGNETITE ORE IN PRECAMBRIAN AMPHIBOLITE, SAVAGE RIVER. MINERAL CONCENTRATES 100% PURE (PS). | | | | | | | | | | | |
| 100621 | PY | 1266 | 1394 | 1229 | 1353 | 0.91 | | | | | * 22900N 21370E RL 1030 |
| 100621 | MG | 39 | 768 | 38 | 740 | 0.05 | | | | | |
| 100622A | PY | 1093 | 1257 | 1083 | 1245 | 0.87 | | | | | |
| 100622A | MG | 36 | 1607 | 35 | 1564 | 0.02 | | | | | |
| 100622B | PY | 1155 | 1118 | 1146 | 1109 | 1.03 | | | | | |
| 100622B | MG | 29 | 1388 | 29 | 1360 | 0.02 | | | | | |
| 100662 | PY | 2180 | 2495 | 2176 | 2490 | 0.87 | 63 | 11.80 | | | * 23560N 21180E RL 1070 |
| 100662 | MG | 20 | 370 | 19 | 362 | 0.05 | | | | | |
| 100663 | PY | 2582 | 763 | 2577 | 761 | 3.39 | | | | | |
| 100663 | MG | 33 | 514 | 33 | 509 | 0.06 | | | | | |
| 100664 | PY | 2067 | 2715 | 2059 | 2704 | 0.76 | | | | | |
| 100664 | MG | 21 | 226 | 21 | 222 | 0.09 | | | | | |
| 100665 | PY | 2549 | 2564 | 2522 | 2536 | 0.99 | 20 | 3.75 | | | |
| 100665 | MG | 36 | 277 | 35 | 270 | 0.13 | | | | | |
| 100666 | PY | 2118 | 921 | 2083 | 906 | 2.30 | 24 | 4.49 | | | * 23110N 21370E RL 1030 |
| 100666 | MG | 33 | 612 | 32 | 588 | 0.05 | | | | | |

| SAMPLE | MIN | CO1 | NI1 | CO2 | NI2 | CO/NI | SE | SE/S | DS34 | FT | COMMENT |
|---|---|---|---|---|---|---|---|---|---|---|---|
| 100667 | PY | 2026 | 2087 | 2023 | 2083 | 0.97 | 29 | 5.43 | | | |
| 100667 | MG | 27 | 380 | 27 | 371 | 0.07 | | | | | |
| 100668 | PY | 2061 | 1122 | 2031 | 1106 | 1.84 | 54 | 10.11 | | | |
| 100668 | MG | 37 | 773 | 34 | 718 | 0.05 | | | | | |
| 100669 | PY | 1931 | 832 | 1905 | 821 | 2.32 | | | | | |
| 100669 | MG | 28 | 583 | 27 | 563 | 0.05 | | | | | |
| 19. PENTLANDITE-PYRRHOTITE ORE ASSOCIATED WITH THE CAMBRIAN SERPENTINE HILL ULTRAMAFIC COMPLEX, CUNI, FIVE MILES FROM ZEEHAN. TASMANIAN MINES DEPT. DRILLCORE. | | | | | | | | | | | |
| 100658A | ORE | 1938 | 53205 | 1857 | 50968 | 0.04 | 165 | | * | 42 | DDH M15, VANDEAU SECTION |
| 100658B | ORE | 1871 | 52442 | 1764 | 49429 | 0.04 | | | | | |
| 100659A | ORE | 2170 | 61424 | 1895 | 53658 | 0.04 | 159 | | * | 42 | DDH M15, VANDEAU SECTION |
| 100659B | ORE | 2119 | 58549 | 1783 | 49264 | 0.04 | | | | | |
| 100660A | ORE | 2342 | 68696 | 2004 | 58784 | 0.03 | 188 | | * | 53 | DDH M19 |
| 100660B | ORE | 2345 | 61448 | 2086 | 54682 | 0.04 | | | | | |
| 20. NODULE IN AMYGDALOIDAL CAMBRIAN SPILITE, BALD HILL COMPLEX, MT. STEWART TRACK, HALF MILE SOUTH OF CORINNA ROAD. | | | | | | | | | | | |
| 100674 | PY | 324 | 155 | 259 | 124 | 2.09 | | | | | TEXTURE SUGGESTS GREW FROM CENTRAL NUCLEUS |
| 21. MAGNETITE ASSOCIATED WITH THE CAMBRIAN MCIVOR HILL GABBRO, FIVE MILES WEST OF ZEEHAN. TENTH LEGION DEPOSIT. TASMANIAN MINES DEPT. DRILLCORE. | | | | | | | | | | | |
| 100661A | MG | 28 | 352 | 23 | 297 | 0.08 | | | | | |
| 100661B | MG | 25 | 74 | 22 | 66 | 0.33 | | | | | |
| 22. DISSEMINATIONS IN THE CAMBRIAN MURCHISON GRANITE, TULLAH. H.E.C. DRILLCORE. | | | | | | | | | | | |
| 11211A | PY | | | | | | | | + 8.1 | 635 | DDH 6630 |
| 11211B | PY | | | | | | | | + 7.9 | 635 | DDH 6630 |
| 11211C | PY | 21 | 26 | 20 | 24 | 0.83 | 20 | 3.75 | | 204 | DDH 6639 |
| 11212 | PY | 90 | 55 | 84 | 52 | 1.64 | 23 | 4.31 | + 8.6 | 204 | DDH 6639 |
| 100409 | PY | 382 | 58 | 355 | 54 | 6.56 | | | | 607 | DDH 6627 |
| 100451 | PY | 57 | 43 | 51 | 38 | 1.33 | | | | 235 | DDH 6630 |
| 100452 | PY | 72 | 38 | 66 | 35 | 1.91 | 8 | 1.50 | | 235 | DDH 6630 |
| 100453 | PY | 216 | 80 | 187 | 70 | 2.69 | | | | 12 | DDH 6630 |
| 100454 | PY | 251 | 50 | 227 | 45 | 5.00 | | | | 7 | DDH 6630 |
| 100455 | PY | 96 | 37 | 90 | 35 | 2.60 | | | | 204 | DDH 6639 |

| SAMPLE | MIN | CO1 | NI1 | CO2 | NI2 | CO/NI | SE | SE/S | DS34 | FT | COMMENT |
|---|---|---|---|---|---|---|---|---|---|---|---|
| 23. PYRITE-HEMATITE VEINS, POWERFUL MINE, CAMBRIAN DOVE GRANITE, LORINNA. | | | | | | | | | | | |
| 100353 | PY | 7791 | 674 | 7472 | 647 | 11.55 | 29 | 5.43 | | | |
| 100353 | HM | 12 | 29 | 10 | 24 | 0.41 | | | | | |
| 100599 | PY | 7672 | 726 | 7534 | 713 | 10.57 | 13 | 2.43 | | | |
| 100599 | HM | 4 | 7 | 3 | 5 | 0.53 | | | | | |
| 100600 | PY | 8749 | 698 | 8632 | 689 | 12.53 | 27 | 5.06 | | | |
| 100600 | HM | 9 | 10 | 6 | 7 | 0.90 | | | | | |
| 24. PYRITE-HEMATITE-CHALCOPYRITE VEIN, PENDERS PROSPECT, CAMBRIAN VOLCANICS, TWO ML. N. OF LOW ROCKY POINT, S.W. TAS. | | | | | | | | | | | |
| 100470 | PY | 723 | 12 | 685 | 12 | 58.01 | 33 | 6.18 | | | |
| 100471A | PY | 747 | 6 | 736 | 6 | 129.47 | | | | | |
| 100471B | PY | 678 | 7 | 652 | 7 | 94.86 | 44 | 8.24 | | | |
| 100471C | PY | 808 | 5 | 802 | 5 | 153.37 | | | | | |
| 100471D | PY | 857 | 305 | 846 | 301 | 2.81 | | | | | |
| 100471D | HM | 18 | 18 | 17 | 17 | 1.00 | | | | | |
| 100831 | PY | 927 | 59 | 922 | 59 | 15.76 | | | | | |
| 100831 | HM | 18 | 43 | 18 | 41 | 0.43 | | | | | |
| 25. DISSEMINATED MINERALIZATION IN CAMBRIAN (?) MOUNT READ VOLCANICS. FOOTWALL OF ROSEBERY MINE. DRILLHOLES AND CROSSCUT. | | | | | | | | | | | |
| 33952 | PY | 205 | 9 | 163 | 7 | 23.76 | 16 | 3.00 | +12.1 | 918 | DDH R1452 |
| 100552 | PY | 44 | 4 | 38 | 4 | 9.98 | | | | 1184 | DDH R1440 |
| 100553 | PY | 73 | 14 | 71 | 14 | 5.27 | 14 | 2.62 | | 1185 | DDH R1440 |
| 100554 | PY | 185 | 11 | 179 | 10 | 17.23 | 19 | 3.56 | | 1263 | DDH R1440 |
| 100555 | PY | 239 | 3 | 228 | 3 | 70.90 | | | | 1273 | DDH R1440 |
| 100556 | PY | 501 | 2 | 464 | 2 | 237.97 | | | | 920 | DDH R1452 |
| 100708 | PY | 7 | 7 | 7 | 6 | 1.14 | | | | 60 | DDH R1254 |
| 100709 | PY | 26 | 3 | 25 | 3 | 7.90 | | | | 68 | DDH R1254 |
| 100710 | PY | 70 | 14 | 68 | 13 | 5.07 | | | | | 14 LEVEL 760S 730E RL 9820 |
| 26. VEIN IN CAMBRIAN(?) MOUNT READ VOLCANICS, HANGINGWALL OF ROSEBERY MINE. 14 LEVEL, D5N N DRIVE, 910N 2173E RL 9825. | | | | | | | | | | | |
| 33955 | PY | 1172 | 103 | 1055 | 93 | 11.38 | | | +16.1 | | |
| 27. CUBES FROM DUMP, PHAR LAP PROSPECT, 200 YD. S.W. OF LONG TUNNEL PORTAL, CENTRAL WORKINGS, FEDERATION MINE, HEEMSKIRK GRANITE. DEVONIAN. | | | | | | | | | | | |
| 100379 | PY | 8 | 14 | 5 | 9 | 0.56 | | | | | * WHITE SERIES GRANITE |
| 100380 | PY | 11 | 7 | 11 | 7 | 1.65 | 26 | 4.87 | | | |

| SAMPLE | MIN | CO1 | NI1 | CO2 | NI2 | CO/NI | SE | SE/S | DS34 | FT | COMMENT |
|---|---|---|---|---|---|---|---|---|---|---|---|
| 100382 | PY | 4 | 5 | 4 | 5 | 0.96 | | | | | |
| 100390 | PY | 6 | 25 | 6 | 24 | 0.25 | | | | | |
| 100391 | PY | 5 | 6 | 5 | 6 | 0.87 | 19 | 3.56 | | | |
| 100392 | PY | | | | | | 21 | 3.93 | | | |
| 100393 | PY | 5 | 47 | 5 | 47 | 0.11 | | | | | |
| 100394 | PY | 7 | 17 | 7 | 17 | 0.41 | | | | | |
| 100395 | PY | 7 | 6 | 7 | 6 | 1.16 | | | | | |
| 100407 | PY | 7 | 7 | 6 | 6 | 1.04 | | | | | |
| 28. IN LODES IN HEEMSKIRK GRANITE. DEVONIAN. | | | | | | | | | | | |
| 11232 | PY | 56 | 4 | 51 | 4 | 13.32 | | | + 7.2 | | * WHITE SERIES GRANITE |
| 100466 | PY | 0 | 5 | 0 | 4 | 0.0 | 28 | 5.24 | | | |
| 100467 | PY | 17 | 7 | 16 | 6 | 2.61 | 26 | 4.87 | +13.9 | | * RED SERIES GRANITE |
| 100468 | PY | 22 | 7 | 19 | 6 | 3.02 | 12 | 2.25 | | | |
| 29. IN PORPHYRY DYKE, BROWN FACE, MT. BISCHOFF OPEN CUT. DEVONIAN. | | | | | | | | | | | |
| 100576B | PO | 10 | 13 | 8 | 11 | 0.76 | | | | | |
| 100577B | PO | 13 | 11 | 11 | 9 | 1.17 | | | | | |
| 30. WHITE FACE PORPHYRY DYKE. MT. BISCHOFF OPEN CUT. DEVONIAN. | | | | | | | | | | | |
| 100256 | PY | 3 | 9 | 3 | 9 | 0.36 | | | | | * IN ELUVIAL GRAVEL, |
| 100257 | PY | 6 | 28 | 6 | 28 | 0.22 | 14 | 2.62 | | | WHITE FACE |
| 100258 | PY | 3 | 10 | 3 | 10 | 0.35 | | | | | |
| 100259 | PY | 3 | 12 | 3 | 12 | 0.28 | | | | | |
| 100260 | PY | | | | | | 27 | 5.06 | | | |
| 100261 | PY | 4 | 16 | 4 | 16 | 0.27 | | | | | |
| 100263 | PY | 3 | 10 | 3 | 10 | 0.26 | | | | | |
| 100264 | PY | 4 | 14 | 4 | 14 | 0.29 | | | | | |
| 100265 | PY | 2 | 8 | 2 | 8 | 0.20 | 20 | 3.75 | | | |
| 100266 | PY | 1 | 8 | 1 | 8 | 0.06 | | | | | |
| 100271 | PY | 6 | 14 | 6 | 14 | 0.41 | 16 | 3.00 | | | |
| 100272 | PY | 3 | 16 | 3 | 16 | 0.20 | | | | | |
| 100273 | PY | 3 | 9 | 3 | 9 | 0.28 | | | | | |
| 1413 | PO | 11 | 14 | 10 | 13 | 0.79 | | | | | * IN WHITE FACE DYKE |

| SAMPLE | MIN | LCO1 | LNI1 | LCO2 | LNI2 | NI/CO | FR | WT1 | WT2 | PREPARATION |
|---|---|---|---|---|---|---|---|---|---|---|
| 100382 | PY | 0.65 | 0.67 | 0.65 | 0.66 | 1.04 | 1 | 10 | | IA |
| 100390 | PY | 0.79 | 1.40 | 0.78 | 1.39 | 4.08 | 6 | 10 | | IA |
| 100391 | PY | 0.73 | 0.80 | 0.73 | 0.79 | 1.15 | 2 | 10 | | IA |
| 100932 | PY | | | | | | 6 | 10 | | IA |
| 100393 | PY | 0.71 | 1.67 | 0.70 | 1.67 | 9.28 | 6 | 10 | | IA |
| 100394 | PY | 0.85 | 1.23 | 0.84 | 1.22 | 2.42 | 6 | 10 | | IA |
| 100395 | PY | 0.87 | 0.81 | 0.87 | 0.81 | 0.86 | 3 | 10 | | IA |
| 100407 | PY | 0.85 | 0.84 | 0.81 | 0.79 | 0.96 | 5 | 10 | | IA |
| 28. IN LODES IN HEEMSKIRK GRANITE. DEVONIAN. | | | | | | | | | | |
| 11232 | PY | 1.75 | 0.62 | 1.71 | 0.59 | 0.08 | M | MH | | DNMA |
| 100466 | PY | - | 0.69 | - | 0.58 | - | 2 | 2H | | DNMA |
| 100467 | PY | 1.23 | 0.82 | 1.22 | 0.80 | 0.38 | 1 | H | | DNMFA |
| 100468 | PY | 1.33 | 0.85 | 1.28 | 0.80 | 0.33 | 1 | H | | DNMFA |
| 29. IN PORPHYRY DYKE, BROWN FACE, MT. BISCHOFF OPEN CUT. DEVONIAN. | | | | | | | | | | |
| 100576B | PO | 1.00 | 1.12 | 0.93 | 1.05 | 1.32 | M | 3000 | | DNMFA |
| 100577B | PO | 1.10 | 1.03 | 1.04 | 0.97 | 0.85 | M | 3000 | | DNMFA |
| 30. WHITE FACE PORPHYRY DYKE, MT. BISCHOFF OPEN CUT. DEVONIAN. | | | | | | | | | | |
| 100256 | PY | 0.52 | 0.97 | 0.52 | 0.97 | 2.80 | 1 | 90 | | NDEN |
| 100257 | PY | 0.79 | 1.44 | 0.79 | 1.44 | 4.50 | 1 | 50 | | NDEN |
| 100258 | PY | 0.53 | 0.98 | 0.53 | 0.98 | 2.84 | 1 | 40 | | NDEN |
| 100259 | PY | 0.53 | 1.08 | 0.53 | 1.07 | 3.52 | 1 | 30 | | NDEN |
| 100260 | PY | | | | | | 1 | 30 | | NDEN |
| 100261 | PY | 0.65 | 1.21 | 0.65 | 1.21 | 3.67 | 1 | 30 | | NDEN |
| 100263 | PY | 0.41 | 0.99 | 0.41 | 0.99 | 3.83 | 1 | 20 | | NDEN |
| 100264 | PY | 0.62 | 1.16 | 0.62 | 1.16 | 3.49 | 1 | 20 | | NDEN |
| 100265 | PY | 0.21 | 0.91 | 0.21 | 0.91 | 5.00 | 1 | 15 | | NDEN |
| 100266 | PY | 0.00 | 0.92 | 0.00 | 0.92 | 15.91 | 1 | 15 | | NDEN |
| 100271 | PY | 0.76 | 1.15 | 0.76 | 1.15 | 2.44 | 1 | 12 | | NDEN |
| 100272 | PY | 0.50 | 1.19 | 0.49 | 1.19 | 4.98 | 1 | 12 | | NDEN |
| 100273 | PY | 0.42 | 0.96 | 0.41 | 0.96 | 3.51 | 1 | 12 | | NDEN |
| 1413 | PO | 1.04 | 1.14 | 1.01 | 1.11 | 1.26 | 1 | | 1 | ILI*** |

| SAMPLE | MIN | CO1 | NI1 | CO2 | NI2 | CO/NI | SE | SE/S | DS34 | FT | COMMENT |
|---|---|---|---|---|---|---|---|---|---|---|---|
| 1435 | PO | 0 | 74 | 0 | 64 | 0.0 | | | | | |
| 31. CUBES IN NORTH-EASTERN PORPHYRY DYKE, NORTH VALLEY ROAD, MT. BISCHOFF. DEVONIAN. | | | | | | | | | | | |
| 100237 | PY | 2 | 5 | 2 | 5 | 0.46 | 18 | 3.37 | | | |
| 100241 | PY | 2 | 8 | 2 | 8 | 0.28 | | | | | |
| 100242 | PY | 5 | 17 | 4 | 16 | 0.28 | | | | | |
| 100243 | PY | 1 | 6 | 1 | 6 | 0.19 | | | | | |
| 100244 | PY | 6 | 19 | 5 | 18 | 0.29 | 12 | 2.25 | | | |
| 100245 | PY | 3 | 7 | 3 | 7 | 0.42 | 33 | 6.18 | | | |
| 100248 | PY | 3 | 11 | 3 | 10 | 0.30 | | | | | |
| 100249 | PY | 3 | 9 | 3 | 8 | 0.36 | | | | | |
| 100251 | PY | 4 | 25 | 4 | 23 | 0.16 | | | | | |
| 100252 | PY | 5 | 11 | 4 | 10 | 0.41 | | | | | |
| 100254 | PY | | | | | | 13 | 2.43 | | | |
| 32. MASSIVE, REPLACING DOLOMITE, BROWN FACE, MT. BISCHOFF OPEN CUT. DEVONIAN. | | | | | | | | | | | |
| 100060B | PO | 20 | 7 | 18 | 6 | 2.99 | | | | | |
| 100061 | PO | 1 | 11 | 1 | 10 | 0.12 | | | | | |
| 100143 | PO | 14 | 7 | 11 | 6 | 1.87 | | | | | |
| 100573 | PO | 3 | 5 | 3 | 5 | 0.59 | | | | | |
| 100574 | PO | 3 | 6 | 3 | 5 | 0.54 | 18 | 4.56 | | | SE IN DUPLICATE |
| 100575 | PO | 7 | 10 | 6 | 8 | 0.69 | | | | | |
| 33. MASSIVE, REPLACING DOLOMITE, SLAUGHTERYARD FACE, MT. BISCHOFF OPEN CUT. DEVONIAN. | | | | | | | | | | | |
| 100062 | PO | | | | | | 20 | 5.10 | | | |
| 100063 | PO | 21 | 6 | 20 | 5 | 3.74 | | | | | |
| 100064 | PO | | | | | | 0 | 0.0 | | | |
| 100066 | PO | 7 | 8 | 6 | 7 | 0.87 | | | | | |
| 100067A | PO | 7 | 15 | 5 | 13 | 0.42 | | | | | |
| 100067B | PO | 1 | 5 | 1 | 5 | 0.25 | | | | | |
| 34. POSSIBLY MIXED REPLACEMENT-VEIN SYSTEM, AND SECONDARY PYRITE, SLAUGHTERYARD LODE, MT. BISCHOFF OPEN CUT. DEVONIAN. | | | | | | | | | | | |
| 100136A | ASPY | 107 | 13 | 106 | 12 | 8.53 | | | | | * SAMPLED WITHIN 1 INCH |
| 100136B | ASPY | 114 | 7 | 113 | 7 | 16.47 | | | | | |

| SAMPLE | MIN | CO1 | NI1 | CO2 | NI2 | CO/NI | SE | SE/S | DS34 | FT | COMMENT |
|---|---|---|---|---|---|---|---|---|---|---|---|
| 100136C | PY | 7 | 47 | 6 | 46 | 0.14 | | | | | |
| 100136D | PY | 8 | 4 | 8 | 4 | 1.89 | | | | | |
| 100140A | PO | 1 | 10 | 1 | 10 | 0.06 | | | | | |
| 100140B | PO | 1 | 2 | 1 | 2 | 0.25 | | | | | |
| 100578 | PY | 6 | 17 | 5 | 14 | 0.34 | | | | | * SECONDARY IN VUGS |
| 100579 | PY | 16 | 42 | 14 | 37 | 0.38 | 16 | 3.00 | | | |
| 100580 | PY | 6 | 31 | 5 | 29 | 0.18 | 32 | 5.99 | | | |
| 35. MASSIVE, REPLACING DOLOMITE, GREISEN FACE, MT. BISCHOFF OPEN CUT. DEVONIAN. | | | | | | | | | | | |
| 100070 | PO | 18 | 5 | 18 | 5 | 3.38 | | | | | * SURFACE SAMPLES |
| 100071 | PO | 21 | 5 | 21 | 5 | 4.35 | | | | | |
| 100073A | PO | 15 | 28 | 15 | 28 | 0.55 | | | | | |
| 100073B | PO | | | | | | 18 | 4.56 | | | |
| 100074A | PO | 9 | 9 | 8 | 8 | 1.01 | | | | | |
| 100074B | PO | | | | | | 34 | 8.61 | | | |
| 100075 | PO | | | | | | 31 | 7.85 | | | |
| 100124 | PO | 29 | 18 | 28 | 18 | 1.61 | | | | 174 | DDH NO. 3 |
| 100125 | PO | 5 | 6 | 4 | 6 | 0.78 | | | | 110 | DDH B9 |
| 36. MASSIVE, REPLACING DOLOMITE, PIG FLAT, MT. BISCHOFF OPEN CUT. DEVONIAN. | | | | | | | | | | | |
| 100076 | PO | | | | | | 11 | 2.78 | | | |
| 100077A | PO | 4 | 20 | 4 | 20 | 0.21 | | | | | |
| 100077B | PO | | | | | | 9 | 2.28 | | | |
| 100080 | PO | 1 | 26 | 1 | 26 | 0.03 | | | | | |
| 100081 | PO | 4 | 5 | 4 | 5 | 0.76 | | | | | |
| 100083A | PO | 2 | 5 | 1 | 5 | 0.29 | | | | | |
| 100083B | PO | | | | | | 18 | 4.57 | | | |
| 100141 | PO | 11 | 11 | 11 | 11 | 1.02 | | | | | |
| 37. MASSIVE, REPLACING DOLOMITE, SOUTH END, MT. BISCHOFF OPEN CUT. DEVONIAN. | | | | | | | | | | | |
| 100011A | PY | 16 | 13 | 14 | 12 | 1.18 | | | | | |
| 100011B | SL | | | | | | 17 | 5.15 | | | |
| 100012A | PY | 11 | 13 | 11 | 13 | 0.85 | | | | | |
| 100012B | SL | | | | | | 14 | 4.24 | | | |

| SAMPLE | MIN | CO1 | NI1 | CO2 | NI2 | CO/NI | SE | SE/S | DS34 | FT | COMMENT |
|---|---|---|---|---|---|---|---|---|---|---|---|
| 100146 | PY | 1 | 5 | 1 | 5 | 0.23 | | | | | |
| 100152 | PY | 6 | 5 | 6 | 5 | 1.09 | | | | | |
| 38. MASSIVE, PROBABLY MIXED REPLACEMENT-VEIN SYSTEM, HAPPY VALLEY, MT. BISCHOFF OPEN CUT. DEVONIAN. | | | | | | | | | | | |
| 100679 | PY | 13 | 16 | 13 | 16 | 0.81 | | | | | |
| 100680 | PY | 6 | 20 | 6 | 20 | 0.32 | | | | | |
| 100681A | PO | 2 | 25 | 2 | 25 | 0.09 | | | | | |
| 100681B | PY | 210 | 43 | 209 | 43 | 4.88 | | | | | |
| 100681B | PO | 2 | 13 | 2 | 13 | 0.17 | | | | | |
| 100682 | PY | 14 | 44 | 14 | 44 | 0.32 | | | | | |
| 100682 | PO | 1 | 11 | 1 | 11 | 0.10 | | | | | |
| 39. VEINS, IN DRILLHOLES, BROWN FACE, MT. BISCHOFF OPEN CUT. DEVONIAN. | | | | | | | | | | | |
| 100795A | PO | 2 | 75 | 2 | 73 | 0.02 | | | | 270 | DDH B50 |
| 100795B | PO | 4 | 82 | 4 | 82 | 0.05 | | | | | |
| 100796 | PO | 22 | 56 | 21 | 52 | 0.40 | | | | 270 | DDH B50 |
| 100798A | ASPY | 209 | 134 | 205 | 131 | 1.56 | | | | 60 | DDH B52 |
| 100798B | ASPY | 207 | 137 | 204 | 135 | 1.51 | | | | | |
| 100813A | PY | 18 | 28 | 17 | 28 | 0.62 | | | | | DDH B57 |
| 100813B | PY | 14 | 26 | 14 | 25 | 0.54 | | | | | |
| 40. VEINS IN PORPHYRY (CF. SET 29), BROWN FACE, MT. BISCHOFF OPEN CUT. DEVONIAN. | | | | | | | | | | | |
| 100576A | PY | 11 | 51 | 11 | 48 | 0.22 | 23 | 5.82 | | | |
| 100577A | PY | 10 | 46 | 9 | 44 | 0.21 | | | | | |
| 41. VEIN IN WHITE FACE PORPHYRY DYKE, IN GREISEN FACE DRILLHOLE, MT. BISCHOFF OPEN CUT. DEVONIAN. | | | | | | | | | | | |
| 100126 | PY | 13 | 8 | 13 | 8 | 1.65 | | | | 589 | DDH B9 |
| 42. VEIN, IN DRILLHOLE, GREISEN FACE, MT. BISCHOFF OPEN CUT. DEVONIAN. | | | | | | | | | | | |
| 100127A | PO | 7 | 92 | 7 | 92 | 0.08 | | | | 723 | DDH B9 |
| 100127B | PO | 7 | 109 | 7 | 108 | 0.07 | | | | | |
| 100127C | PO | 5 | 71 | 5 | 69 | 0.07 | | | | | |
| 100127D | PO | 9 | 87 | 9 | 85 | 0.11 | | | | | |

| SAMPLE | MIN | CO1 | NI1 | CO2 | NI2 | CO/NI | SE | SE/S | DS34 | FT | COMMENT |
|---|---|---|---|---|---|---|---|---|---|---|---|
| 43. VEIN, GIBLIN LODE, SW. CORNER, MT. BISCHOFF OPEN CUT. DEVONIAN. | | | | | | | | | | | |
| 100703 | PY | 82 | 168 | 79 | 161 | 0.49 | | | | | |
| 100704 | PY | 73 | 142 | 72 | 139 | 0.52 | | | | | |
| 44. VEIN, IN DRILLHOLE, NEAR DON HILL, S. OF MT. BISCHOFF OPEN CUT. DEVONIAN. | | | | | | | | | | | |
| 100793A | PY | 4 | 15 | 4 | 15 | 0.26 | | | | | |
| 100793B | PY | 5 | 15 | 5 | 15 | 0.33 | | | | | |
| 45. VEIN, THOMPSONS LODE, SW. OF MT. BISCHOFF OPEN CUT. DEVONIAN. | | | | | | | | | | | |
| 100017 | SL | | | | | | 11 | 3.33 | | | DISSEMINATED IN CARBONATE |
| 46. VEIN, ANTIMONIAL LODE, TINSTONE CREEK, SW. OF MT. BISCHOFF OPEN CUT. DEVONIAN. | | | | | | | | | | | |
| 100027 | SL | | | | | | 22 | 6.67 | | | MASSIVE |
| 100028 | SL | | | | | | 0 | 0.0 | | | MASSIVE |
| 100705 | PY | 2 | 9 | 2 | 9 | 0.25 | | | | | |
| 100706 | PY | 3 | 9 | 3 | 8 | 0.41 | | | | | |
| 100707 | PY | 3 | 4 | 3 | 4 | 0.76 | | | | | |
| 47.VEIN, SILVER CLIFFS MINE, W. OF MT. BISCHOFF OPEN CUT. DEVONIAN. | | | | | | | | | | | |
| 100029 | SL | | | | | | 9 | 2.27 | | | |
| 100030 | SL | | | | | | 9 | 2.27 | | | |
| 48. VEIN, FOOKS LODE, SE. OF MT. BISCHOFF OPEN CUT. DEVONIAN. | | | | | | | | | | | |
| 100013 | SL | | | | | | 17 | 5.15 | | | MASSIVE |
| 100015 | SL | | | | | | 12 | 3.64 | | | MASSIVE |
| 100699 | PY | 2 | 13 | 2 | 13 | 0.18 | | | | | ACICULAR IN QUARTZ |
| 100700 | PY | 2 | 27 | 2 | 26 | 0.06 | | | | | DISSEMINATED IN QUARTZ |
| 100701 | PY | 36 | 37 | 33 | 34 | 0.97 | | | | | WITH SL IN QUARTZ |
| 100702 | PY | 70 | 103 | 69 | 101 | 0.68 | | | | | WITH CARBONATE |
| 49. VEIN, NORTH VALLEY LODE, N. OF MT. BISCHOFF OPEN CUT. DEVONIAN. | | | | | | | | | | | |
| 100009 | SL | | | | | | 11 | 3.33 | | | |
| 100010 | SL | | | | | | 19 | 5.76 | | | |
| 100675 | PY | 100 | 82 | 94 | 77 | 1.21 | | | | | |
| 100676 | PY | 7 | 74 | 7 | 72 | 0.10 | | | | | |

| SAMPLE | MIN | CO1 | NI1 | CO2 | NI2 | CO/NI | SE | SE/S | DS34 | FT | COMMENT |
|---|---|---|---|---|---|---|---|---|---|---|---|
| 100677 | PY | 57 | 66 | 40 | 47 | 0.86 | | | | | |
| 100678 | PY | 23 | 34 | 21 | 30 | 0.70 | | | | | |
| 50. VEIN, N. OF WARATAH RIVER, N. OF MT. BISCHOFF OPEN CUT. DEVONIAN. | | | | | | | | | | | |
| FOR FURTHER MT. BISCHOFF RESULTS SEE SET 129 ETC. | | | | | | | | | | | |
| 100162 | PY | 2 | 16 | 2 | 16 | 0.12 | | | | | BANDED PY-SL-CARBONATE |
| 51. MASSIVE, REPLACEMENT, BATTERY WORKINGS, RENISON BELL. DEVONIAN. | | | | | | | | | | | |
| 100023 | SL | | | | | | 11 | 3.33 | | | |
| 100024 | SL | | | | | | 20 | 6.06 | | | |
| 100026 | SL | | | | | | 4 | 1.21 | | | |
| 52. MASSIVE, REPLACEMENT, NO. 1 HORIZON, BATTERY WORKINGS, RENISON BELL. DEVONIAN. | | | | | | | | | | | |
| 100118A | PO | 10 | 15 | 9 | 14 | 0.68 | | | | | |
| 100118C | PO | 10 | 18 | 10 | 17 | 0.58 | | | | | |
| 100118D | PO | | | | | | 36 | 9.16 | | | |
| 100120A | PY | 23 | 25 | 22 | 24 | 0.90 | | | | | |
| 100120A | PO | 5 | 17 | 5 | 17 | 0.31 | | | | | |
| 100120B | PY | 28 | 28 | 28 | 27 | 1.01 | | | | | |
| 100120B | PO | 3 | 13 | 3 | 12 | 0.21 | | | | | |
| 100121A | PO | | | | | | 14 | 3.56 | | | |
| 100121B | PY | 35 | 52 | 34 | 51 | 0.67 | | | | | |
| 100121C | PY | 53 | 51 | 52 | 50 | 1.04 | | | | | |
| 100121D | PO | 1 | 11 | 1 | 11 | 0.05 | | | | | |
| 100121E | PO | 1 | 14 | 1 | 13 | 0.08 | | | | | |
| 100121F | PO | 1 | 13 | 1 | 12 | 0.04 | | | | | |
| 100123A | PO | | | | | | 11 | 2.80 | | | |
| 100123C | PO | 0 | 11 | 0 | 10 | 0.0 | | | | | |
| 53. MASSIVE, REPLACEMENT, NO.2 HORIZON, BATTERY WORKINGS, RENISON BELL. DEVONIAN. | | | | | | | | | | | |
| 10901A | PO | | | | | | 2 | 0.51 | | | |
| 10901B | PO | | | | | | | | + 6.0 | | |
| 19797A | PY | 65 | 30 | 64 | 30 | 2.13 | | | | | |
| 19797B | PY | 134 | 41 | 132 | 40 | 3.32 | | | | | |
| 19797C | PY | 139 | 28 | 139 | 28 | 5.00 | | | | | |

| SAMPLE | MIN | CO1 | NI1 | CO2 | NI2 | CO/NI | SE | SE/S | DS34 | FT | COMMENT |
|---|---|---|---|---|---|---|---|---|---|---|---|
| 19797D | PY | 138 | 46 | 137 | 45 | 3.03 | 14 | 2.62 | | | |
| 19797E | PY | | | | | | 27 | 5.06 | | | |
| 19797F | PO | 3 | 14 | 3 | 13 | 0.20 | | | | | |
| 19797G | PO | 3 | 3 | 3 | 3 | 0.98 | | | | | |
| 19797H | PO | 3 | 10 | 3 | 10 | 0.33 | | | | | |
| 19797I | PO | 3 | 6 | 3 | 6 | 0.44 | | | | | |
| 19797J | PO | | | | | | 14 | 3.56 | | | |
| 100093A | PO | | | | | | 0 | 0.0 | | | |
| 100093B | PO | 6 | 14 | 6 | 13 | 0.43 | | | | | |
| 100095A | PO | | | | | | 0 | 0.0 | | | |
| 100095B | PO | 53 | 7 | 50 | 7 | 7.36 | | | | | |
| 100095B | ASPY | 103 | 5 | 96 | 5 | 19.87 | | | | | |
| 100096 | PO | 7 | 9 | 6 | 9 | 0.74 | | | | | |
| 100097A | PO | | | | | | 18 | 4.58 | | | |
| 100097B | PO | 28 | 19 | 26 | 18 | 1.47 | | | | | |
| 100099 | PO | 22 | 6 | 22 | 6 | 3.44 | | | | | |
| 54. DISSEMINATED IN QUARTZ GANGUE, NO. 6 CROSSCUT, FEDERAL LODE, RENSION BELL, DEVONIAN. | | | | | | | | | | | |
| 100102A | PO | 7 | 59 | 7 | 56 | 0.13 | | | | | |
| 100102B | PO | 8 | 57 | 8 | 54 | 0.15 | | | | | |
| 100104A | PO | 15 | 86 | 14 | 81 | 0.17 | | | | | |
| 100104B | PO | 15 | 93 | 14 | 88 | 0.16 | | | | | |
| 100105 | PO | 21 | 103 | 19 | 95 | 0.20 | | | | | |
| 100107 | PO | 36 | 105 | 33 | 94 | 0.35 | 18 | 4.58 | | | |
| 100108A | PO | 12 | 111 | 12 | 109 | 0.11 | | | | | |
| 100108B | PO | 12 | 107 | 11 | 105 | 0.11 | | | | | |
| 100108C | PO | | | | | | 18 | 4.58 | | | |
| 100115A | PO | 62 | 95 | 53 | 81 | 0.65 | | | | | |
| 100115B | PO | | | | | | 7 | 1.78 | | | |
| 55. VEIN TRANSECTING AND PROBABLY REPLACING SHALE. BATTERY OPEN CUT, RENISON BELL. DEVONIAN. | | | | | | | | | | | |
| 100284 | PY | 2 | 28 | 2 | 28 | 0.08 | 18 | 3.37 | | | * VEIN |
| 100291 | PY | 16 | 35 | 15 | 33 | 0.45 | 15 | 2.83 | | | |
| 100292 | PY | 14 | 25 | 13 | 25 | 0.54 | 20 | 3.75 | | | |

| SAMPLE | MIN | CO1 | NI1 | CO2 | NI2 | CO/NI | SE | SE/S | DS34 | FT | COMMENT |
|---|---|---|---|---|---|---|---|---|---|---|---|
| 100293 | PY | 6 | 19 | 6 | 19 | 0.35 | | | | | |
| 100295 | PY | 6 | 46 | 6 | 45 | 0.13 | | | | | |
| 100297 | PY | 1 | 16 | 1 | 15 | 0.08 | | | | | |
| 100303 | PY | 8 | 91 | 8 | 90 | 0.09 | | | | | |
| 100635A | PY | 12 | 12 | 12 | 12 | 1.00 | | | | | |
| 100635B | PY | 1 | 24 | 1 | 20 | 0.03 | | | | | REPLACING SHALE |
| 100635C | PY | 12 | 24 | 12 | 23 | 0.50 | | | | | VEIN |
| 100635D | PY | 1 | 30 | 1 | 25 | 0.05 | | | | | REPLACING SHALE |
| 100636A | PY | 7 | 41 | 6 | 40 | 0.16 | | | | | VEIN |
| 100636B | PY | 10 | 33 | 9 | 30 | 0.29 | | | | | REPLACING SHALE |
| 100636C | PY | 10 | 25 | 9 | 23 | 0.41 | | | | | REPLACING SHALE |
| 100637A | PY | 0 | 12 | 0 | 10 | 0.0 | | | | | * REPLACING SHALE |
| 100637B | PY | 2 | 11 | 2 | 9 | 0.19 | | | | | |
| 100638A | PY | 3 | 8 | 2 | 6 | 0.37 | | | | | |
| 100638B | PY | 2 | 2 | 2 | 2 | 0.92 | | | | | |
| 56. MASSIVE IN VEINS. UNKNOWN LOCALITIES, ZEEHAN. DEVONIAN. | | | | | | | | | | | |
| 10501 | SL | | | | | | 19 | 5.76 | | | |
| 10503 | SL | | | | | | 27 | 8.18 | | | |
| 57. MASSIVE, IN VEIN. SWANSEA MINE, ZEEHAN. DEVONIAN. | | | | | | | | | | | |
| 10509 | SL | | | | | | 17 | 5.15 | | | |
| 58. VEIN, ZEEHAN-MONTANA MINE, ZEEHAN. DEVONIAN. | | | | | | | | | | | |
| 11175 | PY | 5 | 25 | 4 | 23 | 0.19 | 18 | 3.37 | | | CO-NI: AV. OF 8 REPLICATES |
| 59. BANDED VEIN, ROAD-LEVEL ADIT, TRIAL HARBOUR ROAD, ZEEHAN-QUEEN MINE, ZEEHAN. DEVONIAN. | | | | | | | | | | | |
| 100354 | PY | 6 | 22 | 6 | 22 | 0.29 | | | | | * FROM DUMP |
| 100355 | PY | 14 | 20 | 14 | 20 | 0.72 | | | | | |
| 100356 | PY | 1 | 14 | 1 | 14 | 0.11 | 23 | 4.31 | | | |
| 100357 | PY | 3 | 31 | 2 | 30 | 0.08 | | | | | |
| 100359 | PY | 1 | 9 | 1 | 9 | 0.16 | 27 | 5.06 | | | |
| 100360 | PY | 2 | 33 | 2 | 32 | 0.06 | | | | | |
| 100361 | PY | | | | | | 27 | 5.06 | | | |

| SAMPLE | MIN | CO1 | NI1 | CO2 | NI2 | CO/NI | SE | SE/S | DS34 | FT | COMMENT |
|---|---|---|---|---|---|---|---|---|---|---|---|
| 100362 | PY | | | | | | 33 | 6.18 | | | |
| 100363 | PY | | | | | | 14 | 2.62 | | | |
| 100364 | PY | | | | | | 8 | 1.50 | | | |
| 100365 | PY | 3 | 17 | 2 | 16 | 0.15 | | | | | |
| 60. VEIN, COMET MINE, DUNDAS. DEVONIAN. | | | | | | | | | | | |
| 100226 | PY | 16 | 40 | 15 | 39 | 0.39 | 6 | 1.12 | | | DISSEMINATED IN SIDERITE |
| 61. VEIN, SOUTH COMET MINE, DUNDAS. DEVONIAN. | | | | | | | | | | | |
| 100406 | PY- | 10 | 40 | 10 | 39 | 0.25 | 13 | 2.43 | | | FROM DUMP |
| 62. VEIN, WEST COMET MINE, DUNDAS. DEVONIAN. | | | | | | | | | | | |
| 100457 | PY | 90 | 350 | 80 | 311 | 0.26 | | | | | FROM DUMP |
| 63. VEIN, KAPI MINE, NORTH DUNDAS. DEVONIAN. | | | | | | | | | | | |
| 100224 | PY | 5 | 49 | 5 | 46 | 0.10 | 19 | 3.56 | | | * FROM DUMP |
| 100456 | PY | 4 | 93 | 4 | 92 | 0.05 | 0 | 0.0 | | | |
| 64. MASSIVE, IN VEINS, MCKIMMIE MINE, NORTH DUNDAS. DEVONIAN. | | | | | | | | | | | |
| 100037 | SL | | | | | | 26 | 7.88 | | | |
| 100038A | SL | | | | | | 43 | 13.03 | | | |
| 100038B | SL | | | | | | 39 | 11.82 | | | |
| 100039 | SL | | | | | | 20 | 6.06 | | | |
| 100040 | SL | | | | | | 57 | 17.27 | | | |
| 65. VEIN, RAMSDALE PROSPECT, NORTH-EAST DUNDAS. DEVONIAN. | | | | | | | | | | | |
| 100405 | PY | 4 | 251 | 4 | 236 | 0.02 | 24 | 4.49 | | | |
| 66. VEIN, CURTIN DAVIS MINE, NORTH-EAST DUNDAS. DEVONIAN. | | | | | | | | | | | |
| 100404 | PY | 23 | 43 | 21 | 39 | 0.54 | 14 | 2.62 | | | * FROM DUMP |
| 100601 | PY | 47 | 74 | 43 | 67 | 0.64 | 19 | 3.56 | | | |

| SAMPLE | MIN | CO1 | NI1 | CO2 | NI2 | CO/NI | SE | SE/S | DS34 | FT | COMMENT |
|---|---|---|---|---|---|---|---|---|---|---|---|
| 67. VEIN, FAHL MINE, NORTH-EAST DUNDAS. DEVONIAN. | | | | | | | | | | | |
| 100602 | PY | 39 | 456 | 38 | 444 | 0.08 | 32 | 5.99 | | | FROM DUMP |
| 68. VEINS, AND WALLROCK. STORYS CREEK MINE, NE. TASMANIA. DEVONIAN. | | | | | | | | | | | |
| 100384 | PY | 5 | 32 | 5 | 30 | 0.16 | 26 | 4.87 | | | * FROM DUMP |
| 100385 | PY | 4 | 29 | 3 | 25 | 0.14 | | | | | |
| 100386 | PY | 5 | 39 | 5 | 36 | 0.14 | 35 | 6.55 | | | |
| 100387 | PY | 4 | 26 | 4 | 22 | 0.16 | | | | | |
| 100388 | PY | 3 | 30 | 3 | 27 | 0.11 | | | | | |
| 100389 | PY | 4 | 225 | 3 | 188 | 0.02 | 21 | 3.93 | | | |
| 100652A | PY | 5 | 12 | 5 | 12 | 0.38 | | | | | * WALLROCK, 11 LEVEL |
| 100652B | PY | 2 | 13 | 2 | 13 | 0.14 | | | | | |
| 100653 | PY | 16 | 59 | 15 | 57 | 0.27 | | | | | |
| 100654 | PY | 12 | 50 | 12 | 49 | 0.24 | | | | | |
| 100655 | PY | 3 | 15 | 3 | 14 | 0.23 | | | | | VEIN, 9 LEVEL |
| 100656 | PY | 115 | 256 | 115 | 255 | 0.45 | | | | | VEIN, 9 LEVEL, BOXWORKS |
| 100735 | PY | 58 | 25 | 50 | 21 | 2.35 | | | | | VEIN, ADIT LEVEL |
| 100736 | PY | 80 | 25 | 71 | 22 | 3.18 | | | | | VEIN, 4 LEVEL |
| 100737 | PY | 74 | 50 | 59 | 40 | 1.47 | | | | | VEIN, 4 LEVEL |
| 100738 | PY | 132 | 34 | 112 | 29 | 3.87 | | | | | VEIN, 7 LEVEL |
| 100739 | PY | 138 | 39 | 123 | 35 | 3.52 | | | | | VEIN, 9 LEVEL |
| 100739 | CPY | 53 | 26 | 52 | 26 | 2.00 | | | | | VEIN, 9 LEVEL |
| 100740 | PY | 110 | 36 | 110 | 35 | 3.11 | | | | | VEIN, 9 LEVEL |
| 100741 | PY | 163 | 443 | 150 | 406 | 0.37 | | | | | VEIN,11 LEVEL |
| 69. HENRYS LODE, CLEVELAND MINE, LUINA. DEVONIAN. PYRRHOTITE AND CHALCOPYRITE DISSEMINATED IN QUARTZ-CARBONATE GANGUE; SPHALERITE MASSIVE. FURTHER CLEVELAND RESULTS IN SET 128. | | | | | | | | | | | |
| 100084 | PO | | | | | | 20 | 5.09 | | | S. END |
| 100085 | PO | 7 | 24 | 6 | 22 | 0.29 | 22 | 5.60 | | | NE. END |
| 100086A | PO | 38 | 48 | 33 | 42 | 0.79 | 36 | 9.16 | | | B LODE, R X-CUT |
| 100086B | CPY | | | | | | 40 | 11.43 | | | |
| 100087 | PO | 52 | 88 | 45 | 75 | 0.59 | 32 | 8.14 | | | R X-CUT |
| 100088 | PO | 128 | 103 | 107 | 86 | 1.24 | 7 | 1.78 | | | 100 FT. SW. R X-CUT |
| 100089 | PO | 54 | 51 | 45 | 43 | 1.06 | 32 | 8.14 | | | 200 FT. SW. R X-CUT |
| 100018 | SL | | | | | | 10 | 3.03 | | | |
| 100019 | SL | | | | | | 18 | 5.45 | | | |

| SAMPLE | MIN | CO1 | NI1 | CO2 | NI2 | CO/NI | SE | SE/S | DS34 | FT | COMMENT |
|---|---|---|---|---|---|---|---|---|---|---|---|
| 100020 | SL | | | | | | 35 | 10.61 | | | |
| 100022 | SL | | | | | | 7 | 2.12 | | | |
| 70. CU-PB-ZN LODE, ROUND HILL MINE, GOWRIE PARK. DEVONIAN. | | | | | | | | | | | |
| 100834 | PY | 167 | 157 | 166 | 156 | 1.07 | | | | | * COARSE GRAINED VEIN |
| 100835 | PY | 211 | 138 | 210 | 137 | 1.53 | | | | | |
| 100836 | PY | 11 | 19 | 11 | 18 | 0.60 | | | | | MIXED SULPHIDES, REPL.(?) |
| 71. VEINS, ADJACENT TO DYKE, QUARRY ON A.P.P.M. ROAD, NEAR VALENTINES PEAK. DEVONIAN. | | | | | | | | | | | |
| 100730 | PY | 294 | 48 | 283 | 46 | 6.11 | | | | | |
| 100731 | PY | 98 | 44 | 97 | 43 | 2.23 | | | | | |
| 100732 | PY | 391 | 54 | 372 | 51 | 7.30 | | | | | |
| 72. PYRITE FROM TOP OF MASSIVE OREBODY, BLOW OPEN CUT, AT WATER LEVEL. MT. LYELL. 5220S 700E. | | | | | | | | | | | |
| 11242A | PY | 255 | 77 | 252 | 76 | 3.31 | | | | | |
| 11242B | PY | 260 | 82 | 261 | 83 | 3.15 | 200 | 37.45 | | | SE IN DUPLICATE |
| 100473 | PY | 700 | 77 | 697 | 77 | 9.05 | | | | | |
| 11243 | PY | 362 | 24 | 360 | 23 | 15.40 | | | | | |
| 100475 | PY | 214 | 79 | 197 | 73 | 2.70 | | | | | |
| 32664 | SL | | | | | | 9 | 2.73 | | | BLOW OREBODY |
| 73. REPLACEMENT BANDS, PARALLEL TO THE SCHISTOSITY, 6 FT. ABOVE SET 72, NORTH FACE, BLOW OPEN CUT, MT. LYELL. 5220S 700E. | | | | | | | | | | | |
| 100476 | PY | 64 | 22 | 62 | 21 | 2.90 | | | | | |
| 100477 | PY | 43 | 21 | 41 | 20 | 2.02 | | | | | |
| 100478 | PY | 55 | 20 | 54 | 19 | 2.78 | 211 | 39.51 | | | SE IN DUPLICATE |
| 100479A | PY | 75 | 24 | 73 | 23 | 3.18 | | | | | |
| 100479B | PY | 98 | 35 | 97 | 35 | 2.80 | | | | | |
| 11244 | PY | 168 | 54 | 155 | 50 | 3.13 | | | | | |
| 74. AS SET 73, PARALLEL TO IT, 15 FT. WEST. | | | | | | | | | | | |
| 11245 | PY | 18 | 10 | 16 | 9 | 1.82 | | | | | |
| 100482 | PY | 255 | 57 | 253 | 57 | 4.45 | | | | | |
| 100483 | PY | 10 | 23 | 10 | 22 | 0.43 | | | | | |
| 100484 | PY | 146 | 26 | 143 | 26 | 5.59 | | | | | |

| SAMPLE | MIN | CO1 | NI1 | CO2 | NI2 | CO/NI | SE | SE/S | DS34 | FT | COMMENT |
|---|---|---|---|---|---|---|---|---|---|---|---|
| 100485 | PY | 25 | 13 | 24 | 12 | 2.03 | | | | | |
| 75. AS SET 74, PARALLEL TO IT, 10 FT. FURTHER WEST. | | | | | | | | | | | |
| 100486 | PY | 128 | 121 | 124 | 117 | 1.06 | | | | | |
| 100487 | PY | 87 | 74 | 84 | 72 | 1.17 | | | | | |
| 100488 | PY | 224 | 114 | 217 | 110 | 1.96 | | | | | |
| 100489 | PY | 108 | 97 | 102 | 92 | 1.12 | | | | | |
| 100490 | PY | 72 | 105 | 69 | 100 | 0.69 | | | | | |
| 76. AS SET 75, TOP BENCH, BLOW OPEN CUT, MT. LYELL. 5100S 500E RL 1375. | | | | | | | | | | | |
| 100569 | PY | 99 | 49 | 97 | 48 | 2.04 | | | | | |
| 100570 | PY | 224 | 98 | 222 | 97 | 2.28 | 311 | 58.24 | | | SE IN DUPLICATE |
| 100571 | PY | 113 | 50 | 111 | 49 | 2.26 | | | | | |
| 100572 | PY | 250 | 108 | 240 | 104 | 2.31 | 325 | 60.86 | | | |
| 77. DISSEMINATIONS IN SCHIST, PRINCE LYELL OREBODY, WEST LYELL OPEN CUT, MT. LYELL. RL 1140 AND 1185 BENCHES. | | | | | | | | | | | |
| 100501 | PY | 421 | 1560 | 404 | 1496 | 0.27 | | | | | |
| 100502 | PY-CPY | 1062 | 264 | 1027 | 256 | 4.02 | | | | | |
| 100503 | PY | 1633 | 420 | 1559 | 401 | 3.89 | | | | | |
| 100504 | PY-CPY | 1824 | 190 | 1738 | 181 | 9.59 | 76 | 15.20 | | | |
| 100505 | PY-CPY | 1346 | 269 | 1252 | 250 | 5.00 | | | | | |
| 100506 | PY-CPY | 1168 | 99 | 1118 | 95 | 11.77 | | | | | |
| 78. DISSEMINATIONS IN SCHIST, PRINCE LYELL OREBODY, DDH WL 229 BENEATH WEST LYELL OPEN CUT, MT. LYELL. COLLAR 4685S 1492W RL 1325, GEOLOGICAL CROSS SECTION NO. 15. | | | | | | | | | | | |
| 100410 | PY | 662 | 77 | 634 | 74 | 8.58 | | | | 686 | |
| 100411 | PY | 631 | 169 | 600 | 161 | 3.73 | | | | 713 | |
| 100412 | PY | 216 | 47 | 200 | 44 | 4.60 | | | | 782 | |
| 100413 | PY | 623 | 395 | 585 | 371 | 1.58 | | | | 832 | |
| 11230 | PY | 705 | 78 | 671 | 75 | 8.98 | | | + 9.7 | 713 | 92% PY, 5% CPY. XRF |
| 100415 | PY | 968 | 91 | 896 | 85 | 10.60 | | | | 686 | |
| 100416 | PY | 1266 | 143 | 1175 | 133 | 8.83 | | | | 663 | 87% PY, 5% CPY. XRF |
| 100418 | PY-CPY | 628 | 122 | 528 | 102 | 5.16 | | | | 713 | 78% PY,10% CPY. XRF |
| 100419 | PY | 1006 | 60 | 853 | 51 | 16.86 | | | | 639 | 87% PY, 2% CPY. XRF |
| 100443 | PY-CPY | 929 | 191 | 868 | 179 | 4.86 | | | | | 86% PY,14% CPY. XRF |

| SAMPLE | MIN | CO1 | NI1 | CO2 | NI2 | CO/NI | SE | SE/S | DS34 | FT | COMMENT |
|---|---|---|---|---|---|---|---|---|---|---|---|
| 100444 | PY-CPY | 308 | 109 | 275 | 97 | 2.83 | | | | 814 | 84% PY,16% CPY. XRF |
| 100445 | PY-CPY | 756 | 124 | 690 | 113 | 6.12 | | | | 763 | 73% PY,23% CPY. XRF |
| 100446 | PY | 835 | 24 | 758 | 22 | 35.20 | | | | 806 | 89% PY, 6% CPY. XRF |
| 100447 | PY-CPY | 1072 | 97 | 992 | 90 | 11.03 | | | | 923 | 85% PY,12% CPY. XRF |
| 100448 | PY | 539 | 314 | 495 | 289 | 1.71 | | | | 832 | 82% PY, 7% CPY. XRF |
| 10736 | PY=CPY | 657 | 62 | 631 | 59 | 10.68 | | | + 5.8 | 889 | 47% PY,46% CPY. XRF |
| 100450 | PY | 1334 | 61 | 1204 | 55 | 21.73 | | | | 984 | 83% PY, 9% CPY. XRF |
| 100624 | PY | 685 | 425 | 672 | 417 | 1.61 | | | | 832 | |
| 100672 | PY | 2260 | 150 | 2157 | 144 | 15.02 | | | | 792 | 96% PY, 4% CPY. PS |
| 100672 | CPY-PY | 521 | 48 | 450 | 42 | 10.84 | | | | | 12% PY,88% CPY. PS |
| 100673 | PY | 2358 | 150 | 2277 | 145 | 15.70 | | | | 800 | 100%PY. PS |
| 100673 | CPY | 330 | 36 | 302 | 33 | 9.18 | | | | | 6% PY,94% CPY. PS |
| 79. DISSEMINATIONS IN SCHIST. PRINCE LYELL OREBODY.DDH WL 146 BENEATH WEST LYELL OPEN CUT. MT. LYELL. COLLAR 1451W RL 729, GEOLOGICAL CROSS SECTION NO. 15. | | | | | | | | | | | |
| 100434 | PY-CPY | 1185 | 31 | 972 | 26 | 37.76 | 43 | 8.60 | | 473 | 78% PY, 12% CPY. XRF |
| 100436 | PY | 1178 | 20 | 1113 | 18 | 60.17 | | | | 665 | 87% PY, 0% CPY. XRF |
| 100437 | PY | 1074 | 17 | 991 | 16 | 63.47 | | | | 432 | 95% PY, 1% CPY. XRF |
| 100438 | PY | 761 | 146 | 661 | 127 | 5.23 | | | | 497 | 87% PY, 3% CPY. XRF |
| 100439 | PY-CPY | 249 | 16 | 238 | 16 | 15.28 | | | | 422 | 43% PY,31% CPY. XRF |
| 11231 | PY | 208 | 63 | 195 | 59 | 3.29 | | | +10.0 | 347 | 98% PY, 2% CPY. XRF |
| 100441 | PY | 299 | 69 | 250 | 58 | 4.34 | | | | 707 | 67% PY, 3% CPY. XRF |
| 80. DISSEMINATIONS IN SCHIST. PRINCE LYELL OREBODY. DDH WL 150 BENEATH WEST LYELL OPEN CUT. MT. LYELL. COLLAR 4580S 1452W RL 730, GEOLOGICAL CROSS SECTION NO. 15. | | | | | | | | | | | |
| 100421 | PY-CPY | 1017 | 153 | 751 | 113 | 6.65 | 84 | 18.26 | | 1200 | 56% PY,22% CPY. XRF |
| 100422 | PY-CPY | 1330 | 141 | 1168 | 123 | 9.47 | | | | 857 | 79% PY,16% CPY. XRF |
| 100423 | PY | 1382 | 114 | 1271 | 105 | 12.13 | | | | 950 | 92% PY, 2% CPY. XRF |
| 100424 | PY | 916 | 185 | 747 | 151 | 4.95 | | | | 1050 | 76% PY, 7% CPY. XRF |
| 100425 | PY | 921 | 366 | 858 | 341 | 2.52 | 87 | 17.40 | | 1234 | 83% PY, 7% CPY. XRF |
| 100426 | PY | 299 | 37 | 289 | 36 | 8.05 | 46 | 9.02 | | 964 | 67% PY, 4% CPY. XRF |
| 100427 | PY-CPY | 734 | 92 | 698 | 88 | 7.97 | | | | 1341 | 87% PY,13% CPY. XRF |
| 11229 | PY | 543 | 55 | 487 | 50 | 9.79 | | | + 8.7 | 927 | 86% PY, 5% CPY. XRF |
| 11228 | PY | 82 | 14 | 75 | 13 | 5.99 | | | + 6.5 | 997 | 76% PY, 3% CPY. XRF |
| 100430 | PY | 1774 | 244 | 1638 | 225 | 7.27 | | | | 1206 | 96% PY, 1% CPY. XRF |
| 11227 | PY-CPY | 1487 | 138 | 1296 | 121 | 10.75 | | | + 6.3 | 1180 | 71% PY,25% CPY. XRF |

| SAMPLE | MIN | CO1 | NI1 | CO2 | NI2 | CO/NI | SE | SE/S | DS34 | FT | COMMENT |
|---|---|---|---|---|---|---|---|---|---|---|---|
| 100432 | PY | 484 | 56 | 456 | 53 | 8.64 | | | | 1273 | 94% PY, 6% CPY. XRF |
| 100433 | CPY-PY | 367 | 123 | 337 | 113 | 2.97 | | | | 1234 | 24% PY,68% CPY. XRF |
| 100625 | PY | 1710 | 197 | 1266 | 146 | 8.69 | | | | 1155 | |
| 100626 | PY | 1393 | 313 | 1377 | 310 | 4.45 | | | | 1234 | |
| 100626 | CPY | 471 | 148 | 456 | 143 | 3.18 | | | | | |
| 100670 | PY | 2193 | 380 | 1678 | 291 | 5.76 | | | | 1235 | 87% PY,13% CPY. PS |
| 100670 | CPY | 50 | 21 | 45 | 19 | 2.33 | | | | | 2% PY,98% CPY. PS |
| 100671 | PY | 1458 | 333 | 1327 | 303 | 4.38 | | | | 1236 | 99% PY, 1% CPY. PS |
| 100671 | CPY | 99 | 32 | 85 | 28 | 3.05 | | | | | 4% PY,96% CPY. PS |
| 81. IN QUARTZ VEINS IN PRINCE LYELL OREBODY,DRILLHOLES BENEATH WEST LYELL OPEN CUT, MT. LYELL. | | | | | | | | | | | |
| 100417 | CPY | 5 | 5 | 5 | 5 | 0.95 | | | | 816 | DDH WL229 |
| 100442 | CPY | 1 | 6 | 1 | 6 | 0.17 | 41 | 11.71 | | 718 | DDH WL229 93%CPY,1%PY.XRF |
| 10737 | CPY | 4 | 6 | 4 | 6 | 0.65 | 82 | 23.43 | + 6.2 | 675 | DDH WL146 |
| 100420 | CPY | 4 | 10 | 4 | 10 | 0.37 | 53 | 15.14 | | 1203 | DDH WL150 |
| 82. IN QUARTZ VEINS IN PRINCE LYELL OREBODY, WEST LYELL OPEN CUT, MT. LYELL. | | | | | | | | | | | |
| 19798A | CPY | | | | | | 55 | 15.71 | | | |
| 19798B | CPY | | | | | | 59 | 16.86 | | | |
| 19798C | CPY | | | | | | 72 | 20.57 | | | |
| 19798D | CPY | | | | | | 60 | 17.14 | | | |
| 19911A | CPY | | | | | | 58 | 16.57 | | | |
| 19911B | CPY | | | | | | 57 | 16.29 | | | |
| 83. IN QUARTZ VEINS, WEST LYELL OPEN CUT, MT. LYELL. | | | | | | | | | | | |
| 10719A | CPY | | | | | | 35 | 10.00 | | | |
| 10719B | CPY | | | | | | 33 | 9.43 | | | |
| 10719C | CPY | | | | | | 29 | 8.29 | | | |
| 10733A | CPY | | | | | | 25 | 7.14 | | | |
| 10733B | CPY | | | | | | 61 | 17.43 | | | |
| 19763 | CPY | | | | | | 35 | 10.00 | | | |

| SAMPLE | MIN | CO1 | NI1 | CO2 | NI2 | CO/NI | SE | SE/S | DS34 | FT | COMMENT |
|---|---|---|---|---|---|---|---|---|---|---|---|
| 84. IN QUARTZ VEINS, S.E. CORNER, WEST LYELL OPEN CUT, MT. LYELL. | | | | | | | | | | | |
| 100312A | PY | 72 | 58 | 72 | 58 | 1.25 | | | | | |
| 100312B | PY | 63 | 63 | 63 | 63 | 1.00 | | | | | |
| 100312C | PY | 66 | 76 | 65 | 75 | 0.87 | 114 | 21.35 | | | |
| 100313A | PY | 111 | 47 | 111 | 47 | 2.38 | | | | | |
| 100313B | PY | 39 | 60 | 39 | 60 | 0.64 | | | | | |
| 100313C | PY | 40 | 57 | 40 | 57 | 0.70 | | | | | |
| 100314 | PY | 38 | 151 | 38 | 151 | 0.25 | | | | | |
| 100315 | PY | 80 | 48 | 80 | 48 | 1.66 | | | | | |
| 100317 | PY | | | | | | 121 | 22.66 | | | |
| 100320 | PY | | | | | | 139 | 26.03 | | | |
| 100832A | PY | 86 | 250 | 84 | 243 | 0.34 | | | | | 100% PY. PS |
| 100832A | CPY | 4 | 23 | 4 | 22 | 0.17 | | | | | 3% PY, 97% CPY. PS |
| 100832B | PY | 82 | 153 | 80 | 151 | 0.53 | | | | | 100% PY. PS |
| 100832B | CPY | 1 | 7 | 1 | 7 | 0.09 | | | | | 100% CPY. PS |
| 100833A | PY | 107 | 178 | 104 | 174 | 0.60 | | | | | 98% PY, 2% CPY. PS |
| 100833A | CPY | 75 | 86 | 74 | 86 | 0.87 | | | | | 38% PY, 62% CPY. PS |
| 100833B | PY | 113 | 100 | 105 | 92 | 1.14 | | | | | 97% PY, 3% CPY. PS |
| 100833B | CPY | 55 | 5 | 54 | 5 | 11.60 | | | | | 1% PY, 99% CPY. PS |
| 85. DISSEMINATED IN BANDS IN THE SCHISTOSITY, GULLET (RL 1320) BENCH, NORTH FACE OF WEST LYELL OPEN CUT, MT. LYELL. 3500S 1600W. | | | | | | | | | | | |
| 100509 | PY | 483 | 92 | 457 | 87 | 5.25 | | | | | |
| 100510 | PY | 250 | 51 | 232 | 47 | 4.90 | 98 | 18.35 | | | |
| 100511 | PY | 248 | 66 | 233 | 62 | 3.74 | | | | | |
| 100512 | PY | 678 | 94 | 632 | 88 | 7.19 | | | | | |
| 86. AS SET 85, 10 FT. WEST. | | | | | | | | | | | |
| 100513 | PY | 459 | 136 | 442 | 131 | 3.37 | | | | | |
| 100514 | PY | 476 | 128 | 456 | 123 | 3.71 | | | | | |
| 100515 | PY | 554 | 147 | 521 | 138 | 3.76 | | | | | |
| 100516 | PY | 623 | 145 | 582 | 135 | 4.29 | | | | | |
| 87. AS SET 86, 42 FT. FURTHER WEST. | | | | | | | | | | | |
| 100517 | PY | 233 | 114 | 221 | 108 | 2.04 | | | | | |
| 100518 | PY | 436 | 101 | 420 | 97 | 4.32 | | | | | |

| SAMPLE | MIN | CO1 | NI1 | CO2 | NI2 | CO/NI | SE | SE/S | DS34 | FT | COMMENT |
|---|---|---|---|---|---|---|---|---|---|---|---|
| 100519 | PY | 130 | 40 | 126 | 38 | 3.27 | | | | | |
| 100520 | PY | 376 | 119 | 362 | 115 | 3.16 | | | | | |
| 88. DISSEMINATED IN BANDS IN THE SCHISTOSITY, HONEYPOT OREBODY, GULLET(RL 1320)BENCH, NORTH FACE OF WEST LYELL OPEN CUT, MT. LYELL. 3000S 1150W. | | | | | | | | | | | |
| 100507 | PY | 532 | 42 | 510 | 40 | 12.68 | | | | | |
| 100508 | PY | 442 | 38 | 421 | 36 | 11.59 | 47 | 8.80 | | | |
| 89. DISSEMINATIONS IN SCHIST, CAPE HORN PYRITE BODY, COMSTOCK TRACK, NORTH OF WEST LYELL OPEN CUT, MT.LYELL. 1000N 2100W RL 1925. | | | | | | | | | | | |
| 100372A | PY | 143 | 68 | 99 | 47 | 2.09 | 38 | 7.12 | | | |
| 100372B | PY | 7 | 23 | 6 | 22 | 0.29 | | | | | |
| 100372C | PY | 118 | 60 | 93 | 47 | 1.98 | | | | | |
| 100372E | PY | 184 | 67 | 127 | 46 | 2.75 | 35 | 6.55 | | | |
| 100373A | PY | 185 | 79 | 134 | 57 | 2.34 | | | | | |
| 100373C | PY | | | | | | 40 | 7.47 | | | |
| 100373D | PY | 159 | 76 | 132 | 63 | 2.10 | | | | | |
| 100374A | PY | 216 | 78 | 147 | 54 | 2.75 | | | | | |
| 100374B | PY | | | | | | 41 | 7.68 | | | |
| 90. DISSEMINATIONS IN QUARTZOSE SEGREGATIONS IN THE SCHISTOSITY, ASSOCIATED WITH SET 89. | | | | | | | | | | | |
| 100559 | PY | 393 | 269 | 381 | 262 | 1.46 | | | | | |
| 100560 | PY | 240 | 147 | 230 | 141 | 1.63 | | | | | |
| 91. DISSEMINATIONS IN SERICITIC SCHIST, CROWN LYELL OREBODY IOE, MT. LYELL. | | | | | | | | | | | |
| 100496 | PY | 1498 | 122 | 1393 | 114 | 12.24 | | | | | |
| 100497 | PY | 1611 | 99 | 1539 | 95 | 16.22 | 98 | 18.35 | | | |
| 100498 | PY | 953 | 17 | 874 | 16 | 54.83 | 85 | 15.92 | | | |
| 100499 | PY | 1152 | 137 | 1053 | 125 | 8.39 | | | | | |
| 100500 | PY | 1041 | 112 | 988 | 107 | 9.26 | | | | | |
| 92. MASSIVE, WITH BORNITE, NORTH LYELL, MT. LYELL. | | | | | | | | | | | |
| 19796A | CPY | | | | | | 82 | 23.43 | | | |
| 19796B | CPY | | | | | | 80 | 22.86 | | | |

| SAMPLE | MIN | CO1 | NI1 | CO2 | NI2 | CO/NI | SE | SE/S | DS34 | FT | COMMENT |
|---|---|---|---|---|---|---|---|---|---|---|---|
| 93. MASSIVE ORE, CROWN LYELL, MT. LYELL. | | | | | | | | | | | |
| 10738-2 | CPY | | | | | | 326 | 93.14 | | | |
| 10739-2 | PY-CP | | | | | | 116 | 22.31 | | | |
| 31805A | CPY | | | | | | | | - 3.6 | | |
| 31805C | CPY | | | | | | | | - 2.5 | | |
| 31805E | CPY | | | | | | | | - 2.8 | | |
| 31805I | CPY | | | | | | 43 | 12.29 | | | |
| 31805J | CPY | | | | | | 38 | 10.86 | | | |
| 100042 | SL | | | | | | 31 | 9.39 | | | |
| 94. MASSIVE, SECOND BENCH, LYELL COMSTOCK OPEN CUT, MT. LYELL. 5600N 800W RL 1650. | | | | | | | | | | | |
| 11234 | PY | 58 | 52 | 54 | 49 | 1.12 | 10 | 1.87 | + 6.1 | | |
| 11235 | PY | 62 | 57 | 58 | 53 | 1.10 | | | + 6.7 | | |
| 11236 | PY | 42 | 54 | 38 | 49 | 0.79 | | | + 6.6 | | |
| 11237 | PY | 50 | 51 | 45 | 46 | 0.98 | | | + 6.3 | | |
| 100495 | PY | 40 | 44 | 37 | 41 | 0.90 | | | | | |
| 95. MASSIVE, DUMP AT COLLAR OF TASMAN AND CROWN LYELL SHAFT, MT. LYELL. 6060N 420W RL 1380. | | | | | | | | | | | |
| 100369A | PY | | | | | | 77 | 14.42 | | | SE IN DUPLICATE |
| 100369B | PY | 9 | 24 | 9 | 23 | 0.40 | | | | | |
| 100369D | PY | 6 | 17 | 6 | 17 | 0.38 | | | | | |
| 100369E | PY | 14 | 28 | 14 | 28 | 0.51 | | | | | |
| 11219A | PY | 149 | 77 | 116 | 59 | 1.95 | | | | | |
| 11219B | PY | | | | | | 130 | 24.34 | | | |
| 11219E | PY | 4 | 17 | 4 | 17 | 0.22 | | | | | |
| 11219F | PY | | | | | | | | + 5.8 | | |
| 100371E | PY | | | | | | 141 | 26.40 | | | |
| 100403 | PY | 6 | 18 | 4 | 14 | 0.31 | | | | | |
| 11238 | PY | 4 | 9 | 4 | 9 | 0.44 | | | + 6.7 | | |
| 11239 | PY | 8 | 25 | 7 | 22 | 0.33 | | | + 8.4 | | |
| 11240 | PY | 12 | 22 | 10 | 20 | 0.52 | | | + 8.3 | | |
| 11241 | PY | 1 | 5 | 1 | 5 | 0.13 | 88 | 16.48 | + 6.6 | | SE IN DUPLICATE |

| SAMPLE | MIN | CO1 | NI1 | CO2 | NI2 | CO/NI | SE | SE/S | DS34 | FT | COMMENT |
|---|---|---|---|---|---|---|---|---|---|---|---|
| 96. MASSIVE, UNKNOWN LOCALITIES, ROSEBERY MINE. | | | | | | | | | | | |
| 10535A | CPY | | | | | | | | + 9.6 | | |
| 10535D | CPY | | | | | | | | + 9.0 | | |
| 10535I | CPY | | | | | | 8 | 2.29 | | | |
| 10535J | CPY | | | | | | 24 | 6.86 | | | |
| 10535K | CPY | | | | | | 8 | 2.29 | | | |
| 10535B | SL | | | | | | | | + 9.9 | | |
| 10535E | SL | | | | | | | | + 10.0 | | |
| 10535L | SL | | | | | | 8 | 2.42 | | | |
| 10535G | SL | | | | | | 14 | 4.24 | | | |
| 10535H | SL | | | | | | 10 | 3.03 | | | |
| 19764A | CPY | | | | | | | | +13.5 | | |
| 19764D | CPY | | | | | | | | +10.0 | | |
| 19764G | CPY | | | | | | 27 | 7.71 | | | |
| 19764B | SL | | | | | | | | +12.2 | | |
| 19764E | SL | | | | | | | | +12.6 | | |
| 19764F | SL | | | | | | 12 | 3.64 | | | |
| 97. BANDED SPHALERITIC ORE, 9 LEVEL, B LENS, ROSEBERY MINE. K35N STOPE, 3450N 75E RL 558. | | | | | | | | | | | |
| 100055 | SL | | | | | | 16 | 4.85 | | | |
| 100056 | SL | | | | | | 2 | 0.61 | | | |
| 100057 | SL | | | | | | 20 | 6.06 | | | |
| 98. BANDED SPHALERITIC ORE, 11 LEVEL, D LENS, ROSEBERY MINE. M10N STOPE, 970N 320E RL 285. | | | | | | | | | | | |
| 100052 | SL | | | | | | 6 | 1.82 | | | |
| 99. MASSIVE PYRITIC ORE, 12 LEVEL, HANGINGWALL OF B LENS, ROSEBERY MINE. 040N STOPE, 4030N 490E RL 30. | | | | | | | | | | | |
| 100548 | PY | 4 | 6 | 3 | 5 | 0.76 | | | | | |
| 100549 | PY | 5 | 9 | 4 | 8 | 0.51 | | | | | |
| 100550 | PY | 4 | 6 | 3 | 5 | 0.63 | | | | | |
| 100551 | PY | 3 | 4 | 3 | 4 | 0.77 | 5 | 0.94 | | | |
| 100. MASSIVE PYRITIC ORE, 12 LEVEL, FOOTWALL OF E LENS, ROSEBERY MINE. S. DRIVE 00N 700E RL 61. | | | | | | | | | | | |
| 100349 | PY | 1 | 9 | 1 | 9 | 0.10 | 12 | 2.25 | | | |
| 100350A | PY | 1 | 8 | 1 | 8 | 0.11 | 0 | 0.0 | | | |

| SAMPLE | MIN | CO1 | NI1 | CO2 | NI2 | CO/NI | SE | SE/S | DS34 | FT | COMMENT |
|---|---|---|---|---|---|---|---|---|---|---|---|
| 100350B | PY | 0 | 5 | 0 | 5 | 0.0 | | | | | |
| 100350C | PY | 0 | 16 | 0 | 16 | 0.0 | 7 | 1.31 | | | |
| 100350D | PY | 0 | 14 | 0 | 14 | 0.0 | | | | | |
| 100350H | PY | 1 | 17 | 1 | 17 | 0.09 | | | | | |
| 100350I | PY | 3 | 18 | 3 | 17 | 0.16 | | | | | |
| 100350J | PY | 2 | 18 | 2 | 18 | 0.13 | | | | | |
| 100350L | PY | | | | | | 13 | 2.43 | | | |
| 101. MEDIUM GRAINED PYRITIC ORE, 13 LEVEL, FOOTWALL OF D LENS, ROSEBERY MINE. N DRIVE 1100N 720E RL 9940. NOTE: SL=RL 10000. | | | | | | | | | | | |
| 100536 | PY | 2 | 3 | 2 | 3 | 0.55 | | | | | |
| 100537 | PY | 3 | 6 | 2 | 6 | 0.41 | | | | | |
| 100538 | PY | 4 | 6 | 3 | 5 | 0.69 | 14 | 2.62 | | | |
| 100539 | PY | 2 | 5 | 2 | 4 | 0.39 | 15 | 2.81 | | | |
| 102. MASSIVE PYRITIC ORE, 13 LEVEL, HANGINGWALL OF D LENS, ROSEBERY MINE. 8N X-CUT 720N 680E RL 9938. | | | | | | | | | | | |
| 100540 | PY | 42 | 1 | 42 | 1 | 68.09 | | | | | |
| 100541 | PY | 68 | 1 | 67 | 1 | 105.19 | 12 | 2.25 | | | |
| 100542 | PY | 652 | 1 | 636 | 1 | 469.81 | | | | | |
| 100543 | PY | 52 | 9 | 50 | 8 | 6.08 | | | | | |
| 103. MEDIUM GRAINED PYRITIC ORE, 13 LEVEL, FOOTWALL OF E LENS, ROSEBERY MINE. 100N 830E RL 9940 | | | | | | | | | | | |
| 100544 | PY | 5 | 9 | 4 | 7 | 0.61 | | | | | |
| 100545 | PY | 442 | 6 | 433 | 6 | 74.29 | | | | | |
| 100546 | PY | 330 | 10 | 322 | 10 | 32.84 | | | | | |
| 100547 | PY | 380 | 10 | 364 | 9 | 38.95 | 41 | 7.68 | | | |
| 104. BANDED COARSE GRAINED PYRITIC ORE, 13 LEVEL, WITHIN F LENS, ROSEBERY MINE. 300N 1030E RL 9939. | | | | | | | | | | | |
| 100523 | PY | 49 | 6 | 43 | 5 | 8.70 | | | | | |
| 100524A | PY | 64 | 6 | 62 | 6 | 10.57 | 10 | 1.87 | | | SE IN DUPLICATE |
| 100524B | PY | 65 | 14 | 62 | 13 | 4.74 | | | | | |
| 100525 | PY | 22 | 97 | 15 | 69 | 0.22 | | | | | |
| 100526 | PY | 51 | 7 | 47 | 6 | 7.33 | 16 | 3.00 | | | |

| SAMPLE | MIN | CO1 | NI1 | CO2 | NI2 | CO/NI | SE | SE/S | DS34 | FT | COMMENT |
|---|---|---|---|---|---|---|---|---|---|---|---|
| 105. FINE GRAINED PYRITIC ORE, 13 LEVEL, FOOTWALL OF F LENS, ROSEBERY MINE. 350S 895E RL 9942. | | | | | | | | | | | |
| 100616 | PY | 3 | 3 | 3 | 3 | 1.11 | | | | | |
| 100617 | PY | 4 | 5 | 4 | 5 | 0.73 | 7 | 1.31 | | | |
| 100618 | PY | 1 | 3 | 1 | 3 | 0.22 | | | | | |
| 100528 | PY | 11 | 7 | 8 | 5 | 1.69 | 26 | 4.87 | | | |
| 106. DISSEMINATED IN SCHIST, 13 LEVEL, FOOTWALL OF F LENS, ROSEBERY MINE. 309S 890E RL 9942. | | | | | | | | | | | |
| 100532 | PY | 3 | 17 | 3 | 16 | 0.18 | 5 | 0.94 | | | |
| 100533 | PY | 3 | 11 | 3 | 11 | 0.24 | | | | | |
| 100534 | PY | 2 | 14 | 2 | 14 | 0.15 | | | | | |
| 100535 | PY | 2 | 14 | 2 | 13 | 0.13 | | | | | |
| 107. INTERGROWN MEDIUM GRAINED PYRITE AND HEMATITE, 13 LEVEL, ABOVE F LENS, ROSEBERY MINE. 750S 740E RL 9945. | | | | | | | | | | | |
| 100530 | PY | 21 | 120 | 20 | 111 | 0.18 | | | | | |
| 100530 | HM | 2 | 11 | 2 | 10 | 0.16 | | | | | |
| 100531 | PY | 1 | 3 | 1 | 3 | 0.42 | 23 | 4.31 | | | |
| 100531 | HM | 1 | 3 | 1 | 3 | 0.22 | | | | | |
| 100734 | PY | 4 | 17 | 3 | 17 | 0.20 | | | | | |
| 100734 | HM | 2 | 4 | 2 | 4 | 0.46 | | | | | |
| 108. BANDED SPHALERITIC ORE, 13 LEVEL, D LENS, STOPES Q5NS AND P8NS, ROSEBERY MINE. | | | | | | | | | | | |
| 100050 | SL | | | | | | 16 | 4.85 | | | 450S 760E RL 9958 |
| 100053 | SL | | | | | | 4 | 1.21 | | | 750N 635E RL 9956 |
| 109. CHIP SAMPLES AT 18 IN. INTERVALS ACROSS ROSEBERY OREBODY, 14 LEVEL, E LENS, 14S2NN STOPE, 210N RL 9868, FOOTWALL 855E. | | | | | | | | | | | |
| 100711 | PY | 5 | 9 | 5 | 9 | 0.51 | | | | 1 FT. INTO FOOTWALL. | 100%PY. PS |
| 100712 | ORE | 4 | 16 | 3 | 13 | 0.26 | | | | AT FOOTWALL. | 24% PY, 8% CPY, 34% SL. XRF |
| 100712 | PY | 9 | 36 | 6 | 26 | 0.24 | | | | | 93% PY, 2% SL, 5% GA. PS |
| 100713 | ORE | 148 | 5 | 147 | 5 | 30.91 | | | | | 58% PY, 15% CPY,25% SL. XRF |
| 100713 | PY | 190 | 6 | 189 | 6 | 29.91 | | | | | 97% PY. PS |
| 100714 | ORE | 3 | 6 | 3 | 5 | 0.60 | | | | | 34% PY, 1% CPY,53% SL. XRF |
| 100714 | PY | 8 | 8 | 8 | 8 | 0.99 | | | | | 85% PY. PS |
| 100715 | ORE | 8 | 15 | 7 | 13 | 0.55 | | | | | 24% PY, 2% CPY,46% SL. XRF |
| 100715 | PY | 23 | 31 | 21 | 28 | 0.74 | | | | | 85% PY. PS |
| 100716 | ORE | 8 | 9 | 7 | 8 | 0.86 | | | | | 43% PY, 2% CPY,33% SL. XRF |

| SAMPLE | MIN | CO1 | NI1 | CO2 | NI2 | CO/NI | SE | SE/S | DS34 | FT | COMMENT |
|---|---|---|---|---|---|---|---|---|---|---|---|
| 100716 | PY | 25 | 18 | 9 | 6 | 1.42 | | | | | 80% PY. PS |
| 100717 | ORE | 33 | 7 | 31 | 6 | 4.93 | | | | | 81% PY,10% CPY, 7% SL. XRF |
| 100717 | PY | 29 | 7 | 26 | 7 | 3.96 | | | | | 100%PY. PS |
| 100718 | ORE | 108 | 11 | 88 | 9 | 10.19 | | | | | 45% PY, 2% CPY,15% SL. XRF |
| 100718 | PY | 80 | 22 | 27 | 7 | 3.68 | | | | | |
| 100719 | ORE | 107 | 11 | 64 | 7 | 9.41 | | | | | 26% PY,11% CPY,11% SL. XRF |
| 100719 | PY | 143 | 17 | 102 | 12 | 8.39 | | | | | 89% PY, 9% GA. PS |
| 100720 | ORE | 13 | 9 | 7 | 5 | 1.41 | | | | | 10% PY,12% CPY,19% SL. XRF |
| 100720 | PY | 21 | 9 | 15 | 7 | 2.26 | | | | | 85% PY. PS |
| 100721 | ORE | 36 | 17 | 29 | 14 | 2.11 | | | | | 88% PY, 9% CPY. XRF |
| 100721 | PY | 60 | 15 | 59 | 15 | 3.94 | | | | AT HANGINGWALL. | 100%PY. PS |
| 110. CHIP SAMPLES AT 18 IN. INTERVALS ACROSS ROSEBERY OREBODY, 14 LEVEL, E LENS, 14S2NS STOPE, 130N RL 9868, FOOTWALL 855E. | | | | | | | | | | | |
| 100722 | ORE | 185 | 18 | 166 | 16 | 10.25 | | | | AT FOOTWALL. | 86% PY,<1% CPY,<1% SL. XRF |
| 100722 | PY | 153 | 11 | 135 | 10 | 13.57 | | | | | 100%PY. PS |
| 100723 | ORE | 12 | 26 | 9 | 19 | 0.46 | | | | | 20% PY,<1% CPY,51% SL. XRF |
| 100723 | PY | 26 | 82 | 23 | 73 | 0.32 | | | | | 75% PY. PS |
| 100724 | ORE | 246 | 21 | 242 | 20 | 11.81 | | | | | 81% PY, 8% CPY, 5% SL. XRF |
| 100724 | PY | 321 | 16 | 316 | 15 | 20.41 | | | | | 95% PY, 2% CPY, 2% SL. PS |
| 100725 | ORE | 25 | 18 | 18 | 13 | 1.38 | | | | | 47% PY, 9% CPY,12% SL. XRF |
| 100725 | PY | 42 | 29 | 42 | 29 | 1.46 | | | | | 98% PY, 1% CPY, 1% SL. PS |
| 100726 | ORE | 96 | 13 | 88 | 12 | 7.52 | | | | | 52% PY,12% CPY,27% SL. XRF |
| 100726 | PY | 145 | 21 | 143 | 20 | 6.98 | | | | | 93% PY, 7% SL. PS |
| 100727 | ORE | 159 | 14 | 152 | 13 | 11.73 | | | | | 65% PY,22% CPY, 3% SL. XRF |
| 100727 | PY | 240 | 37 | 197 | 30 | 6.52 | | | | | 96% PY, 2% CPY, 2% SL. PS |
| 100728 | ORE | 353 | 19 | 349 | 19 | 18.16 | | | | | 72% PY, 7% CPY,14% SL. XRF |
| 100728 | PY | 253 | 33 | 251 | 33 | 7.70 | | | | | 90% PY,10% SL. PS |
| 100729 | ORE | 250 | 12 | 248 | 12 | 20.32 | | | | | 68% PY, 7% CPY,20% SL. XRF |
| 100729 | PY | 285 | 23 | 284 | 23 | 12.15 | | | | | 80% PY. PS |
| 111. MASSIVE PYRITIC ORE, 14 LEVEL, FOOTWALL OF E LENS, ROSEBERY MINE. S DRIVE, 250N, 900E RL 9815. | | | | | | | | | | | |
| 100339 | PY | 7 | 10 | 6 | 10 | 0.64 | 31 | 5.81 | | | |
| 100340 | PY | 3 | 10 | 3 | 10 | 0.27 | | | | | |
| 100341 | PY | 38 | 11 | 35 | 10 | 3.43 | | | | | |

| SAMPLE | MIN | CO1 | NI1 | CO2 | NI2 | CO/NI | SE | SE/S | DS34 | FT | COMMENT |
|---|---|---|---|---|---|---|---|---|---|---|---|
| 100342 | PY | 4 | 5 | 4 | 5 | 0.87 | | | | | |
| 100343 | PY | 24 | 9 | 22 | 9 | 2.58 | | | | | |
| 100344A | PY | 5 | 9 | 4 | 8 | 0.49 | | | | | |
| 100344B | PY | 4 | 5 | 4 | 5 | 0.73 | | | | | |
| 100345A | PY | 3 | 4 | 2 | 4 | 0.63 | | | | | |
| 100345B | PY | | | | | | 10 | 1.87 | | | |
| 100347A | PY | | | | | | 2 | 0.37 | | | |
| 112. COARSE GRAINED BANDED PY-CPY ORE, 14 LEVEL, FOOTWALL OF F LENS, ROSEBERY MINE. S4SN SUBLEVEL 320S 1010E RL 9840. | | | | | | | | | | | |
| 100565 | PY | 39 | 5 | 37 | 5 | 8.05 | | | | | |
| 100566 | PY | 107 | 6 | 105 | 6 | 17.87 | | | | | |
| 100567 | PY | 9 | 2 | 9 | 2 | 3.98 | 32 | 5.99 | | | |
| 100568 | PY | 9 | 2 | 9 | 2 | 4.84 | | | | | |
| 113. BANDED SPHALERITIC ORE, AND CROSSCUTTING MASSIVE PYRRHOTITE, 14 LEVEL, F LENS, ROSEBERY MINE. | | | | | | | | | | | |
| 100054 | SL | | | | | | 20 | 6.06 | | | 320S 1010E RL 9840 |
| 100619A | PO | | | | | | 5 | 1.27 | | | * 260S 1020E RL 9840 |
| 100619B | PO | | | | | | 16 | 4.07 | | | |
| 100619C | PO | | | | | | 11 | 2.80 | | | |
| 100620A | PO | | | | | | 16 | 4.07 | | | * 800S 880E RL 9820 |
| 100620B | PO | | | | | | 22 | 5.60 | | | |
| 100620C | PO | | | | | | 16 | 4.07 | | | |
| 114. BANDED PY-CPY ORE, 17 LEVEL, FOOTWALL OF E LENS, ROSEBERY MINE. 547N 1305E RL 9370. | | | | | | | | | | | |
| 100527A | PY-CP | 212 | 6 | 197 | 5 | 36.52 | | | | | |
| 100527B | PY-CP | 223 | 7 | 209 | 6 | 32.41 | | | | | |
| 100527C | PY-CP | 263 | 5 | 248 | 4 | 58.10 | | | | | |
| 100527D | PY-CP | 202 | 8 | 189 | 8 | 25.14 | | | | | |
| 115. BRECCIATED CARBONATE, MARGINAL TO FOOTWALL OF B LENS, 8 LEVEL, ROSEBERY MINE. 3750N, 64E, RL 545. | | | | | | | | | | | |
| 100627 | PY | 1 | 7 | 1 | 7 | 0.10 | | | 32 | DDH | R1596 |

| SAMPLE | MIN | CO1 | NI1 | CO2 | NI2 | CO/NI | SE | SE/S | DS34 | FT | COMMENT |
|---|---|---|---|---|---|---|---|---|---|---|---|
| 116. VEIN CUTTING ROSEBERY HANGINGWALL DARK GREY SHALE (SET 6), ROSEBERY MINE. | | | | | | | | | | | |
| 100657 | PO | 160 | 848 | 119 | 630 | 0.19 | | | | 720 | DDH R1651 |
| 117. PYRITIC ORE, COARSE GRAINED MASSIVE SPHALERITE AND BANDED SPHALERITE, AND MASSIVE CHALCOPYRITE. HERCULES MINE, WILLIAMSFORD, 4 ML. S. OF ROSEBERY. | | | | | | | | | | | |
| 33887A | PY | 3 | 6 | 3 | 5 | 0.59 | 5 | 0.96 | | | * PYRITIC ORE |
| 33887B | PY | 4 | 11 | 3 | 10 | 0.32 | 19 | 3.56 | +11.7 | | |
| 33888A | PY | 2 | 198 | 2 | 195 | 0.01 | 8 | 1.50 | +12.8 | | |
| 33888B | PY | 3 | 19 | 3 | 19 | 0.15 | | | +13.2 | | |
| 100043 | SL | | | | | | 18 | 5.45 | | | * COARSE GRAINED, MASSIVE |
| 100044 | SL | | | | | | 0 | 0.0 | | | |
| 100045 | SL | | | | | | 6 | 1.82 | | | |
| 100046 | SL | | | | | | 6 | 1.82 | | | * BANDED |
| 100047 | SL | | | | | | 0 | 0.0 | | | |
| 100048 | SL | | | | | | 11 | 3.33 | | | |
| 100049 | SL | | | | | | 4 | 1.21 | | | |
| 100201A | CPY | 33 | 9 | 33 | 9 | 3.76 | | | | | * MASSIVE |
| 100201B | CPY | | | | | | 4 | 1.14 | | | |
| 100196 | PY | 0 | 6 | 0 | 6 | 0.0 | | | | | PYRITIC ORE |
| 118. BANDED SPHALERITE-GALENA VEIN IN CAMBRIAN DYKE, MAGNET MINE, 2 ML. WSW. OF MT. BISCHOFF. | | | | | | | | | | | |
| 100032 | SL | | | | | | 17 | 5.15 | | | |
| 100033 | SL | | | | | | 8 | 2.42 | | | |
| 100034 | SL | | | | | | 8 | 2.42 | | | |
| 119. LARGE CUBES IN SKARN, SHEPHERD AND MURPHY MINE, MOINA. | | | | | | | | | | | |
| 100585 | PY | 243 | 108 | 233 | 104 | 2.25 | | | | | |
| 100586 | PY | 298 | 92 | 287 | 88 | 3.25 | 17 | 3.18 | | | |
| 120. MT. REMUS MO PROSPECT. | | | | | | | | | | | |
| 100623A | PY | 3030 | 19 | 2885 | 18 | 156.37 | | | | | |
| 100623B | PY | 3034 | 21 | 2928 | 20 | 147.31 | | | | | |
| 100623C | PY | 3042 | 19 | 2935 | 18 | 164.05 | | | | | |

| SAMPLE | MIN | CO1 | NI1 | CO2 | NI2 | CO/NI | SE | SE/S | DS34 | FT | COMMENT |
|---|---|---|---|---|---|---|---|---|---|---|---|
| 121. VEINS IN CAMBRIAN(?) SHALES, STIRLING VALLEY MINE, S. OF TULLAH. NO. 1 LEVEL ADIT DUMP. | | | | | | | | | | | |
| 100649A | PY | 9 | 37 | 9 | 36 | 0.25 | | | | | BRECCIA-VEIN IN SHALE |
| 100649B | ASPY | 33 | 41 | 30 | 38 | 0.81 | | | | | |
| 100650A | PY | 488 | 1247 | 478 | 1221 | 0.39 | | | | | MILKY QUARTZ VEIN |
| 100650B | PY | 356 | 1453 | 345 | 1408 | 0.24 | 81 | 15.17 | | | |
| 122. VEIN IN MT. READ VOLCANICS, TULLAH AG-PB MINE, S. OF TULLAH. UPPER NO. 1 ADIT DUMP. | | | | | | | | | | | |
| 100651 | PY | 449 | 530 | 375 | 443 | 0.85 | | | | | |
| 123. VEIN IN CAMBRIAN(?) SHALES, MURCHISON MINE, S. OF TULLAH. 2 LEVEL. | | | | | | | | | | | |
| 10528 | PY | 11 | 7 | 8 | 5 | 1.69 | | | | | |
| 124. VEINS IN CAMBRIAN(?) SHALES, NEW NORTH MT. FARRELL MINE, TULLAH. | | | | | | | | | | | |
| 10438A | CPY | | | | | | | | +15.3 | | |
| 10438B | CPY | | | | | | | | +15.6 | | |
| 10438C | CPY | | | | | | 17 | 4.86 | | | |
| 10523A | CPY | | | | | | 321 | 91.71 | | | * 9 LEVEL |
| 10523B | SL | | | | | | 10 | 3.03 | | | |
| 10730 | CPY | | | | | | 6 | 1.71 | | | * 8 LEVEL |
| 100035 | SL | | | | | | 15 | 4.55 | | | |
| 100036 | SL | | | | | | 0 | 0.0 | | | |
| 100645 | PY | 29 | 283 | 28 | 267 | 0.10 | | | | | * 7-9 LEVELS DUMP |
| 100646 | PY | 80 | 804 | 78 | 779 | 0.10 | 23 | 4.31 | | | |
| 100647 | PY | 29 | 243 | 28 | 236 | 0.12 | 32 | 5.99 | | | |
| 100648 | PY | 72 | 861 | 70 | 835 | 0.08 | | | | | |
| 125. VEINS IN MT. READ VOLCANICS, BLACK P.A., W. OF ROSEBERY MINE. | | | | | | | | | | | |
| 31434 | PY | 8 | 35 | 7 | 32 | 0.22 | 18 | 3.37 | | | |
| 100558 | PY | 1 | 5 | 1 | 4 | 0.13 | 13 | 2.43 | | | |
| 126. DISSEMINATED IN THE NATONE VOLCANICS, ROSEBERY SERIES. WILLIAMSFORD ROAD, 2 ML. S. OF ROSEBERY. | | | | | | | | | | | |
| 100557 | PY | 73 | 277 | 66 | 250 | 0.26 | 6 | 1.12 | | | |

| SAMPLE | MIN | CO1 | NI1 | CO2 | NI2 | CO/NI | SE | SE/S | DS34 | FT | COMMENT |
|---|---|---|---|---|---|---|---|---|---|---|---|
| 127. DISSEMINATED IN SHALE, AND MASSIVE, LAKE GEORGE MINE, CAPTAINS FLAT, NEW SOUTH WALES. | | | | | | | | | | | |
| 100603 | PY | 183 | 26 | 176 | 25 | 6.98 | | | | | BANDED IN SHALE |
| 100604 | PY | 23 | 15 | 18 | 12 | 1.55 | | | | | * MEDIUM-FINE GRAINED |
| 100605 | PY | 39 | 17 | 37 | 16 | 2.36 | | | | | |
| 100606 | PY | 78 | 25 | 64 | 20 | 3.19 | | | | | BANDED IN SHALE |
| 100607 | PY | 67 | 23 | 64 | 21 | 2.96 | | | | | MASSIVE WITH CARBONATE |
| 100608 | PY | 47 | 21 | 41 | 18 | 2.27 | | | | | BANDED IN SHALE |
| 100609 | PY | 53 | 12 | 53 | 12 | 4.27 | | | | | MASSIVE |
| 100610 | PY | 27 | 9 | 27 | 9 | 2.91 | | | | | DISSEMINATED IN SHALE |
| 128. VARIOUS LODES, CLEVELAND MINE, LUINA. DEVONIAN. DISSEMINATED IN QUARTZ-CARBONATE GANGUE. NUMBERS REFER TO THE ROCK COLLECTION, TASMANIAN DEPARTMENT OF MINES. | | | | | | | | | | | |
| 62-404 | PO | 122 | 69 | 114 | 64 | 1.78 | | | | | *DRILLCORE |
| 62-405A | PO | 182 | 68 | 164 | 62 | 2.67 | | | | | |
| 62-405B | PO | 204 | 75 | 173 | 64 | 2.72 | | | | | |
| 62-406 | PO | 187 | 80 | 173 | 74 | 2.34 | | | | | |
| 62-406A | PO | 186 | 75 | 174 | 70 | 2.47 | | | | | |
| 62-406B | PO | 195 | 74 | 177 | 67 | 2.64 | | | | | |
| 62-409 | PO | 106 | 61 | 92 | 53 | 1.72 | | | | | |
| 62-413 | PO | 63 | 88 | 56 | 78 | 0.71 | | | | | |
| 129. PRIMARY BEDDED DOLOMITE HOST-ROCK, MT. BISCHOFF OPEN CUT. DEVONIAN. | | | | | | | | | | | |
| 100207 | DOL | 13 | 25 | 12 | 24 | 0.50 | | | | 13 | DDH NO. 5 |
| 100208 | DOL | 13 | 22 | 12 | 21 | 0.59 | | | | | S. END, OPEN CUT |
| 130. MASSIVE, REPLACING DOLOMITE, S. END, MT. BISCHOFF OPEN CUT. DEVONIAN. | | | | | | | | | | | |
| 100209 | CA-R | 14 | 12 | 14 | 12 | 1.15 | | | | | * MANGANIFEROUS SIDERITE |
| 100210 | CA-R | 20 | 20 | 19 | 19 | 1.02 | | | | | |
| 100211 | CA-R | 9 | 14 | 8 | 13 | 0.61 | | | | | * MANGANIFEROUS PISTOMACITE |
| 100219 | CA-R | 14 | 15 | 14 | 14 | 0.96 | | | | | |
| 101028A | PY | 12 | 5 | 12 | 5 | 2.20 | | | | 90 | DDH B2, GREISEN FACE |
| 101028B | PY | 8 | 7 | 8 | 7 | 1.12 | | | | | |
| 101030A | PY | 0 | 4 | 0 | 4 | 0.0 | | | | 10 | DDH B24, S. END, OPEN CUT |
| 101030B | PY | 1 | 3 | 1 | 3 | 0.28 | | | | | |
| 101032A | ASPY | 73 | 4 | 73 | 4 | 20.08 | | | | | SLAUGHTERYARD LODE |
| 101032B | ASPY | 75 | 8 | 74 | 7 | 9.88 | | | | | |

| SAMPLE | MIN | CO1 | NI1 | CO2 | NI2 | CO/NI | SE | SE/S | DS34 | FT | COMMENT |
|---|---|---|---|---|---|---|---|---|---|---|---|
| 131. VEINS, IN DRILLHOLES, MT. BISCHOFF OPEN CUT. DEVONIAN. | | | | | | | | | | | |
| 101026A | PO | 5 | 55 | 5 | 55 | 0.09 | | | | 275 | DDH B50 NEAR GIBLIN LODE |
| 101026B | PO | 3 | 53 | 3 | 53 | 0.06 | | | | | |
| 101024A | PO | 4 | 7 | 3 | 7 | 0.49 | | | | 436 | DDH B22 S. END, OPEN CUT |
| 101024B | PO | 8 | 7 | 8 | 7 | 1.18 | | | | | |
| 101015A | PO | 2 | 29 | 2 | 29 | 0.06 | | | | 17 | DDH B54 NEAR BROWN FACE |
| 101015B | PO | 3 | 30 | 3 | 30 | 0.10 | | | | | |
| 101016B | PO | 2 | 5 | 2 | 5 | 0.33 | | | | 23 | DDH B49 NEAR GIBLIN LODE |
| 101016C | ASPY | 35 | 16 | 35 | 16 | 2.24 | | | | | |
| 101018A | ASPY | 99 | 7 | 98 | 7 | 13.77 | | | | 593 | DDH B54 BENEATH DOLOMITE |
| 101018B | ASPY | 104 | 16 | 102 | 16 | 6.37 | | | | | |
| 101022 | ASPY | 28 | 3 | 28 | 3 | 8.77 | | | | 283 | DDH B50 NEAR GIBLIN LODE |
| 132. VEIN CARBONATE, LODES S. AND W. OF MT. BISCHOFF OPEN CUT. DEVONIAN. | | | | | | | | | | | |
| 100217 | CA-V | 23 | 17 | 23 | 17 | 1.36 | | | | | SIDERITE. THOMPSONS LODE |
| 100218 | CA-V | 14 | 16 | 14 | 16 | 0.88 | | | | | MANGANOSIDERITE. SILVER CLIFFS MINE |

## COBALT AND NICKEL ANALYSES

### Sedimentary-Diagenetic

Pyrite which was confidently interpreted from field and textural evidence to have been originally syngenetic with host sediments was sampled from Tasmanian rocks of different ages, lithologies and degrees of lithification and metamorphism. A summary of the field and textural data is given in Table 6.1 (sets 2-17) and in Table 6.2. All samples were shown by X-ray diffraction or mineragraphy to be pyrite, except for one specimen in set 2 which contained some marcasite.

Some of the samples are somewhat unusual:

(a) The South Mt. Cameron (set 15) and King Island (set 17) samples were included only for comparative purposes; both are terrestrial, whereas all the other pyrites are thought to be marine, and the King Island pyrite at least is probably not syngenetic.

(b) There is a possibility that not all the pyrite in some of the Rosebery hangingwall shale samples (set 6) is primary sedimentary, as it proved difficult to remove all traces of minute cross-cutting pyritic quartz veinlets. However sample nos. 100521-100522 are of pure segregated lenses.

The Co and Ni analyses are illustrated in Figure 6.1. Many of the fields are elongate approximately parallel to lines of constant Co/Ni ratio, indicating intake of Co and Ni by the crystallizing or re-crystallizing sulphide from a constant Co-Ni supply. Because of the wide sample spacing (tens of yards) within many sample sets, this must

Figure 6.1

Co and Ni in sedimentary-diagenetic pyrites.

(a) The pyrite sets illustrated in Figure 6.2.

5 : Hangingwall shale, Hercules Mine, Williamsford. Cambrian (?).

9 : Munro Creek Slate and Quartzite, Rosebery. Cambrian (?).

12 : Siltstone, Que River. Middle Cambrian.

14 : Woody Island Siltstone, Woody Island and Florentine Valley. Permian.

16 : Unconsolidated sands, Great Mussel Roe Bay. Recent (?).

(b) The remaining pyrite sets, with Trend I being defined by all the sedimentary-diagenetic pyrites.

2 : Siltstone, Rocky Cape Group, Cowrie Point. Precambrian.

3 : Siltstone, Rocky Cape Group, Arthur River. Precambrian.

4 : Siltstone and sandstone, Franklin River. Precambrian.

6 : Hangingwall shale, Rosebery Mine, Rosebery. Cambrian (?).

7 : Host-rock shale, Rosebery Mine, Rosebery. Cambrian (?).

8 : Slate, New North Mt. Farrell Mine, Tullah. Cambrian (?).

10 : Sandstone, near Valentine's Peak. Cambrian (?).

11 : Carbonaceous shale, Branch Creek. Cambrian (?).

13 : Gordon Limestone, Lyell Highway east of Queenstown. Ordovician.

15 : Deep-lead gravel, South Mt. Cameron. Middle Tertiary.

17 : Base of raised beach, King Island. Recent (?).

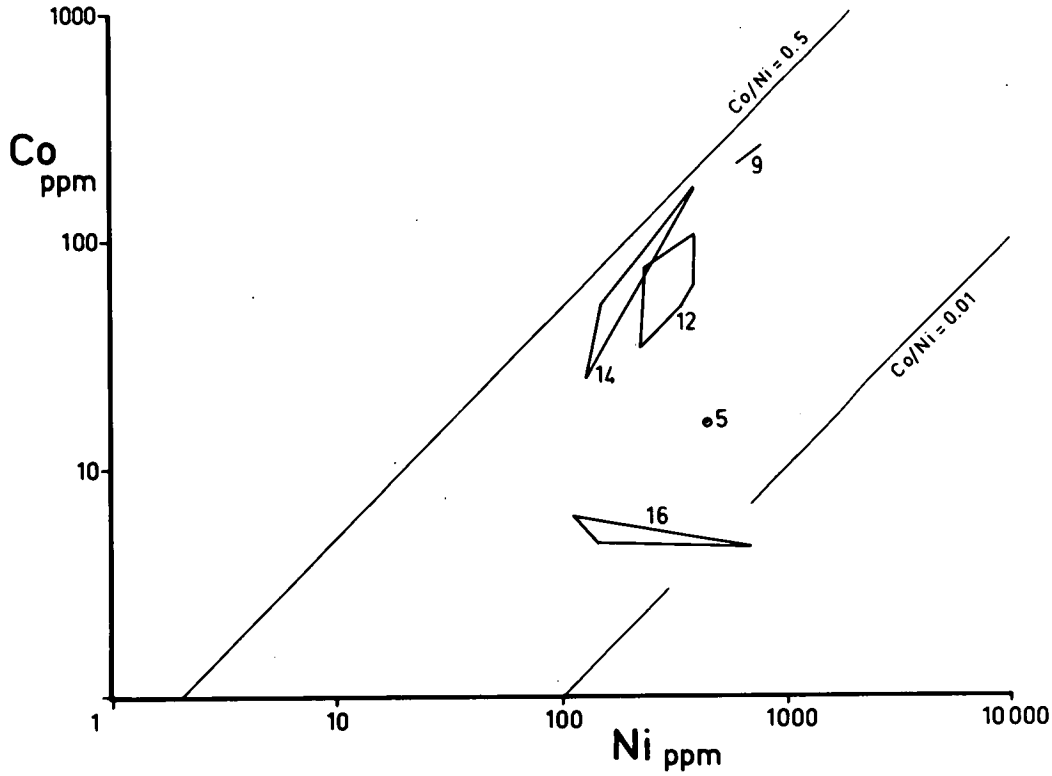
1000
100
10
1
Co
ppm
Co/Ni = 0.5
Co/Ni = 0.01
9
12
14
5
16
10
100
1000
10 000
Ni ppm

(a)

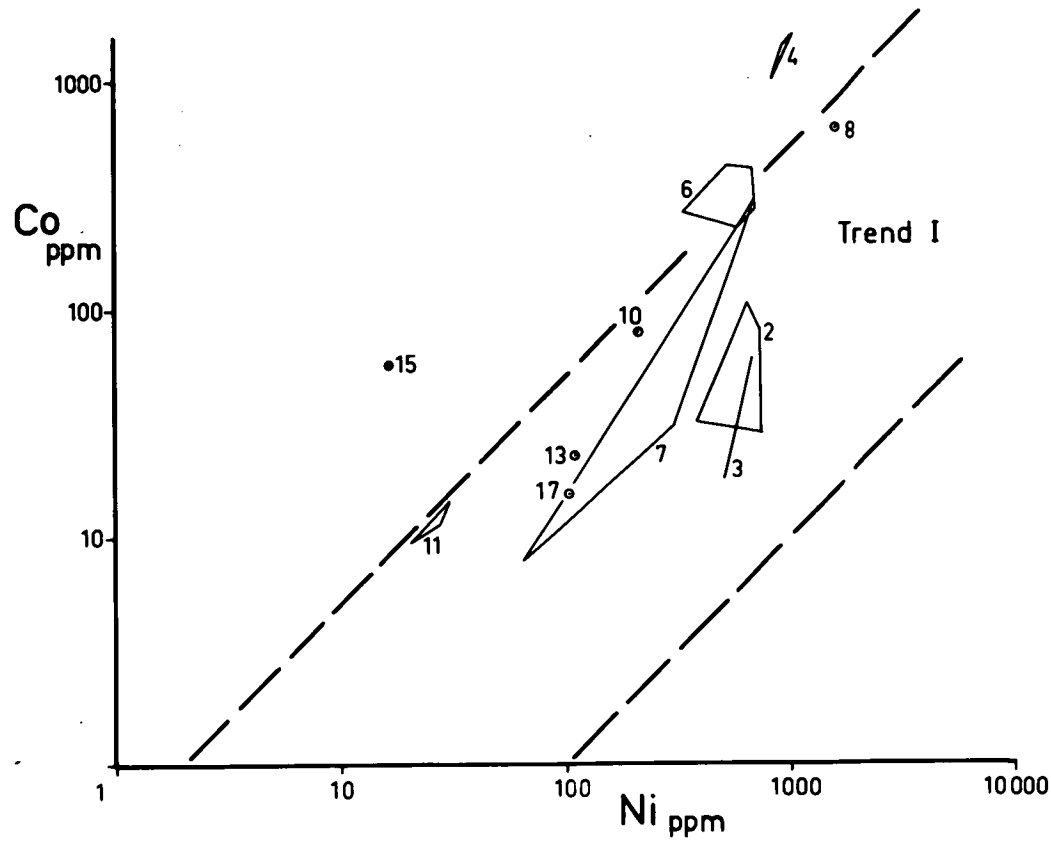
1000
100
10
1
Co
ppm
4
8
6
Trend I
10
2
15
13
7
3
17
11
10
100
1000
10 000
Ni ppm

(b)

TABLE 6.2

TEXTURAL DATA FOR SEDIMENTARY-DIAGENETIC PYRITES

| Set | Name/Locality | Age | Host Rock | Bedding-plane sulphide | Accretions & Nodules | Associated segregations | Metamorphic recrystallization |
|---|---|---|---|---|---|---|---|
| 2,3 | Rocky Cape Gp. | Precamb. | Siltstone | Coarse g. | - | Qtz., chlorite | ? |
| 4 | Franklin River | Precamb. | Shale-sandst. | Coarse g. | - | - | ? |
| 5 | Hercules shale | Camb. | Shale | - | C.-f.g., pure py | - | Yes |
| 6 | Rosebery shale | Camb. | Shale | Fine g. | F.g. lenses | - | No |
| 7 | Rosebery hostrock | Camb. | Shale | - | C.g., pure py | - | ? |
| 8 | Farrell Slate | Camb. | Shale | Very f.g. | - | - | No |
| 9 | Munro Creek | Camb. | Shale | - | F.g., pure py | Qtz., chlorite | ? |
| 10 | Valentine's Pk. | Camb. | Sandstone | Coarse g. | - | - | No |
| 11 | Branch Creek | Camb. | Carb. shale | Medium g. | - | - | Py in joints |
| 12 | Que River | Camb. | Siltstone | Framboids only | Complex, almost pure py | Qtz., chlorite | No |
| 13 | Gordon Limest. | Ordovic. | Limestone | - | F.g. | - | No |
| 14 | Woody Island | Permian | Siltstone | - | Very f.g., impure | - | No |
| 15 | Sth. Mt. Cameron | Tertiary | Gravel | F.g., interstitial | | - | No |
| 16 | Gt. Mussel Roe Bay | Recent ? | Sand | - | 50% qtz. sand | - | No |
| 17 | King Island | Recent ? | C.g. silt | - | 10% qtz. silt | - | No |

reflect quite a large scale uniformity of trace element availability within some sediments. This conclusion is supported by the similarity of Co-Ni values in Rocky Cape Group pyrites samples 16 miles apart (sets 2 and 3).

The fields lie below the line Co/Ni = 0.5, with the exception of sets 4 and 15, which are discussed below:

(i) The Franklin River samples (set 4) are from three different rock types containing pyrite of different grain-size, yet all show a major enrichment in Co. Although dolerite, presumably Precambrian, intrudes the Precambrian sediments within 400 yards of the sampling site (A.B. Gulline, pers. comm.), no satisfactory explanation can at present be given for this enrichment. The only other Tasmanian pyrite with similar composition is that from the Savage River magnetite deposit (set 18), the host rocks of which are probably metamorphosed Precambrian dolerites.

(ii) Interpretation of the Co-rich deep-lead pyrite from South Mt. Cameron (set 15) must await further analyses of this material.

Apart from the above sets, the Co-Ni concentrations generally fall within the ranges listed in Chapter 3 (Table 3.3) for sedimentary pyrites. The marked exception is that pyrite from the highly carbonaceous shale at Branch Creek (set 11) shows very low Co and Ni values. Although this anomaly requires further investigation with more samples, the following possible explanation is proposed. In Table 6.3 are listed some preliminary analyses by C.E. Gee (Geology Department, University of Tasmania) of the sedimentary formations from which sample sets 6, 12 and 11 were taken. Assuming that all the Fe in the sediment was present as $FeS_2$ which had the average Ni composition determined in this study, partition

TABLE 6.3

ANALYTICAL DATA - ROSEBERY MINE HANGINGWALL SHALE, QUE RIVER SILTSTONE, AND BRANCH CREEK SHALE

WHOLE ROCK : Analyses by C.E. Gee. The Fe and C analyses have been verified by independent analyses by CSIRO, Melbourne.
Fe, Co, and Ni by XRF Spectrography.
C = non-carbonate C, from total $CO_2$ (combustion at 1100°C) minus carbonate $CO_2$ (phosphoric acid method).

| | Rosebery hanging-wall shale | Que River siltstone | Branch Creek shale | |
|---|---|---|---|---|
| WHOLE ROCK | | | BC9 | BC15 |
| Fe% | 5.02 (20)* | 5.56 (3) | 2.98 | 7.13 |
| C% | 0.45 (15) | 0.82 (2) | 7.84 | 23.30 |
| Co ppm | < 20 (20) | < 20 (3) | < 20 | < 20 |
| Ni ppm | 63 (20) | 84 (3) | 93 | 280 |
| PYRITE | Set 6 (5) | Set 12 (9) | Set 11 (2) | |
| Co ppm | 315 | 64 | 12 | |
| Ni ppm | 557 | 320 | 25 | |
| PARTITION** | | | | |
| $Ni_{non\text{-}py}$ | 3 | 52 | 186 | |
| $\frac{Ni_{non\text{-}py}}{Ni_{py}}$ | 0.01 | 0.16 | 7.44 | |

* Number of samples averaged.

** Calculated assuming all Fe occurs as $FeS_2$.

of Ni between the pyrite and non-pyrite fractions could be calculated. Two correlations are evident:

(a) In the Branch Creek shale, the total Ni content is approximately proportional to the non-carbonate C content.

(b) The partition factor $Ni_{non\text{-}py}/Ni_{py}$ in the three rocks is also approximately proportional to the non-carbonate C content.

This preliminary evidence not only supports the contention that the original Ni content of a carbonaceous shale can be mainly a function of the content of carbonaceous material, but suggests that for constant Fe content and metamorphic grade (as allowed by this study) the pyrite phase will sequester a successively smaller proportion of the available Ni as the carbonaceous content increases, the balance presumably being bonded to the carbonaceous fraction.

The Co-Ni values do not appear to correlate with the age of the sediments, but in view of the results of previous workers, correlations were sought between trace element content and metamorphic grade. As most of the sediments studied were relatively unmetamorphosed, an attempt was made to relate Co-Ni content to the extent of recrystallization of pyrite nodules. Because of the great variation observed in original sedimentary textures, criteria for the extent of modification of the textures during diagenesis or metamorphism were almost impossible to define. Progressive increase in grain size and ejection of impurities from nodules and crystals probably occur during recrystallization (Pettijohn, 1956, p.203), but the initial variability of these parameters precludes the assigning of a texture to a particular stage of recrystallization. This study suggests that very little modification

of original textures occurs until the sediment is quite strongly metamorphosed, because examples "a" (Recent) to "d" (Cambrian) in Figure 6.2 could all be original textures, and framboids are preserved in the Cambrian sediments (and of course in much older sediments elsewhere). On the other hand, it is only in some of the older rocks (Que River siltstone; Munro Creek Slate and Quartzite; Rocky Cape Group) that chlorite* (and sometimes quartz*, and possibly carbonaceous material) is found intimately associated with the pyrite, sometimes in the form of pressure shadows. These may be segregated impurities ejected from the pyrite crystals and nodules during recrystallization, which has also been responsible in some of these older rocks for rotating the bedding-plane pyrite into the cleavage. The sequence a-b, c-d, e, in Figure 6.2 could then represent a trend of increasing purification with recrystallization, but such a trend shows no particular correlation with the Co-Ni values.

Metamorphism as distinct from diagenetic recrystallization of a pyrite nodule was established with some certainty in the case of the large nodule in the Hercules shale (set 5; Fig. 6.2e). Plates 6.1 and 6.2 show textures in the outer rim of this nodule which were revealed only after electrolytic etching. Euhedral cores of growth-zoned pyrite occur in grains which may themselves be growth-zoned (Plate 6.2), may show a rim zone (Plates 6.1, 6.2), and often meet at triple-junction points at approximately 120° (Plate 6.1). More than one core may be present in a grain (Plate 6.2). Han (1968) considered textures similar to these (his Figs. 8a, b) to have formed by supergene alteration of

---

* determined by X-ray diffraction.

Figure 6.2

Textures of polished sections of some sedimentary pyrite nodules analysed in this study. The scale bar for each specimen is 0.25 in.

(a) Spherical nodule, Great Mussel Roe Bay; Recent (?); set 16. Black : angular quartz grains. White : pyrite. The nodule is cracked in the centre.

(b) Tubular nodule; Woody Island Siltstone, Woody Island; Permian; set 14. Black : fine-grained quartz. Dark grey : very fine-grained quartz and carbonaceous material. White : pyrite.

(c) Discoidal, flanged (?) recrystallized nodules, with associated siliceous segregations; Que River siltstone; Cambrian; set 12.

(d) (i) Left nodule : Black dots : very fine-grained quartz, possibly with some carbonaceous material. Fine black lines : pyrite crystals. Dark grey : aligned prismatic quartz (by XRD). Hachuring : similarly oriented chlorite (by XRD).

(ii) The right nodule has been micro-faulted and veined by quartz and chlorite in at least two stages.

(d) Typical twin (?) recrystallized nodules from the Munro Creek Slate and Quartzite; Cambrian (?); set 9. Hachuring : chlorite. Dark grey : quartz. Black : carbonaceous material (?).

(e) Large spherical recrystallized nodule; Hercules slate; Cambrian (?); set 5. Heavy black : cracking. Fine black lines : pyrite crystals.

(a)

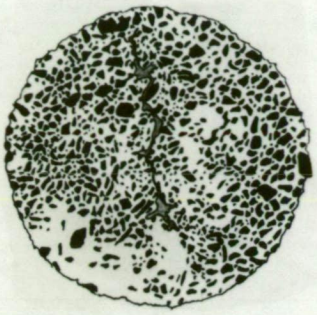

(b)

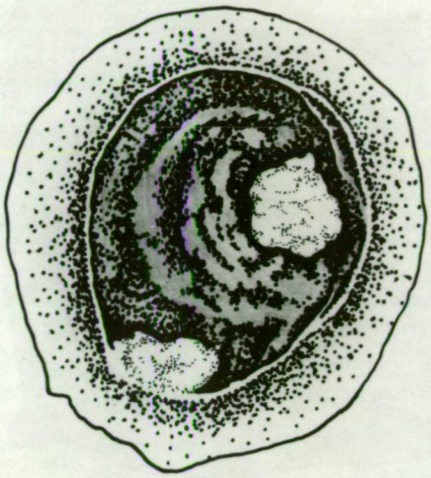

(c)

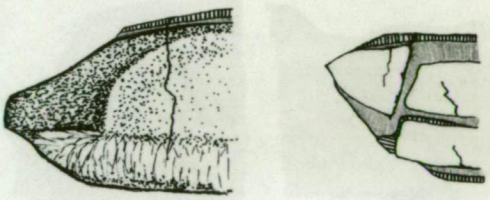

(d)

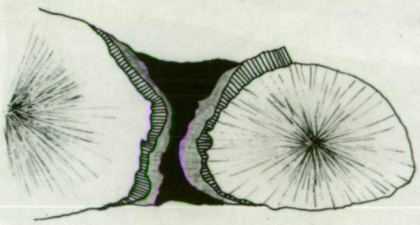

(e)

Plate 6.1

Textures in a sedimentary pyrite nodule (33886) from the Hercules Mine hangingwall shale (set 5). The polished sections have been electrolytically etched.

TOP Pyrite grains, showing rim zones, and a growth-zoned core (x 350).

BOTTOM Enlargement of the growth-zoned core in the top illustration (x 1030).

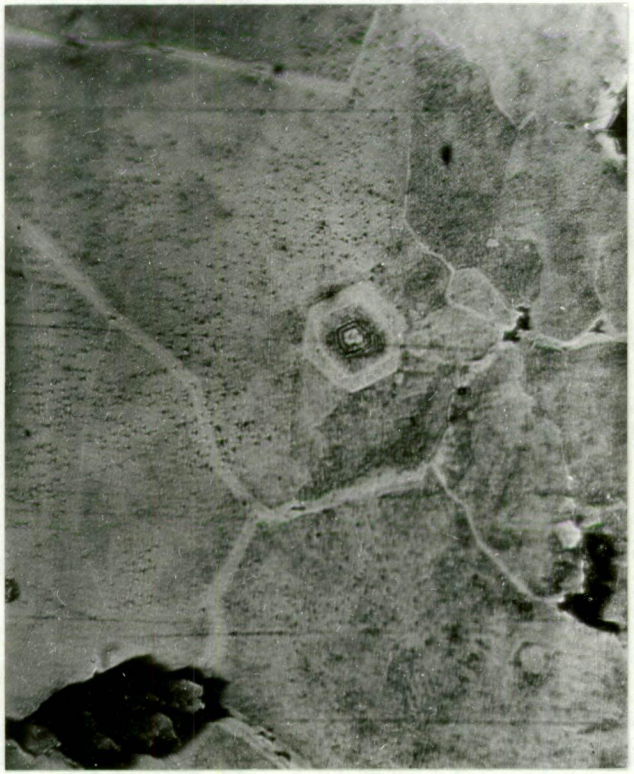

Plate 6.2

Textures in a sedimentary pyrite nodule (33886) from the Hercules Mine hangingwall shale (set 5). The polished sections have been electrolytically etched.

TOP Growth-zoning in both the core and main grain, and thick rim zones. The black areas are cracks, as illustrated in Figure 6.2e (x 425).

BOTTOM Twin growth-zoned cores within one grain (x 755).

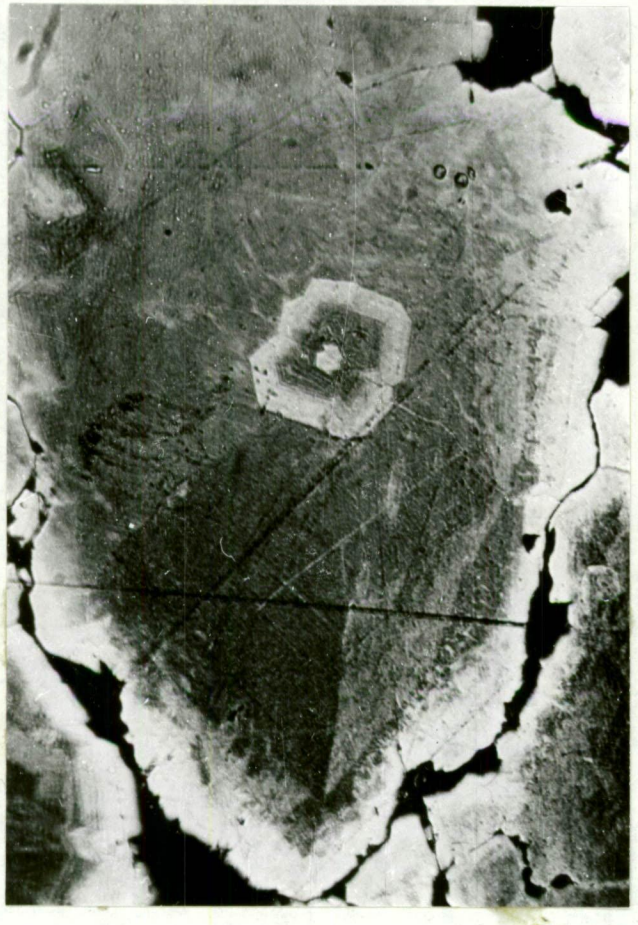

pre-existing core material to form the outer grain. However in the present example it is thought that the euhedral cores, the continuity of the cores with the grain, and the 120° triple-junction points all indicate that the texture is crystalloblastic, developed from an original sedimentary-diagenetic texture, out of which all impurities have been ejected during recrystallization. The central and rim zoning is probably due to compositional variations (cf. Cu-deficient rim zones, in Frenzel and Otteman, 1967, Figs. 2-4), but electron microprobe analysis (Mrs. J.R. Widdowson, for Dr. J.F. Lovering, A.N.U.) revealed Co, Ni and Se contents generally too low for quantitative analysis, the actual values (Table 6.4) showing no correlation with the composition of the sample as a whole (set 5). The cause of the zoning remains undetermined. The metamorphism has not produced atypical Co-Ni values in the nodule, and there is little scope for any Co-enrichment similar to that reported by Cambel and Jarkovsky (1967).

TABLE 6.4

ELECTRON MICROPROBE ANALYSES - HERCULES SHALE PYRITE NODULE

Analyses performed on area of Plate 6.2 (bottom)

| | Co | Ni | Se |
|---|---|---|---|
| Left hand core | 0.08 ± 0.05% | < 0.06% | < 0.11% |
| Right hand core | 0.07 ± 0.05% | < 0.06% | 0.12 ± 0.11% |
| Main unzoned grain | 0.06 ± 0.05% | < 0.06% | 0.25 ± 0.11% |
| Lower limit of detection | 0.04% | 0.06% | 0.11% |

The generalized trend for the Co-Ni values of the Tasmanian sedimentary pyrites is here designated Trend I, and is illustrated in Figure 6.1.

## Precambrian (?) Intramagmatic

The only Tasmanian mineralization which can probably be referred to a Precambrian episode is that at Savage River. Analyses of pyrite and magnetite from the ore are presented in set 18 and Figure 6.3.

## Cambrian Intramagmatic

### Acid-intermediate rocks

Sets 22-24 contain pyrite and hematite from the Cambrian Mt. Read Volcanics, and from veins and disseminations in coeval subvolcanic granites. Of less certain origin are the pyrites in sets 25-26, which are in the Mt. Read Volcanics adjacent to the Rosebery orebody. However all the pyrites form a trend (Trend II in Figure 6.4) of high to very-high Co values, and high Co-Ni ratios. The 0.8% Co in the pyrite from the Powerful Mine is apparently not present as a discrete mineral phase, as no sign of trace minerals could be found by mineragraphic and X-ray diffraction examination.

### Mafic-ultramafic rocks

Ratios of Co/Ni comparable with those obtained by Vogt (1923) and Noddack and Noddack (1931) for primary magmatic sulphides were found in the Cuni pyrrhotite-pentlandite ores (Figure 6.4). The magnetites from

Figure 6.3

Co and Ni in pyrites and magnetites from Savage River (set 18).

Figure 6.4

Co and Ni in pyrites, magnetites, and Cu-Ni ore, from mineralization in Cambrian igneous rocks.

19 : Cu-Ni ore, Cuni.

20 : Pyrite, spilite, Corinna Road.

21 : Magnetite, Tenth Legion, McIvor Hill Gabbro, Zeehan.

22 : Pyrite, Murchison Granite.

23 : Pyrite, Dove Granite (hematite not plotted).

24 : Pyrite, Pender's Prospect, Low Rocky Point (hematite not plotted).

25 : Pyrite, footwall of schisted pyroclastics, Rosebery Mine.

26 : Pyrite, hangingwall massive volcanics of Rosebery Mine.

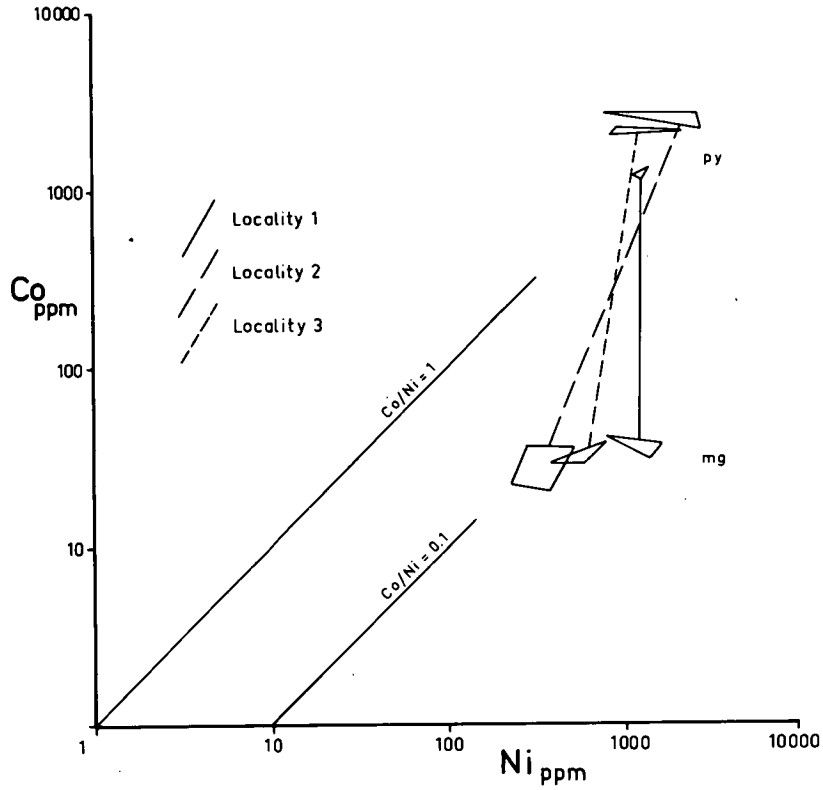
10000
1000
100
10
1
Co ppm
Locality 1
Locality 2
Locality 3
Co/Ni = 1
Co/Ni = 0.1
py
mg
10
100
1000
10000
Ni ppm

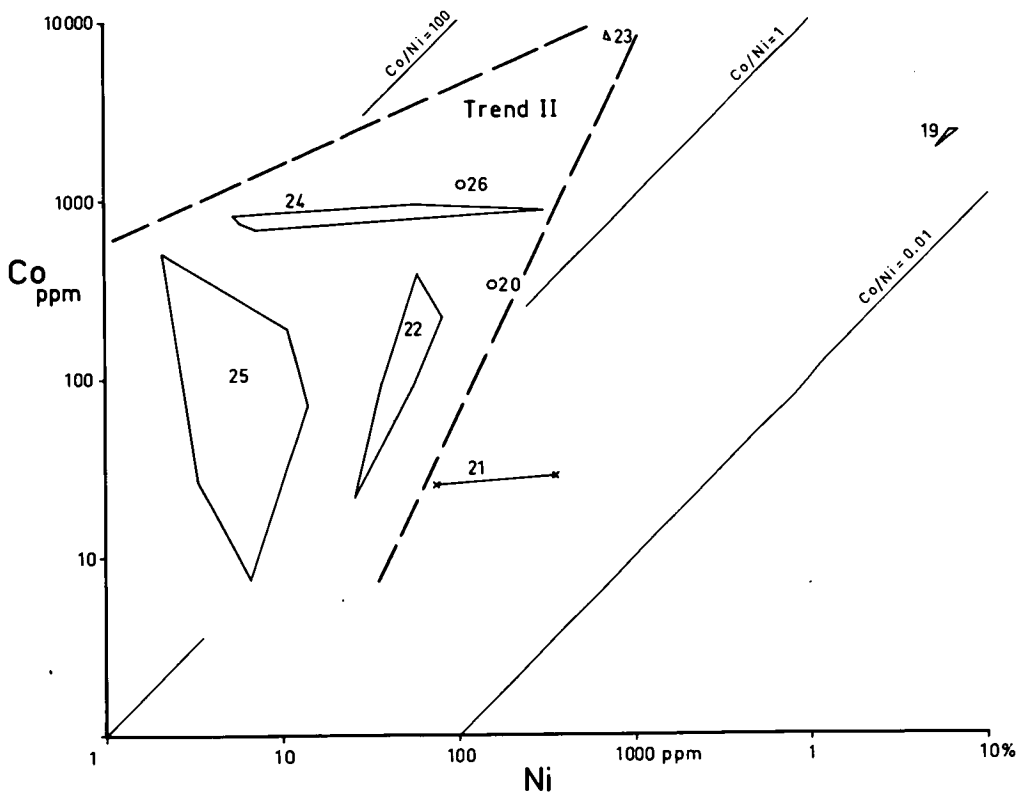
10000
1000
100
10
1
Co ppm
Co/Ni = 100
Trend II
23
Co/Ni = 1
19
24
26
20
22
25
21
Co/Ni = 0.01
10
100
1000 ppm
1
10%
Ni

the Tenth Legion deposit have similar Co/Ni ratios, but the Co and Ni contents are much more like those in the magnetites at Savage River. The spilite pyrite nodules, however, in accordance with their later stage of derivation, are Co-enriched, and actually fall into Trend II defined for the pyrites in acid-intermediate rocks.

## Devonian Intramagmatic and Hydrothermal

The Devonian intramagmatic and hydrothermal vein and replacement deposits are more numerous and cover a wider area than any other category of deposit sampled in this study. Analyses of pyrite, pyrrhotite, and chalcopyrite are summarized in Figures 6.5-6.6, but pyrrhotite and arsenopyrite analyses from Mt. Bischoff and Renison Bell are plotted in Figures 6.21 and 6.22.

These deposits show trends (Fig. 6.6b) to high Ni with low Co/Ni ratio (III), to medium Co with Ni approximately constant (IV), and a negative correlation trend (V). Trend V is followed only by the Heemskirk and Zeehan analyses. Although the analyses of Zeehan pyrites by the writer and Williams (1968) are not coincident, their trends are very similar. The extension of Trends III and V to high Ni values is consistent with (although not caused by) the occurrence of Ni arsenides and sulpharsenides in the Zeehan-Dundas area (Petterd, 1910; Stillwell, 1935; Williams, 1958, 1968; Both, 1966). As Williams (1958) noted, this Ni enrichment could be due to contamination of the Devonian mineralizing fluids by the nickeliferous Cambrian igneous country rocks in the area.

Figure 6.5

Co and Ni in pyrites and pyrrhotites from Devonian ores.

(a) Pyrites from all environments of deposition at Mt. Bischoff (B) and at Renison Bell (R), and pyrrhotites from Cleveland (C). For details see Figures 6.21, 6.22.

(b) Pyrites from the Zeehan-Dundas area.

W : Results of analyses of pyrites from Zeehan by Williams (1968). More details are given in Figure 6.29.

27, 28 : Lodes in the Heemskirk Granite.

58 : Vein, Zeehan-Montana Mine, Zeehan.

59 : Vein, Zeehan-Queen Mine, Zeehan.

60 : Vein, Comet Mine, Dundas.

61 : Vein, South Comet Mine, Dundas.

62 : Vein, West Comet Mine, Dundas.

63 : Vein, Kapi Mine, north Dundas.

65 : Vein, Ramsdale Prospect, north-east Dundas.

66 : Vein, Fahl Mine, north-east Dundas.

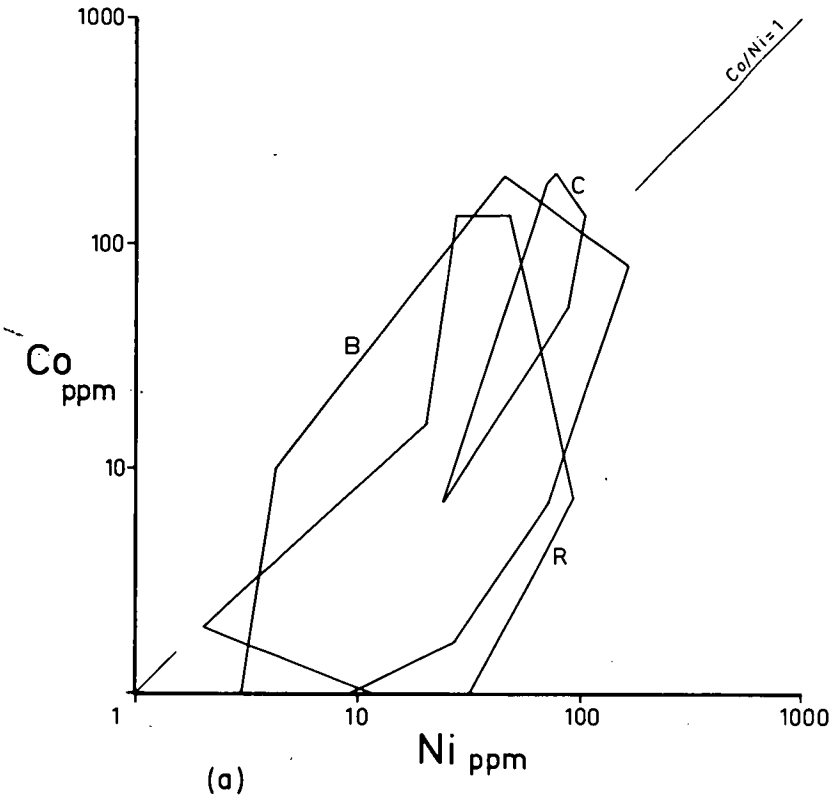
1000
100
10
1
Co ppm
Ni ppm
1
10
100
1000
Co/Ni=1
B
C
R

(a)

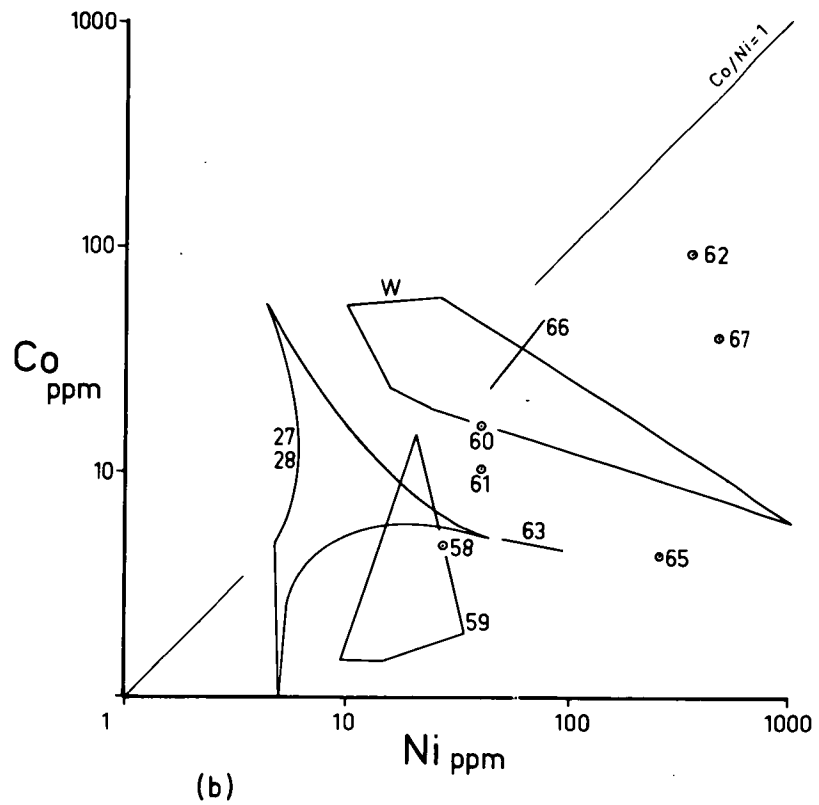
1000
100
10
1
Co ppm
Ni ppm
1
10
100
1000
Co/Ni=1
W
66
62
67
60
61
27
28
63
58
65
59

(b)

Figure 6.6

Co and Ni in pyrites from Devonian ores.

(a) 68 : Vein, Story's Creek, north-eastern Tasmania.

70 : Vein and replacement (?), Round Hill Mine, Moina.

71 : Skarn, Shepherd and Murphy Mine, Moina.

(b) Trends III, IV and V, summarizing the fields of concentration of Co and Ni in pyrites from all the Devonian ores. "C & J" is the field for Czechoslovakian "plutogene hydrothermal" deposits from Cambel and Jarkovsky (1967, Fig. 126).

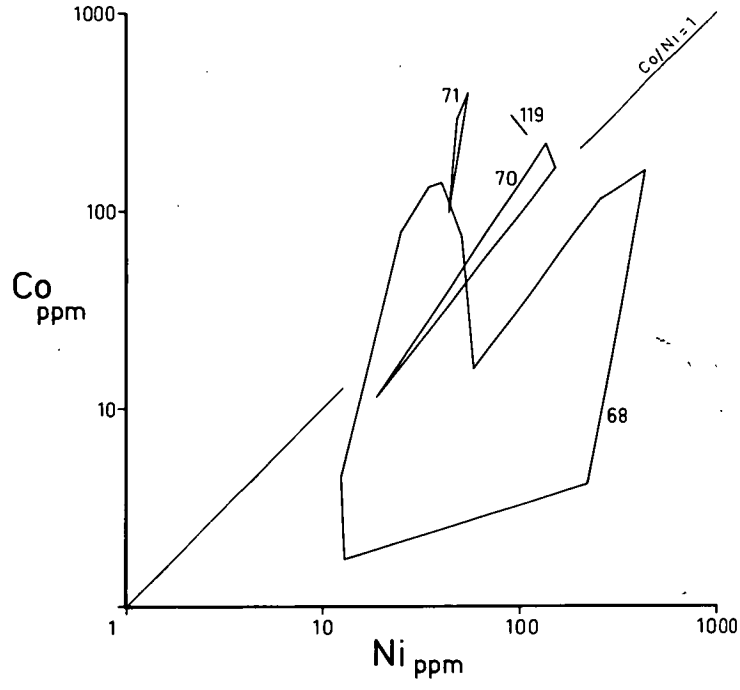
1000
100
10
1
Co ppm
10
100
1000
Ni ppm
Co/Ni = 1
71
119
70
68

(a)

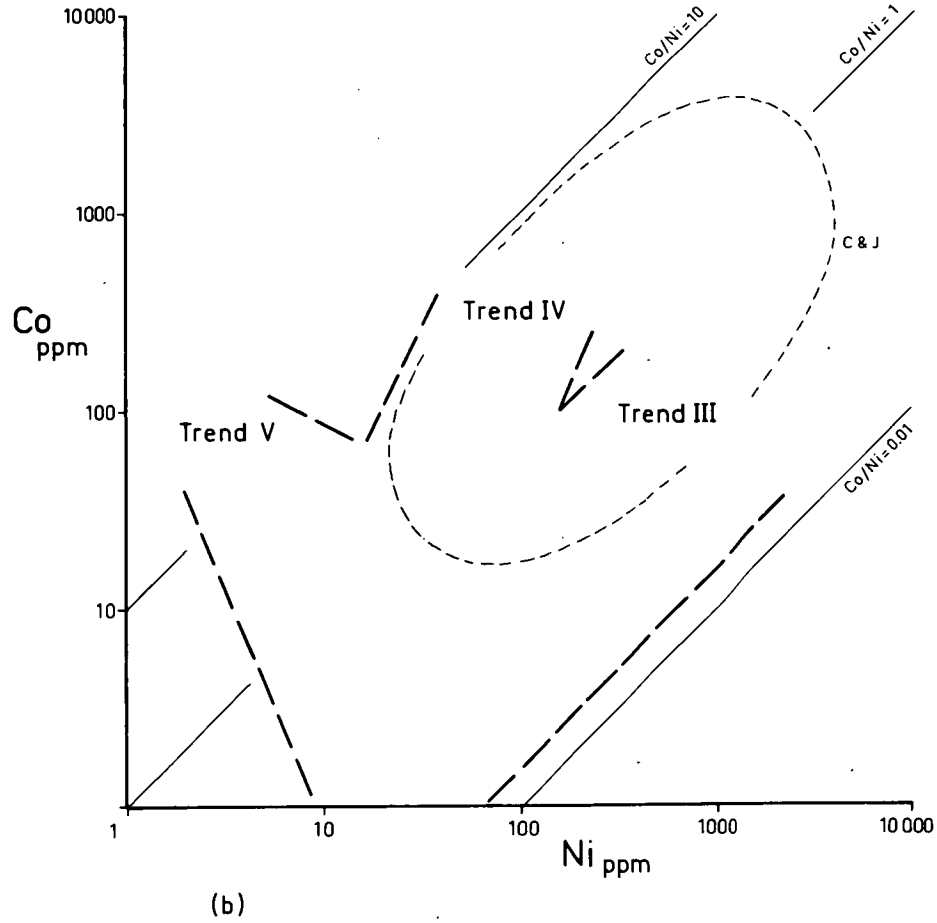
10000
1000
100
10
1
Co ppm
10
100
1000
10 000
Ni ppm
Co/Ni=10
Co/Ni = 1
C & J
Trend IV
Trend III
Trend V
Co/Ni=0.01

(b)

Included in Figure 6.6b for comparison is the trend for Czechoslovakian hydrothermal deposits given by Cambel and Jarkovsky (1967, fig. 126). Their trend is between trends III and IV, and the Tasmanian pyrites have a relative deficiency in both Co and Ni.

## Mt. Lyell

The analyses of pyrites and chalcopyrites have been grouped geographically, then subdivided with respect to mode of occurrence, in Figures 6.7 - 6.8. Although the overall trend shows Co > Ni, both linnaeite and pentlandite have been recorded from these ores (Edwards, 1939). Figure 6.8c includes the trend for Czechoslovakian volcanic pyritic-Cu ores (Cambel and Jarkovsky, 1967, fig. 124).

## Rosebery-Hercules District

The analyses for the sample sets from the main Zn-Pb-Cu lode are given in Figure 6.9. Sets 109-110 are plotted in full in Figure 6.32. The lode analyses have then been generalized and compared with the other mineralization surrounding the lode, in Figure 6.10a. In Figure 6.10b are included the analyses of the Hercules lode, and of the samples from the Black P.A. and the Natone Volcanics.

Figure 6.7

Co and Ni in pyrites and chalcopyrites from the West Lyell area.

(a) Disseminations in schist:

77 : Prince Lyell orebody, Open Cut.

78 : Prince Lyell orebody, DDH WL 229, beneath Open Cut.

79 : Prince Lyell orebody, DDH WL 146, beneath Open Cut.

80 : Prince Lyell orebody, DDH WL 150, beneath Open Cut.

(b) Disseminations in bands in the schistosity:

85 : West of Honeypot orebody (Fig. 5.5), Open Cut.

86 : 10 ft. west of 85.

87 : 42 ft. west of 86.

88 : Honeypot orebody, Open Cut.

(c) Quartz veins formed by remobilization:

81 : Prince Lyell orebody, DDH WL 146, 150, 229.

84 : South-east corner, Open Cut.

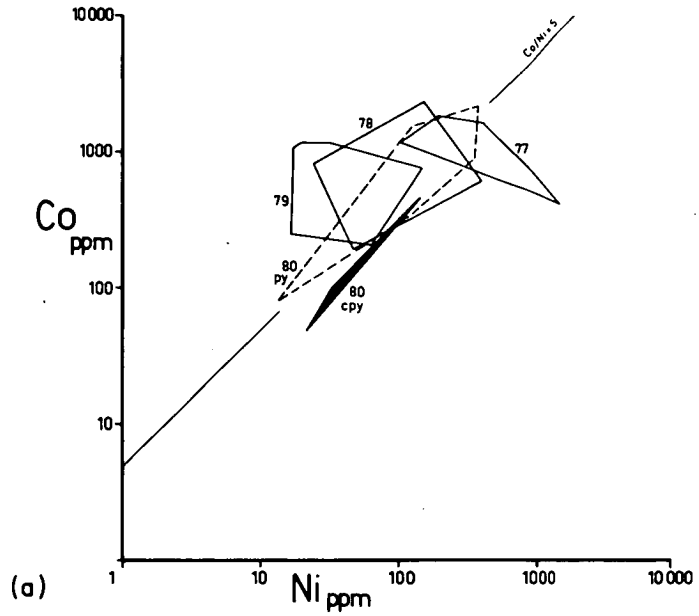
10000
1000
100
10
Co ppm
Co/Ni=5
78
77
79
80 py
80 cpy
1
10
100
1000
10000
Ni ppm

(a)

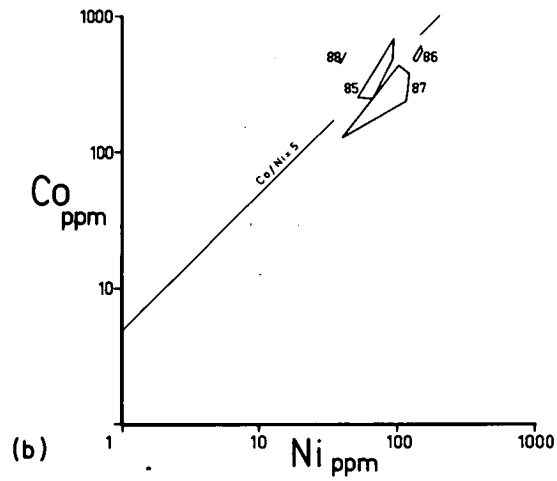
1000
100
10
Co ppm
Co/Ni=5
88
86
85
87
1
10
100
1000
Ni ppm

(b)

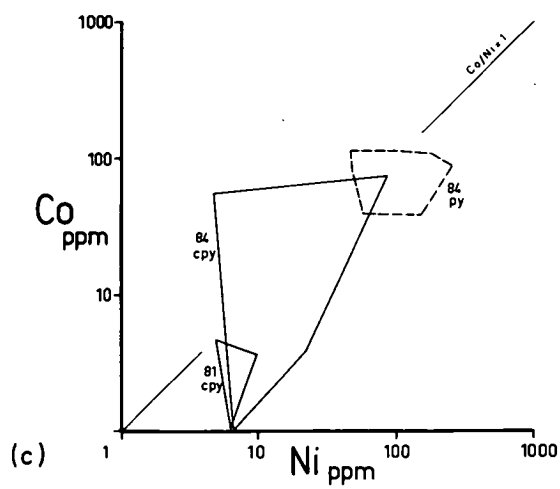
1000
100
10
Co ppm
Co/Ni=1
84 py
84 cpy
81 cpy
1
10
100
1000
Ni ppm

(c)

Figure 6.8

Co and Ni in pyrites from Mt. Lyell lodes other than in the West Lyell area.

(a) The Blow (Mt. Lyell) Open Cut:

72 : Top of massive Blow orebody.

73 : Replacement band parallel to schistosity, 6 ft. above 72.

74 : 15 ft. west of 73.

75 : 10 ft. west of 74.

76 : Replacement band parallel to schistosity, about 50 ft. above 72.

(b) Mineralization to the north of the West Lyell Open Cut:

89 : Disseminations in schist, Cape Horn pyrite body.

90 : Quartzose bands in the schist associated with 89.

91 : Disseminations in schist, Crown Lyell.

(c) Mineralization in the Comstock area:

94 : Massive, Comstock Open Cut.

95 : Massive, Tasman and Crown Lyell.

"C & J" is the general trend for epizonally metamorphosed "volcanic-exhalative" pyritic Cu ores from Smolnik and Mnisek, Czechoslovakia (Cambel and Jarkovsky, 1967, Fig. 124). About 25% of the analyses are outside the field as given, with higher Ni contents up to 300 ppm.

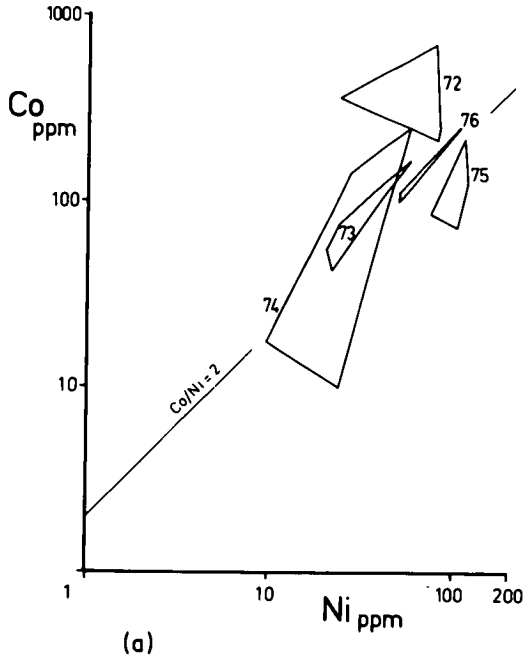
1000
100
10
Co ppm
72
76
75
73
74
Co/Ni = 2
1
10
100
200
Ni ppm

(a)

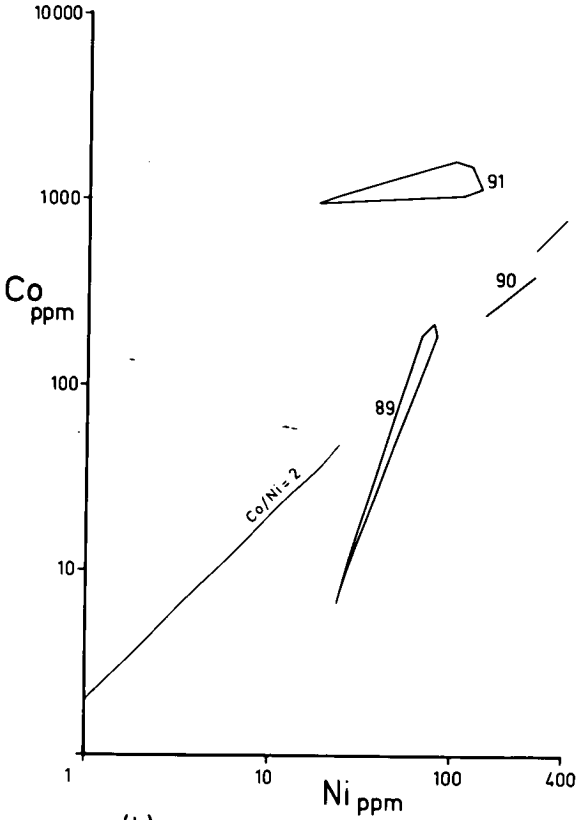
10000
1000
100
10
Co ppm
91
90
89
Co/Ni = 2
1
10
100
400
Ni ppm

(b)

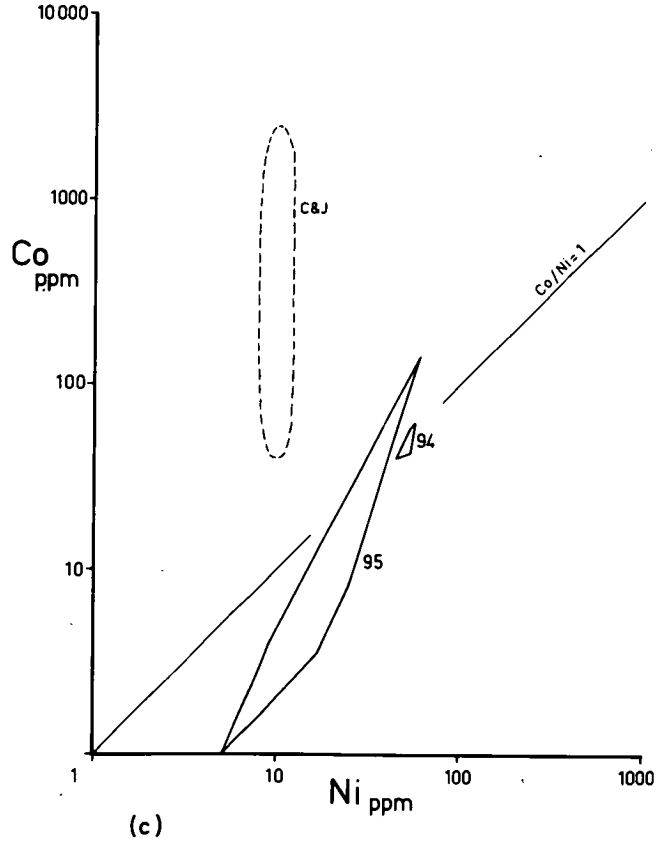
10000
1000
100
10
Co ppm
C&J
Co/Ni = 1
94
95
1
10
100
1000
Ni ppm

(c)

Figure 6.9

Co and Ni in pyrites and pyritic ore from the main lode, Rosebery Mine. The "lenses" refer to steeply pitching, thicker portions of the folded orebody, which have previously been considered to be en echelon replacement lodes. "B" lens is at the north of the mine, "F" lens at the south. "Footwall" and "hangingwall" below refer to the "bottom" and "top" portions of the lode itself.

B lens : 99 : Massive pyritic ore, hangingwall, 12 level.

115 : In brecciated carbonate, marginal to footwall, 8 level.

D lens : 101 : Medium-grained pyritic ore, footwall, 13 level.

102 : Massive pyritic ore, hangingwall, 13 level.

E lens : 100 : Massive pyritic ore, footwall, 12 level.

103 : Medium-grained pyritic ore, footwall, 13 level.

109, 110 : Those samples from 14 level S2N stope which were purified >95% pyrite (see also Fig. 6.32).

111 : Massive pyritic ore, footwall, 14 level, 80 ft. from 109.

114 : Banded pyrite-chalcopyrite ore, footwall, 17 level. This field represents four quarters of a 4.6 g specimen.

F lens : 104 : Banded coarse-grained pyritic ore, centre of lode, 13 level.

105 : Fine-grained pyritic ore, footwall, 13 level.

106 : Disseminated in schist, footwall, 13 level.

112 : Coarse-grained banded pyrite-chalcopyrite ore, footwall, 14 level.

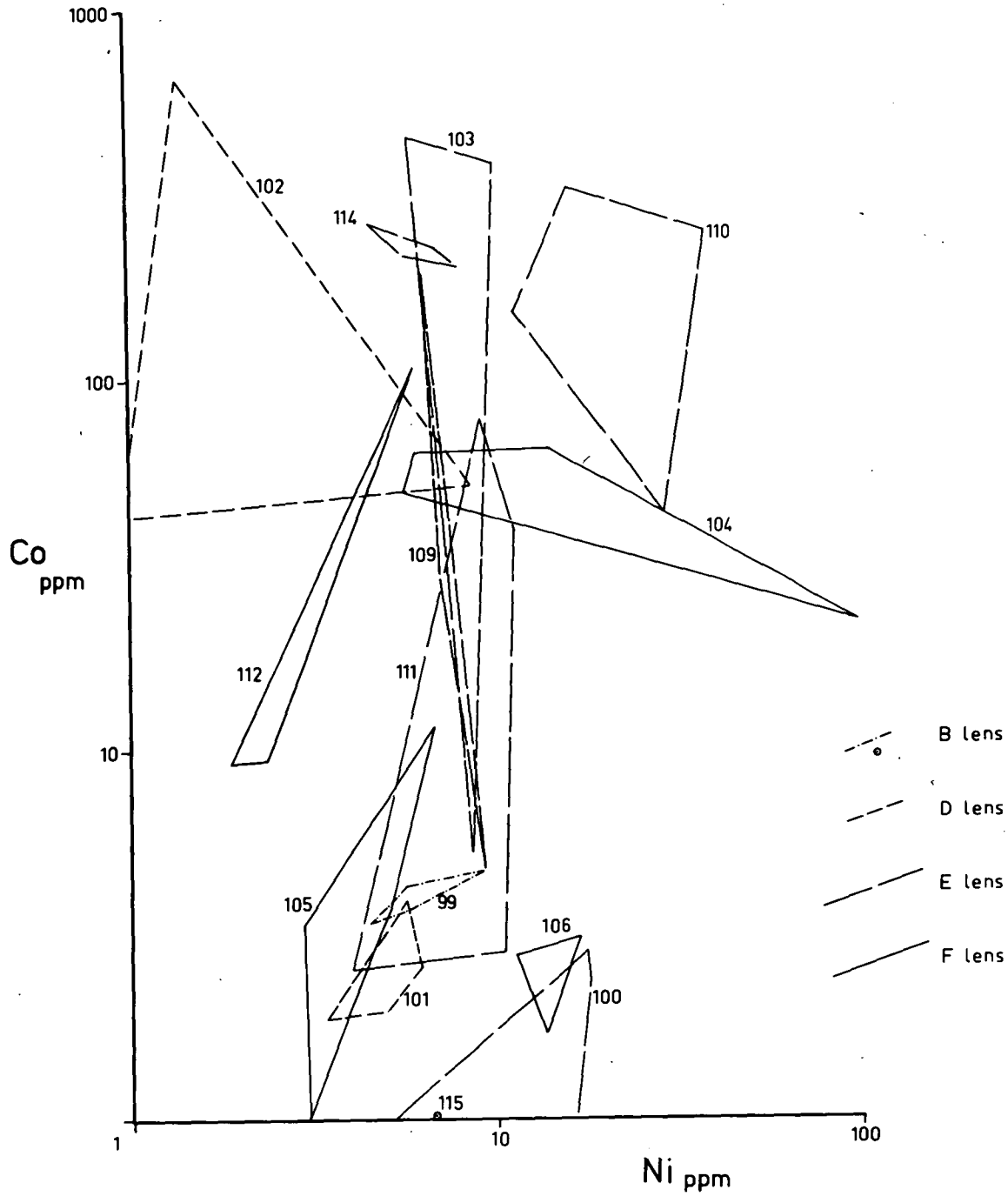
1000
100
10
1
Co ppm
1
10
100
Ni ppm
102
103
114
110
104
109
112
111
105
99
106
101
100
115
B lens
D lens
E lens
F lens

Figure 6.10

Co and Ni in pyrites and pyritic ore, Rosebery-Hercules area.

(a) Summary of results for samples across the section of the Rosebery Mine (see Fig. 5.7b):

(i) Footwall of the mine : disseminated and veinlet pyrite in schisted pyroclastics (25).

(ii) Main Lode (from Fig. 6.9).

(iii) Host rock shale, sedimentary pyrite (7).

(iv) Pyrite from the pyrite-hematite lode (107).

(v) Sedimentary pyrite, and pyrrhotite veinlets (triangles) from the hangingwall dark grey shale (6, 116).

(vi) Pyrite vein in the hangingwall massive volcanics (26).

(b) (i) Pyrite from the Hercules Lode (117), and sedimentary pyrite from the "slate" in the hangingwall of the lode (5).

(ii) Pyrite from the Black P.A. Mine (125) and the Natone Volcanics (126).

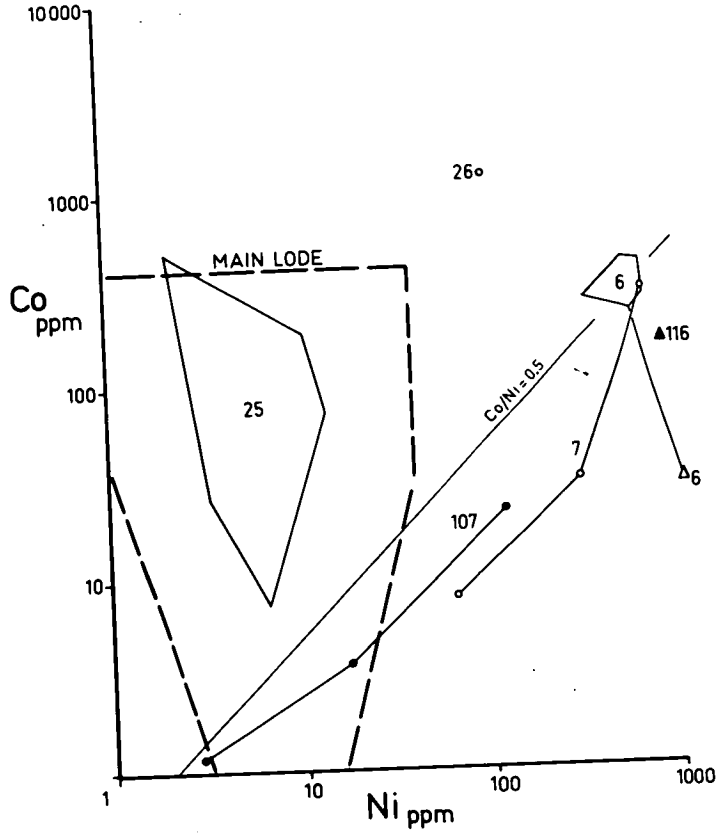
10000
1000
100
10
1
Co ppm
Ni ppm
1
10
100
1000
MAIN LODE
25
26
6
116
7
6
107
Co/Ni = 0.5

(a)

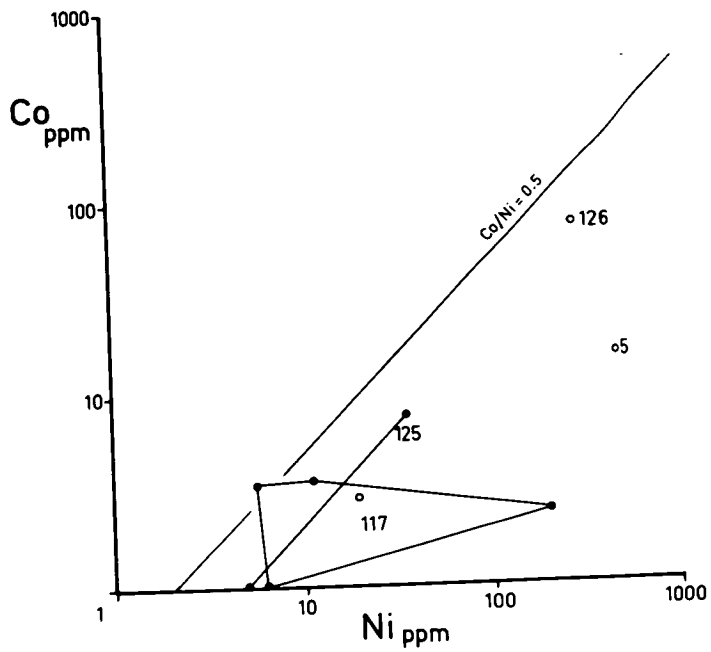
1000
100
10
1
Co ppm
Ni ppm
1
10
100
1000
Co/Ni = 0.5
126
5
125
117

(b)

## Mt. Farrell group, Mt. Remus

All analyses from the Mt. Farrell group of mines, including an analysis of sedimentary pyrite, are plotted in Figure 6.11a.

Figure 6.11b includes the values for pyrites from the Mt. Remus prospect.

## Lake George, Captain's Flat, N.S.W.

As a test of the possible correlation of Co-Ni relationships in stratiform banded Zn-Pb-Cu deposits within one geosyncline, specimens (set 127) were collected on the surface and from drill core at the Lake George Mine for comparison with the Rosebery specimens. The two mines are 500 miles apart.

The genesis of the Lake George orebodies has been discussed by Glasson and Paine (1965). While these authors maintain that in its present position the ore is structurally controlled, there is also strong evidence of stratigraphic control. As the ore is associated with acid volcanics, and some at least of the pyrite is obviously syngenetic, the possibility exists of a volcanic-sedimentary origin for all the ore (Stanton and Rafter, 1966).

The Co-Ni results are plotted in Figure 6.11b.

Figure 6.11

(a) Co and Ni in pyrite (and arsenopyrite) from the mines in the Tullah area (Mt. Farrell group):

8 : Sedimentary pyrite, New North Mt. Farrell Mine.

121 : Stirling Valley Mine.

122 : Tullah Ag-Pb Mine.

123 : Murchison Mine.

124 : New North Mt. Farrell Mine.

(b) Co and Ni in pyrite from the Mt. Remus prospect (120), and from the Lake George Mine, Captain's Flat, N.S.W. (127).

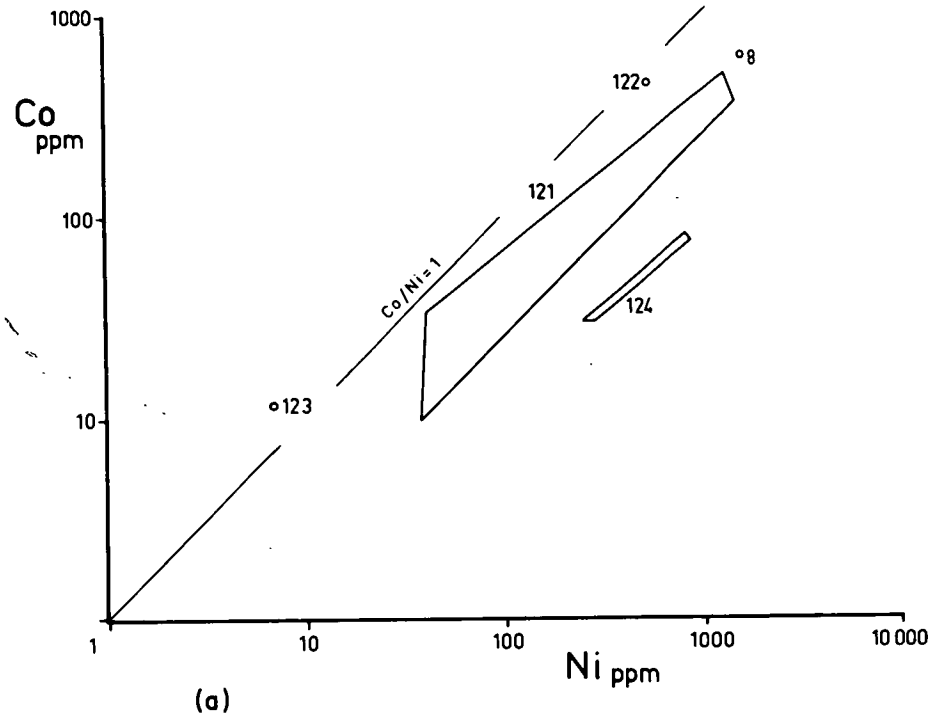
1000
Co
ppm
100
10
1
10
100
1000
10 000
Ni ppm
Co/Ni=1
°8
122°
121
124
°123

(a)

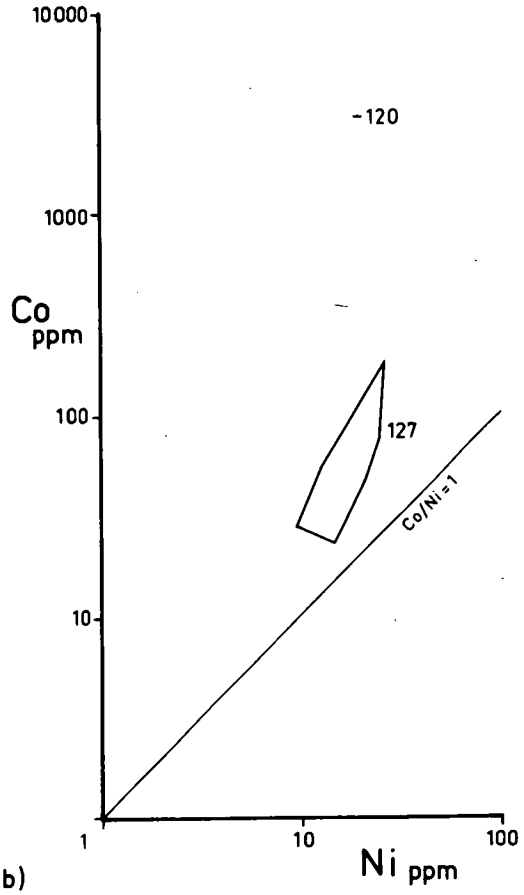
10000
1000
Co
ppm
100
10
1
10
100
Ni ppm
-120
127
Co/Ni=1

(b)

## SELENIUM ANALYSES

All the Se results summarized in Figure 6.12 are differentiated with respect to host mineral. The sedimentary pyrites have Se contents which are high for a province which in general shows no gross Se enrichment, and are much higher than the concentrations found in pyrites from Victoria analyzed by Edwards and Carlos (1954), which have been plotted at the top of Figure 6.12. Possible explanations are that most of the pyrites occur in shales, some of then carbonaceous, and several of the pyrites may be recrystallized.

The Cambrian pentlandite-pyrrhotite ores from Cuni have consistently high Se contents, although these are four times greater than those found by Edwards and Carlos (1954) in a similar specimen from the same deposit. The high values are consistent with enrichment of Se in similar veins associated with magmatic Cu-Ni mineralization, as observed in the Noril'sk group of deposits (Sindeeva, 1964, p.185). Pyrites in the Savage River ortho-amphibolite are slightly enriched in Se, but all other classes of deposit show about the same range in concentration, except for the notably enriched Mt. Lyell deposits.

Because of the variable partition of Se between different sulphides, pyrite is used here as an index mineral for detailed comparison of the sample populations using the F variance ratio test of Snedecor (1946, p.218). Selenium contents of the pyrites from the Devonian Pb-Zn-Ag deposits and cassiterite-sulphide deposits are not significantly different. The Devonian pyrites as a group do not differ significantly from the pyrites syngenetic in the Cambrian acid-intermediate igneous rocks, but

Figure 6.12

Histogram of Se analyses of pyrite, chalcopyrite, sphalerite, pyrrhotite and Cu-Ni ore.

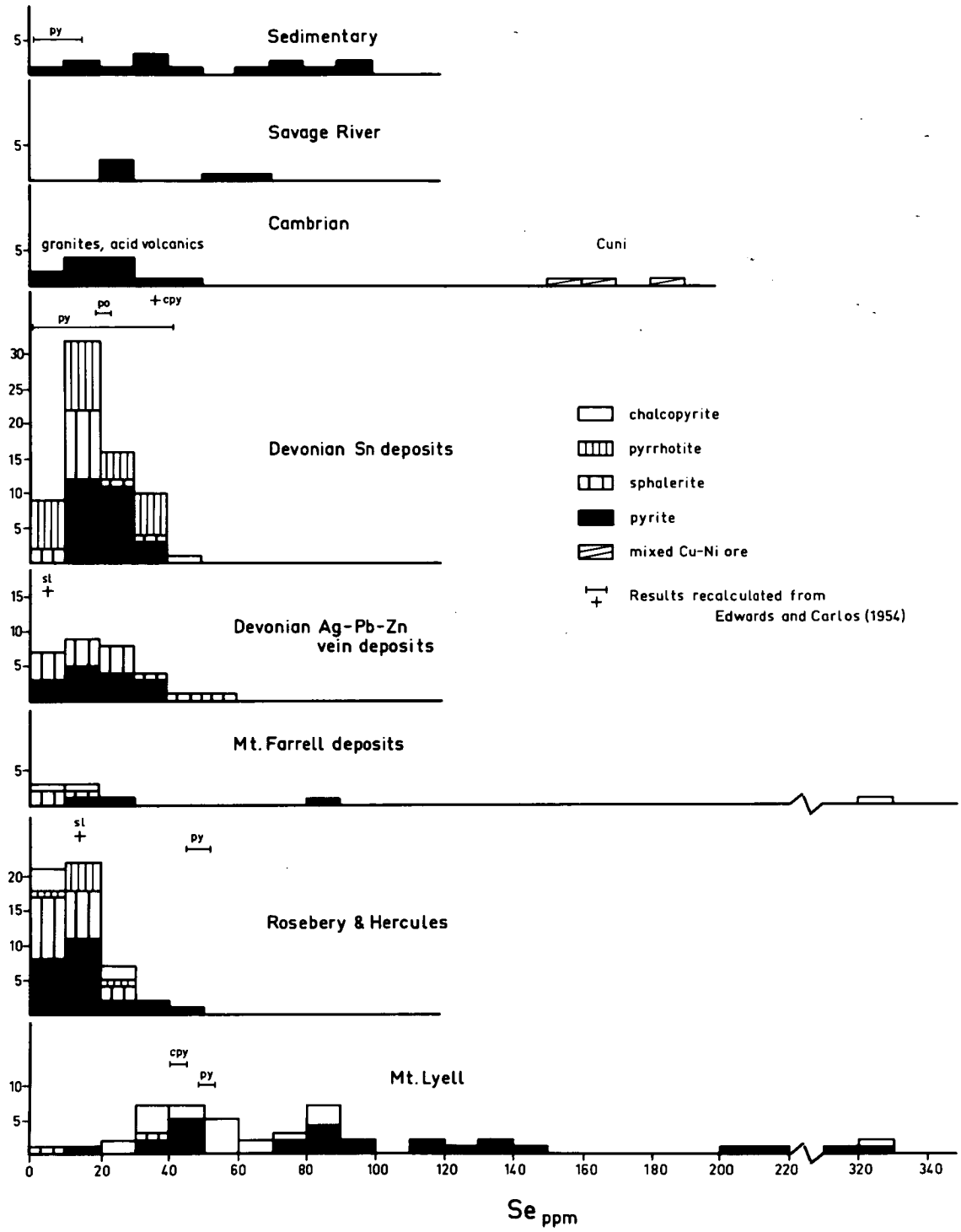
Sedimentary
py
5
Savage River
5
Cambrian
granites, acid volcanics
Cuni
5
Devonian Sn deposits
py
po
+cpy
30
25
20
15
10
5
chalcopyrite
pyrrhotite
sphalerite
pyrite
mixed Cu-Ni ore
Results recalculated from
Edwards and Carlos (1954)
Devonian Ag-Pb-Zn
vein deposits
sl
15
10
5
Mt. Farrell deposits
5
Rosebery & Hercules
sl
py
20
15
10
5
Mt. Lyell
cpy
py
10
5
0
20
40
60
80
100
120
140
160
180
200
220
320
340
Se ppm

the Se contents of Rosebery-Hercules pyrites are significantly less than both these groups, at the 99% and 95% confidence levels respectively. The samples from the Mt. Farrell mines differ from all these groups, except possibly Mt. Lyell, but there are insufficient results for statistical analysis. No pyrites were available from the Magnet Mine, but the Se contents of sphalerites were the same as those in the other (Devonian) Pb-Zn-Ag deposits in the area around Mt. Bischoff.

It appears from these results that there was a uniform availability of Se in mineralizing fluids derived from acid-intermediate igneous activity in Cambrian and Devonian times, but that the Savage River magnetite ore, the Cuni Cu-Ni ore, and particularly the Mt. Lyell pyritic Cu ore were all enriched in Se, whereas the Rosebery ore was impoverished. The enrichment at Mt. Lyell is consistent with the tentative identification in the ore of berzelianite, $Cu_{2-x}Se$ (Edwards, 1939).

## ANALYSES OF CADMIUM IN SPHALERITE

The distribution of Cd in sphalerites from the Devonian Pb-Zn-Ag deposits (Fig. 6.13) is not significantly different (by F test) from that in the Devonian cassiterite-sulphide deposits, and the average Cd content of all these deposits is approximately equal to the average Cd content of all sphalerites (Ivanov, 1964). These results indicate a generally uniform availability of Cd during Devonian mineralization over the sampled area. The Cd contents of sphalerites from Tullah and Magnet are similar to those for the Devonian deposits.

Figure 6.13

Histogram of Cd in sphalerites from Devonian cassiterite-sulphide lodes and Pb-Zn-Ag fissure veins, and from Rosebery-Hercules and Mt. Lyell (Groves and Loftus-Hills, in press).

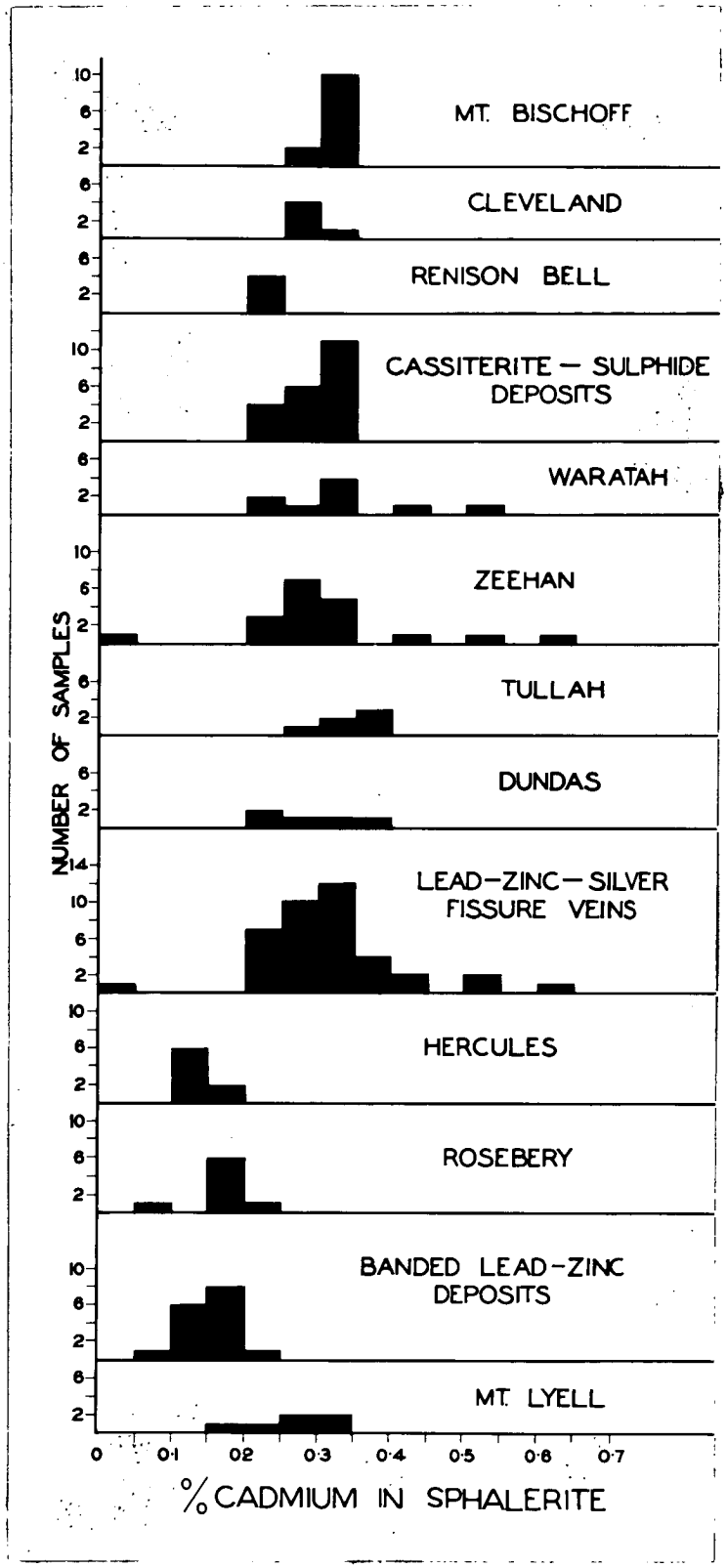
MT. BISCHOFF
CLEVELAND
RENISON BELL
CASSITERITE — SULPHIDE DEPOSITS
WARATAH
ZEEHAN
TULLAH
DUNDAS
LEAD–ZINC— SILVER FISSURE VEINS
HERCULES
ROSEBERY
BANDED LEAD–ZINC DEPOSITS
MT. LYELL
NUMBER OF SAMPLES
0
0·1
0·2
0·3
0·4
0·5
0·6
0·7
% CADMIUM IN SPHALERITE

There is a marked difference between Cd contents of sphalerite from the Devonian deposits and from the Rosebery-Hercules ores, implying distinctly different Zn/Cd ratios during deposition. The Cd values in the Rosebery-Hercules sphalerites vary 0.09 - 0.20%, with an average value of 0.15%, approximately half that for the Devonian deposits.

The few available sphalerite specimens from the Mt. Lyell area show a variation 0.18 - 0.30% Cd, and average 0.26% Cd. Although this range differs from those of both the Rosebery-Hercules deposits and the Devonian ores, it is based on insufficient samples for confident interpretation.

## DEPOSITIONAL AND POST-DEPOSITIONAL VARIATIONS

### Distribution Functions

The two largest homogeneous sample populations - 23 pyrites from the dykes, and 26 pyrrhotites from the replacement deposits at Mt. Bischoff - were examined for distribution patterns of Co and Ni. Histograms of the distributions are plotted in Figure 6.14, on both linear and logarithmic scales. All the Co and Ni values, when plotted on linear scales, reveal the positively skewed distributions to be expected for trace element data. However the logarithmic-scale plots of the same data do not produce normal distributions, three of the distributions retaining some positive skewness, and the Co data from the dyke pyrites acquiring a negative skew, which is very different from the equivalent Co distribution in the replacement deposits.

Figure 6.14

Co and Ni distribution histograms for two homogeneous sample populations, plotted on linear and logarithmic scales.

(a) Pyrite, porphyry dykes, Mt. Bischoff.

(b) Pyrrhotite, replacement deposits, Mt. Bischoff.

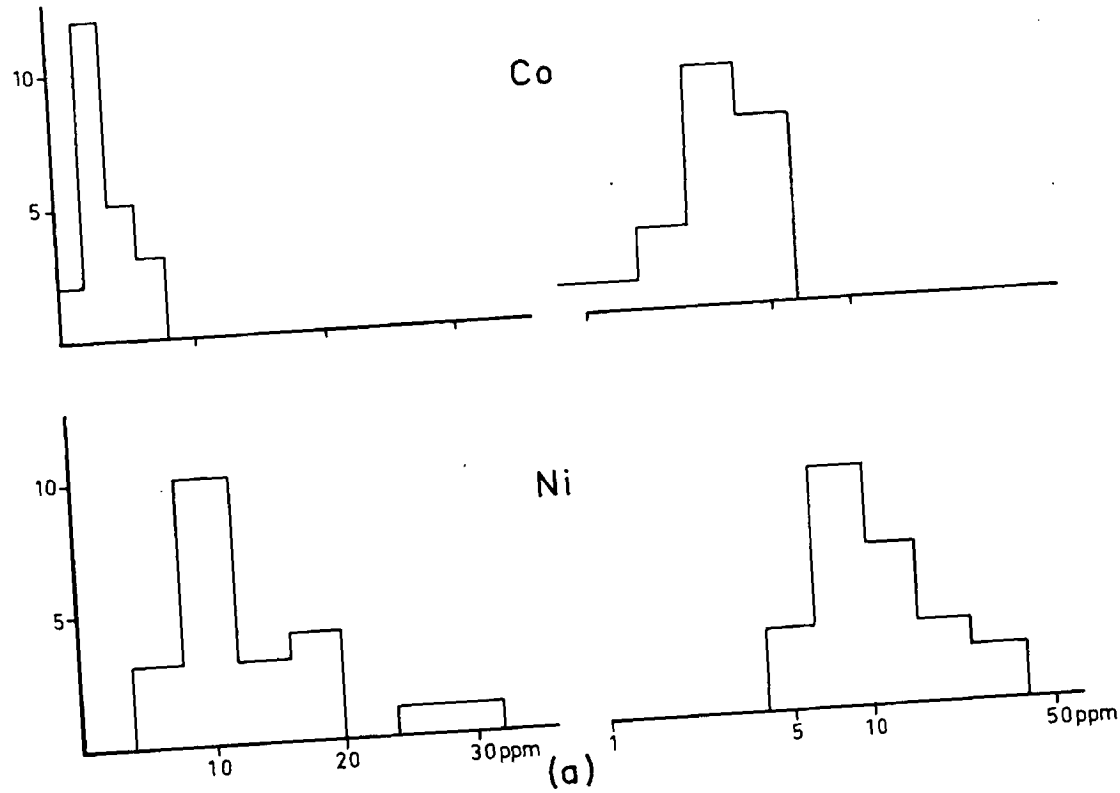
Co
10
5
Ni
10
5
10
20
30ppm
1
5
10
50ppm
(a)

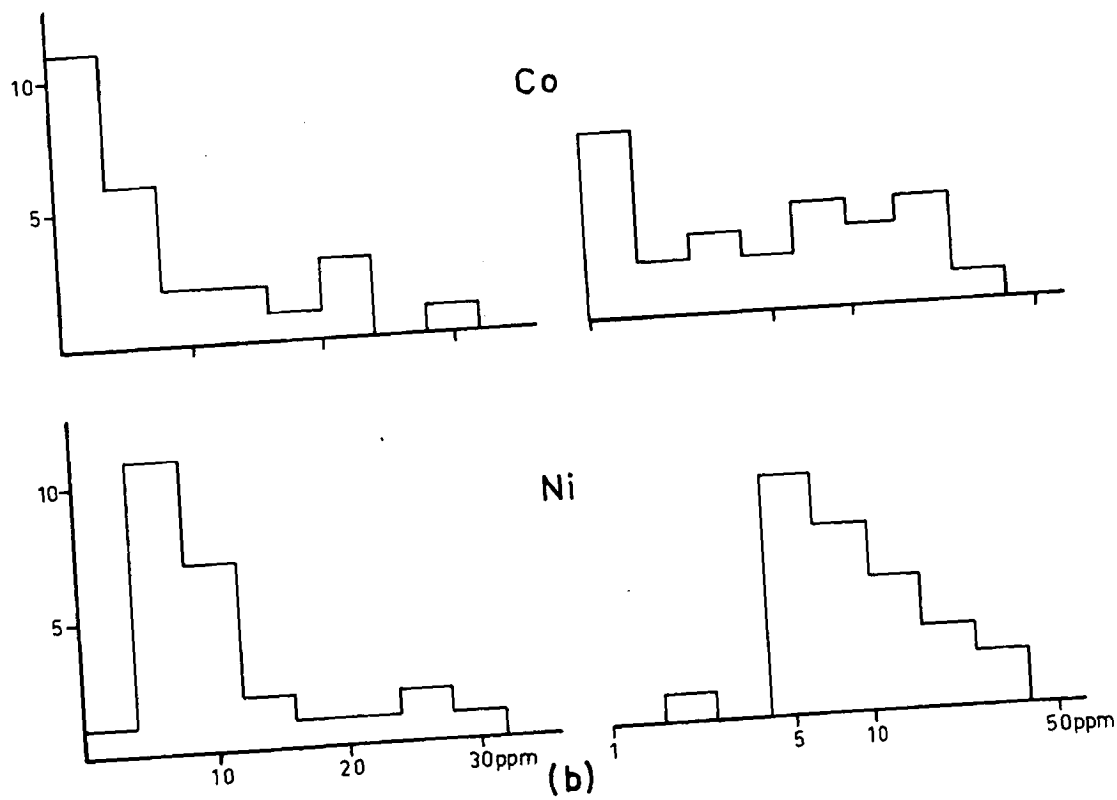
Co
10
5
Ni
10
5
10
20
30ppm
1
5
10
50ppm
(b)

The distribution functions for the Ni data are, however, remarkably similar for the two modes of occurrence. The dissimilarity in Co distribution functions is much more likely to be related to the mode of occurrence than to the host mineralogy, but as there is no theoretical basis for element distribution functions in general, the observations must remain empirical. Overall, the basic distribution functions for Co and Ni in these sulphides approach more closely to lognormal than to normal distributions, but they are not lognormal.

## Variation within Single Minerals

In Figure 6.15 are plotted the Co-Ni analyses of those groups of two, three or four samples of the same mineral, which were taken from one hand specimen. The ranges of the groups do not vary greatly between deposit types, which is contrary to the results of Rose (1967), who reported a greater specimen-scale variation of trace elements in vein deposits than in replacement deposits. The exceptions are the groups from the Savage River, which show somewhat smaller ranges, possibly due to local homogenization of trace element values during at least two metamorphisms. The ranges in different minerals also appear to be about the same.

The type of variation, however, can in some cases be correlated with the mode of occurrence. Although there is an unexpected tendency for variations of the type Co or Ni = k (k = a constant), this is more marked in the vein deposits than in the replacement deposits, the latter trending towards variations of the type Co/Ni = k (parallel

Figure 6.15

Variation in Co and Ni concentrations in one mineral within single specimens:

(a) Sedimentary-diagenetic.

(b) Savage River.

(c) All the vein deposits (other than at Mt. Lyell).

(d) All the replacement deposits (other than at Mt. Lyell).

(e) Mt. Lyell.

(f) Rosebery.

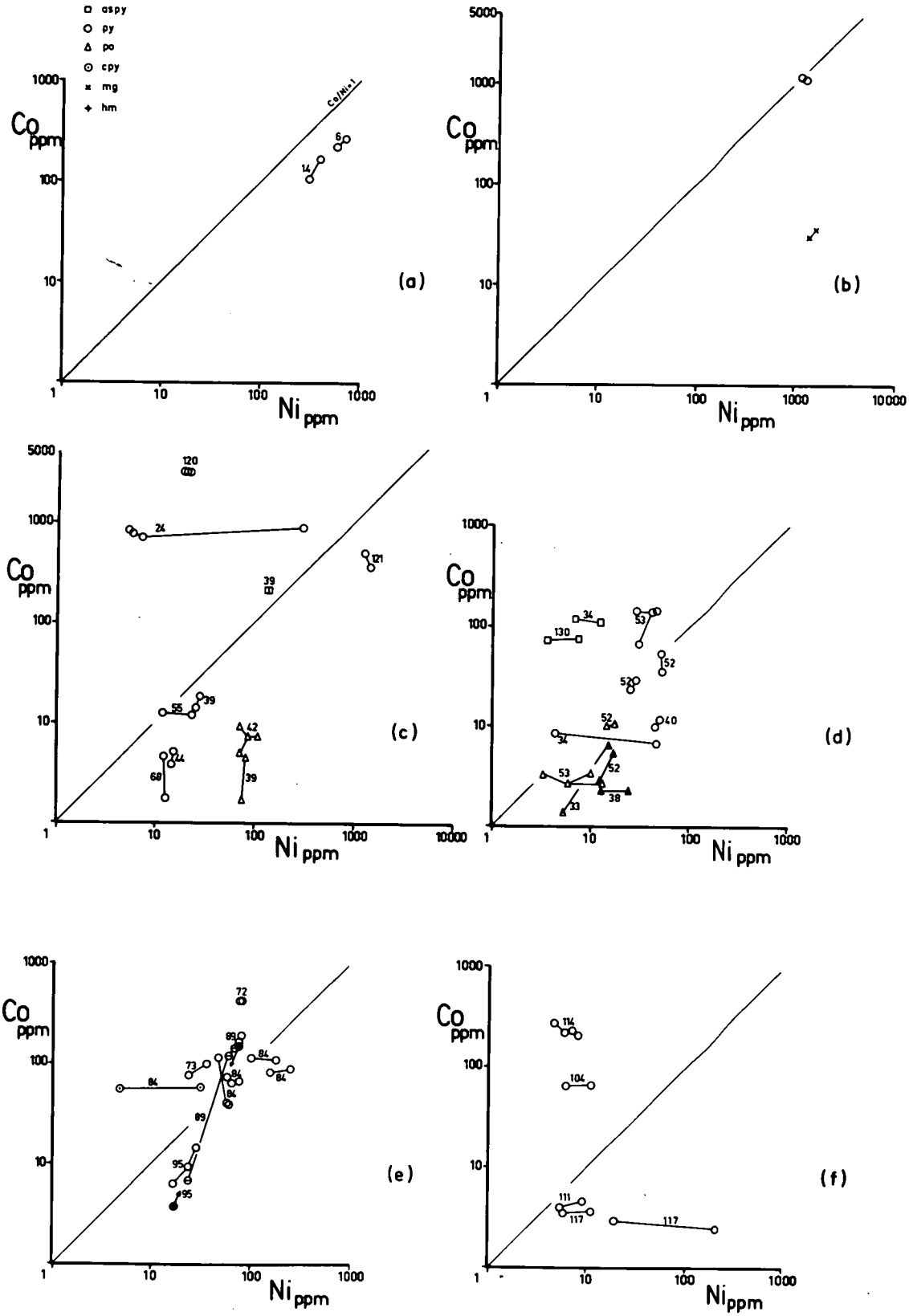
aspy
py
po
cpy
mg
hm
Co/Ni=1
Co ppm
Ni ppm
(a)
(b)
(c)
(d)
(e)
(f)

straight lines at 45° to the axes). This holds true both for the Cambrian and Devonian veins, and for the Mt. Lyell replacement deposits and remobilized veins (Fig. 6.15e). The Rosebery groups show a consistent variation of the type Co = k. On the other hand, the two sedimentary groups (Fig. 6.15a) show a very strong Co/Ni = k tendency.

A quanlitative explanation of these variation-types is that the formation of sedimentary and replacement minerals occurs in solid media, where the available Co and Ni, bound in a slowly diffusing, mainly intergranular dispersed phase, are physically restrained from large independent concentration variations, and will tend to vary sympathetically. In the vein situation, however, where the system is open, Co and Ni can be incorporated into minerals independently, on the specimen scale at least. A similar explanation was given by Rose (1967) for the smaller trace-element variations he found in replacement deposits than in vein deposits.

The types of specimen-scale Co-Ni variations outlined above are reflected in the overall Co-Ni variations for whole sampling sites, and for whole deposits. Thus several of the sedimentary pyrite fields in Figure 6.1 are of the type Co/Ni = k; many of the Devonian hydrothermal vein fields, and also trend IV, (Figs. 6.5 - 6.6), are of the type Ni or Co = k.

In Figure 6.16 are plotted the Se analyses of groups of two, three and four samples of the same mineral taken from the same specimen. The ranges of the groups appear to be about the same for different minerals. These analyses show, however, a much greater tendency than the Co-Ni groups for the absolute variation within the groups to remain

Figure 6.16

Variation of Se concentration in one mineral within single specimens.

Figure 6.17

Distribution of Se concentrations in the different ore-types at Mt. Lyell.

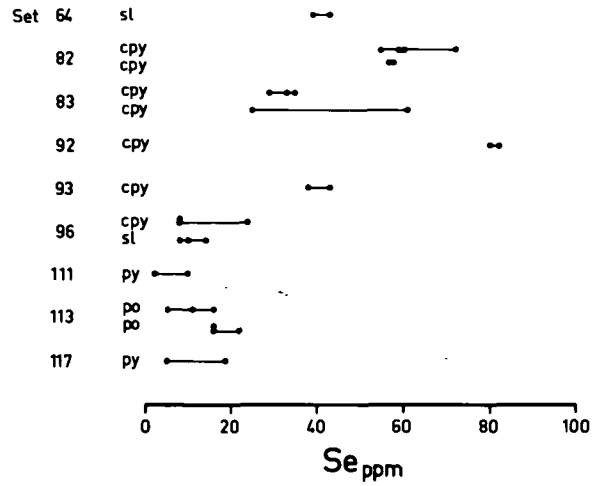
Set 64 sl
82 cpy
cpy
83 cpy
cpy
92 cpy
93 cpy
96 cpy
sl
111 py
113 po
po
117 py
0 20 40 60 80 100
Se ppm

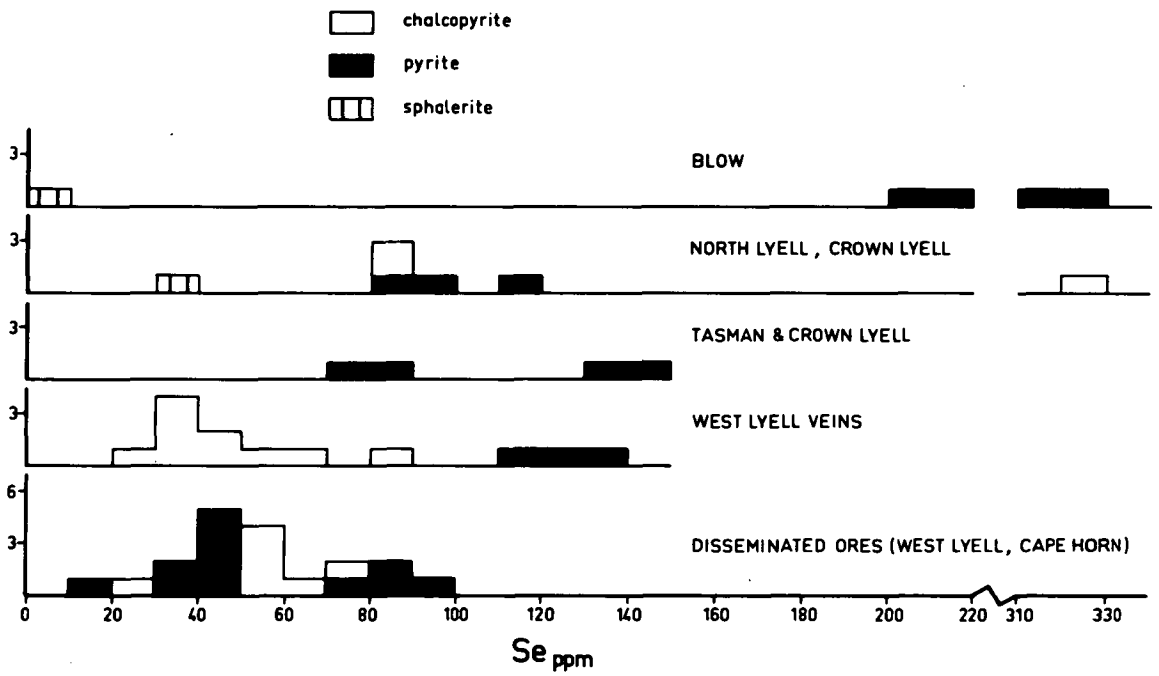
chalcopyrite
pyrite
sphalerite
BLOW
NORTH LYELL , CROWN LYELL
TASMAN & CROWN LYELL
WEST LYELL VEINS
DISSEMINATED ORES (WEST LYELL, CAPE HORN)
0 20 40 60 80 100 120 140 160 180 200 220 310 330
Se ppm

constant, giving a generally decreasing percentage variation about the group-mean with increasing mean.

## Correlations with Mode of Emplacement

### Massive - disseminated

The main trend evident in the wide range of Se concentrations in pyrite, chalcopyrite and sphalerite from Mt. Lyell (Fig. 6.17) is a general enrichment in the massive ore-bodies close to the stratigraphic top of the volcanics i.e. close to the upturned unconformity with the Owen Conglomerate (Blow, North Lyell, Crown Lyell, Tasman and Crown Lyell), compared with the disseminated ores a few hundred feet further into the volcanics (West Lyell Open Cut, Cape Horn). This gross trend cuts across mineralogical and textural types of ore, and its genetic significance is discussed under "Mt. Lyell".

### Vein - replacement

At the mineralogically and structurally similar Mt. Bischoff (Figs. 6.18, 6.19) and Renison Bell (Fig. 6.20) cassiterite-sulphide deposits, it was possible to sample both vein and replacement lodes, and at Mt. Bischoff, disseminated mineralization in the porphyry dykes. The veins and dykes are essentially vertical, whereas the replacement lodes are mainly stratiform, and at Mt. Bischoff there are distinct time differences between the vein and replacement mineralizations. It was hoped that any empirical inferences obtained from analyses of these specimens could be used to help elucidate the origin of the Federal Lode at Renison Bell, which from purely geological criteria is not apparent.

Figure 6.18

(a) Locality map of the Mt. Bischoff Open Cut area (Groves, 1968).

(b) Geological map of Mt. Bischoff and the surrounding area (Groves and Solomon, 1964). The line of section of Figure 6.19 is shown as A–B.

(a)

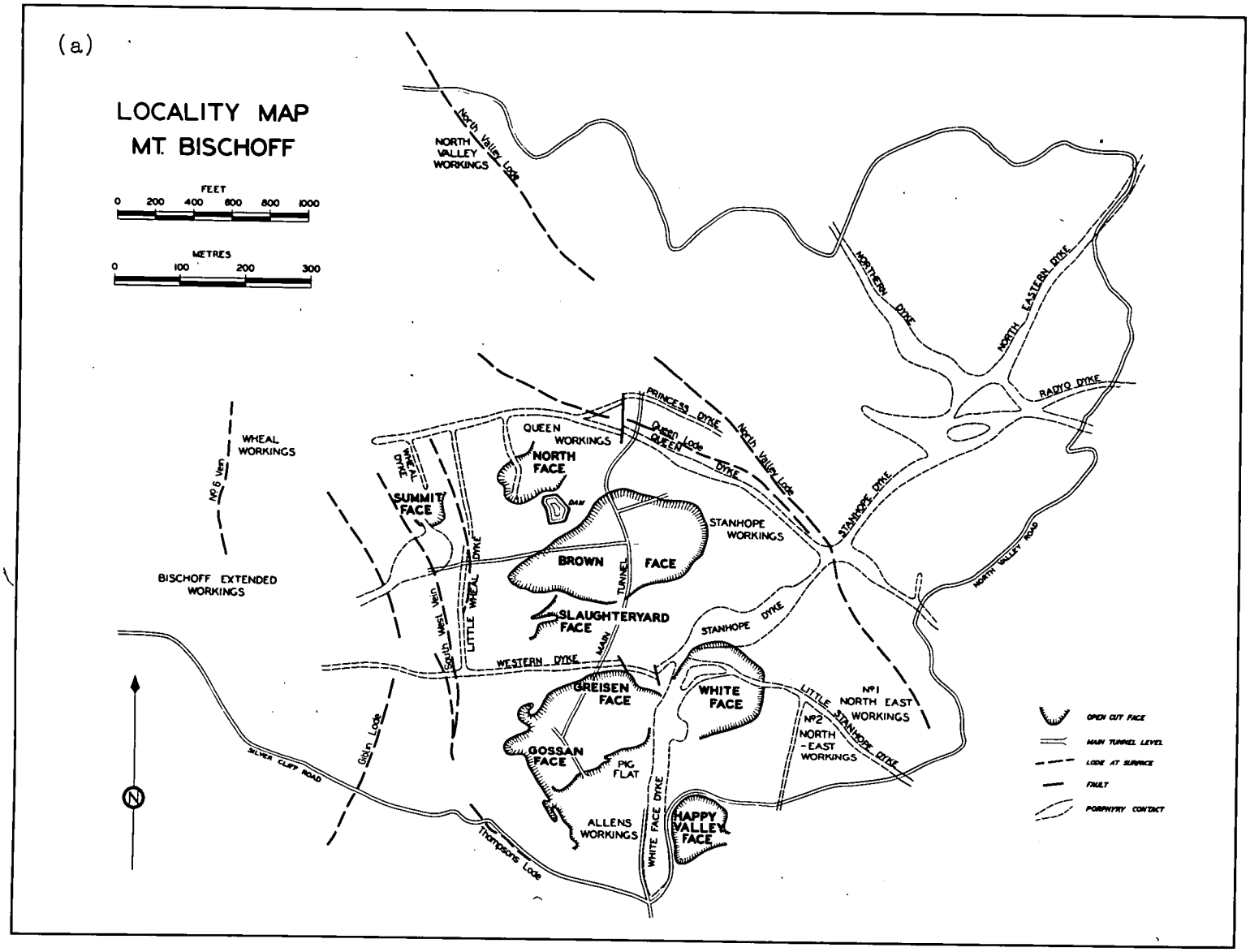
LOCALITY MAP
MT. BISCHOFF
FEET
0 200 400 600 800 1000
METRES
0 100 200 300
NORTH VALLEY WORKINGS
North Valley Lode
NORTHERN DYKE
NORTH EASTERN DYKE
RADYO DYKE
PRINCESS DYKE
North Valley Lode
Queen Lode
QUEEN DYKE
QUEEN WORKINGS
NORTH FACE
WHEAL WORKINGS
No 6 Vein
WHEAL DYKE
SUMMIT FACE
STANHOPE WORKINGS
STANHOPE DYKE
BROWN FACE
TUNNEL
LITTLE WHEAL DYKE
BISCHOFF EXTENDED WORKINGS
SLAUGHTERYARD FACE
MAIN
WESTERN DYKE
STANHOPE DYKE
NORTH VALLEY ROAD
GREISEN FACE
WHITE FACE
No1 NORTH EAST WORKINGS
No2 NORTH - EAST WORKINGS
LITTLE STANHOPE DYKE
GOSSAN FACE
PIG FLAT
ALLENS WORKINGS
HAPPY VALLEY FACE
WHITE FACE DYKE
SILVER CLIFF ROAD
Glen Lode
Thompsons Lode
OPEN CUT FACE
MAIN TUNNEL LEVEL
LODE AT SURFACE
FAULT
PORPHYRY CONTACT

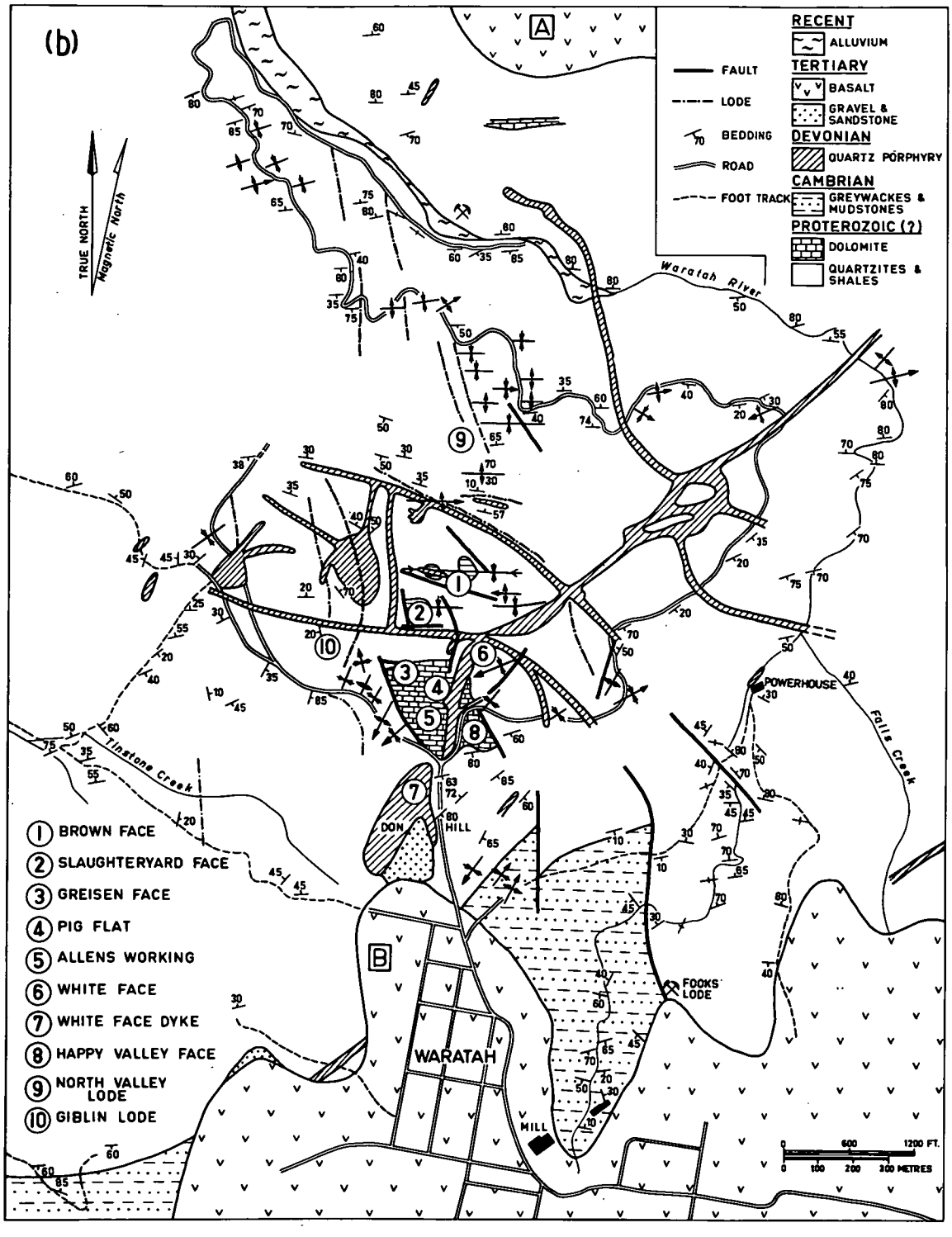
(b)
RECENT
ALLUVIUM
TERTIARY
BASALT
GRAVEL & SANDSTONE
DEVONIAN
QUARTZ PORPHYRY
CAMBRIAN
GREYWACKES & MUDSTONES
PROTEROZOIC (?)
DOLOMITE
QUARTZITES & SHALES
FAULT
LODE
BEDDING
ROAD
FOOT TRACK
TRUE NORTH
Magnetic North
Waratah River
Tinstone Creek
Falls Creek
POWERHOUSE
DON HILL
WARATAH
MILL
FOOKS LODE
A
B
1 BROWN FACE
2 SLAUGHTERYARD FACE
3 GREISEN FACE
4 PIG FLAT
5 ALLENS WORKING
6 WHITE FACE
7 WHITE FACE DYKE
8 HAPPY VALLEY FACE
9 NORTH VALLEY LODE
10 GIBLIN LODE
0 600 1200 FT.
0 100 200 300 METRES

Figure 6.19

North-south cross-section through Mt. Bischoff (Groves and Solomon, 1964). The line of section is shown on Figure 6.18.

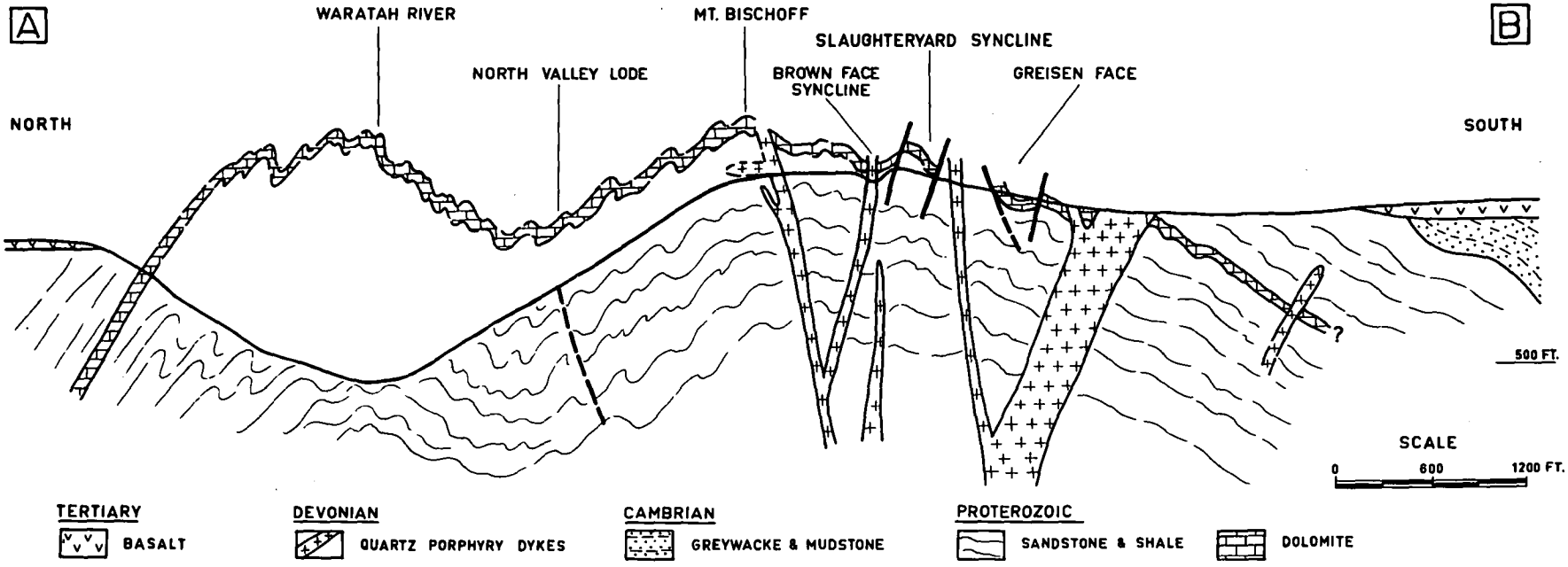
A
B
WARATAH RIVER
MT. BISCHOFF
SLAUGHTERYARD SYNCLINE
NORTH VALLEY LODE
BROWN FACE SYNCLINE
GREISEN FACE
NORTH
SOUTH
?
500 FT.
SCALE
0
600
1200 FT.
TERTIARY
BASALT
DEVONIAN
QUARTZ PORPHYRY DYKES
CAMBRIAN
GREYWACKE & MUDSTONE
PROTEROZOIC
SANDSTONE & SHALE
DOLOMITE

Figure 6.20

Cross-sections through the Renison Bell Mine (Groves, 1968), showing Nos. 1 and 2 Horizons (replacement lodes), and the Federal lode.

# CROSS-SECTIONS RENISON BELL

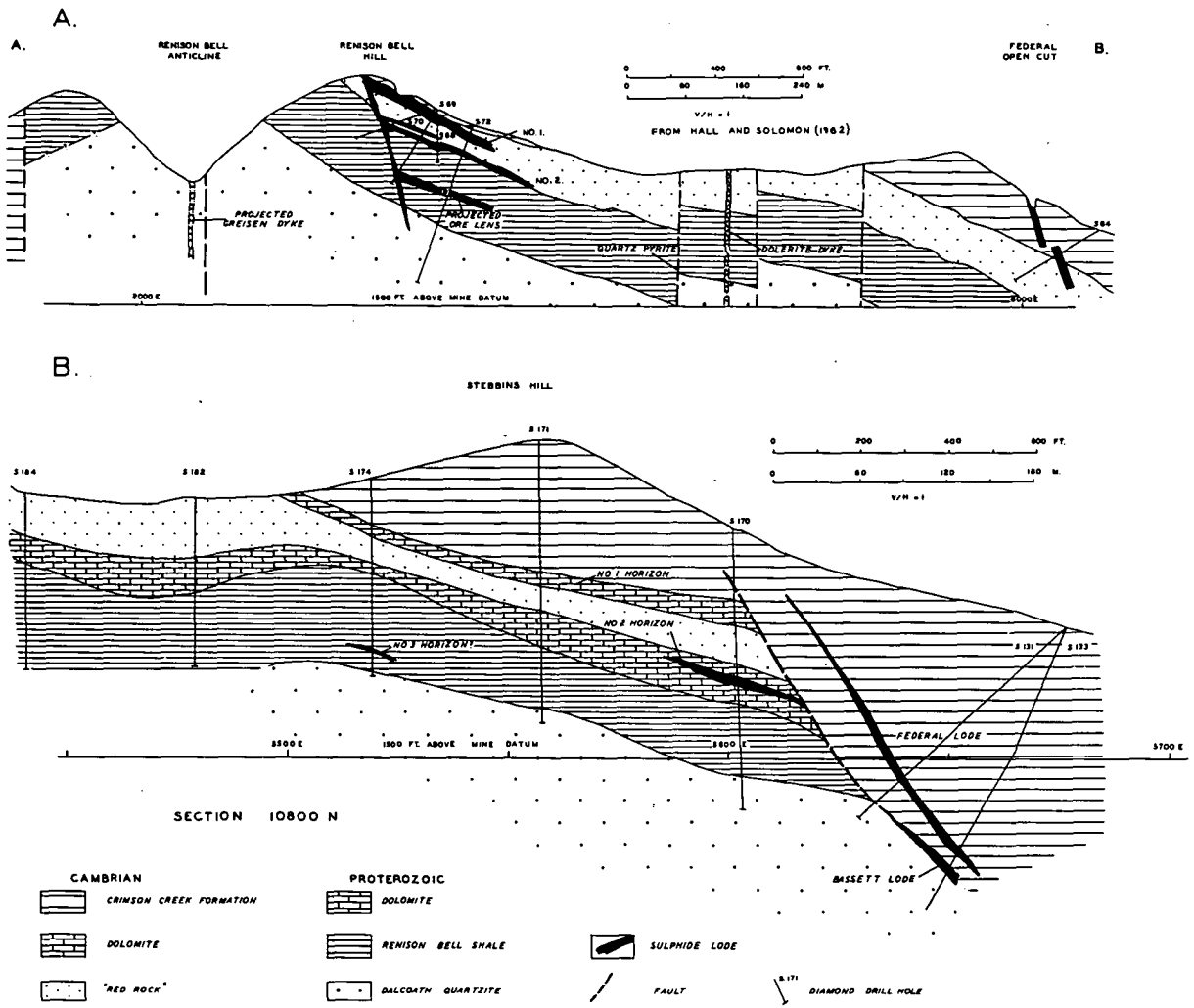

The analyses of arsenopyrite, pyrite and pyrrhotite at Mt. Bischoff (Fig. 6.21a, c; Fig. 6.22a) reveal major differences between samples from the vein, replacement and dyke mineralization.

(i) In the replacement deposits pyrrhotite has less Ni, and arsenopyrite and pyrite less Co and Ni, than the same mineral in the veins. The pyrite in the dykes contains even less Co and Ni than the replacement pyrite.

(ii) There is less variation of Co and Ni content in the replacement deposits than in the vein deposits. The variation in the dyke pyrite is smaller still.

The vein-replacement relationship was tested at Renison Bell in the Battery Open Cut, where a pure pyrite vein a few inches wide cuts siltstones containing pyrite selectively replacing the beds (Plate 6.3). The two types of pyrite are penecontemporaneous, a thin selvage of replacement pyrite along the borders of the veins having been remobilized into the vein. The analyses of these materials (Figs. 6.21b, 6.22b) give results consistent with those from Mt. Bischoff.

The apparent difference between the Co and Ni contents of pyrites from the replacement ores of Nos. 2 and 1 Horizons at Renison Bell (Fig. 6.21b) requires verification, as only one and two specimens respectively were used. However the replacement pyrrhotites (Fig. 6.21d) have similar ranges to those at Mt. Bischoff.

The equivalence of Co-Ni distributions in replacement pyrrhotites and in replacement and vein pyrites at Renison Bell and Mt. Bischoff strongly suggests that identical variables are controlling the concentrations of Co and Ni in the replacement and vein depositional environments. The control could be (a) a fortuitously similar temporal

Figure 6.21

Co and Ni in pyrite, pyrrhotite and arsenopyrite from vein and replacement deposits at Mt. Bischoff and Renison Bell.

(a) Pyrites and arsenopyrites from vein and replacement deposits, and from the porphyry dykes, Mt. Bischoff.

(b) Pyrite from Nos. 1 and 2 Horizons (replacement), arsenopyrite from No. 2 Horizon, and pyrite from the vein-replacement samples in the Battery Open Cut (set 55; Plate 6.3).

(c) Pyrrhotites from vein and replacement deposits, Mt. Bischoff and from the replacement deposit at Cleveland (sets 69, 128).

(d) Pyrrhotites from Nos. 1 and 2 Horizons (replacement), and from the Federal Lode.

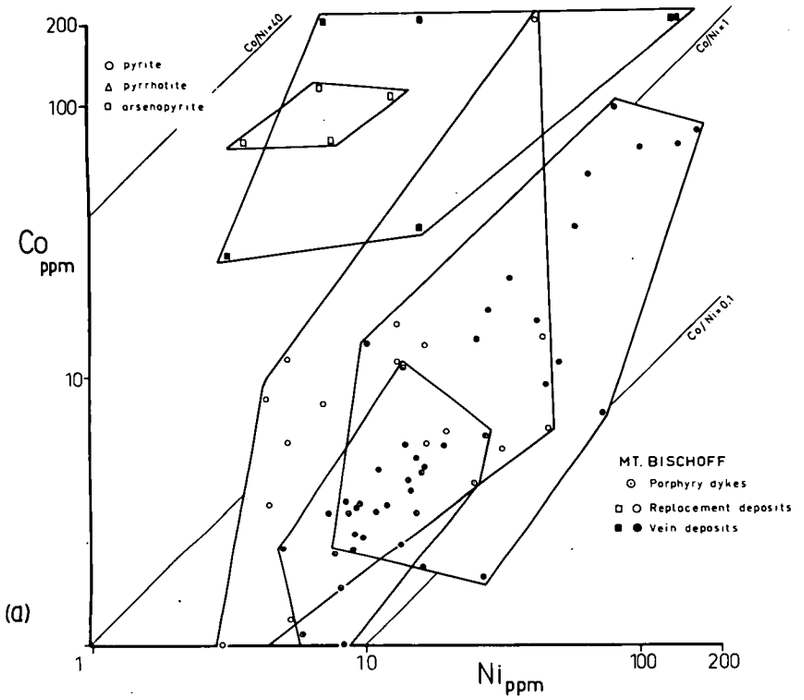
200
100
10
1
10
100
200
Co ppm
Ni ppm
Co/Ni=10
Co/Ni=1
Co/Ni=0.1
pyrite
pyrrhotite
arsenopyrite
MT. BISCHOFF
Porphyry dykes
Replacement deposits
Vein deposits
(a)

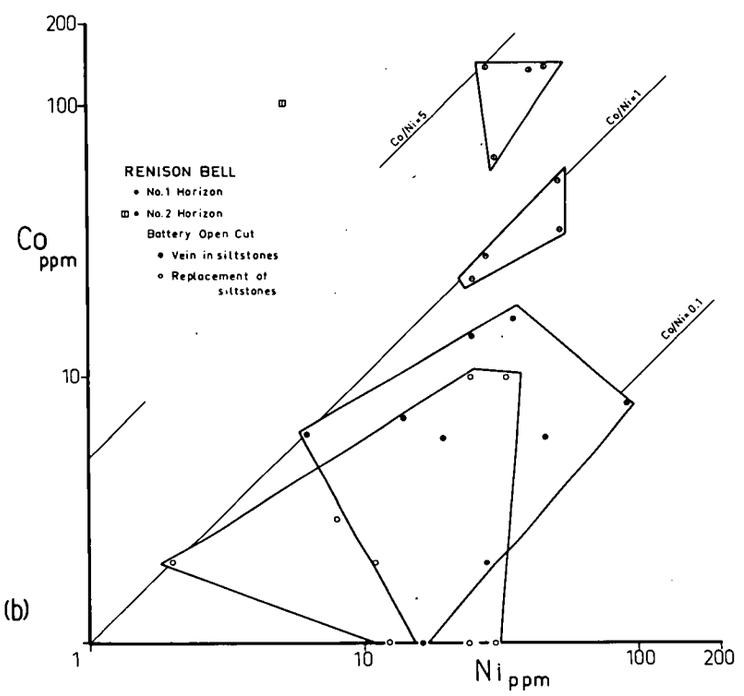
200
100
10
1
10
100
200
Co ppm
Ni ppm
Co/Ni=5
Co/Ni=1
Co/Ni=0.1
RENISON BELL
No.1 Horizon
No.2 Horizon
Battery Open Cut
Vein in siltstones
Replacement of siltstones
(b)

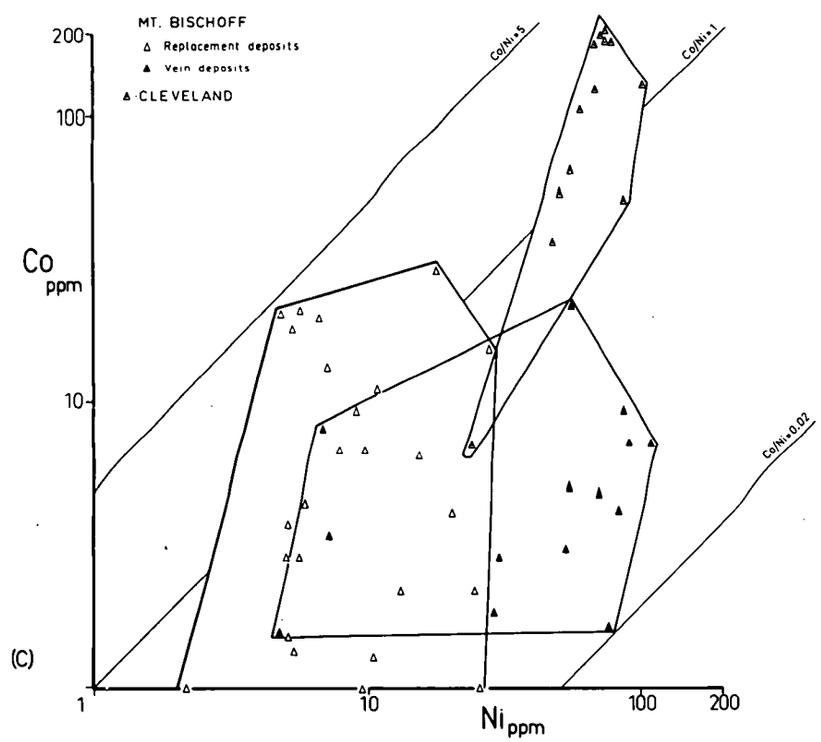
200
100
10
1
10
100
200
Co ppm
Ni ppm
Co/Ni=5
Co/Ni=1
Co/Ni=0.02
MT. BISCHOFF
Replacement deposits
Vein deposits
CLEVELAND
(c)

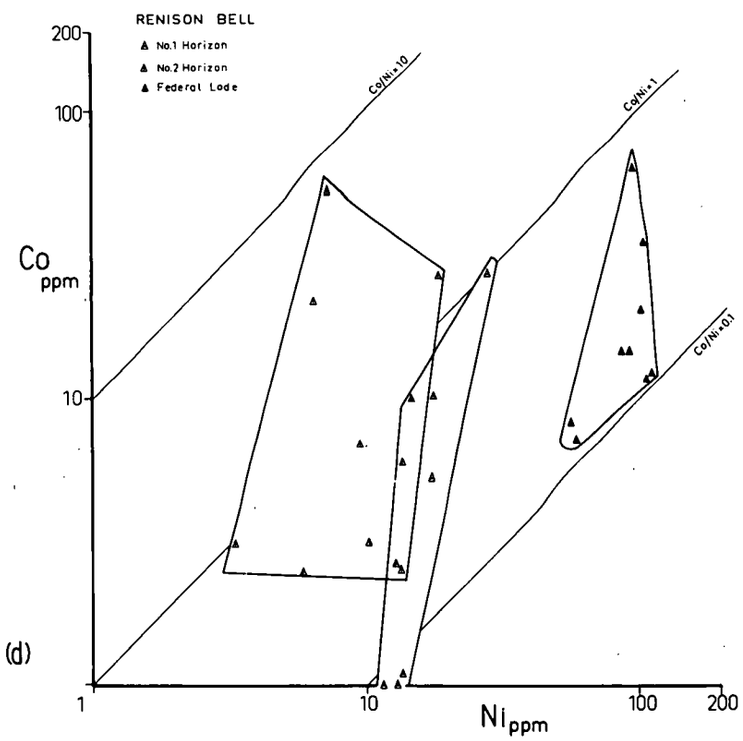
200
100
10
1
10
100
200
Co ppm
Ni ppm
Co/Ni=10
Co/Ni=1
Co/Ni=0.1
RENISON BELL
No.1 Horizon
No.2 Horizon
Federal Lode
(d)

Figure 6.22

Co and Ni at Mt. Bischoff and Renison Bell - deposit averages and within-specimen variation. R = replacement, V = vein.

(a) Averages for the Mt. Bischoff deposit (from Figure 6.21) of pyrite, arsenopyrite and pyrrhotite in replacement and vein deposits.

(b) Averages for the Renison Bell deposit (from Figure 6.21) of pyrite, arsenopyrite and pyrrhotite from the No. 2 Horizon, pyrite and pyrrhotite from the No. 1 Horizon, pyrite from the Battery Open Cut, and pyrrhotite from the Federal Lode.

(c) Within-specimen variation, Mt. Bischoff.

(d) Within-specimen variation, Renison Bell.

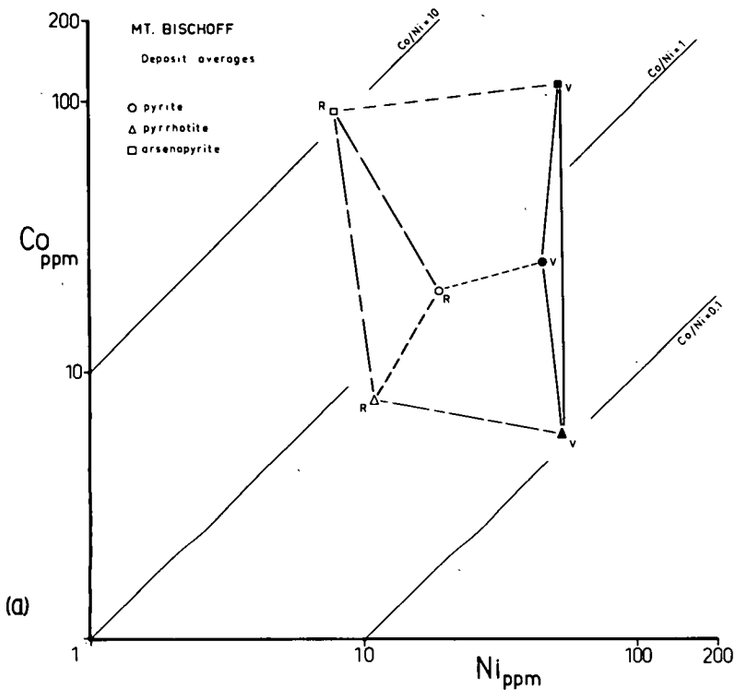
MT. BISCHOFF
Deposit averages
pyrite
pyrrhotite
arsenopyrite
Co/Ni=10
Co/Ni=1
Co/Ni=0.1
Co ppm
Ni ppm
200
100
10
1
10
100
200
(a)

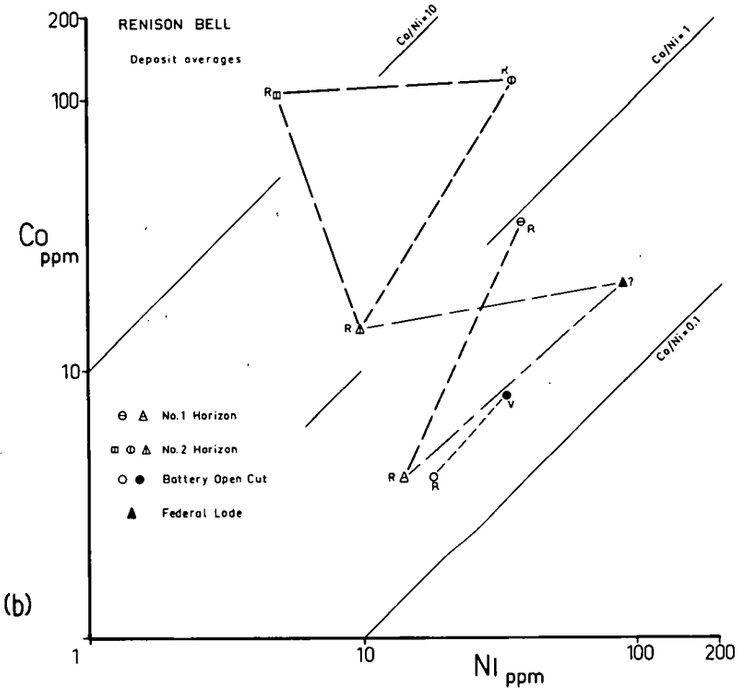
RENISON BELL
Deposit averages
No.1 Horizon
No.2 Horizon
Battery Open Cut
Federal Lode
Co/Ni=10
Co/Ni=1
Co/Ni=0.1
Co ppm
Ni ppm
200
100
10
1
10
100
200
(b)

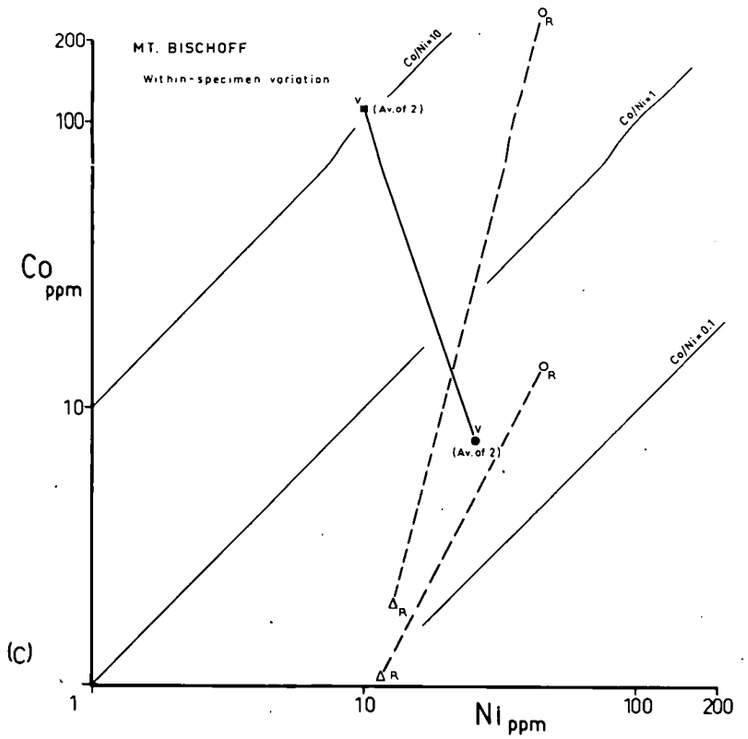
MT. BISCHOFF
Within-specimen variation
(Av. of 2)
(Av. of 2)
Co/Ni=10
Co/Ni=1
Co/Ni=0.1
Co ppm
Ni ppm
200
100
10
1
10
100
200
(c)

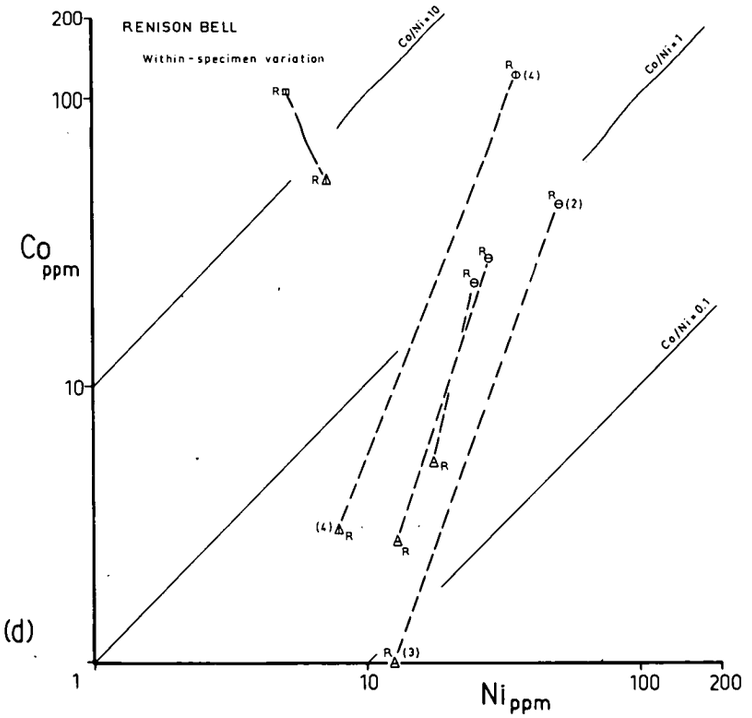
RENISON BELL
Within-specimen variation
(4)
(2)
(4)
(3)
Co/Ni=10
Co/Ni=1
Co/Ni=0.1
Co ppm
Ni ppm
200
100
10
1
10
100
200
(d)

Plate 6.3

Fissure vein - replacement relationships in the Battery Open Cut, Renison Bell (set 55). The main pyrite vein is approximately vertical, cutting and selectively replacing gently dipping fine-grained siltstones and shales. Selvages of pyrite adjacent to the veins have been remobilized, apparently back into the veins, the width of the selvages being approximately proportional to the width of the veins.

TOP 100636 : Two larger and one smaller pyrite veins, one filling a small fault, with associated replacement pyrite, and remobilization selvages of several sizes (x 1.5).

BOTTOM 100635 : Replacement, and a remobilization selvage, adjacent to the main pyrite vein (x 1.5).

variation in availability; or (b) a difference in physicochemical processes between replacement and vein deposition. Because the two deposits are 25 miles apart, and there is no previous documentation of Ni-enrichment with time of mineralizing solutions, variation in depositional processes appears to be the more likely explanation. The Ni-enrichment in the Federal Lode at Renison Bell (Fig. 6.22b) would then be empirical support for the lode being at least in part a vein deposit.

If Ni (and Co) have been lost from the sulphide phases during replacement reactions, possible repositories are carbonates and silicates in the host rock. However, analyses of primary dolomite, and of secondary carbonate and vein carbonate (sets 129, 130, 132) reveal no differences in Co-Ni contents between these minerals, and the whereabouts of any elements which may have been subtracted remains speculative.

The pyrites at Mt. Bischoff and Renison Bell belong in Trend IV along with other Devonian vein deposits (Fig. 6.6b). It may be noted that replacement pyrrhotites from the Cleveland cupriferous cassiterite-sulphide deposit have a quite different Co-Ni content to the Mt. Bischoff and Renison Bell replacement pyrrhotites, being enriched about five-fold in both elements.

Vein - sedimentary

The writer was requested by Dr. R.J. George (University of Adelaide) to compare the trace-element content of two sets of sulphides from the Nairne Pyrite deposit, South Australia, which occurred respectively in bedding, and in cross-cutting "shear" veins.

The Nairne Pyrite Member of the Brukunga Formation of the Upper Proterozoic-Cambrian (?) metamorphosed Kanmantoo Group (Thomson, 1965)

is a thick, lenticular unit, originally shale-greywacke, 20 miles long, containing disseminated pyrite and pyrrhotite. The Nairne deposit consists of three ore beds containing stratiform pyrite, separated by predominantly greywacke waste beds. George (1967) has established from rock analyses and mineralogical and textural studies that the ore beds are significantly different from the waste beds only in their Fe and S content. All rocks have undergone sillimanite-muscovite grade metamorphism, which has produced a dominant assemblage of quartz-muscovite-albite-microcline.

The sulphides occur in three modes that are of interest in the present study: primary sedimentary pyrite; vein pyrite and pyrrhotite in tension gashes, remobilized from the sedimentary material; and coarse-grained pyrrhotite-pyrite, with galena, chalcopyrite, sphalerite, arsenopyrite, and Ag-Sb sulphosalts, in cross-cutting "shear" veins about 8 in. wide. George (1967) has convincingly demonstrated the remobilized nature of the tension gash sulphides, but his evidence for the "shear" veins also being "lateral secretions" is not as conclusive. LaGanza (1959) considered the base metal traces to represent a later mineralization. This interpretation is supported by extensive regional geochemical sampling by the South Australian Geological Survey, which has shown that (a) other pyrite members to the north and south are low in base metal content; and (b) Cu, Pb and Hg trace anomalies occur where cross-cutting structures intersect the pyrite horizon (Thomson, 1965).

The results (set 1) of seven sedimentary pyrite analyses are compared with analyses of seven pyrites from the "shear" veins in

Figure 6.23

Co and Ni in pyrites and pyrrhotites from the Nairne Deposit, South Australia (set 1).

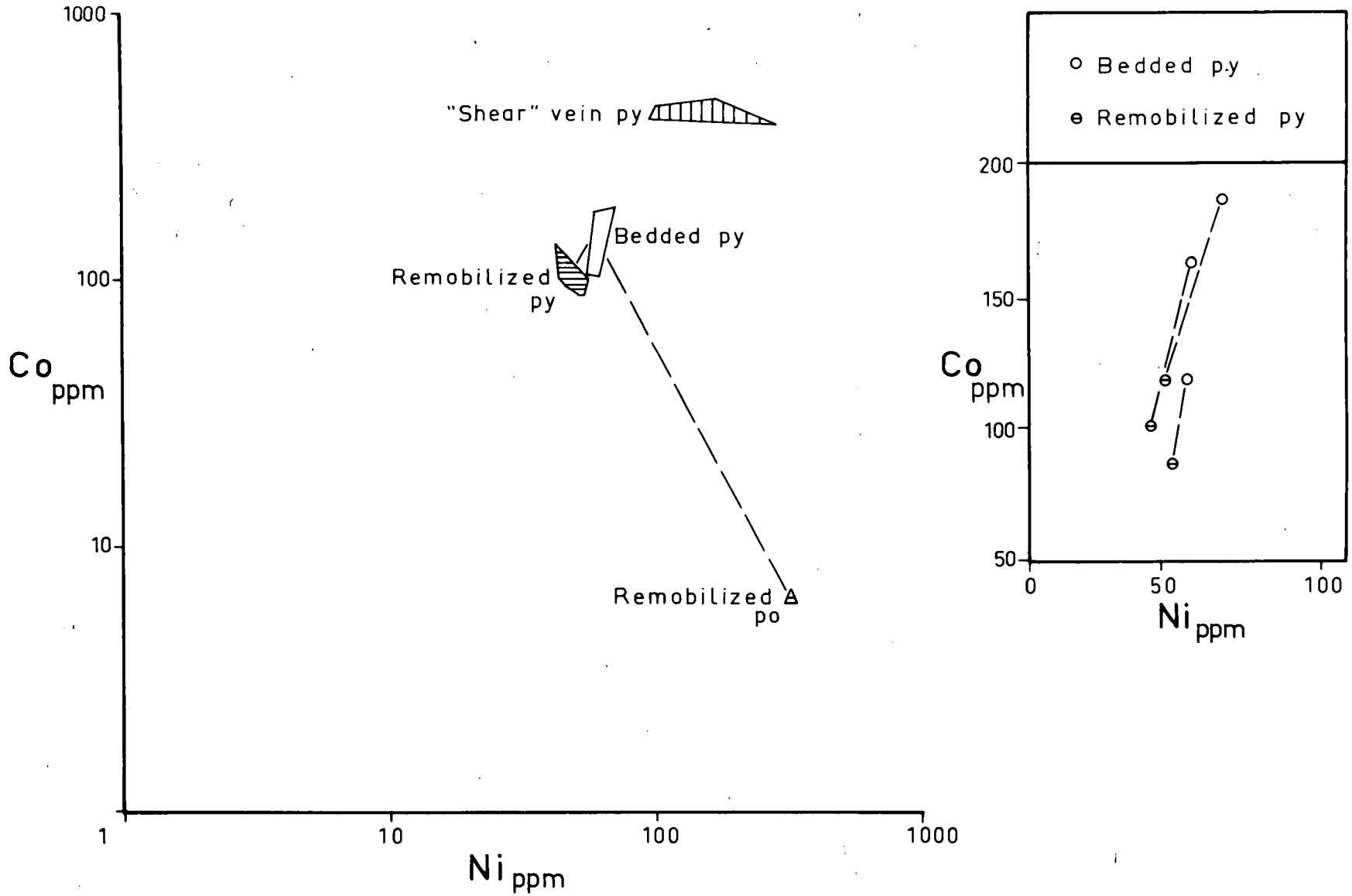
1000
100
10
1
Co ppm
1
10
100
1000
Ni ppm
"Shear" vein py
Bedded py
Remobilized py
Remobilized po
Bedded py
Remobilized py
200
150
100
50
Co ppm
0
50
100
Ni ppm

Figure 6.23. The two groups obviously belong to different populations, but the "shear" veins have a higher concentration of both Co and Ni than the sedimentary material, which is a trend opposite to that for remobilization at Nairne as established in the next section. It would appear that this constitutes further empirical evidence against the sedimentary and "shear" vein minerals being genetically related.

## Remobilization

One of the few Tasmanian ores studied which shows clear evidence of remobilization is that in the West Lyell Open Cut at Mt. Lyell, where discontinuous quartz-chalcopyrite-pyrite lenses (sets 81-84) up to several feet in circumference, which have been derived from the country rock (schist with disseminated sulphides: sets 77-80), occur at the nodes of large-scale cleavage boudins in the schist (Solomon et al., in press). The scale of the remobilization implies secondary hydrothermal transport. The reduction of both the Co and Ni content during remobilization of both pyrite and chalcopyrite can be observed on a deposit scale by comparing Figures 6.7a and 6.7c. However, as many of the samples on which those figures were based are < 95% single-mineral, another set of samples was more carefully processed to give pyrite and chalcopyrite concentrates, the purity of which was estimated mineragraphically by counting > 400 grains. The analyses of these concentrates were then cross-corrected to give the concentrations in the pure sulphides. The results, presented in Table 6.5, and plotted in Figure 6.24, verify the previously observed trend, and also reveal that a greater proportion of Co is lost than of Ni, particularly in the pyrite.

TABLE 6.5

MT. LYELL PYRITES AND CHALCOPYRITES : CROSS-CORRECTION PROCEDURE

| Number | Pyrite concentrate | | | Chalcopyrite concentrate | | | Cross-correction | | | |
|---|---|---|---|---|---|---|---|---|---|---|
| | Co 1 | Ni 1 | Py:Cpy* | Co 1 | Ni 1 | Py:Cpy* | $Co_{py}$ | $Co_{cpy}$ | $Ni_{py}$ | $Ni_{cpy}$ |
| SCHIST | | | | | | | | | | |
| 100670 | 2193 | 380 | 87:13 | 50 | 21 | 2:98 | 2521 | 0 | 435 | 13 |
| 100671 | 1458 | 333 | 99:1 | 99 | 32 | 4:96 | 1470 | 44 | 336 | 19 |
| 100672 | 2260 | 150 | 96:4 | 521 | 48 | 12:88 | 2343 | 273 | 155 | 33 |
| 100673 | 2358 | 150 | 100:0 | 330 | 36 | 6:94 | 2358 | 201 | 150 | 29 |
| QUARTZ VEINS | | | | | | | | | | |
| 100832A | 86 | 250 | 100:0 | 4 | 23 | 3:97 | 86 | 1 | 250 | 16 |
| 100832B | 82 | 153 | 100:0 | 1 | 7 | 0:100 | 82 | 1 | 153 | 7 |
| 100833A | 107 | 178 | 98:2 | 75 | 86 | 38:62 | 108 | 58 | 181 | 31 |
| 100833B | 113 | 100 | 97:3 | 55 | 5 | 1:99 | 115 | 54 | 103 | 4 |

* Counting > 400 grains mineragraphically.

Figure 6.24

The effect of remobilization on the Co and Ni contents of pyrite and chalcopyrite, West Lyell Open Cut. Analyses plotted have been cross-corrected (Table 6.5).

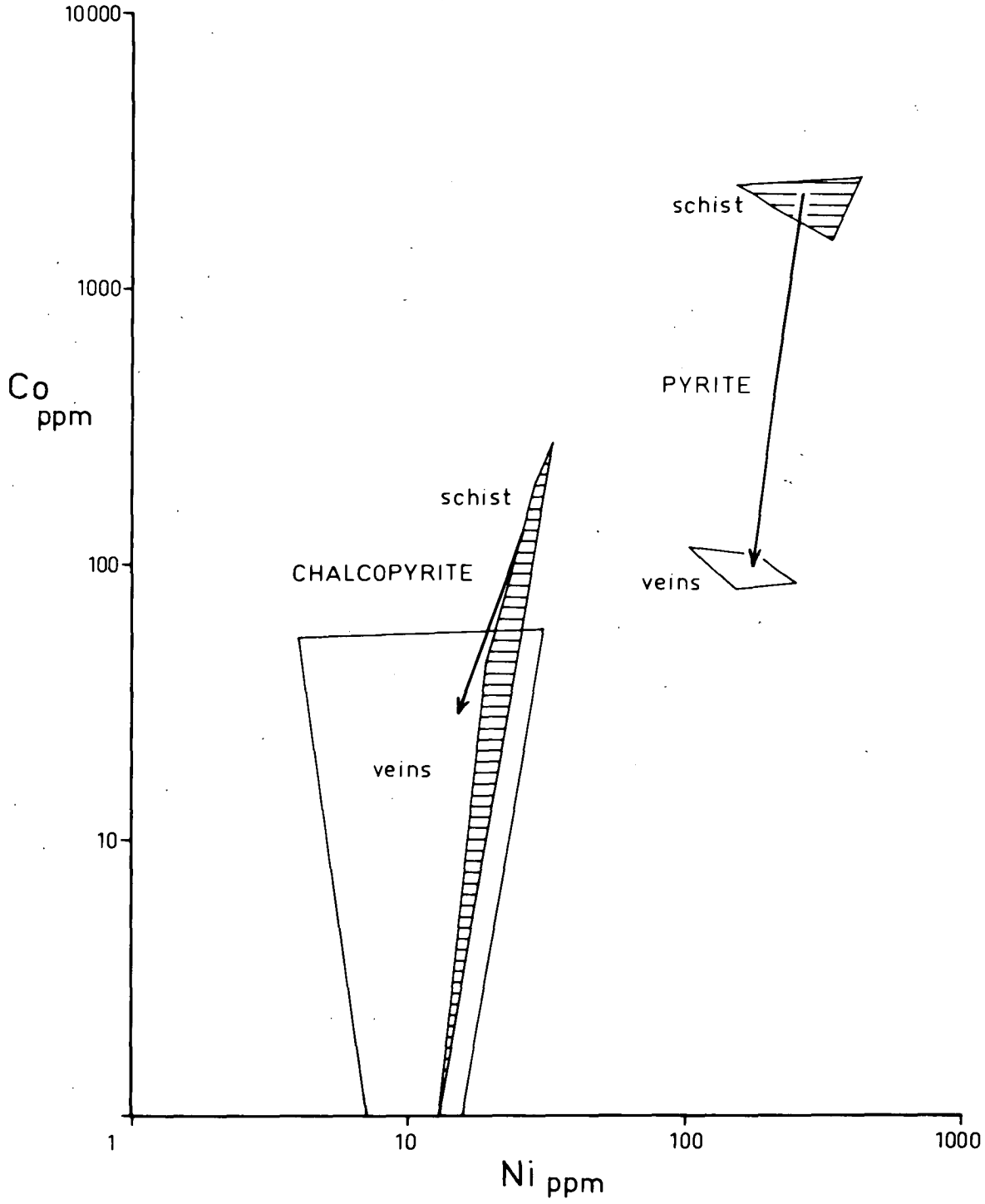
10000
1000
100
10
Co ppm
schist
PYRITE
veins
schist
CHALCOPYRITE
veins
1
10
100
1000
Ni ppm

The above result was checked by investigating an occurrence of remobilization on the specimen scale, where there was a reasonable probability that both the parent and daughter minerals were being sampled, and the remobilization need only have involved solid diffusion. The specimens used, from Nairne, are illustrated in Plates 6.4 and 6.5, and the results of the analyses (set 1) are plotted in Figure 6.23. The results are consistent with those from Mt. Lyell. Again, a slightly greater proportion of Co is lost than of Ni, but the impoverishment in Co is an order of magnitude less, which probably reflects the different scales of remobilization in the two deposits. At Chvalitice, Czechoslovakia (Cambel and Jarkovsky, 1967, p.244), there occurs similar impoverishment of Co and Ni in pyrites remobilized from a metamorphosed Proterozoic sedimentary pyrite-manganese ore.

The West Lyell quartz-chalcopyrite-pyrite veins show a different behaviour with respect to Se (Fig. 6.17). Selenium in the disseminated sulphides in the schist is irregularly distributed between pyrite and chalcopyrite, but after remobilization the pyrite is enriched and the chalcopyrite impoverished, in Se. This could imply that the remobilization has allowed a closer approach to equilibrium partitioning, but an alternative explanation is given below.

The impoverishment of Co (and Ni) during remobilization contrasts with the enrichment of Co in metamorphosed pyrites found by Cambel and Jarkovsky (1967), and implied by the high Co/Ni ratios in the Nairne bedding-plane pyrites. In general, both major and trace elements should be repartitioned during <u>in situ</u> recrystallization, especially if the original sulphide - non-sulphide assemblage was formed under sedimentary

Plate 6.4

Remobilization textures in specimens (set 1) from the metamorphosed Nairne pyrite deposit, South Australia. (Specimens by courtesy of Dr. R. George).

TOP 100630 : Coarse-grained metamorphic segregations of bedding-plane pyrite (white) with a little pyrrhotite (medium grey in top band), and of quartz (second band from the top) (x 2.4).

BOTTOM 100633 : Coarse-grained metamorphic segregation of pyrite (dull white) in the bedding planes, with a wide remobilization selvage adjacent to a tension gash containing pyrrhotite (bright white) (x 1.3). The Co and Ni concentrations show sharp gradients across this specimen:

| | po | selvage py | segregated py |
|---|---|---|---|
| Co ppm | 6 | 17 | 177 |
| Ni ppm | 314 | 63 | 59 |

Plate 6.5

Remobilization textures in specimens (set 1) from the metamorphosed Nairne pyrite deposit, South Australia. (Specimens by courtesy of Dr. R. George).

TOP 100634 : Bedding-plane pyrite segregations cut by two pyrite (white) - pyrrhotite (grey) remobilization veins in tension gashes parallel to the axial plane of a fold in the ore bed. Note the well developed remobilization selvages, which George (1967) has calculated (from point-counting) to be of the appropriate size to account for the amounts of sulphides in the veins.

BOTTOM 100631 : Similar to 100634, but coarser-grained, the remobilization selvage being defined mainly by the absence of the finer-grained pyrite (x 1.5).

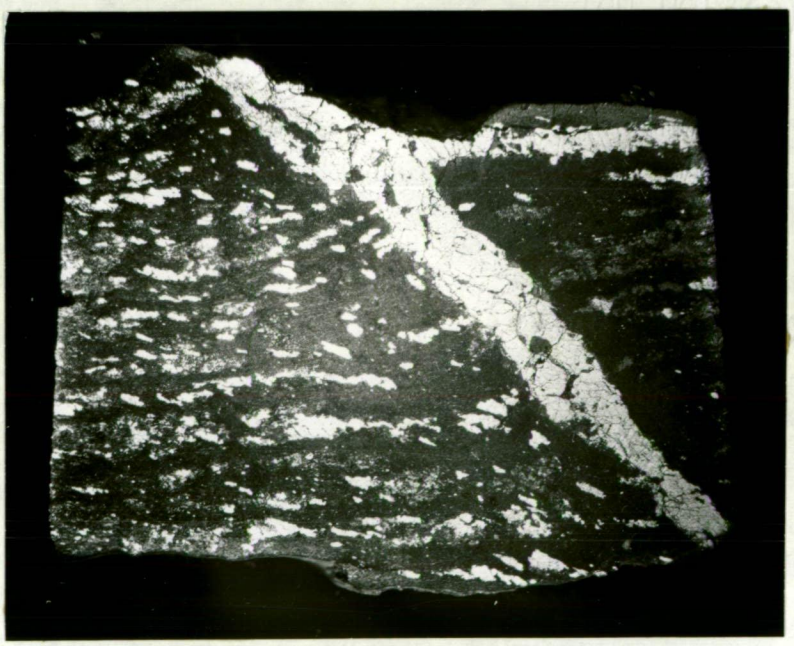

regimes of T, P, Eh, and pH. At Nairne, the trace Ti in the original clays has crystallized under high grade metamorphism as rutile (Edwards, 1949), and the major Fe has repartitioned between the sulphide and silicate phases (George, 1967).

Remobilization, on the other hand, probably involves diffusion, or hydrothermal transport, along structurally produced pressure gradients (Reitan, 1960; Ramberg, 1961; Gresens, 1966), and changes in Co, Ni and Se concentrations could be kinetic effects due to differential mobility of elements in the "dispersed phase".

## Partition between Minerals

Although the textures of most associated minerals examined in this study show that they were not deposited contemporaneously, the generalized distribution of Co and Ni between analyzed pairs (separated from single crushed samples) of associated minerals (Figs. 6.22c, d, 6.25, 6.26) agrees quite well with the distribution in Figure 3.1. Evidence particularly significant for pyrite-pyrrhotite partition is given by the analyses of the specimen from Nairne shown in Plate 6.4 (bottom), which are presented in the caption, and in Figure 6.23. The Co and Ni concentrations in the specimen have steep gradients with respect to the pyrrhotite vein. Further, the relative Co-Ni concentrations in remobilized pyrrhotite and remobilized pyrites from other specimens are almost identical with those suggested in Figure 3.1 on generally less satisfactory evidence.

Figure 6.25

Partition of Co and Ni between associated minerals. For examples from Mt. Bischoff and Renison Bell see Figure 6.22 (c, d). V = vein, L = Mt. Lyell, S = Savage River, O = Rosebery. Numbers are set numbers.

(a) Arsenopyrite-pyrrhotite, arsenopyrite-pyrite, pyrite-pyrrhotite.

(b) Pyrite-chalcopyrite.

(c) Pyrite-magnetite.

(d) Pyrite-hematite.

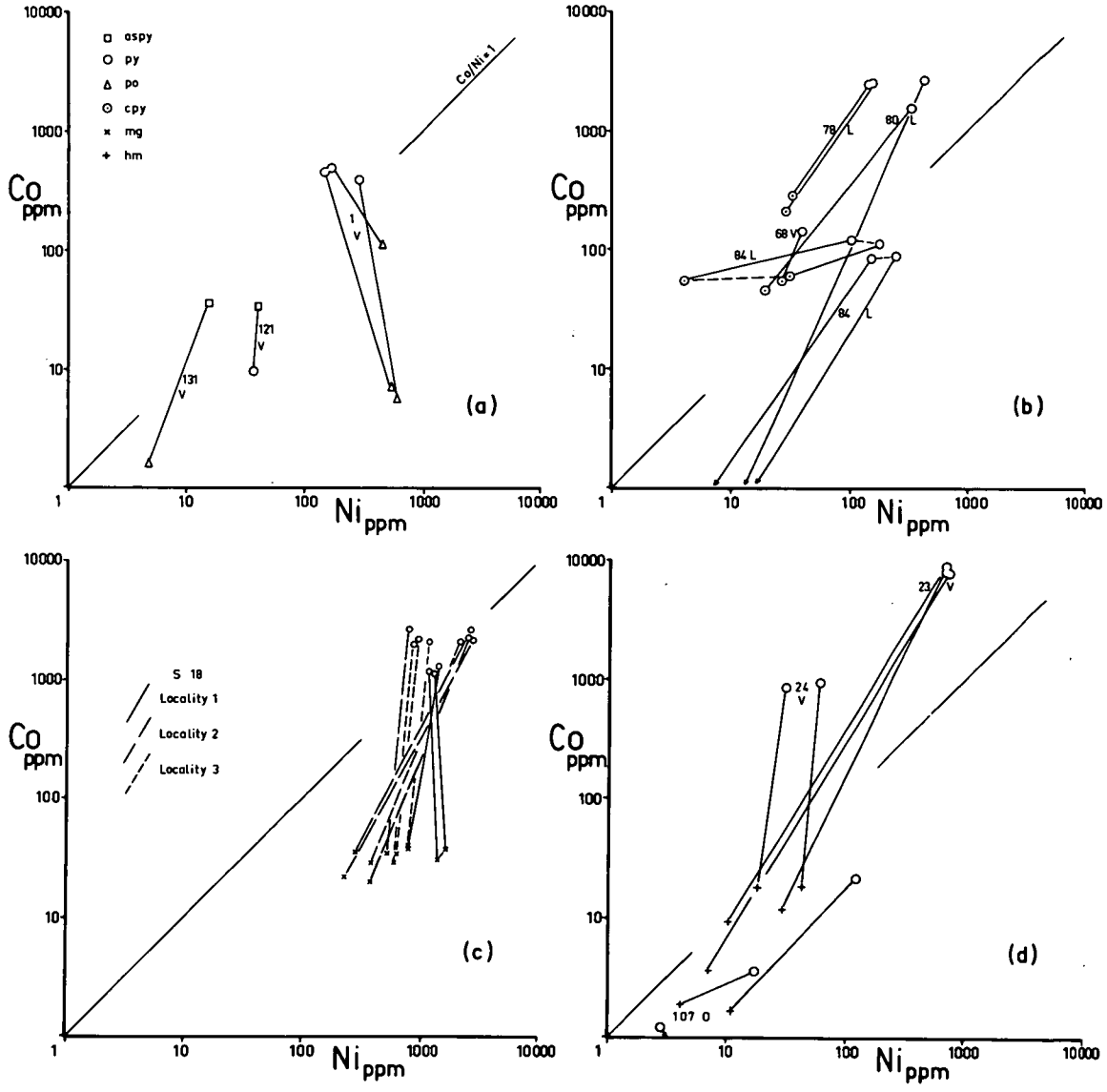
aspy
py
po
cpy
mg
hm
Co/Ni=1
Co ppm
Ni ppm
10000
1000
100
10
1
131 V
121 V
1 V
(a)
79 L
80 L
68 V
84 L
84 L
(b)
S 18
Locality 1
Locality 2
Locality 3
(c)
23 V
24 V
107 0
(d)

Figure 6.26

Averaged results of the partitioning of Co and Ni between pyrite and other associated minerals in this study (cf. Fig. 3.1).

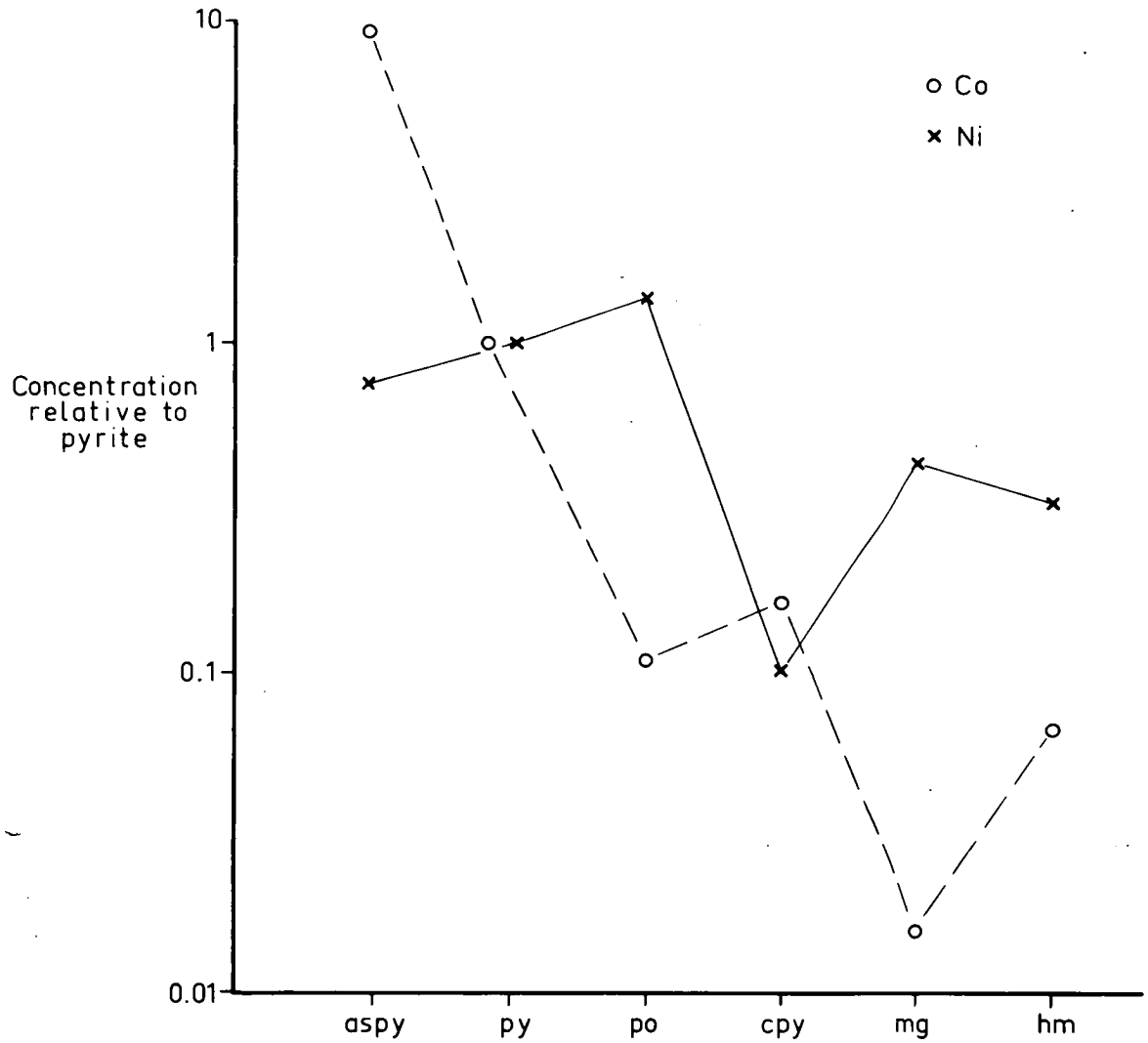
10
1
0.1
0.01
Concentration relative to pyrite
o Co
× Ni
aspy
py
po
cpy
mg
hm

There are, however, some disagreements with predicted partitioning relationships:

(i) All the hematites have Ni > Co, which may partly be explained in sets 24 and 107 by known magnetite contamination.

(ii) The pyrite-pyrrhotite relationships at Mt. Bischoff and Renison Bell are anomalous, as the pyrrhotite in the replacement deposits contains less Ni than the pyrite. Although this is consistent with the textural disequilibrium between the two minerals in both deposits (D.I. Groves, pers. comm), there is both a remarkable similarity between the pyrite-pyrrhotite partitioning in the two deposits (Figs. 6.22a, b), and a constant partition within the deposits (Figs. 6.22c, d). As with the replacement-vein relationships discussed previously, the similarities could be caused by similarly varying availability during paragenesis, or by a common mechanism of emplacement, perhaps involving a constantly biased disequilibrium partitioning. The latter alternative is unlikely, but a third possibility, at present untestable, is that the Co-Ni partitioning was actually in equilibrium under the prevailing physicochemical conditions of deposition. If this hypothesis can also be discounted, similarly varying availability is the most likely explanation, which would be compelling evidence against the tentative conclusion previously drawn for a process-controlled impoverishment of Ni during replacement reactions.

Despite the above anomalous effects, the three specimens, from Savage River and Mt. Lyell, which were analyzed in duplicate to test for internal consistency of Co-Ni partition, gave positive results [Fig. 6.25: (b) 84L, (c) locality 1]. The tie lines were parallel,

and in the direction predicted in Figure 3.1, and the partition ratios of both Co and Ni for the mineral pairs were very similar for adjacent pairs, thus suggesting equilibrium partitioning on a hand-specimen scale. The partitions were derived from analyses which had either been cross-corrected (Mt. Lyell, Table 6.5), or which were of > 99.5% pure mineral (Savage River).

The consistency of variations at the specimen-scale and the deposit-scale at Savage River and Mt. Lyell may be partly due to the relatively large intrinsic difference in Co-Ni accommodation between pyrite-chalcopyrite and pyrite-magnetite. Such large intrinsic differences probably constitute the best explanation for the reasonable agreement which is found between the results of workers analyzing Co-Ni in ores which often are known to be in textural disequilibrium, and between these results and the theoretical predictions. Because there is not the same agreement between the results of investigations of Se in different minerals, it is probable that any intrinsic differences in Se accommodation between ore minerals is small. In this study, although there are discernible trends of impoverishment of Se in sphalerite (Fig. 6.12), the distribution between pyrite and chalcopyrite appears to be variable (Figs. 6.12; 6.17 - West Lyell veins).

## Dilution

Only in samples from the Stirling Valley Mine (set 121, Fig. 6.11) were there observed effects which could best be explained by variable abundance of suitable host minerals. There is a 20 to 30-fold enrichment

of Co and Ni in pyrite from the quartz veins compared with that in the pyrite veins, which is probably due to the negligible tendency of the $SiO_2$ structure to accommodate these trace elements, causing their concentration in the pyrite.

## Zoning

Three excellent opportunities existed in Tasmanian deposits for testing the spatial distribution of Co and Ni in sulphides - at Mt. Bischoff, Zeehan, and Story's Creek.

(i) At Mt. Bischoff (Fig. 6.18), Groves (1968) and Groves and Solomon (in press) have established, from several criteria, a temperature gradient from the central part of the dyke swarm (Brown Face) outwards (Fig. 6.27). There are no uniform gradients of Co-Ni values over the same interval (Fig. 6.28), but within the replacement lodes the pyrrhotites show an increase in Ni from the Brown Face outwards accompanied by an increase, and then a larger decrease, in Co (Fig. 6.28, inset). The peculiar Co trend (which is similar to Se zoning at the McIntyre Mine, Canada, noted on p.34) is paralled by a decrease, and then a larger increase, in the $\delta S^{34}$ values (Rafter and Solomon, 1967) , the apex of both distributions occurring in the same area (Greisen Face - Pig Flat). This suggests that overall zoning trends of decreasing Co and increasing $\delta S^{34}$ values are complicated by additional unknown local variables.

(ii) Williams (1968) has analyzed pyrites from Zeehan, sampled from the pyritic, sidero-pyritic, and sideritic zones, which are

Figure 6.27

Variation of parameters of possible thermometric significance with spatial position at Mt. Bischoff (Groves, 1968).

A. Formation temperatures of fluorite and quartz from fluid inclusion studies.

B. FeS content of sphalerite, expressed as mole %.

C. Composition of pyrrhotite, expressed as atomic % Fe.

D. Isotopic composition of sulphur, expressed as $\delta S^{34}$.

A
FORMATION TEMP °C OF FLUORITE AND QUARTZ (Fluid inclusions)
600
500
400
300
200
100
RANGE
MEAN
B
MOLE % FeS IN SPHALERITE
25
20
15
10
SINGLE ANALYSIS
TWO ANALYSES
C
ATOMIC % Fe IN PYRRHOTITE
47·6
47·4
47·2
47·0
46·8
46·6
46·4
4
2
6
7
8
SINGLE ANALYSIS OF HEXAGONAL PYRRHOTITE
TWO ANALYSES OF HEXAGONAL PYRRHOTITE
RANGE OF COMPOSITION AND NUMBER OF SAMPLES OF MONOCLINIC PYRRHOTITE
D
δ 34S VALUES IN SULPHIDES
+6
+4
+2
0
−2
PYRRHOTITE
PYRITE
SPHALERITE
PORPHYRY DYKES
BROWN FACE
SLAUGHTERYARD FACE
GREISEN FACE
PIG FLAT
SOUTH END OF OPEN CUT
THOMPSON'S LODE
NORTH VALLEY AND GIBLIN LODE
ANTIMONIAL LODES
LODE NORTH OF WARATAH RIVER
FOOKS LODE
SILVERCLIFFS LODE
MAGNET LODE
INCREASING DISTANCE FROM CENTRE OF MOUNT BISCHOFF

Figure 6.28

Spatial distribution of Co and Ni in pyrite, pyrrhotite and arsenopyrite at Mt. Bischoff. The lode sequence is the same as that used in Figure 6.27 to illustrate the zoning across the deposit, the Brown Face being the area of highest temperatures of deposition. The inset shows the Co-Ni concentration trend for pyrrhotite in the replacement deposits across the lode sequence.

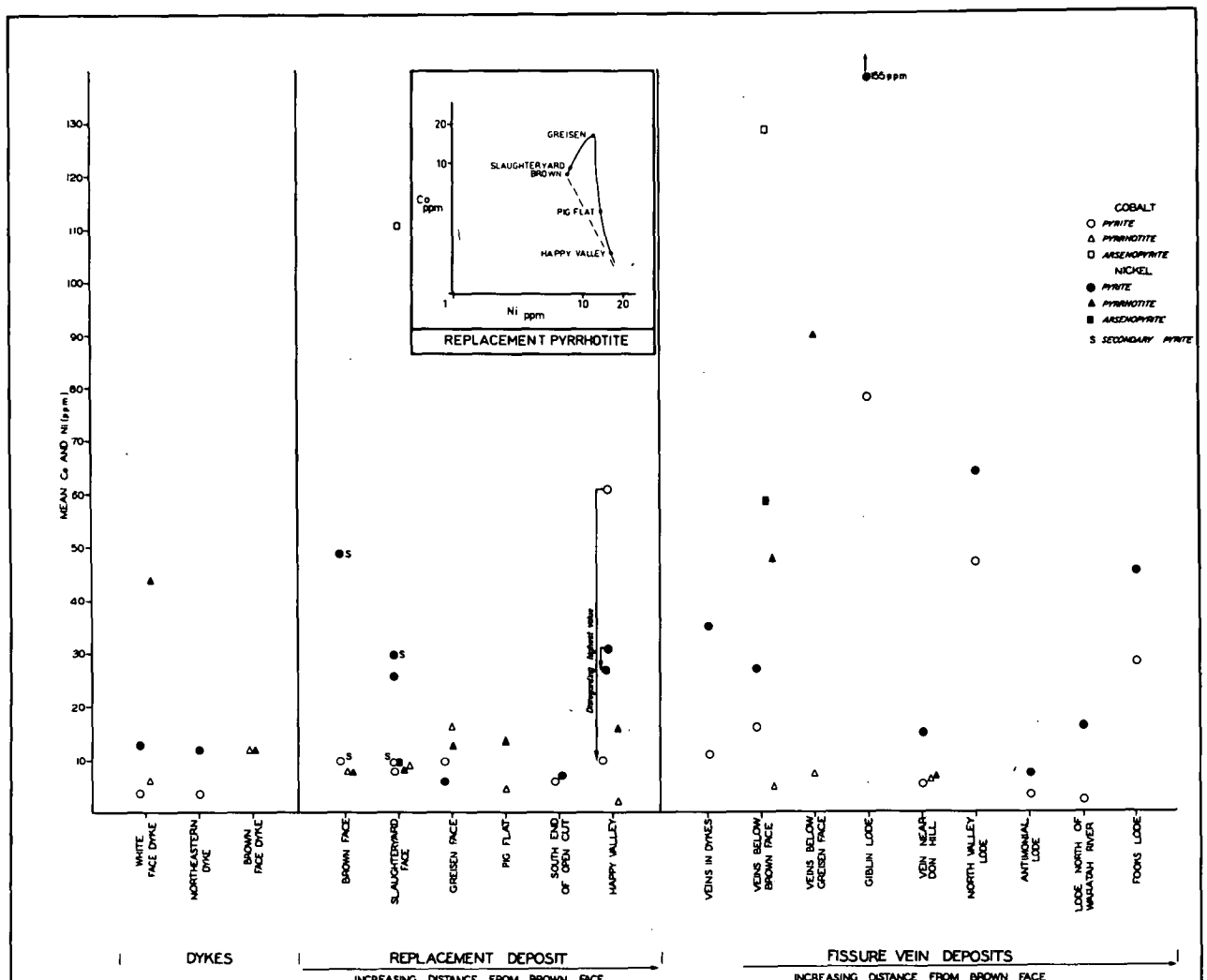


DISTRIBUTION OF Co AND Ni IN Fe-SULPHIDES MT. BISCHOFF

believed to represent zones of decreasing temperature of deposition (Both and Williams, 1968). The Co-Ni analyses are plotted in Fig. 6.29a. Williams found the pyritic and intermediate zone pyrites to have significantly different Co contents (by F-test), and he also calculated Co-Ni correlation coefficients of -0.58 and -0.84 for normal and logarithmic coordinates respectively. He concluded that the limited data supported the idea of Co content of pyrite decreasing with decreasing temperature; and on the basis of the negative correlations, he inferred an opposite, if less pronounced trend for Ni. He emphasised that temperature was probably not the direct control of Co concentration.

(iii) At the Story's Creek Mine, the vein system is underlain 620 ft underground by an aplite cupola of the parent granite (Kingsbury, 1965). The (Sn + W) content and the Sn/W ratio are zoned with respect to the granite, and it seems likely that a temperature gradient was present during the formation of the veins. This is supported by fluid inclusion studies (D. Patterson, pers. comm.). A preliminary survey of the Co-Ni values in pyrite (set 68) shows an inverse relationship between Co concentration and distance from the igneous source (Fig. 6.29b), for an interval over which the fluid inclusion studies indicate a temperature difference of 80°C.

In at least two of the three samples studied, therefore, there are indications of a decrease in Co content of sulphides with increasing distance from the igneous source and/or lower temperature-type of deposit. These results support the inverse relationships between Co concentration (in pyrite and sphalerite) and various parameters related to "distance from the source" (e.g. inferred temperature, Zn/Pb ratios)

Figure 6.29

Zoning of Co and Ni at Zeehan and Story's Creek.

(a) Results of pyrite analyses from the Heemskirk Granite (sets 27, 28) and some peripheral Zeehan lodes (sets 58, 59), compared with independent analyses by Williams (1968) of pyrites from the Zeehan lodes subdivided with respect to the mineralogical zoning. Note that the regression line for the analyses of set 59 has an opposite slope to the overall trend.

(b) Zoning at Story's Creek, showing a general decrease in Co concentration away from the source granite.

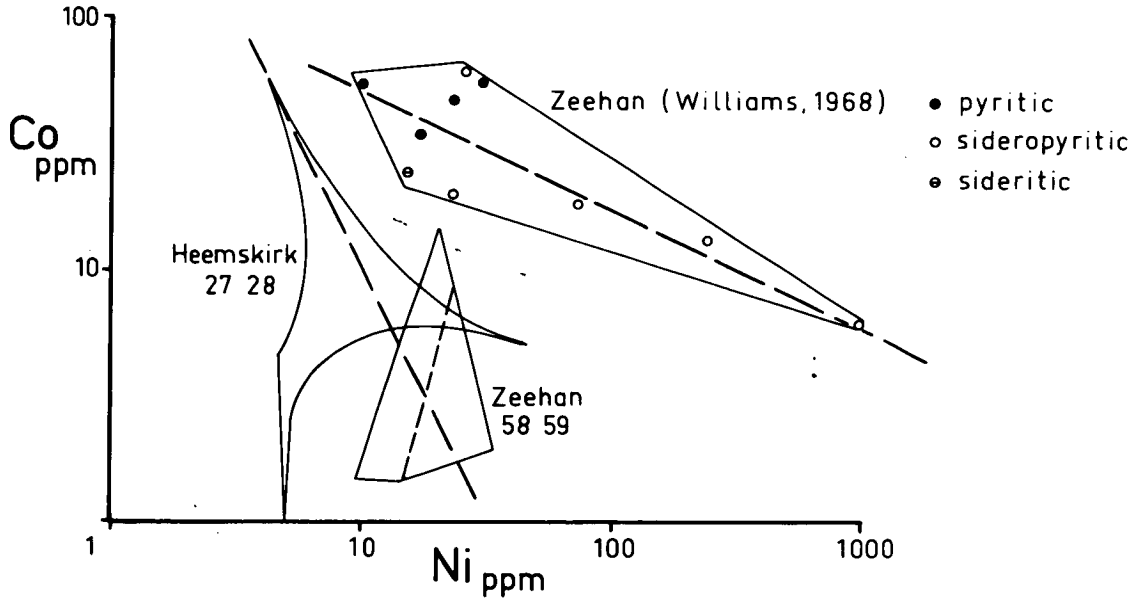
100
Co
ppm
10
Heemskirk
27 28
Zeehan (Williams, 1968)
pyritic
sideropyritic
sideritic
Zeehan
58 59
1
10
100
1000
Ni ppm

(a)

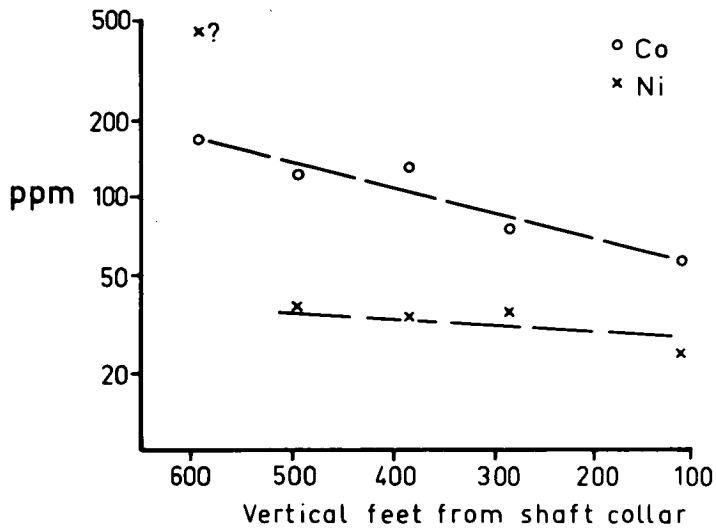
500
200
ppm
100
50
20
×?
Co
Ni
600
500
400
300
200
100
Vertical feet from shaft collar

(b)

previously established by Gavelin and Gabrielson (1947), Bjørlykke and Jarp (1950), Hawley (1952), and Rose (1967). A direct relationship between Ni content and these parameters is suggested by the Mt. Bischoff and Zeehan results.

Because of the controversy over the relationship between Cd content of sphalerite and its Fe content and temperature of formation, the data of Appendix 2 have been tested for the significance of such correlations. A plot of average Fe content against average Cd content, and the ranges of contents, of sphalerites from the different areas is shown in Figure 6.30. There is no simple relationship between Fe and Cd if all the deposits are considered together, and the Devonian cassiterite-sulphide deposits and Pb-Zn-Ag fissure veins show opposite trends if grouped separately. If, however, the spatial distribution is considered, i.e. Waratah, Mt. Bischoff and Cleveland are grouped in one district (group 1), and Zeehan, north-east Dundas and Renison Bell in another (group 2), there is a negative correlation within each district between the average Cd and Fe values for each deposit. The negative correlation becomes even clearer when the Zeehan values are divided between the pyritic and sideritic zones, and averaged. Further, Williams (1968) has found a good negative correlation ($r = -0.92$) between average Cd and Fe in sphalerites from the Zeehan lodes (25 analyses from 14 localities).

The negative correlations of the averages within the two district sets is not, however, shown by the individual analyses, as correlation coefficients calculated for the latter are not significant at the 95% level of confidence. Thus in western Tasmania Cd and Fe are dependent variables on a regional scale, on a deposit scale (Zeehan), but not on

Figure 6.30

Plot of averaged Cd and Fe in sphalerites from the Devonian lodes, and from Rosebery-Hercules and Mt. Lyell (Groves and Loftus-Hills, in press). The bars represent the ranges of values, the individual analyses being given in Appendix 2.

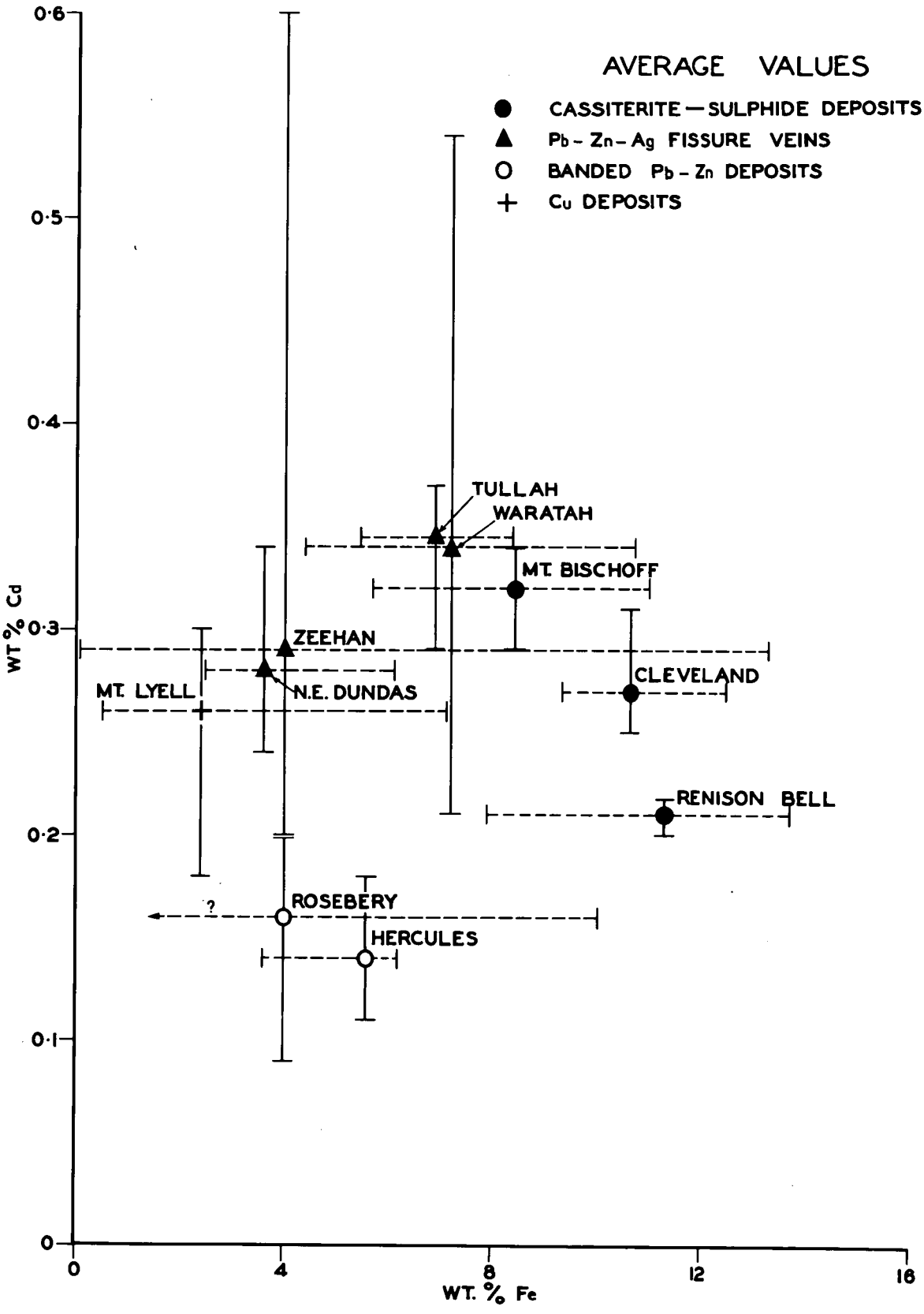
AVERAGE VALUES
CASSITERITE — SULPHIDE DEPOSITS
Pb - Zn - Ag FISSURE VEINS
BANDED Pb - Zn DEPOSITS
Cu DEPOSITS
0·6
0·5
0·4
0·3
0·2
0·1
0
WT % Cd
0
4
8
12
16
WT. % Fe
TULLAH
WARATAH
MT. BISCHOFF
ZEEHAN
N.E. DUNDAS
MT. LYELL
CLEVELAND
RENISON BELL
ROSEBERY
?
HERCULES

a specimen scale. This discrepancy could be partly due to insufficiently large sample populations, but the large ranges of concentrations for each deposit (Fig. 6.30) suggest that additional local specimen-scale variables are masking the regional correlation. The regional trends are most simply ascribed to a varying availability of Cd in the ore forming fluid related to distance from the source of the fluid.

## Discussion

Trends I to V, defined from the undifferentiated Co-Ni analyses of pyrites, contain the following components due to depositional and post-depositional processes:

(i) The trends to high Co, with Co/Ni > 1 (trends II and IV), contain components due to remobilization (Mt. Lyell) and to zoning (Story's Creek). The remobilization effect, although large, may be disregarded in discussions of availability, and the zoning effect does not substantially contribute to the outline of trend IV.

(ii) The trend to high Ni, with Co/Ni < 1 (trend III), contains components due to differential enrichment in veins and replacement lodes (Mt. Bischoff, Renison Bell), and to a large mineralogical dilution effect within the Stirling Valley deposit. Neither of these components is inconsistent with the trend as established by other Devonian ores.

(iii) The negative correlation trend between Co and Ni (trend V) is wholly due to zoning of lodes across the Heemskirk-Zeehan field. Further, the one lode for which several analyses are available (Zeehan-Queen, set 59) follows trend III, normal to trend V (Fig. 6.29a).

Trend V cannot therefore be used as a basis for comparison of fundamental availability in other deposits.

Although the range of Cd values in the Devonian sphalerites is partly caused by a district-scale zoning, this range is still quite distinct from that of the Rosebery-Hercules sphalerites. Similarly, the correlation of Se abundance with type of mineralization at Mt. Lyell does not invalidate the comparisons already made between the range of Se values in this deposit and in other deposits.

Thus, with the exception of Co-Ni trend V, the variations of concentrations of Co, Ni, Se and Cd due to the recognizable depositional and post-depositional processes have contributed little to the boundaries of the originally defined trends and groupings, which may therefore be interpreted as reflecting fundamental availability.

## METALLOGENIC SUBPROVINCES

The Co-Ni and Se analyses of pyrites from the Devonian deposits cannot be systematically subdivided on the basis of geographic distribution. There appears to have been a uniform availability of these elements during this epoch across Tasmania, in agreement with the consanguinity of the east and west coast Devonian granites evident from petrologic and radiometric relationships (Spry, 1962b; McDougall and Leggo, 1965).

The values of Cd-Fe averaged for the different areas, as plotted in Figure 6.30, suggest a varying availability of Cd between district groups 1 and 2. This variation was tested by covariance analysis of Cd

on Fe for the individual analyses (Snedecor, 1946, p.318). It was established at the 95% confidence level that the Fe content of the sphalerites did not explain the difference in Cd content between the two districts; after Cd was adjusted to a common Fe basis, the Cd contents were still different. This small initial difference in availability of Cd between the Zeehan-Renison Bell and the Mt. Bischoff-Cleveland districts is not shown by Co and Ni.

## ORES OF UNCERTAIN ORIGIN

### Savage River

The Co and Ni values in pyrite (Fig. 6.3) lie about the line Co/Ni = 1, Co ranging 1000-2600 ppm and Ni 760-2700 ppm. They are unlike the values in any other Tasmanian pyrites, thus precluding empirical correlation with local ores of known origin. However, the ranges of values are not incompatible with data from other countries. Ortho-amphibolites in general, like the original mafic ingeous rocks, have high Co and Ni, and Ni > Co (Taylor, 1965). Evans and Leake (1960) give an example from Ireland with Co approximately constant at 10-46 ppm, and Ni ranging 6-465 ppm. The Ni values in the amphibolites of the Savage River similarly range 50-200 ppm* (E.B. Corbett, pers. comm.), and if the Co values are assumed to be < 50 ppm, the enrichments of Co and Ni in the pyrite are by approximate factors of 50 and

---

* Analyses by XRF spectrograph, University of Tasmania.

20 respectively relative to the present host rock. The different partition ratios for Co and Ni are consistent with the crystallochemical properties of pyrite, and are similar to ratios (Fe-sulphide liquid/silicate liquid) calculated for Skaergaard by Wager et al. (1957). Cambel and Jarkovsky (1967, p.435) also consider that Ni concentrations in certain pyrites averaging 1680 ppm were derived from ortho-amphibolites averaging 199 ppm Ni.

It has already been suggested that the ore was metamorphosed at least twice, which may explain the apparent trace-element equilibrium on a hand-specimen scale between pyrite and magnetite. Figure 6.3 shows that, in the data averaged for three localities, an increase in $Co_{py}$ is accompanied by a decrease in $Ni_{mg}$. This effect is as great between localities as within localities (Fig. 6.25c), and is ascribed to variation of Co and Ni during the original mineralization.

The Se values in the pyrites (Fig. 6.12) are too few for statistical comparison with the other groups, but they are very much less than the values in the pyrrhotite-pentlandite ore associated with the mafic-ultramafic complex at Cuni.

There are insufficient trace element results to give a detailed indication of mechanisms of emplacement of the Savage River ores, but the data are consistent with abundances in sulphides in other ortho-amphibolites.

## Mt. Lyell

The results of the analyses (Figs. 6.7, 6.8) may be summarized as follows. Pyrite from disseminated and massive cupriferous mineralization (Figs. 6.7a, 6.8a - 72, 6.8b - 91) contains high Co and low Ni. Chalcopyrite from the same ores contains less Co and Ni than the pyrite. Pyrite from disseminated non-cupriferous mineralization (Figs. 6.7b - 85 to 88, 6.8a - 73 to 76, 6.8b - 89 to 90) also contains somewhat less Co and Ni, and that from the Pb-Zn ore at Tasman and Crown Lyell (Fig. 6.8c - 95) contains little of either Co or Ni. As already discussed, pyrite and chalcopyrite remobilized from disseminated mineralization (Fig. 6.7c) become impoverished in both Co and Ni.

These results indicate that Co in pyrite correlates grossly with the Cu concentration, the lowest Co values being recorded either in pyritic disseminations spatially separated from the Cu ore (as at the Blow), or in areas which are generally Cu-deficient (as in the Cape Horn pyrite body, and at Comstock). This phenomenon does not, however, apply over a wider area, because although there are other Cu ores in the Cambrian acid-intermediate igneous suite which are Cu-rich and Co-rich (set 24), there are Co-rich mineralizations that lack Cu (sets 22, 23). It is interesting to note that Se is dispersed in this igneous suite quite differently, being enriched only at Mt. Lyell, but not showing the same correlation with Cu across the area.

Spatial distribution was tested by sampling several specimens from each of four adjacent pyritic shoots in the schistosity at the Blow (sets 73-76; Fig. 6.8a); several specimens from each of three

similar shoots in the West Lyell Open Cut (sets, 85-87; Fig. 6.7b); and irregularly distributed specimens from each of three diamond-drill holes through the Prince Lyell orebodies (sets 71-80; Figs. 6.7a, 6.31). The results show that the Co/Ni ratio remains approximately constant within individual shoots, but that successive shoots are demarcated over distances as small as 10 ft by variable Ni, and to a much less extent variable Co. This implies stratification of Ni (and Co) in the plane of the shoots. In the larger-scale Prince Lyell ore lenses (Fig. 6.31), the Co and Ni concentrations have been averaged over 25 ft intervals along the drill holes, and the resulting values define a limiting volume for mutual dependence of Co and Ni concentrations of about 200 ft normal to the lenses, and up to at least 1200 ft parallel to the lenses, once again indicating gross stratification. However, the large-scale isopleths of Ni, Co, and Cu values (the latter indicated by the lens outlines in Fig. 6.31) are not quite parallel, which suggests either that the stratification of elements is less likely to have been caused by simple sedimentation than by large scale replacement, or possibly that later metamorphism has slightly modified the dispersion patterns. The tendency for Co to be enriched within the lenses of higher Cu-concentration is further evidence for the correlation of Co and Cu within the deposit.

The banded Pb-Zn ores at Tasman and Crown Lyell, which are somewhat similar to the ore at Rosebery, display a variety of empirical correlations. On the basis of Se, and of S-isotope analyses (Solomon *et al.*, in press), these ores are little different from the other Mt. Lyell mineralization, and quite different to the results for Rosebery. In their Co and Ni values, however (Fig. 6.8c), they differ markedly from

Figure 6.31

Co and Ni contents of pyrite (chalcopyrite) concentrates from three diamond-drill holes through B, C and D lenses of the Prince Lyell orebody, Mt. Lyell.

(a) Cross-section through the ore lenses (redrawn from a tracing supplied by courtesy of the Mt. Lyell Co.). The profile of the West Lyell Open Cut is that at 30/6/67. The dip of the schistosity is approximately parallel to that of the lenses.

(b) Co and Ni analyses (sets 78, 79, 80) averaged over 25 ft. intervals. A few individual analyses may be up to 20% low (compared with pure pyrite) because of dilution of the pyrite concentrates with chalcopyrite. The solid-dashed lines represent interpreted trends in Co and Ni concentrations, the solid segments representing the lens positions.

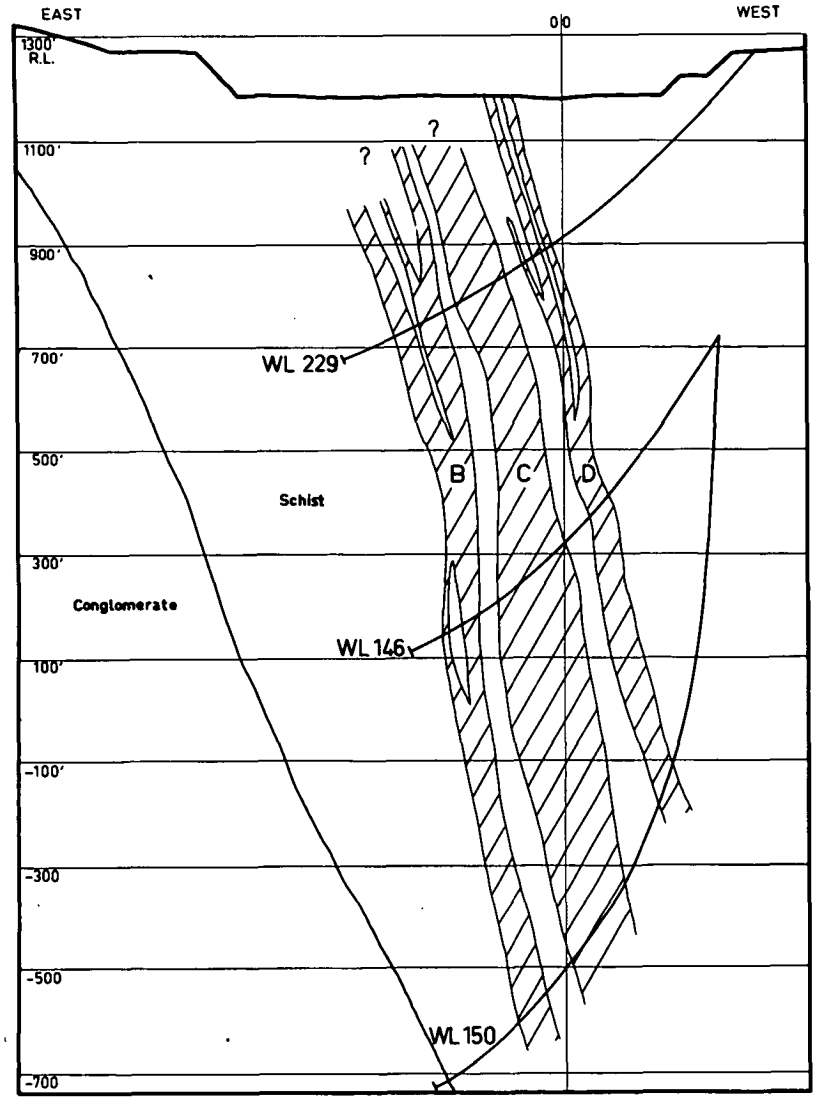
EAST
0|0
WEST
1300'
R.L.
1100'
900'
700'
500'
300'
100'
-100'
-300
-500
-700
?
?
WL 229
WL 146
WL 150
B
C
D
Schist
Conglomerate

(a)

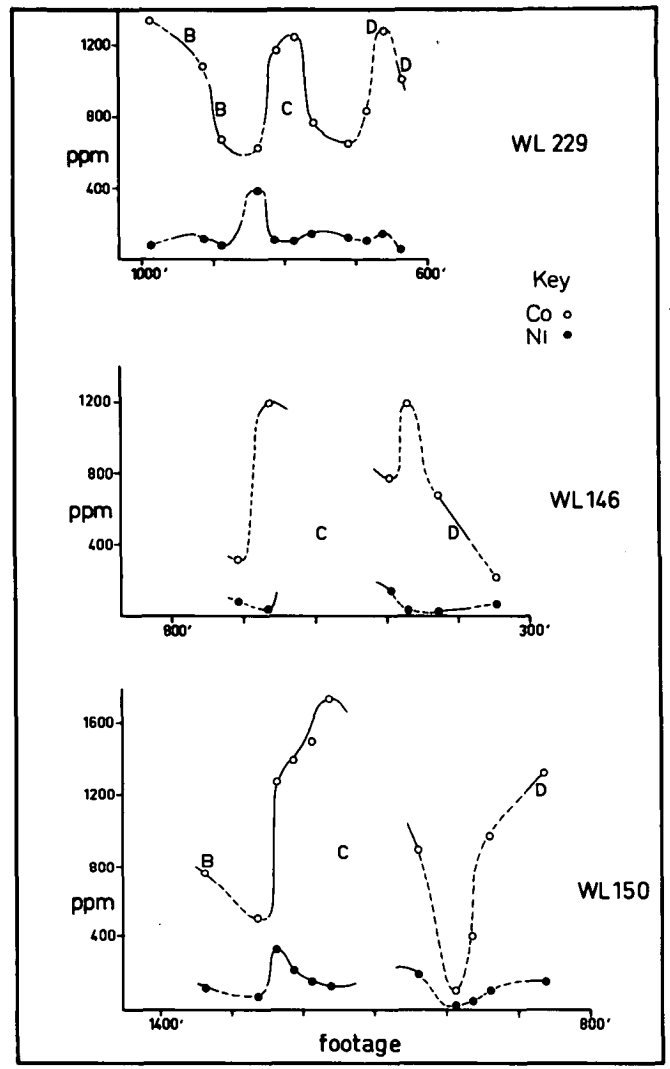
1200
800
ppm
400
B
B
C
D
D
WL 229
1000'
600'
Key
Co ○
Ni ●
1200
800
ppm
400
C
D
WL 146
800'
300'
1600
1200
800
ppm
400
B
C
D
WL 150
1400'
800'
footage

(b)

the other Mt. Lyell ores, and lie within the range of values shown by the Rosebery ores (Fig. 6.9).

The overall trend of the Co-Ni values in the Mt. Lyell deposit is coincident with trend II, which was defined from the concentrations in pyrites coeval with the Cambrian acid-intermediate igneous activity. This correlation is strong empirical support for a similar origin for the Mt. Lyell ores. Evidence from this study that the mineralization was due to the volcanic phase of this ingeous activity is based on comparisons with data from ores in other countries:

(i) The Co-Ni values in the Cu ores, and the relative impoverishment in the associated Pb-Zn ores, are consistent with values in several similar ores in Europe and Canada for which a volcanic source of the metals has been postulated (see Chapter 3).

(ii) The high concentrations of Se in sulphides at Mt. Lyell (Fig. 6.12), in an otherwise low- to normal-Se province, are consistent with enrichment in pyritic-Cu deposits in volcanic rocks elsewhere in the world (Sindeeva, 1964). However, the pyrites from the Cambrian volcanic rocks and sub-volcanic granites away from the Mt. Lyell area are all low in Se, and it would appear that whatever process resulted in Cu-rich ore fluids at Mt. Lyell also caused a concentration of Se.

(iii) The Se dispersion pattern (Fig. 6.17) is best explained by a volcanic origin for the ores. As Se is particularly enriched in surficial volcanic processes, its concentration in the massive orebodies at Mt. Lyell (including the banded Pb-Zn deposit at Tasman and Crown Lyell), which occur at the stratigraphic top of the Cambrian volcanic sequence, is consistent with the surface origin which has previously been suggested

for several of these lodes, and for hematite-chert bodies at the same horizon (Solomon, 1967; Markham, 1968; Solomon et al., in press).

## Rosebery-Hercules District

Samples, mainly of purified pyritic ore, from the Rosebery and Hercules banded Zn-Pb-Cu lodes, show an enrichment in Co from 0 ppm to 650 ppm, but an extreme deficiency in Ni, most of the analyses falling below 20 ppm (Fig. 6.9). The maximum Co values are one-third, and the average Ni values one-twentieth, those at Mt. Lyell. The Se values, and the Cd concentrations in sphalerites, are also significantly impoverished with respect to all the other ores analyzed, most significantly the Devonian ores. The Se values are very much less than in the similar Tasman and Crown Lyell ore at Mt. Lyell.

A spatial distribution within the Rosebery lodes of increasing Co from footwall to hangingwall was tentatively postulated from preliminary analyses, and this was tested by systematic chip sampling across the lode at two sections 80 feet apart (sets 109, 110), one of these sections also extending 1 ft into the footwall schist. These samples were analyzed whole ("ORE" in sets 109, 110), and an attempt was then made to extract pure pyrite concentrates ("PY" in sets 109, 110). All original and purified samples were analyzed for Fe, Zn, Cu, Co and Ni, and the proportions of sphalerite, pyrite and chalcopyrite calculated. The trends of Co-Ni (Co2, Ni2) concentrations in ore (of variable mineralogy) were then tested by comparing the Co-Ni (Co1, Ni1) concentrations in those purified samples which were > 95% pyrite, with the results given in Figure 6.32a, b.

Figure 6.32

Co and Ni analyses of Rosebery ore, and of pyrite concentrates (>95% pure), with pyrite, chalcopyrite, and sphalerite contents of the ore calculated from Fe, Cu and Zn analyses (sets 109, 110). Chip samples (100-900 g) were taken at 18 in. intervals across the lode, normal to the banding, in E lens, 14 level. Sections are east-west, looking north.

(a) 14S2NS stope.

(b) 14S2NN stope, 80 ft. north along strike from (a).

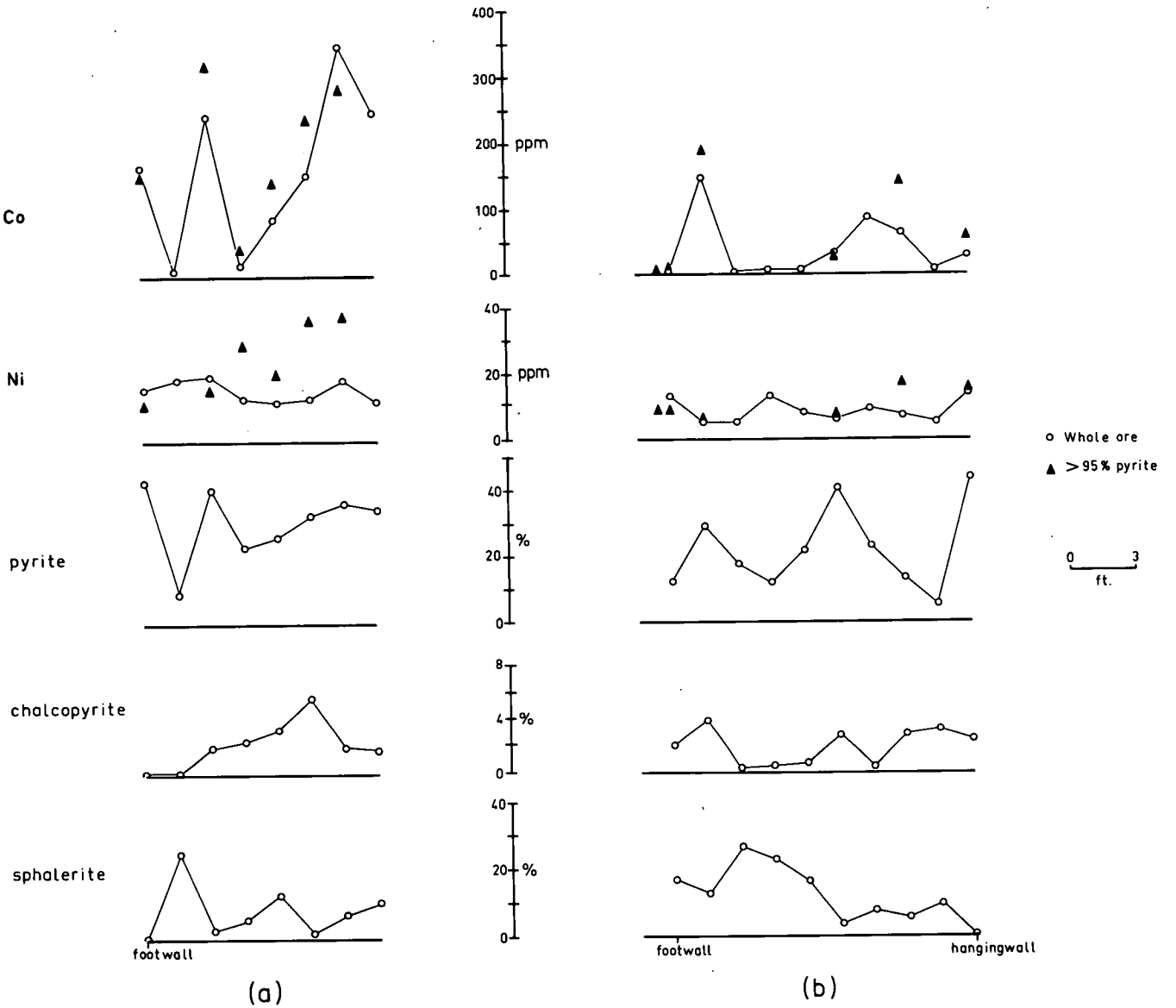
Co
Ni
pyrite
chalcopyrite
sphalerite
400
300
200
100
0
ppm
40
20
0
ppm
40
20
0
%
8
4
0
%
40
20
0
%
footwall
(a)
footwall
hangingwall
(b)
o Whole ore
▲ >95% pyrite
0
3
ft.

The Co-Ni trends for the purified samples are not markedly different to those for the whole ore, apparently because pyrite constituted such a large proportion of the ore, and contained most of the Co. The sphalerite contains only about 10 ppm Co (McLeod, 1965), even though sphalerite can incorporate up to 21% Co (Hall, 1961). In both sections, Ni in pyrite shows a general increase in concentration from footwall to hangingwall, and Co shows two concentration peaks, approximately 5 and 18 feet from the footwall. Both Co and Ni values are somewhat lower in set 109 than set 110. It may be concluded that Co and Ni varied independently during mineralization, but that both are highly stratified in the plane of the orebody. The volume defining the limits of mutual dependence of Co concentrations has dimensions of less than 6 ft normal to the banding, and probably not much greater than 80 ft parallel to the banding along strike. That the third dimension, parallel to the banding, may also be large, is indicated (Fig. 6.9) by the equivalence of set 109 values with those in set 111, 80 ft away down a $45^{\circ}$ pitch to the north. Although the stratification of trace elements across the two measured sections is more consistent than that of the major elements, this is a direct consequence of the sampling interval, which exceeds the wavelengths of variation (for the sample-size used) of the major elements, but not those of Co and Ni. These Co-Ni distributions are further evidence for the chemical layering of the ore parallel to the host rock contacts.

The Co-enrichment gives the Rosebery-Hercules ores a trend similar to trend II, which is empirical support for association of the ores with Cambrian igneous activity. That the mineralization was associated with the volcanic phase of this activity is suggested by the

striking similarity of the Co-Ni distributions with those in ores in other countries which have been genetically linked with volcanic rocks. Further, some of these other ores show the same relative Co-Ni relationships in their pyritic-Cu and Pb-Zn ores as are shown by Mt. Lyell and Rosebery-Hercules.

Evidence from this study that the Rosebery ore was sedimentary is as follows:

(i) The trace elements, as well as the major elements, are highly stratified, as at Rammelsberg (see p.28).

(ii) There is a large-scale zonation of Co-Ni values through the mine suggestive of gradations between normal and abnormal sedimentary environments (Fig. 6.10a). The hangingwall shale contains pyrite and pyrrhotite (sets 6, 116) with normal sedimentary Co-Ni values. The pyrite in the host-rock shale (set 7) also appears to be sedimentary, but the Co-Ni values show large and variable impoverishment. Overlapping the latter values are those from the pyrite-hematite lode (set 107), just above F lens of the main lode. These in turn pass into the Co-Ni field for the main lode. Taken in reverse sequence, the gradual change in Co-Ni values could represent a gradual reestablishment of normal sedimentary trace-element concentrations after an episode of highly abnormal availability of metals to the sedimentary basin. The equivalence of Co-Ni values in the footwall schist (set 25) and the main lode further reinforces the interpretation of ore solutions rising through the footwall to the site of open-cast deposition. The distinctiveness of Co-Ni values in pyrite in the hangingwall volcanics (set 26) can be explained by a separate mineralization in younger rocks.

None of the zonations described above is reflected in the Se or $\delta S^{34}$ values.

If the ore is indeed sedimentary, the impoverishment in Ni, unusual in normal sediments, requires explanation. At the time of deposition, the normal agents of transport of Co and Ni in the sedimentary basin may have been completely excluded from the depositional site. This is consistent with the massive nature of the ore, even at its strike extremities. The high Co and low Ni could therefore be wholly due to the volcanic exhalations.

The origin of the mineralization at the Black P.A. Mine, to the west of the Rosebery Mine, is not revealed by the Co and Ni values (set 125), which are both low, and therefore ambiguous. However the pyrite in the Natone Volcanics (set 126) has Co-Ni values similar to trend III, and is therefore probably Devonian.

## Mt. Farrell

Minerals from the group of mines at Mt. Farrell contain Co-Ni values (Fig. 6.11a) belonging to the Devonian trend III, and the Cd concentrations in sphalerite (Appendix 2) fall within the range of the Devonian deposits. Thus two independent empirical correlations point to a Devonian age for this mineralization. The spread of Se values (Fig. 6.12), however, is similar to that at Mt. Lyell. Solomon *et al.* (in press) have suggested that a volcanic (Cambrian) origin for the S at Mt. Farrell is a distinct possibility, and the Se may have a similar origin. Nevertheless, the Se enrichment would still remain essentially

unexplained, as the Mt. Farrell ores are not cupriferous, and Rosebery, which is mineralogically more similar and geographically closer to Mt. Farrell than is Mt. Lyell, shows an impoverishment in Se.

## Magnet

The Cd and Se contents of sphalerite from the Magnet Mine are similar to those in the sphalerites from the other (Devonian) Pb-Zn-Ag deposits in the area around Mt. Bischoff, which supports the consanguinity of these ores.

## Mt. Remus

The high Co values found in the pyrite (Fig. 6.11b) seem not to be contained in independent minerals, as none of the latter were found by mineragraphic examination by Stillwell (1932) or by mineragraphic and X-ray diffraction examination by the author. The Co-Ni values belong to trend II, and this mineralization is therefore probably related to the Cambrian acid-intermediate igneous activity.

## Lake George Mine, Captain's Flat, N.S.W.

The Co-Ni values from these samples have not been compared with values in other minerals of known origin in the same area. However there is a striking similarity between the trend of Co-Ni values from this deposit (Fig. 6.11b), from Rosebery (Fig. 6.9), and especially from

Tasman and Crown Lyell (Fig. 6.8c). If this trend remains distinctive after further investigation of other types of mineralization in the Captain's Flat area, it would be suggestive of a common mineralizing process for the three deposits.

## Discussion

In three places - the Rosebery, Hercules, and New North Mt. Farrell Mines - contiguous lode and sedimentary pyrites were analyzed for Co and Ni, and only at the last of these mines was there an overlap of trends for the two types. The freedom from ambiguity shown by the other two occurrences reflects the most striking difference in trends revealed by this study - between the sedimentary-diagenetic trend I, and the Cambrian acid-intermediate igneous trend II. The Devonian intramagmatic and hydrothermal minerals, showing more diverse trends, are less easily used for unambiguous empirical correlations.

The data of this study indicate significant differences in the dispersion characteristics of Co-Ni, Se, and $S^{32}$-$S^{34}$. The overall availability trends of Co and Ni are alike for deposits of similar genesis (e.g. the sedimentary pyrites; the volcanic pyrites). The gross availability of Se, however, seems to be much more closely related to the composition of the mineralizing fluid (e.g. Mt. Lyell and Rosebery are very different, which was already known), and the $\delta S^{34}$ values either tend to be different for each deposit (Mt. Lyell, Rosebery, Mt. Farrell; Fig. 5.6) or fortuitously alike for unrelated deposits (Mt. Lyell and Renison Bell: Rafter and Solomon, 1967; Both et al., 1967). Further,

differences in depositional variables within deposits are reflected in detail by the Co-Ni concentrations, but only in a general way by the Se concentrations (at Mt. Lyell) and by the $\delta S^{34}$ values (zoning at Mt. Bischoff and Heemskirk-Zeehan: Rafter and Solomon, 1967; Both et al., 1967). The practical consequence for genetic interpretation is that neither the Se nor $\delta S^{34}$ values are as useful as the Co-Ni values in drawing empirical correlations within deposits, and between nearby deposits. One is forced instead to rely on empirical correlations with deposits in other metallogenic provinces, which for trace element studies at least is less satisfactory, because ideally this requires establishment of the background dispersion patterns in each area.

## CONCLUSIONS

### Processes

1. Distribution functions. Cobalt and nickel in the two largest homogeneous sample populations (23 and 26 samples) show positively skewed distributions which are not, however, exactly lognormal.

2. Variation within single minerals. The ranges of specimen-scale variation of Co and Ni are similar for different types of deposits and different minerals. However, in replacement and sedimentary-diagenetic minerals, on both the hand-specimen and deposit scale, variations tend towards the type Co/Ni = k, whereas the variation in veins is more like Co or Ni = k.

The range of specimen-scale variation of Se tends to remain constant for all mean Se concentrations.

3. Massive vs. disseminated. Selenium at Mt. Lyell is more concentrated in the massive orebodies at the stratigraphic top of the Mt. Read Volcanics than in the stratigraphically lower disseminated mineralization. This is interpreted in 17 (below).

4. Vein vs. replacement. From the strikingly similar distributions of Co and Ni between vein and replacement deposits at Mt. Bischoff and Renison Bell, 25 miles apart, it is tentatively concluded that the replacement process results in an impoverishment of Ni, and to a less extent of Co.

5. Vein vs. sedimentary. The results of analyses from the sedimentary pyrite-pyrrhotite deposit at Nairne, South Australia, do not support the contention of George (1967) that cross-cutting "shear" veins represent remobilized bedded sulphides.

6. Metamorphism. The Savage River magnetite deposit, probably the most metamorphosed ore in Tasmania, shows homogenization of Co-Ni values, and apparent specimen-scale equilibrium partitioning of Co and Ni between pyrite and magnetite.

7. Remobilization. Analyses from Nairne and Mt. Lyell indicate that both solid-state and hydrothermal remobilization of pyrite and chalcopyrite involve the expulsion of Co, and to a less extent Ni.

8. Partition between minerals. The irregularity of Se partitioning is confirmed, and it is concluded that the differences in intrinsic accommodation capabilities of the sulphides are probably small. There is some evidence, however, for a general impoverishment in sphalerite.

Cobalt and nickel show quite consistent partitioning, particularly strong evidence being adduced for pyrite-pyrrhotite, pyrite-magnetite, and pyrite-chalcopyrite relationships. Anomalous pyrite-pyrrhotite partitioning at Mt. Bischoff and Renison Bell could not be satisfactorily explained.

9. Dilution. There is a 20 to 30-fold impoverishment of Co and Ni in pyrite from quartz veins compared with that from pure pyrite veins at the Stirling Valley Mine, Tullah.

10. Zoning. Data from mineralogically (and in at least two cases, thermally) zoned mineral deposits at Zeehan, Mt. Bischoff and Story's Creek indicate general gradients of decreasing Co (two examples) and increasing Ni (two examples) away from the centres.

A regional zonation of Cd with respect to Fe in sphalerites was detected in the Devonian deposits, but it was heavily masked by local variables. The zonation is interpreted as an increase in the Cd content of the ore fluid with increasing distance from the source.

11. Effects of the processes. Except for the Co-Ni zoning at Zeehan, the variations of the concentrations of Co, Ni, Se and Cd due to the above depositional and post-depositional processes have contributed little to the boundaries of the overall trends, which may be interpreted as reflecting fundamental availability.

## Mineralization of Known Origin

12. Sedimentary-diagenetic (Precambrian-Recent). The Tasmanian samples contain normal Co-Ni values, with Co/Ni < 0.5 in most cases (Trend I). There is no correlation of the Co-Ni values with age or degree of recrystallization, although criteria for the latter were found difficult to establish. Large-scale uniformity of Co/Ni ratios are found in the pyrites within several sedimentary formations. The proportion of Ni in the non-pyrite fraction of shales may be proportional to the carbonaceous content, for constant Fe content and metamorphic grade.

The range of Se values is unusually large for a province which in general shows little Se enrichment.

13. Cambrian. Pyrites in acid-intermediate volcanics and sub-volcanic granites contain high Co/Ni ratios, ranging 1-150 (Trend II).

Pyrrhotite-pentlandite ore associated with the Serpentine Hill mafic-ultramafic complex is enriched in Se, and contains Co/Ni = 0.04, but magnetite from the McIvor Hill gabbro, with the same Co/Ni ratio, contains much less Co and Ni. Pyrite from a spilite in the Bald Hill complex is enriched in Co, and falls into trend II.

14. Devonian. The vein and replacement deposits show three trends: to high Ni with low Co/Ni ratio (trend III), to medium Co with Ni approximately constant (trend IV), and a negative correlation trend (trend V). Trend III could be partly due to contamination of Devonian mineralizing fluids by nickeliferous Cambrian igneous country rocks.

15. Metallogenic subprovinces. There may have been a slight difference in the availability of Cd in the Devonian ore fluids in the

Zeehan-Renison Bell and Mt. Bischoff-Cleveland areas. No systematic subdivision in terms of Co-Ni or Se is possible.

## Mineralization of Uncertain Origin

16. Savage River (Fe). The Co and Ni contents of the pyrite both range 1000-2500 ppm, unlike any other Tasmanian hypogene pyrites. These values are not unreasonable for sulphides in an ortho-amphibolite, but they give no indication of the mechanism of ore emplacement.

17. Mt. Lyell (pyritic-Cu). The Co and Ni values lie within trend II, indicating association of the ores with the Cambrian igneous activity. The high Se, and high Co/Ni ratios, indicate a volcanic origin for the ores, as these features are found in similar overseas ores associated with volcanic rocks. The enrichment of Se in the stratigraphically higher ores is consistent with their postulated open-cast environment of deposition. The Co and Ni are even more strongly stratified, but in the disseminated mineralization the large scale Co, Ni and Cu isopleths intersect, which may imply an original replacement origin and/or metamorphic re-dispersion.

Within the deposit, Co correlates with Cu between ore shoots. In the extreme case, the Tasman and Crown Lyell Pb-Zn ore is very different in Co-Ni values from the rest of the Mt. Lyell lodes, but is similar to Rosebery. On the other hand, the Se and $\delta S^{34}$ values for the Pb-Zn ore are the same as for the other lodes, but different to Rosebery.

18. Rosebery (Zn-Pb-Cu). The Co and Ni values, although much less than those at Mt. Lyell, lie within trend II, indicating a Cambrian

igneous origin for the ores. The high Co/Ni ratio, and especially the impoverishment in Ni, are typical of several overseas Pb-Zn deposits in volcanic rocks. A sedimentary origin for the ore is supported by the highly stratified distribution of the Co and Ni, and is strongly suggested by the gradations of Co-Ni values between ore and adjacent and overlying sedimentary-diagenetic mineralization. Nickel impoverishment is explained by the exclusion of normal transporting agents of Ni from the depositional site. Selenium and Cd are both impoverished with respect to all other Tasmanian ores, which may also result from a sedimentary environment of deposition.

19. Mt. Farrell (Ag-Pb-Zn). A Devonian origin for these ores is indicated by the Co-Ni and Cd concentrations. The large range of Se values, however, is unlike the range for the other Devonian deposits, and the Se may have a Cambrian volcanic origin, as suggested for the S in these ores by Solomon et al. (in press).

20. Magnet (Ag-Pb-Zn). The Cd and Se values in sphalerite indicate that this ore is Devonian.

21. Mt. Remus (Mo). A Cambrian age is indicated by the Co-Ni contents of pyrites in this mineral deposit.

22. Captain's Flat, N.S.W. (Pb-Zn-Cu). The Co-Ni values for this deposit are remarkably similar to those in the Tasman and Crown Lyell deposit, and fall within the range for the Rosebery ores. This is regarded as preliminary evidence for a common mineralizing process for all these deposits.

## Investigational Procedures

23. Scales of empirical correlations. Genetic studies using trace elements usually require establishment of fundamental availability trends. The closer the deposits whose trends are being compared, the more reliable the correlations. For this reason, comparisons with deposits outside the metallogenic province give less certain correlations than intra-provincial comparisons. Nevertheless, many local studies may eventually define general rules of dispersion (25, below).

24. Usefullness of techniques. Cobalt and nickel are sensitive discriminators of common genesis between deposits, and of processes within deposits. In Tasmania, Se and $\delta S^{34}$ values are more closely controlled in their fundamental availability by other than genetic factors, and within deposits they show little variation due to depositional processes.

## Generalizations

25. Criteria for genesis. It is well established that sedimentary-diagenetic pyrites are characterized by low Co/Ni ratios. In this thesis, the evidence collated from the literature, together with new data, strongly suggest that mineralization genetically associated with geosynclinal vulcanism may also possess characteristic Co-Ni concentrations, with

(a) high to very high Co/Ni ratios, and often marked impoverishment in Ni;

(b) greater Co and Ni concentrations associated with Cu than with Pb-Zn ores, both within and between deposits; and

(c) a tendency for Co to correlate with Cu within deposits.

# REFERENCES

Agterberg, F.P., 1965: The technique of serial correlation applied to continuous series of element concentration values in homogenous rocks. J. Geol., 73, 142-154.

Andermann, G., and Kemp, J.W., 1958: Scattered X-rays as internal standards in X-ray emission spectrography. Analyt. Chem., 30, 1306-1309.

Anger, G., Nielsen, H., Puchelt, H., and Ricke, W., 1966: Sulfur isotopes in the Rammelsberg ore deposit (Germany). Econ. Geol., 61, 511-536.

Auger, P.E., 1941: Zoning and district variations of the minor elements in pyrite of Canadian gold deposits. Econ. Geol., 36, 401-423.

Babcan, J., 1966: Zur Geochemie des Selens des Slovakischen Teils der Westkarpaten. Geol. Sb., Bratisl., 17, 1-6.

Badalova, S.T., Basitova, S.M., and Godunova, L.I., 1962: Distribution of rhenium in the molybdenites of Middle Asia. Geochemistry, 9, 934-939.

Banks, M.R., 1965: Geology and mineral deposits. In Atlas of Tasmania. Ed.: J.L. Davies. Lands and Surveys Department, Hobart.

Barton, P.B., and Skinner, B.J., 1967: Sulfide mineral stabilities. In Geochemistry of Hydrothermal Ore Deposits. Ed. H.L. Barnes. Holt, Rinehart and Winston, New York.

Belcher, C.B., and Kinson, K., 1964: The determination of nickel in iron and steel by atomic absorption spectrophotometry. Analytica chim. Acta, 30, 64-67.

Berg, G., and Friedensburg, F., 1944: Nickel und Kobalt. Die metallischen Rohstoffe, ihre Lagerungsverhältnisse und ihre wirtschaftliche Bedeutung. Enke, Stuttgart.

Bergenfelt, S., 1953: Om förekomsten av selen i Skelleftefaltets sulfidmaliner. Geol. För. Stockh. Förh., 75, 327-359.

Bethke, P.M., and Barton, P.B., 1961: Unit cell dimension verses composition in the systems : PbS-CdS, PbS-PbSe, ZnS-ZnSe, and $CuFeS_{1.90}$-$CuFeSe_{1.90}$. Prof. Pap. U.S. geol. Surv., 424-B, 266-270.

Beyer, M., 1965: The determination of manganese, copper, chromium, nickel and magnesium in cast iron and steel. Atomic Absorption Newsletter 4, 212-223. Perkin Elmer Corporation.

Bilibin, Ye.A., 1955: Metallogenetic Provinces and Epochs. Gosgeoltekhizdat, Moscow (Russian). Translated by the Canadian Geological Survey.

Bjørlykke, H., and Jarp, S., 1950: The content of cobalt in some Norwegian sulphide deposits. Norsk. geol. Tidsskr., 28, 151-156.

Blissett, A.H., 1962: Geology of the Zeehan Sheet, 1 mile Geol. Map Series K 55-5-50. Explan. Rep. geol. Surv. Tasm.

Boorman, R.S., 1967: Subsolidus studies in the ZnS-FeS-$FeS_2$ system. Econ. Geol., 62, 614-632.

Both, R.A., 1966: The zoned ore deposits of the Zeehan mineral field. M.Sc. thesis (unpublished). University of Tasmania.

Both, R.A., Rafter, T.A., and Solomon, M., 1967: Sulphur isotopes and zoning of the Zeehan mineral field. In The Geology of Western Tasmania. A Symposium (unpublished). University of Tasmania.

———— , and Williams, K.L., 1968: Mineralogical zoning in the lead-zinc ores of the Zeehan field, Tasmania. Part I : Introduction and review. J. geol. Soc. Aust., 15, 121-137.

Brathwaite, R.L., 1967: The structure of the Rosebery ore deposit. In The Geology of Western Tasmania. A Symposium (unpublished). University of Tasmania.

Brooks, C., 1966: The rubidium-strontium ages of some Tasmanian igneous rocks. J. geol. Soc. Aust., 13, 457-469.

———— , and Compston, W., 1965: The age and initial $Sr^{87}/Sr^{86}$ of the Heemskirk Granite, western Tasmania. J. geophys. Res., 70, 6249-6262.

Brooks, R.R., and Ahrens, L.H., 1961: Some observations on the distribution of thallium, cadmium and bismuth in silicate rocks and the significance of covalency on their degree of association with other elements. Geochim. cosmochim. Acta, 23, 100-115.

Burnham, C.W., 1959: Metallogenic provinces of the south-western United States and northern Mexico. New Mex. Inst. Min. Tech. Bull. 65.

Burns, R.G., and Fyfe, W.S., 1967: Crystal-field theory and the geochemistry of transition elements. In Researches in Geochemistry, 2. Ed.: Ph.H. Abelson. Wiley, New York.

Byers, H.G., Miller, J.T., Williams, K.T., and Lakin, H.W., 1938: Selenium occurrence in certain soils in the United States, III. U.S. Dep. Agric. Tech. Bull., 60, 1-74.

Cambel, B., and Jarkovsky, J., 1965: Rare elements in pyrites from the Western Carpathians and their possible use in the study of mineralization genesis. Probl. Geochim., Akad. Nauk SSSR, Inst. Geokhim. i Analit. Khim., (1965), 249-66. (Russ.). [Chem. Abs., 64, 6311].

———————————, 1967: Geochemie der Pyrite einiger Lagerstätten der Tschechoslowakei. Slovenska Akademia Vied, Bratislava.

Carr, M.H., and Turekian, K.K., 1961: The geochemistry of cobalt. Geochim. cosmochim. Acta, 23, 9-60.

Carstens, C.W., 1941: Zur Geochemie einiger norwegischen Kiesvorkommen. Kgl. Norske Videnskab. Selsk., Forh. 14, 36-39.

———————————, 1943: Über den Co-Ni-Gehalt norwegischen Schwefelkiesvorkommen. Kgl. Norske Videnskab. Selsk., Forh. 15, 165-168.

Coleman, R.G., 1959: The natural occurrence of galena-clausthalite solid solution series. Am. Miner., 44, 166-175.

———————————, and Delevaux, M., 1957: Occurrence of selenium in sulfides from some sedimentary rocks of the Western United States. Econ. Geol., 52, 499-527.

Cox, R., 1968: The use of comparative sampling methods at Cleveland Mine, Tasmania. Proc. Australas. Inst. Min. Metall., no.226, 17-30.

Dana, J.D., 1944: System of Mineralogy, Volume I. 7th ed., by Palache, C., Berman, H., and Frondel, C. Wiley, New York.

Darnley, A.G., 1966: Sulfur isotopes of some Central African sulfide deposits. Econ. Geol., 61, 409-414.

Davidson, C.F., 1962: On the cobalt:nickel ratio in ore deposits. Min. Mag., Lond., 106, 78-85.

Davidson, D.F., and Powers, H.A., 1959: Selenium content of some volcanic rocks from western United States and Hawaiian Islands. Bull. U.S. geol. Surv., 1084-C, 69-81.

Deans, T., 1950: The Kupferschiefer and the associated lead-zinc mineralization in the Permian of Silesia, Germany and England. Rept. 18th Int. Geol. Congr., 7, 340-352.

Deer, W.A., Howie, R.A., and Zussman, J., 1962: Rock-forming Minerals. 5 : Non-silicates. Longmans, London.

De Launay, L., and Urbain, G., 1910: Recherches sur la metallogenie des blendes et des mineraux qui en dérivant. Soc. géol. France Bull., 10, 789-795.

Degens, E.T., 1965: Geochemistry of Sediments : A Brief Survey. Prentice-Hall Inc., New Jersey.

Dodson, R.W., Forney, G.J., and Swift, E.H., 1936: The extraction of ferric chloride from hydrochloric acid solutions by isopropyl ether. J. Am. chem. Soc., 58, 2573-2577.

Doe, B.R., 1962: Distribution and composition of sulphide minerals at Balmat, New York. Bull. geol. Soc. Am., 73, 833-854.

Earley, J.W., 1949: Studies of natural and artificial selenides : I - Klockmannite, CuSe. Am. Miner., 34, 435-440.

———————, 1950: Description and synthesis of the selenide minerals. Am. Miner., 35, 337-364.

Edwards, A.B., 1939: Some observations on the mineral composition of Mt. Lyell copper ores. Proc. Australas. Inst. Min. Metall., no.114, 67-109.

———————, 1949: Pyrite deposit at Nairne, South Australia. Min. Rev., Adelaide, 90, 89-91.

———————, 1955: Cadmium in the Broken Hill lode. Proc. Australas. Inst. Min. Metall., no.176, 71-96.

———————, and Carlos, G.C., 1954: The selenium content of some Australian sulphide deposits. Proc. Australas. Inst. Min. Metall., no.172, 31-63.

Ehrenberg, H., Pilger, A., and Schroder, F., 1954: Monographie das Schwefelkies-Zinkblende-Schwerspatlager von Meggen (Westfalen). Gesellsch. Dtsch. Metallhütten und Bergleute, Clausthal, Zellerfeld.

El Shazly, E.M., Webb, J.S., and Williams, D., 1957: Trace elements in sphalerite, galena and associated minerals from the British Isles. Trans. Inst. Min. Metall., 66, 241-271.

Elliott, N., 1960: Interatomic distances in $FeS_2$, $CoS_2$ and $NiS_2$. J. chem. Phys., 33, 903-905.

Evans, B.W., and Leake, B.E., 1960: The composition and origin of the striped amphibolites of Connemara, Ireland. J. Petrology, 1, 337-363.

Faramazyan, A.S., and Zar'yan, R.N., 1964: Geochemistry of selenium and tellurium in the ores of the Kadzharan deposit. Geochem. Int., 1, 1103-1105.

Firman, R.J., 1965: Interferences caused by iron and alkalies on the determination of magnesium by atomic absorption spectroscopy. Spectrochim. Acta, 21, 341-343.

Fischer, M., and Hiller, J.E., 1956: Über den thermoelektrischen Effekt des Pyrits. Neues Jb. Miner. Abh., 89, 281-301.

Fleischer, M., 1955: Minor elements in some sulphide minerals. Econ. Geol., 50th Anniv. Vol., 970-1024.

———————, 1959: The geochemistry of rhenium, with special reference to its occurrence in molybdenite. Econ. Geol., 54, 1406-1413.

Frank, C.W., Schrenk, W.G., and Meloan, C.E., 1966: A study of the feasibility of the iron hollow cathode as a multi-element atomic absorption unit. Analyt. Chem., 38, 1005-1008.

Frenzel, G., and Ottemann, J., 1967: Eine Sulfidparagenese mit kupferhaltigem Zonarpyrit von Nukundamu/Fiji. Mineralium Deposita, 1, 307-316.

Friedman, I.I., 1949: A proposed method for the measurement of geologic temperatures. J. Geol., 57, 618-619.

Fruth, I., and Maucher, A., 1966: Spurenelemente und Schwefel-Isotope in Zinkblenden der Blei-Zink-Lagerstätte von Gorno. Mineralium Deposita, 1, 238-250.

Fryklund, V.C., and Fletcher, J.D., 1956: Geochemistry of sphalerite from the Star Mine, Coeur d'Alene District, Idaho. Econ. Geol., 51, 223-247.

———————, and Harner, R.S., 1955: Comments on minor elements in pyrrhotite. Econ. Geol., 50, 339-344.

Gavelin, S., and Gabrielson, O., 1947: Spectrochemical investigations of sulphide minerals from the ores of the Skellefte District. Arsb. Sver. geol. Unders., 41, 1-45.

Gee, R.D., 1967: The Proterozoic rocks of the Rocky Cape Geanticline. In The Geology of Western Tasmania. A Symposium (unpublished). University of Tasmania.

George, R.J., 1967: Metamorphism of the Nairne pyrite deposit. Ph.D. thesis (unpublished). University of Adelaide.

Gilbert, P.T., 1962: Absorption flame photometry. Analyt. Chem., 34, 210R-224R.

Gilfillan, J.F., 1965: Tin ore deposits of Renison Bell. 8th Commonw. Min. Metall. Congr., 1, 495-496.

Gjelsvik, T., 1968: Distribution of major elements in the wall rocks and the silicate fraction of the Skorovass pyrite deposit, Grong Area, Norway. Econ. Geol., 63, 217-231.

Glasson, K.R., and Paine, V.R., 1965: Lead-zinc-copper ore deposits of Lake George Mines, Captain's Flat. 8th Commonw. Min. Metall. Congr., 1, 423-431.

Goldschmidt, V.M., 1954: Geochemistry. Oxford Univ. Press, London.

———————— , and Hefter, O., 1933: Zur Geochemie der Selen. Nachr. Ges. Wiss. Gottingen, 2, 245-252.

———————— , and Strock, L., 1935: Zur Geochemie der Selen. II. Nachr. Ges. Wiss. Gottingen, N.F. Fachgr., 1, 123-142.

Goñi, J., and Guillemin, C., 1964: Sites of trace elements in minerals and rocks. Geochem. Int., 1 (5), 1025-1034.

Graton, L.C., and Harcourt, G.A., 1935: Spectrographic evidence on origin of ores of Mississippi Valley type. Econ. Geol., 30, 800-824.

Green, J., 1959: Geochemical tables of the elements for 1959. Bull. geol. Soc. Am., 70, 1127-1184.

Gresens, R.L., 1966: The effect of structurally produced pressure gradients on diffusion in rocks. J. Geol., 74, 307-321.

Grigor'ev, D.P., 1961: Ontogeniya mineralov [Ontogeny of minerals]. Izdatel. L'vov. Univ., L'vov. 284 pp. (in Russian). English translation, Israel Program for Scientific Translations, Jerusalem, 1965. 250 pp.

Groves, D.I., 1965: The geology of the Heazlewood-Godkin area. Tech. Rep. Dep. Mines Tasm., 10, 27-40.

———————, 1968: The cassiterite-sulphide deposits of western Tasmania. Ph.D. thesis (unpublished). University of Tasmania.

———————, and Loftus-Hills, G., (in press): Cadmium in Tasmanian sphalerites. Proc. Australas. Inst. Min. Metall.

———————, and Solomon, M., 1964: The geology of the Mt. Bischoff district. Pap. Proc. R. Soc. Tasm., 98, 1-22.

———————————————, (in press): Fluid inclusion studies on quartz and fluorite from Mount Bischoff, Tasmania. Trans. Inst. Min. Metall.

Gruszczyk, H., and Pouba, Z., 1968: Stratiform ore deposits of the Bohemian Massif and of the Silesia-Cracow area. 23rd Int. Geol. Congr., Excursion Guide 23 AC.

Hall, G., Cottle, V.M., Rosenhain, P.B., and McGhie, R.R., 1953: The lead-zinc deposits of Read-Rosebery and Mount Farrell. 5th Emp. Min. Metall. Congr., 1, 1145-1159.

Hall, G., Cottle, V.M., Rosenhain, P.B., McGhie, R.R., and Druett, J.G., 1965: Lead-zinc ore deposits of Read-Rosebery. 8th Commonw. Min. Metall. Congr., 1, 485-489.

———— , and Solomon, M., 1962: Metallic mineral deposits. J. geol. Soc. Aust., 9, 285-309.

Hall, W.E., 1961: Unit-cell edges of cobalt and cobalt-iron bearing sphalerites. Prof. Pap. U.S. geol. Surv., 424-B, 271-273.

Han, Tsu-Ming, 1968: Ore mineral relations in the Cuyuna sulfide deposit, Minnesota. Mineralium Deposita, 3, 109-134.

Harris, J.F., 1965: Metallogenic studies in south eastern New South Wales. Ph.D. thesis (unpublished). Australian National University, Canberra.

Hawley, J.E., 1952: Spectrographic studies of pyrite in some Eastern Canadian gold mines. Econ. Geol., 47, 260-304.

———————— , and Nichol, I., 1959: Selenium in some Canadian sulphides. Econ. Geol., 54, 608-628.

———————————————— , 1961: Trace elements in pyrite, pyrrhotite and chalcopyrite of different ores. Econ. Geol., 56, 467-487.

Hegemann, Fr., 1943: Die geochemische Bedeutung von Kobalt und Nickel im Pyrit. Z. angew. Miner., 4, 122-239.

———————— , and Leybold, Chr., 1954: Eine Methode zur quantitativen spektrochemischen Analyse von Pyrit. Z. Erzbergb. MetallhütWes., 7, 108-113.

Hills, E.S., 1965: Tectonic setting of Australian ore deposits. 8th Commonw. Min. Metall. Congr., 1, 3-12.

Hirst, D.M., and Dunham, K.C., 1963: Chemistry and petrography of the Marl Slate of S.E. Durham, England. Econ. Geol., 58, 912-940.

Hughes, T.D., 1961: Savage River iron deposits - progress report. Tech. Rep. Dep. Mines Tasm., 5, 163-179.

Ismailov, M.I., 1965: Distribution of selenium and tellurium in the sulphides of the tungsten-molybdenum deposits of the Zirabulak and Nuratinsk mountains. Geochem. Int., 5, 1014-1016.

Ivanov, V.V., 1964: Distribution of cadmium in ore deposits. Geochemistry, 4, 757-768.

Jack, G., and Groves, D.I., 1964: Geology of the Mt. Meredith-Yellowband Creek area. Tech. Rep. Dep. Mines Tasm., 9, 27-37.

Kalman, Z.H., and Heller, L., 1962: Theoretical study of X-ray fluorescent determinations of traces of heavy elements in a light matrix. Analyt. Chem., 34, 946-951.

Kingsbury, C.J.R., 1965: Cassiterite and wolframite veins of Aberfoyle and Story's Creek. 8th Commonw. Min. Metall. Congr., 1, 506-511.

Knitzschke, G., 1966: Zur Erzmineralisation, Petrographie, Hauptmetall- und Spurenelementführung des Kupferschiefers im SE-Harzvorland. Freiberger ForschHft., 207, 1-147.

Koirtyohann, S.R., and Pickett, E.E., 1966a: Spectral interferences in atomic absorption spectrometry. Analyt. Chem., 38, 585-587.

Koirtyohann, S.R., and Pickett, E.E., 1966b: Light scattering by particles in atomic absorption spectrometry. Analyt. Chem., 38, 1087-1088.

Kolbe, P., and Taylor, S.R., 1966a: Major and trace element relationships in granodiorites and granites from Australia and South Africa. Contr. Miner. Petrol., 12, 202-222.

———————————, 1966b: Geochemical investigation of the granitic rocks of the Snowy Mountains area, New South Wales. J. geol. Soc. Aust., 13, 1-25.

Kraume, E., 1962: The zinc-lead-copper-ore deposits of Rammelsberg. Unpublished excursion notes.

————, Dahlgrun, F., Ramdohr, P., and Wilke, A., 1955: Die Erzlager des Rammelsberges bei Goslar. Monogr. Dtsch. Blei-Zink-Erzlagerstatten, Beih. geol. Jb., Heft 18.

Krauskopf, K.B., 1955: Sedimentary deposits of rare metals. Econ. Geol., 50th Anniv. Vol., 411-463.

————————, 1956: Factors controlling the concentrations of thirteen rare metals in sea-water. Geochim. cosmochim. Acta, 9, 1-32.

Kullerud, G., 1953: The FeS - ZnS system : A geological thermometer. Norsk geol. Tidsskr., 32, 61-147.

————, 1959: Sulfide systems as geological thermometers. In Researches in Geochemistry, 1. Ed.: Ph.H. Abelson. Wiley, New York.

————, and Yoder, H.S., 1965: Sulfide-silicate relations. Carnegie Inst. Washington Year Book 64, 192-193.

La Ganza, R.L., 1959: Pyrite investigations at Nairne, South Australia. Econ. Geol., 54, 895-902.

Le Riche, H.H., 1959: The distribution of certain trace elements in the lower Lias of southern England. Geochim. cosmochim. Acta, 16, 101-122.

Liebenberg, C.J., 1961: The trace elements of the rocks of the Bushveld Igneous Complex. Parts I and II. Publs Univ. Pretoria (n.s.), 12 and 13.

Loftus-Hills, G., 1964: The geology of the Dundas-Pieman River area. B.Sc. (Hons.) thesis (unpublished). University of Tasmania.

———————— , and Solomon, M., 1967: Cobalt, nickel and selenium in sulphides as indicators of ore genesis. Mineralium Deposita, 2, 228-242.

———————————————— , and Hall, R.J., 1967: The structure of the bedded rocks west of Rosebery, Tasmania. J. geol. Soc. Aust., 14, 333-338.

Lundegårdh, per H., 1948: Some aspects to the determination and distribution of zinc. K. LantbrHögsk. Annlr, 15.

Markham, N.L., 1968: Some genetic aspects of the Mt. Lyell mineralization. Mineralium Deposita, 3, 199-221.

McCartney, W.D., 1965: Metallogy of post-Precambrian geosynclines. Geol. Surv. Pap. Can., 65-6, 33-42.

McDougall, I., and Leggo, P.J., 1965: Isotopic age determinations on granitic rocks from Tasmania. J. geol. Soc. Aust., 12, 295-333.

McIntyre, W.L., 1963: Trace element partition coefficients - a review of theory and applications to geology. Geochim. cosmochim. Acta, 27, 1209-1264.

McLeod, I.R., 1965: Ferro-alloy metal ore deposits of Australia. 8th Commonw. Min. Metall. Congr., 1, 46-48.

Menzies, A.C., 1960: A study of atomic absorption spectroscopy. Analyt. Chem., 32, 898-904.

Miller, A.R., Densmore, C.D., Degens, E.T., Hathaway, J.C., Manheim, F.T., McFarlin, P.F., Pocklington, R., and Jokela, A., 1966: Hot brines and recent iron deposits in deeps of the Red Sea. Geochim. cosmochim. Acta, 30, 341-359.

Mohr, P.A., 1959: The distribution of some minor elements between sulphide and silicate phases of sediments. Univ. Coll. Addis Ababa, Fac. Sci., Contrib. Geophys. Obs., Ser. A., 2.

Mookherjee, A., 1962: Certain aspects of the geochemistry of cadmium. Geochim. cosmochim. Acta, 26, 351-360.

Muravyeva, L.P., Barabanov, V.F., and Kler, M.M., 1964: Investigation of trace elements in pyrite from the tungsten deposits of Eastern Transbaikaliya. Geochem. Int., 6, 1096-1102.

Nachtrieb, N.H., and Fryxell, R.E., 1948: The extraction of ferric chloride by isopropyl ether, II. J. Am. chem. Soc., 70, 3552-3557.

Neumann, H., 1950: Pseudomorphs of pyrrhotite after pyrite in the Ballachulish slates. Mineralog. Mag., 29, 234-238.

Nicholls, G.D., and Loring, D.H., 1962: The geochemistry of some British Carboniferous sediments. Geochim. cosmochim. Acta, 26, 181-223.

Noddack, I., and Noddack, W., 1931: Die Geochemie des Rheniums. Z. phys. Chem., 154A, 207-244.

Norrish, K., and Chappell, B.W., 1967: X-ray fluorescence spectrography. In Physical Methods in Determinative Mineralogy. Ed.: J. Zussman. Academic Press, London.

Nye, P.B., 1928: Report on the molybdenite prospect at Mt. Remus. Rep. Dep. Mines Tasm., (unpublished).

Paganelli, L., 1963: On the rhenium content of molybdenite of Mount Mulat (Predazzo) and other Italian molybdenites. Geochim. cosmochim. Acta, 27, 401-404.

Park, Jr, C.F., 1955: The zonal theory of ore deposits. Econ. Geol., 50th Anniv. Vol., 226-248.

———————, and MacDiarmid, R.A., 1964: Ore Deposits. Freeman, San Francisco.

Petterd, W.F., 1910: Catalogue of the Minerals of Tasmania. Mines Department, Hobart, Tasmania.

Pettijohn, F.J., 1956: Sedimentary Rocks. 2nd ed. Harper, New York.

Prokhorov, V.G., 1965: Minor elements in pyrites and the use of the pyrites in prospecting for ore deposits. Geologiya Geofiz, Novosibirsk, 9, 67-74. (Russ.). [Chem. Abs., 64, 1820].

Rafter, T.A., and Solomon, M., 1967: Sulphur isotope and oxygen isotope studies of Tasmanian ore deposits. In The Geology of Western Tasmania. A Symposium. (unpublished). University of Tasmania.

Ramberg, H., 1961: A study of veins in Caledonian rocks around Trondheim Fjord, Norway. Norsk. geol. Tidsskr., 41, 1-43.

Rankama, K., and Sahama, Th.G., 1950: Geochemistry. University of Chicago Press, Chicago.

Rann, C.S., and Hambly, A.N., 1965: Distribution of atoms in an atomic absorption flame. Analyt. Chem., 37, 879-884.

Reitan, P.H., 1960: The genetic significance of two kinds of basified zones near small pegmatite veins. Rept. 21st Int. Geol. Congr., 17, 102-107.

Ringwood, A.E., 1956: Melting relationships of Ni-Mg olivines and some geochemical implications. Geochim. cosmochim. Acta, 10, 297-303.

Robinson, B.W., and Strens, R.G.J., 1968: Genesis of concordant deposits of base metal sulphides : an experimental approach. Nature, 217 (5128), 535-536.

Roedder, E., 1960: Studies of primary fluid inclusions in sphalerite crystals from the OH vein, Creede, Colorado (abs.). Econ. Geol., 55, 1337.

Roscoe, S.M., 1965: Geochemical and isotopic studies, Noranda and Matagami areas. Can. Min. metall. Bull., 58 (641), 965-971.

Rose, A.W., 1967: Trace elements in sulfide minerals from the Central district, New Mexico and the Bingham district, Utah. Geochim. cosmochim. Acta, 31, 547-585.

Rosenfeld, I., and Beath, O.A., 1964: Selenium : Geobotany, Biochemistry, Toxicity and Nutrition. Academic Press, New York.

Rost, F., 1939: Spektralanalytische Untersuchungen an Sulfidischen Erzlagerstätten des ostbayerischen Grenzgebirges. Ein Beitrag zur Geochemie von Nickel und Kobalt. Z. angew. Miner., 2, 1-27.

Routhier, P., 1963: Les Gisements Metalliferes. Masson, Paris.

Rubenach, M., 1967: The Serpentine Hill complex. In The Geology of Western Tasmania. A Symposium. (unpublished). University of Tasmania.

Saager, R., and Mihalik, P., 1967: Two varieties of pyrite from the Basal Reef of the Witwatersrand System. Econ. Geol., 62, 719-731.

Sandell, E.B., 1959: Chemical Analysis, Vol. 3 : Colourimetric Determination of Traces of Metals. 3rd ed. Interscience, New York,

———————, and Goldich, S.S., 1943: The rarer metallic constituents of some American igneous rocks. Part I, J. Geol., 51, 99-115. Part II, J. Geol., 51, 167-189.

Schneiderhohn, H., 1962: Erzlagerstatten. Gustav Fischer Verlag, Stuttgart.

Schroll, E., 1950: Spurenelementparagenese (Mikroparagenese) ostalpiner Zinkblenden. Oesterr. Akad. Wiss. Math.-naturwiss. Kl., Anz., 87, 21-25.

———————, 1951: Spurenelementparagenese (Mikroparagenese) alpiner Bleiglanz. Oesterr. Akad. Wiss. Math.-naturwiss. Kl., Anz., 88, 6-12.

Schwarcz, H.P., 1967: The effect of crystal field stabilization on the distribution of transition metals between metamorphic minerals. Geochim. cosmochim. Acta, 31, 503-517.

Scott, S.D., and Barnes, H.L., 1967: Sphalerite geothermometry at 330° to 580°C. Econ. Geol., 62, 874-875.

Sindeeva, N.D., 1964: Mineralogy and types of deposits of selenium and tellurium. John Wiley and Sons, New York.

Singewald, Jr, J.T., 1917: The role of mineralizers in ore segregations in basic igneous rocks. Johns Hopkins Univ. Contr. Geol., (March, 1917), 24-35.

Sisler, H.H., Vanderwerf, C.A., and Davidson, A.W., 1949: General Chemistry. Macmillan, New York.

Slavin, W., 1964: Atomic absorption instrumentation and technique - a review. Atomic Absorption Newsletter 24, 15-31. Perkin Elmer Corporation.

Smith, F.G., 1948: The ore deposition temperature and pressure at the McIntyre Mine, Ontario. Econ. Geol., 43, 627-636.

Snedecor, G.W., 1946: Statistical Methods. 4th ed. Iowa State College Press.

Solomon, M., 1964: The spilite-keratophyre association of west Tasmania and the ore deposits at Mt. Lyell, Rosebery, and Hercules. Ph.D. thesis (unpublished). University of Tasmania.

———— , 1965a: Geology and mineralization of Tasmania. 8th Commonw. Min. Metall. Congr., 1, 464-477.

———— , 1965b: Lead-silver-zinc ore deposits at Mt. Farrell. 8th Commonw. Min. Metall. Congr., 1, 490.

———— , 1967: Fossil gossans (?) at Mt. Lyell, Tasmania. Econ. Geol., 62, 757-772.

———— , and Elms, R.G., 1965: Copper ore deposits of Mt. Lyell. 8th Commonw. Min. Metall. Congr., 1, 478-484.

———— , Rafter, T.A., and Jensen, M.L., (in press): Isotope studies on the Rosebery, Mount Farrell and Mount Lyell ores, Tasmania. Econ. Geol.

Spencer, D., 1966: Factors affecting element distribution in a Silurian graptolite band. Chem. Geol., 1, 221-249.

Spry, A.H., 1962a: Precambrian rocks of Tasmania. J. geol. Soc. Aust., 9, 107-126.

———— , 1962b: Igneous activity. J. geol. Soc. Aust., 9, 255-284.

———— , 1964: The Zeehan-Corinna area. Pap. Proc. R. Soc. Tasm., 91, 95-108.

———— , and Banks, M.R., (Eds.), 1962: The Geology of Tasmania. J. geol. Soc. Aust., 9, 107-362.

Stanton, R.L., and Rafter, T.A., 1966: The isotopic constitution of sulphur in some stratiform lead-zinc sulphide ores. Mineralium Deposita, 1, 16-29.

Steiner, A., and Rafter, T.A., 1966: Sulfur isotopes in pyrite, pyrrhotite, alunite and anhydrite from steam wells in the Taupo volcanic zone, New Zealand. Econ. Geol., 61, 1115-1129.

Stillwell, F.L., 1932: The occurrence of cobalt and vanadium in the Mt. Remus pyritic ore. Rep. Dep. Mines Tasm., (unpublished).

———— , 1935: An occurrence of gersdorffite in north-east Dundas, Tasmania. Proc. Australas. Inst. Min. Metall., no.100, 465-476.

Stoiber, R.E., 1940: Minor elements in sphalerite. Econ. Geol., 35, 501-519.

Sullivan, J.V., Timms, A.B., and Young, P.A., 1968: Atomic absorption analysis for nickel using a resonance detector. Proc. Australas. Inst. Min. Metall., no.226, 31-36.

Suzuki, T., 1963: On the thermoelectric potential of pyrite. Tohoku Univ. Sci. Rep., 8, 317-419.

Suzuoki, T., 1964: A geochemical study of selenium in volcanic exhalation and sulphur deposits. Chem. Soc. Japan, B, 37, 1200-1206.

Tauson, L.V., 1965: Factors in the distribution of the trace elements during the crystallization of magmas. In Physics and Chemistry of the Earth, 6. Pergamon Press, Oxford.

Taylor, S.R., 1965: The application of trace element data to problems in petrology. In Physics and Chemistry of the Earth, 6. Pergamon Press, Oxford.

Tetlow, P., 1960: Savage River iron. Tech. Rep. Dep. Mines Tasm., 4, 106-113.

Thomson, B.P., 1965: Geology and mineralization of South Australia. 8th Commonw. Min. Metall. Congr., 1, 270-284.

Tourtelot, H.A., 1964: Minor-element composition and organic carbon content of marine and nonmarine shales of Late Cretaceous age in the western interior of the United States. Geochim. cosmochim. Acta, 28, 1579-1604.

Troshin, Yu.P., 1962: Gallium-Indium ratios in sphalerites of Transbaikaliya. Geochemistry, no.4, 378-386.

Turekian, K.K., and Wedepohl, K.H., 1961: Distribution of the elements in some major units of the earth's crust. Bull. geol. Soc. Am., 72, 175-192.

Turneaure, F.S., 1955: Metallogenic provinces and epochs. Econ. Geol., 50th Anniv. Vol., 38-98.

Urquhart, G., 1966: The magnetite deposits of the Savage River-Rocky River region. Geol. Surv. Bull. Tasm., 48.

Vincent, E.A., and Bilefield, L.I., 1960: Cadmium in rocks and minerals from the Skaergaard intrusion, East Greenland. Geochim. cosmochim. Acta, 19, 63-69.

Vine, J.D., 1966: Element distribution in some shelf and eugeosynclinal black shales. Bull. U.S. geol. Surv., 1214-E.

Vogt, J.H.L., 1923: Nickel in igneous rocks. Econ. Geol., 18, 307-353.

Wade, M.L., and Solomon, M., 1958: Geology of the Mount Lyell mines, Tasmania. Econ. Geol., 53, 367-416.

Wager, L.R., and Mitchell, R.L., 1951: The distribution of trace elements during strong fractionation of basic magma - a further study of the Skaergaard intrusion, East Greenland. Geochim. cosmochim. Acta, 1, 129-208.

———— , Vincent, E.A., and Smales, A.A., 1957: Sulphides in the Skaergaard intrusion, East Greenland. Econ. Geol., 52, 855-903.

Walsh, A., 1965: Some recent advances in atomic absorption spectroscopy. XII Colloquium Spectroscopicum Internationale. Hilger and Watts, Exeter.

Wampler, J.M., and Kulp, J.L., 1964: An isotopic study of lead in sedimentary pyrite. Geochim. cosmochim. Acta, 28, 1419-1458.

Warren, H.V., and Thompson, R.M., 1945: Sphalerites from western Canada. Econ. Geol., 40, 309-335.

Wazny, H., 1965: Geochemische Untersuchungen der Unterzechsteinsedimente in der Vorsudetischen Zone. Freiberger ForschHft., 193, 169-181.

Webber, G.R., 1965: Second report of analytical data for CAAS syenite and sulphide standards. Geochim. cosmochim. Acta, 29, 229-248.

Wedepohl, K.H., 1964: Untersuchungen am Kupferschiefer in Nordwestdeutschland. Geochim. cosmochim. Acta, 28, 305-364.

———————, 1965: Untersuchungen an Proben von Kupferschiefer aus Nordwestdeutschland und Diskussion seiner Bildungsbedingungen. Freiberger ForschHft., 193, 107-121.

Williams, K.L., 1958: Nickel mineralization in western Tasmania. In F.L. Stillwell Anniversary Volume, Australas. Inst. Min. Metall., Melbourne.

———————, 1968: Hydrothermal zoning : A study of the lead-zinc ores of Zeehan, Tasmania. Ph.D. thesis (unpublished). Australian National University, Canberra.

Williams, K.T., and Byers, H.G., 1934: Occurrence of selenium in pyrites. Ind. Engng. Chem. analyt. Edn, 6, 296-297.

Willis, J.B., 1963: Analysis of biological materials by atomic absorption spectroscopy. In Methods of Biochemical Analysis, 2. Ed.: D. Glick. Interscience, New York.

Wilson, H.D.B., 1953: Geology and geochemistry of base metal deposits. Econ. Geol., 48, 370-407.

———————, and Anderson, D.T., 1959: The composition of Canadian sulphide ore deposits. Can. Min. metall. Bull., 52, 619-631.

Wright, C.M., 1965: Syngenetic pyrite associated with a Precambrian iron ore deposit. Econ. Geol., 60, 998-1019.

Yamaoka, K., 1962: Studies on the bedded cupriferous iron sulfide deposits occurring in the Sambagawa metamorphic zone. Tohoku Univ. Sci. Rep., 8, 317-319.

Zaryan, R.N., 1962: Selenium and tellurium in ores of the Kafan deposit. Geochemistry, no.3, 267-274.

# APPENDIX 1

## CADMIUM AND IRON IN TASMANIAN SPHALERITES : SAMPLE PREPARATION AND ANALYSIS

The Cd and Fe analyses listed in Appendix 2 were performed by three different analysts: Groves, AMDEL for Solomon (1964), and AMDEL for Both (1966).

### Cd Analyses

#### Groves' analyses

After mineragraphic examination, the sphalerite was hand-picked, crushed, sieved (minus 22 plus 44 mesh), and electromagnetically separated. For the fine-grained Rosebery and Hercules ore, the sieve fraction used was minus 85 plus 100 mesh. Microscopic estimates of the impurities ranged from 2% to 5%. The concentrate was finally ground in a gyratory swing-mill with Cr-steel grinding surfaces.

Analyses were carried out on 2 g. pressed pills using a Philips vacuum X-ray spectrograph (PW 1540) with a Mo tube, a $LiF_{200}$ crystal, and a scintillation counter. Standards were prepared by mixing CdS with a low-Fe sphalerite (100041) from the Swansea Mine, Zeehan, in a gyratory swing-mill for 30 seconds.

Doe et al. (1961) have shown that less than 1% Mn does not markedly affect sample absorption. The effect of varying Fe content on the absorption of the sphalerites was tested for each Cd standard with a

series of mineral mixtures with Fe contents of 0, 2, 6, 8, and 10%. The sphalerites were prepared by mechanically mixing crushed pyrite (11247) from Mt. Bischoff with the stock sphalerite (100041). The maximum difference between measured Cd contents for different Fe contents was 0.004%. The results are therefore given to ± 0.01% and the effects of Fe content on the absorption of individual samples have not otherwise been calculated.

Contamination of the sphalerites by other sulphides should depress the Cd results by a maximum of 5% (i.e. 0.005 to 0.03% Cd in the sphalerites analyzed by Groves) from the actual content of the sphalerite alone, as the associated minerals usually have low Cd contents; Ivanov (1964) recorded average values in galena, chalcopyrite and pyrite generally less than 0.01% Cd.

The lower limit of detection (95% confidence) for Cd is 0.0012%. The precision of the results expressed as the relative deviation (see Chapter 4 - Selenium) was 5%.

Solomon's analyses

The analyses quoted by Solomon (1964) were determined using an X-ray spectrographic technique, and several results were checked with polarographic and colorimetric analyses. No accuracy was quoted for the analyses, although the duplicate analyses by different techniques indicate a maximum difference of 30% of the amount present.

Both's analyses

The analyses given by Both (1966) were obtained using an electron microprobe technique, with one accurate spot analysis and several approximate analyses as checks for each result. The analyses are quoted as accurate to ± 30% of the amount present, although K.L. Williams, A.N.U. (personal communication) considers that the results are probably considerably more accurate than this, with the exception of some Cd values close to the detection limit.

## Fe Analyses

The Fe contents of sphalerites from the cassiterite-sulphide deposits and the Pb-Zn-Ag- veins of the Waratah District were computed from cell-sizes of the sphalerites using the equation of Skinner, Barton and Kullerud (1959). Iron contents for the other deposits, excluding Zeehan, Rosebery and Mt. Lyell, were determined by X-ray spectrography using those samples prepared for Cd analysis which were not contaminated with pyrite and/or Fe-rich carbonate. The maximum uncertainty in the analytical determination is ± 1.2 wt.% Fe.

The analyses of sphalerite from Zeehan were given by Both (1966), from Mt. Lyell by Solomon (1964), and from Rosebery by Stillwell (1934).

# APPENDIX 2

## TABLE A2.1

### ANALYSES OF CADMIUM AND IRON IN TASMANIAN SPHALERITES

| Type of deposit | Locality | Number | Wt.% Cd | Wt.% Fe | Analyst |
|---|---|---|---|---|---|
| DEVONIAN | | | | | |
| CASSITERITE-SULPHIDE DEPOSITS | MT. BISCHOFF | | | | |
| | North Valley lode | 100,007 | 0.31 | 6.9 | A |
| | " | 100,008 | 0.32 | 6.3 | A |
| | " | 100.009 | 0.29 | 5.7 | A |
| | " | 100,010 | 0.32 | 7.1 | A |
| | S-end of open cut | 100.012 | 0.31 | | A |
| | Fook's lode | 100,013 | 0.34 | 8.9 | A |
| | " | 100,014 | 0.33 | 10.3 | A |
| | " | 100,015 | 0.34 | 10.6 | A |
| | " | 100,016 | 0.34 | 10.6 | A |
| | Thompson's lode | 100,017 | 0.33 | 11.0 | A |
| | CLEVELAND | | | | |
| | Henry's lode | 100,018 | 0.31 | 12.0 | A |
| | " | 100,019 | 0.25 | 9.3 | A |
| | " | 100,020 | 0.25 | 12.5 | A |
| | " | 100,021 | 0.27 | 10.3 | A |
| | " | 100,022 | 0.29 | 9.9 | A |
| | RENISON BELL | | | | |
| | No. 2 ore-body | 100,023 | 0.21 | 12.1 | A |
| | Battery workings | 100,024 | 0.21 | 11.3 | A |

| Type of deposit | Locality | Number | Wt.% Cd | Wt.% Fe | Analyst |
|---|---|---|---|---|---|
| | Battery workings | 100,025 | 0.21 | 13.7 | A |
| | " | 100,026 | 0.20 | 7.9 | A |
| LEAD-ZINC FISSURE VEINS | WARATAH | | | | |
| | Antimonial lode | 100,028 | 0.31 | 7.1 | A |
| | Silver Cliffs | 10,575 | 0.31 | 6.8 | A |
| | " | 100,029a | 0.34 | 6.0 | A |
| | " | 100,029b | 0.33 | 6.1 | A |
| | " | 100,030 | 0.21 | 9.8 | A |
| | " | 100,031 | 0.27 | 6.3 | A |
| | Magnet | 100,032 | 0.54 | 4.4 | A |
| | " | 100,033 | 0.42 | 8.1 | A |
| | " | 100,034 | 0.32 | 6.4 | A |
| | TULLAH | | | | |
| | New North Mt. Farrell | 100,035 | 0.29 | 5.5 | A |
| | " | 100,036 | 0.30 | 6.0 | A |
| | " | 10,523a | 0.33 | 8.0 | A |
| | " | 10,523b | 0.36 | 8.3 | A |
| | " | 10,528 | 0.36 | | A |
| | Murchison Mine | 11,199 | 0.37 | | A |
| | N.E. DUNDAS | | | | |
| | McKimmie Mine | 100,037 | 0.24 | 6.1 | A |
| | " | 100,038a | 0.31 | 2.6 | A |
| | " | 100,038b | 0.34 | 2.5 | A |
| | " | 100,039 | 0.26 | 2.5 | A |
| | " | 100,040 | 0.24 | 4.5 | A |
| | ZEEHAN | | | | |
| | Swansea Mine | 100,041 | 0.29 | 2.2 | A |
| | " | 10,490 | 0.34 | 1.9 | A |
| | " | P268 | 0.27 | 1.6 | C |
| | Oceana Mine | P254 | 0.6 | 1.7 | C |

| Type of deposit | Locality | Number | Wt.% Cd | Wt.% Fe | Analyst |
|---|---|---|---|---|---|
| | Oonah Mine | P255 | 0.22 | 2.5 | C |
| | Austral Mine | P256 | 0.5 | 6.0 | C |
| | Zeehan Bell | P258 | 0.3 | 5.0 | C |
| | Sunrise Mine | P259 | 0.25 | 0.04 | C |
| | " | P221 | 0.25 | 1.5 | C |
| | Silver King | P260 | 0.25 | 1.1 | C |
| | Montana S.L. | P261 | <0.01 | 1.1 | C |
| | Tasmanian Crown | P262 | 0.4 | 3.1 | C |
| | Junction | P263 | 0.2 | 0.8 | C |
| | No.4 Argent | P264 | 0.3 | 7.8 | C |
| | Stormsdown | P265 | 0.3 | 8.2 | C |
| | Silver Stream | P266 | 0.25 | 13.3 | C |
| | Comstock | P267 | 0.2 | 11.2 | C |
| | T.L.E. Mine | P269 | 0.3 | 5.3 | C |
| | Spray | P270 | 0.27 | 7.7 | C |
| COPPER DEPOSITS IN VOLCANIC ROCKS | MT. LYELL | | | 0.5 - 7.1 (4) | |
| | Crown Lyell | 100,042 | 0.28 | | A |
| | Blow | 32,664 | 0.30 | | A |
| | " | 32,664 | 0.3 | | B |
| | " | 32,980a | 0.18 | | B |
| | " | 32,980b | 0.24 | | B |
| | Lyell Tharsis | 31,709a | 0.27 | | B |
| BANDED LEAD-ZINC DEPOSITS IN VOLCANIC ROCKS | HERCULES | | | 3.6 - 6.2 (7) | |
| | N-K Lode | 100,043 | 0.18 | | A |
| | " | 100,044a | 0.13 | | A |
| | " | 100,044b | 0.13 | | A |
| | N-lode | 100,045 | 0.14 | | A |
| | N-K lode | 100,046 | 0.17 | | A |
| | " | 100,047 | 0.12 | | A |
| | 6.G.4 lode | 100,048 | 0.11 | | A |

| Type of deposit | Locality | Number | Wt.% Cd | Wt.% Fe | Analyst |
|---|---|---|---|---|---|
| | Bell's lode | 100,049 | 0.12 | | A |
| | ROSEBERY | | | 4.0 - 10.0 | |
| | 9 level 9/K-35N stope | 100,051 | 0.15 | | A |
| | 9 level 9/K-38N stope | 100,055 | 0.20 | | A |
| | " | 100,056 | 0.17 | | A |
| | " | 100,057 | 0.17 | | A |
| | 11 level 11/M-10N stope | 100,052 | 0.09 | | A |
| | 13 level 13/P-8NS stope | 100,053 | 0.15 | | A |
| | 13 level 13/Q6NS stope | 100,050 | 0.18 | | A |
| | 14 level 14/T-45N stope | 100,054 | 0.15 | | A |

ANALYSTS

A - D.I. Groves, 1966. X-ray fluorescence spectrography.

B - AMDEL., X-ray fluorescence spectrography, for Solomon (1964).

C - P. Schulz. AMDEL., electron microprobe analysis, for Both (1966). His specimen numbers refer to the polished section collection in the Tasmanian Museum, Hobart, Tasmania.

TABLE A2.2

AVERAGE Cd AND Fe VALUES IN TASMANIAN SPHALERITES

| Type of deposit | Locality | No. of samples | Wt. % Cd | Wt. % Fe |
|---|---|---|---|---|
| CASSITERITE-SULPHIDE DEPOSITS | MT. BISCHOFF | 10 | 0.32 | 8.4 |
| | CLEVELAND | 5 | 0.27 | 10.6 |
| | RENISON BELL | 4 | 0.21 | 11.3 |
| | | 19 | Av. 0.29 | |
| LEAD-ZINC FISSURE VEINS | WARATAH | 9 | 0.34 | 7.2 |
| | TULLAH | 6 | 0.34 | 7.0 |
| | N.E. DUNDAS | 5 | 0.28 | 3.6 |
| | ZEEHAN | 19 | 0.29 | 4.0 |
| | | 39 | Av. 0.31 | |
| BANDED LEAD-ZINC DEPOSITS | HERCULES | 8 | 0.14 | 5.6 |
| | ROSEBERY | 8 | 0.16 | 4.0 |
| | | 16 | Av. 0.15 | |
| COPPER DEPOSITS | MT. LYELL | 6 | 0.26 | 2.4 |

# APPENDIX 3

## SPECTROPHOTOMETRIC DETERMINATION OF Co : 2-NITROSO-1-NAPHTHOL METHOD (AFTER SANDELL, 1959)

### Reagents

2M HCl, 2M NaOH, 3% $H_2O_2$, 40% $Na_3C_6H_5O_7.2H_2O$.

Reagent solution: 1.0 g of 2-nitroso-1-naphthol in 100 ml glacial $CH_3COOH$. Add 1 g activated C. Before use shake the mixture and filter off the required amount.

### Standards

One stock was prepared by dissolving $CoSO_4.7H_2O$ in slightly acidified water. Analar aliquots were taken through the extraction procedure to give standards of 4, 2, 1, 0.5, and 0.2 µg/ml Co, equivalent to concentrations in the solid samples of 200, 100, 50, 25 and 10 ppm Co. Several blanks taken through the same procedure yielded 0.04 µg/ml Co.

### Samples

1. Weigh 1 g dry pyrite powder into a reasonably squat porcelain crucible.
2. Roast very slowly at first with a Meker burner until the powder has blackened, then strongly for at least 10 minutes, agitating the powder at 5 minutes.
3. Transfer the oxide produced to a 250 ml beaker on a sand bath at about 150°C, having added 30-40 ml conc. HCl, some of which was used to clean out the crucible. Wash the crucible into the beaker with distilled water.
4. Heat until all the oxide has dissolved, breaking any lumps with a stirring rod. Evaporate to less than 40 ml.

5. Filter off any residue.
6. Add 30 ml 40% sodium citrate.
7. Dilute to 50-75 ml with distilled water.
8. Bring the pH to 3-4 using $NH_4OH$ or HCl, testing with universal pH paper.
9. Cool to room temperature.
10. Add 10 ml 3% $H_2O_2$. Stand for a short time.
11. Add 2 ml of filtered 2-nitroso-1-naphthol reagent solution. Stand for at least 30 minutes.
12. Transfer to a separating funnel, add 25 ml chloroform, and shake for 1 minute.
13. Draw off the chloroform phase into a 50 ml measuring flask.
14. Add 10 ml chloroform to separating funnel, and shake well for one minute.
15. Draw off the chloroform phase into the 50 ml flask.
16. Repeat steps 12 and 13.
17. Combine the three extracts and dilute to 50 ml with chloroform.
18. Transfer some or all of the chloroform phase to a clean funnel.
19. Add 29 ml 2M HCl and shake well for one minute. (Any Ni complex decomposes, and the Ni dissolves in the HCl).
20. Run the chloroform layer into another funnel.
21. Add 20 ml 2M NaOH, and shake for one minute. (This removes excess reagent).
22. Obtain the absorbance of the clear chloroform phase at 530 millimicrons wavelength.

# APPENDIX 4

## ATOMIC ABSORPTION SPECTROPHOTOMETRIC DETERMINATION OF COBALT AND NICKEL

### Reagents

Di-isopropyl ether, technical grade.

9N HCl, Analar.

5.4N HCl, Analar.

15% w/v $CH_3.COONH_4$.

### Standards

Analar $CoSO_4.7H_2O$ dissolved in water.

B.D.H. Ni "thin sheet" metal, dissolved in aqua regia, taken to dryness, and dissolved in acidified water.

Two mixed Co-Ni stocks were made using the above procedure, one more concentrated (Stock 1), one less (Stock 2).

As well as blanks, the following standards were then prepared by taking aliquots of the stocks and adding the final reagents of the sample preparation procedure:

Stock 1 : 100 µg/ml representing 10,000 ppm

| | |
|---|---|
| 50 | 5,000 |
| 25 | 2,500 |
| 15 | 1,500 |
| 10 | 1,000 |
| 6 | 600 |

Stock 2 : 2 µg/ml representing 200 ppm

| | |
|---|---|
| 1.5 | 150 |
| 1 | 100 |
| 0.5 | 50 |
| 0.3 | 30 |
| 0.1 | 10 |

The two segments of the resulting standard graph were collinear, thus verifying the accuracy of the preparations.

Samples

1. Weigh about 0.5 g (accurately to 3 significant figures) dry mineral powder into a reasonably squat porcelain crucible.
2. Roast very gently at first with a Meker burner or in a furnace, until the powder has blackened, then strongly for 10 minutes.
3. Transfer the oxide produced to a 250 ml beaker on a sand bath at about 150°C, having added 15-20 ml conc. HCl, some of which was used to clean the crucible. Wash the crucible into the beaker with distilled water.
4. Heat until all the oxide has dissolved, breaking any lumps with a stirring rod. Evaporate to about 5 ml.
5. Add 5-10 ml distilled water, agitate, and allow to cool to room temperature.
6. Filter into a 1 inch diameter test tube using Whatman 40 or Greens 801 paper. Wash the residue with copious hot distilled water.
7. Evaporate to dryness (or at least to a moist residue) in a water bath, immersing all but one inch of the test tube. (This requires about 12 hours.)

8. Add 12 ml 9N HCl, and about 20 ml di-isopropyl ether. Shake vigorously 200 times in a darkened room. After the aqueous phase has cleared siphon off the ether with a bulb-actuated graduated pipette, and deposit it into a bottle containing distilled water.
   Add another 15-20 ml ether, and repeat the above. Ether dissolved in the aqueous phase can then be largely eliminated by warming the solution, whereupon ether exsolves and can be removed. (This minimises spitting in the next step.)
9. Warm the test tube gently until all dissolved ether is expelled. Then evaporate to dryness in a water bath. (This requires about 4 hours.)
10. Add 5 ml 5.4N HCl, 10 ml 15% w/v $CH_3.COONH_4$.
    Agitate to dissolve all solids.
11. Wash with 10 ml distilled water into a 25 ml volumetric flask, make up to volume with the water, and transfer to a screw-top polythene bottle. The final solution is pH = 0.6. (Higher pH's than this have been satisfactorily used by other workers.)
12. Weigh the filtered material.
13. Recycle the ether by shaking with distilled water, and separating in a funnel. The iron enters the aqueous phase quantitatively.

Analysis

The hollow-cathode lamps and the burner are lit respectively 15 minutes and 10 minutes before machine calibration is commenced, allowing spectral and thermal stabilization of the equipment. Zeroing at 100% transmission is performed while aspirating distilled water. The sequence of analysis is (i) standard (ii) four samples, directly from bottles (iii) repeat standard (iv) if excessive drift has occurred, rezero. Between each

aspiration the system is purged with distilled water. The standards used are approximately equivalent to the concentrations in the samples, unusual concentrations being immediately covered by aspiration of an appropriate standard. For very high Co and Ni concentrations, the burner is rotated to reduce sensitivity, and thus bring the reading onto the linear part of the standard graph; the resulting determination is less sensitive than readings at lower concentrations, but is reproducible.

The following parameters are then compiled as data for computer processing:

z : sample number

a : original sample weight

b : weight of burnt filtered residue and crucible

c : weight of crucible

i : volume of final sample solution

d : sample percentage transmission

e : blank percentage transmission interpolated graphically to the time of sample aspiration

f : standard percent transmission

g : blank percentage transmission interpolated graphically to the time of standard aspiration

h : value of standard in µg/ml.

# APPENDIX 5

## INDEPENDENT SELENIUM ANALYSES

### Department of Mines, Tasmania

The following summary of the technique of selenium analysis used by the Assay Laboratories of the Department of Mines, Tasmania, has been prepared by Mr. H. Wellington, Chief Chemist and Metallurgist.

The method relies on the formation of a selenium complex with 3,3' diamino benzidene. The selenium is isolated in perchloric acid and the complex developed under controlled pH conditions. The colour is extracted with organic solvents and absorbance measured at 400 mμ.

Reagents

Mixed Acid: 20% $HClO_4$ in $HNO_3$.

Hydrochloric Acid: 50%.

Arsenic Solution: Dissolve 0.25 g $As_2O_3$ with 2 g NaOH in 200 ml water.

Reducing Agent: 25% w/v aqueous $NaH_2PO_2$.

E.D.T.A.: 5% w/v aqueous.

Ammonia Solution: 66% from 0.880 S.G.

Buffer solution: Dissolve 60 g ammonium formate in about 600 ml water, add 200 ml formic acid. Adjust pH to about 1.6 with 50% HCl. Dilute to 1 litre.

3,3' Diamino Benzidene: 0.5% w/v aqueous. Prepare immediately before use. The solution decomposes rapidly at room temperature (may be kept one day if refrigerated). N.B. Avoid contact with skin.

Standard Selenium Solution: Dissolve 50 mg of selenium in 10 ml $HNO_3$, boil to expel $NO_2$ and cool. Dilute to 500 ml giving 100 ppm. From this, prepare a solution of 5 ppm i.e. 5 µg Se/ml.

Indicator Paper: Filter paper soaked in 0.1 per cent Thymol Blue and dried.

A. Separation

1. Weigh 1.0 g of sample (containing up to 200 µg Se) into a 100 ml beaker and add 5 ml water and 5 ml mixed acid. When reaction has ceased add a further 15 ml of acid and evaporate to 1 ml. (Caution: Note 1).
2. Cool, add 50 ml 50% HCl, 2 ml arsenic solution and 15 ml reducing solution. Boil for three minutes or until arsenic has precipitated (black).
3. Filter hot through a porosity 4 sintered glass crucible, washing with 50% HCl. Discard the filtrate.
4. Place a 50 ml beaker under the crucible and without connecting vacuum, rinse sides of crucible with 10 ml mixed acid and original beaker with 5 ml. Add this to the crucible and connect vacuum. Wash three times with distilled water. A pipette was found ideal for the acid washes.
5. Apply vacuum and when filtered wash with distilled water. This should be into a 50 ml beaker.
6. Evaporate to 1 ml. Cool. Note 1.

B. Colour Development

7. Add 1 ml E.D.T.A. and neutralize with ammonia solution using a pointed glass rod to make a small spot on the indicator paper. An orange colour indicates the correct pH.
8. Transfer to test tube (8" x 1") with distilled water and dilute to 10 ml.

9. Add 2 ml buffer solution and 0.5 ml 3,3' diamino-benzidene solution. Stand for ½ - 1 hour.

10. Add 2 ml ammonia solution and 5 ml toluene and shake vigorously. Settle.

11. Pipette off 4 ml into a small test tube containing a few pieces of magnesium perchlorate. Stand for 15 minutes or until turbidity clears, adding more perchlorate if necessary.

12. Read the absorbance of the solution at 400 mμ.

13. Run standards, starting from stage 1. Standards recommended are 0, 10, 25, 50 and 75 μg Se.

Notes

1. Beware of evaporating to dryness or even near dryness as serious loss of selenium occurs.

2. Isolation of the selenium by co-precipitation with arsenic has been used. Of the elements that accompany arsenic there is no interference from tellurium, antimony, bismuth, lead, silver or tin. Copper is masked by E.D.T.A.

3. Solution of the co-precipitated selenium direct from the sintered glass crucible allows the initial filtration of insoluble to be neglected. (In the case of a large insoluble an initial filtration may be necessary). Wash with 50% HCl.

4. Optimum pH for complex development is 1.5-2.7, development taking 30 minutes, no change being observed in the next hour. Optimum pH for extraction is 4.3-10.3. The use of the buffer facilitates the change.

5. The colour may be extracted in toluene and absorbance measured at 400 mμ. An absorbance at 420 mμ has been reported as due to

impurities in the 3,3' diamino benzidene. Benzene was tried (Stanton and McDonald, 1965) but found to be exceptionally prone to turbidity.

6. Turbidity may occur after settling from the extraction. The method used involved removal of the water with magnesium perchlorate, the oxidising agent not attacking the complex. As a matter of procedure this was done with all samples whether apparently turbid or not.
7. The calibration graph is linear to 100 µg selenium at an absorbance of 1.8. Solutions up to 500 µg may be diluted, but it is better to start with a smaller weight. Normally standards to 75 µg selenium are sufficient.

Reproducibility

The replicate determinations are given in the following Table A5.1.

Comparison of independent analyses

Table A5.1 lists the detailed results of the independent analyses by the author, the Tasmanian Mines Department, and the Australian Mineral Development Laboratories.

Table A5.1

| Specimen No. | Min. | This study | Tas. Mines Dept. | AMDEL |
|---|---|---|---|---|
| 11175 | Py | 17 | N.D. | <0.5 |
| 11242b | Py | 200 | 154 (150, 158) | N.D. |
| 32696 | Hm | N.D. | 590 | 250 ± 10 |
| 100015 | Sl | 12 | N.D. | <0.5 |
| 100284 | Py | 18 | 12 | N.D. |
| 100317 | Py | 121 | 122 | N.D. |
| 100369a | Py | 77 | 124 (132, 116) (52, 70, 86, 152)* | N.D. |
| 100421 | Py | 63 | N.D. | 30 ± 5 |
| 100422 | Cpy | 41 | 42 | 5 ± 2 |
| 100456 | Py | 0 | 5 (1, 5, 9) | 0.5 |
| 100478 | Py | 211 | 242 (236, 248) | N.D. |
| 100510a | Py | 90 | N.D. | 50 ± 5 |
| 100510b | Py | 90 | N.D. | 45 ± 5 |
| 100551 | Py | 4 | N.D. | 1 ± 1 |
| 100570 | Py | 311 | 456 (464, 448) (300)* | 150 ± 10 |
| 100572 | Py | 312 | N.D. | 290 ± 10 |
| 100574 | Py | 18 | 16 | 4 ± 1 |
| 100580 | Py | 29 | N.D. | 1 ± 1 |
| 100587a | Po | 90 | 80 | N.D. |

Comparison of independent selenium analyses in ppm. All quoted values for this study are ± 7 ppm. Figures in brackets are replicate analyses and * represents analyses which have been discounted due to alleged interference in colorimetric determination.

N.D. = not determined.

# REFERENCES : APPENDICES


Both, R.A., 1966: The zoned ore deposits of the Zeehan mineral field. M.Sc. thesis (unpublished). University of Tasmania.

Doe, B.R., Chodos, A.A., Rose, A.W., and Godijn, E., 1961: The determination of iron in sphalerite by X-ray fluorescence spectrometry. Am. Miner., 46, 1056-1063.

Ivanov, V.V., 1964: Distribution of cadmium in ore minerals. Geochemistry, 4, 757-768.

Sandell, E.B., 1959: Chemical Analysis, Vol. 3 : Colourimetric Determination of Traces of Metals. 3rd ed. Interscience, New York.

Skinner, B.J., Barton, P.B. Jr., and Kullerud, G., 1959: Effect of FeS on the unit cell edge of sphalerite. A revision. Econ. Geol., 54, 1040-1046.

Solomon, M., 1964: The spilite-keratophyre association of west Tasmania and the ore deposits at Mt. Lyell, Rosebery and Hercules. Ph.D. thesis (unpublished). University of Tasmania.

Stanton, R.E., and McDonald, A.J., 1965: The determination of selenium in soils and sediments with 3,3'-Diamino-benzidine. Analyst, 90, 497-499.

Stillwell, F.L., 1934: Observations on the zinc-lead lode at Rosebery, Tasmania. Proc. Australas. Inst. Min. Metall., no.94, 43-69.

Mineralium Deposita 2, 228–242 (1967)

# Cobalt, Nickel and Selenium in Sulphides as Indicators of Ore Genesis

G. Loftus-Hills and M. Solomon
University of Tasmania, Hobart, Australia

REPRINTED FROM:
*Journal of the Geological Society of Australia*
*Vol.* 14, *Pt* 2, *pp.* 333-338.

# THE STRUCTURE OF THE BEDDED ROCKS WEST OF ROSEBERY, TASMANIA

By G. LOFTUS-HILLS, M. SOLOMON & R. J. HALL



SYDNEY
1967